Regulation of Cytokine mRNA stability

Cheryl Yvette Brown

A thesis submitted for the degree of Doctor of Philosophy of the University of Adelaide (Faculty of Science)

Division of Human Immunology

Hanson Centre for Cancer Research

Institute of Medical and Veterinary Science

and

Department of Microbiology and Immunology

University of Adelaide

Adelaide, South Australia

June 1996

Contents

Summary

The production of cytokines is normally very low in unactivated cells but may be induced by exposure to specific stimuli such as bacterial endotoxin, lectin, antigen or other cytokines. Their expression may be controlled at the level of transcription and by post-transcriptional mechanisms. Upon induction, the mRNA of many cytokines switches from being very unstable to being transiently stabilised. There is still very little known about the mechanisms involved in regulating cytokine mRNA stability and the aim of the work presented in this thesis was to investigate this process.

Many cytokines are involved in orchestrating inflammatory responses but negative regulation plays an essential role in limiting the magnitude and duration of a response. IL-10 is one of a few cytokines that downregulates production of inflammatory cytokines such as G-CSF and GM-CSF and I wished to find out whether IL-10 downregulated their production by modulating the stability of these cytokines. IL-10 downregulated accumulation of G-CSF and GM-CSF mRNAs in LPS-activated monocytes very rapidly, and it also downregulated its own expression, although this was with a considerable delay. Endogenously produced IL-10 also downregulated accumulation of these cytokines but a delay was observed compared with downregulation imposed by exogenously added IL-10. This delay was presumably because endogenously produced IL-10 had to accumulate to a sufficient concentration in the culture medium before its effects were observed. IL-10 did downregulate the accumulation of G-CSF, GM-CSF and IL-10 mRNAs by reducing the stability of their mRNAs but differential regulation of these cytokines by IL-10 was observed. Whereas IL-10 reduced the stability of G-CSF and GM-CSF mRNAs rapidly, it reduced the stability of its own mRNA with some delay. This differential regulation of cytokines by IL-10 might explain its role in modulating the function of monocytes. Production of inflammatory cytokines, such as G-CSF and GM-CSF, occurs rapidly after cellular activation by stimuli such as bacteria. In contrast, IL-10, whose function is to subdue the

primary inflammatory response, is released somewhat later and then negatively regulates its own production.

Stabilisation of cytokine mRNAs in response to cellular activation is an important mechanism for inducing cytokine production but very little is known about the mechanisms involved in increasing the stability of the mRNA. The AU-instability elements (AUIEs), found in many cytokines whose expression is regulated at the level of mRNA stability, play an important role in mediating the rapid decay of an mRNA, but may only have a limited role in mediating stabilisation of the mRNA in response to cellular activation. I used a model system to investigate regulation of GM-CSF mRNA stability in response to IL-1β, TNFα, PMA and calcium ionophore (A23187). Stabilisation of mRNA in response to A23187 was conferred by the AUIEs but they were not sufficient for stabilisation in response to PMA, IL-1β or TNFα. The 3'UTR from human or mouse GM-CSF did not confer response to these agents and although endogenous GM-CSF was induced in response to IL-1β and TNFα, mRNA from a chimeric gene bearing the full cDNA of mouse GM-CSF was still unable to mediate response to these agents.The reason for this lack of stabilisation remains unresolved.

Investigation of the regulation of G-CSF mRNA stability led to the identification of instability elements which are functionally distinct from the AUIEs. mRNA from a chimeric gene containing the AU-rich region of G-CSF was stabilised in response to A23187 treatment of NIH3T3 cells whereas mRNA from a chimeric gene containing the entire 3'UTR of G-CSF was not. Additionally, the mRNA from the chimeric gene containing the AU-rich region of G-CSF was very stable in a bladder carcinoma cell line, 5637, whereas mRNA from the gene containing the entire 3'UTR remained relatively unstable. These results suggested the presence of additional instability elements, and further investigation revealed a region containing 2 putative stem-loop structures conserved between human and mouse. Analysis of these stem-loops indicated that these were instability elements with one of the stem-loops being the predominant destabilising element. This stem-loop destabilising element still functioned when NIH3T3 cells were stimulated with calcium ionophore and it still functioned in the

bladder carcinoma cell line. These results suggest a mechanism to explain the differential expression of some cytokines.

Declaration

This work contains no material which has been accepted for the award of any other degree or diploma in any university or other tertiary institution and, to the best of my knowledge and belief, contains no material previously published or written by any other person, except where due reference has been made in the text.

I give consent to this copy of my thesis, when deposited in the University library, being available for loan and photocopying.

Signed **Date** 5th June '96

Acknowledgements

I would like to thank Professor Mathew Vadas for allowing me to pursue my studies in the Division of Human Immunology at the Hanson Centre for Cancer Research.

I am very grateful for the friendly and relaxed supervision provided by my immediate supervisor Dr. Greg Goodall. His support throughout my project and guidance in preparing this thesis were invaluable.

I would particularly like to acknowledge my fellow workers in the laboratory of Dr. Greg Goodall and throughout the Division of Human Immunology for providing such a stimulating environment in which to work. I am particularly grateful to Cathy Lagnado, for teaching me many of the techniques used during the course of this work and to Cathy, Justin Dibbens and Lara Fitzgerald for much stimulating discussion.

I would like to thank Richard D'Andrea (D.A) for being a very supportive, Paul Moretti for many useful tips and Karen Jones for providing such a lively atmosphere. During my stay here I have been made very welcome by many people including, Jo Woodcock, Chris Ford, Fay Jenkins, Andrew Bert, Cameron Osborne, Roy Himes, Di Miller, Steve Repacholi, Di Favier, Pritinder Kaur, Leanne Coles, Joe Wrin and Fil Occhiodoro. I would like to thank them for their friendship and support.

Thanks also to Cindy Ralph and Brian Walker for providing glassware, tips pipettes and much more. Their patience and tolerance were much appreciated.

I would like to especially thank my partner, Simon Barry for all of his understanding and support over the years and for his belief (much greater than my own) that I really could do it. He has always been there when I have needed help. Finally, to my constant companion, my little dog Bumpy.

Chapter 1

Introduction

1.1 Cytokines

Cytokines are a large family of regulatory molecules produced by many cell types which act on nearly every tissue and organ system. The haemopoietic growth factor family of cytokines, are produced by many cell types including leukocytes, fibroblasts, vascular endothelial cells and mesothelial cells and play an essential role in many aspects of haemopoiesis and immunity. They exhibit considerable functional overlap as well as functional pleiotropy by promoting cell proliferation, survival, differentiation, commitment and they also trigger the functional activation of mature cell responses. Production of these growth factors is normally very low in unactivated cells but may be induced by exposure to specific stimuli such as bacterial endotoxin, lectin, antigen, or other cytokines.

1.2 mRNA stability

The expression of many genes is modulated at the level of transcription but it has become clear that post-transcriptional mechanisms also play an important role. For example, the efficiency of nuclear RNA processing has been suggested to play a regulatory role in the expression of some genes (Prendergast and Cole, 1989) as does intranuclear destabilisation of the primary transcript (Akahane and Pluznik, 1992). For some cytokines the primary mechanism for regulation is at the level of translational efficiency (Han and Beutler, 1990). However, for many cytokine mRNAs regulation of stability is the predominant mechanism for regulating gene expression.

For some time it has been known that in a variety of cell types some mRNAs are short-lived while others persist in the cytoplasm for several hours (Aviv *et al.*, 1976)or in some cases several days (Krowczynska *et al.*, 1985). Many growth factors and proto-oncogenes fall into the class of mRNAs that are expressed only transiently before being

degraded (Greenberg and Ziff, 1984; Berger and Cooper, 1975; Raj and Pitha, 1981). The high rate of growth factor mRNA turnover is consistent with their role of in control of haemopoeisis and immunity. It is important that growth factors are produced rapidly in response to local stimuli so that they can exert their effects almost immediately at their target site. Their production may initiate a cascade of signalling events allowing waves of immune responses. Owing to this role and the fact that they are very potent in their effects, growth factor release is only required for very short bursts. Unregulated production may result in dysregulation of haemopoiesis and immunity and may ultimately lead to malignant transformation. Proto-oncogenes are also induced rapidly and transiently in response to a variety of extracellular stimuli and regulate transcription of diverse genes important for cell growth and differentiation (Chiu *et al.*, 1988). Overexpression of proto-oncogenes may, similarly, lead to tumourogenic transformation (Piechaczyk *et al.*, 1985; Eick *et al.*, 1985).

More recently, it was observed that a region of the 3'UTR of GM-CSF rich in adenosines and uridines was highly conserved (Shaw and Kamen, 1986) and further, that a consensus sequence of 8 nucleotides (TTATTTAT) occurred in the 3'UTRs of several other cytokines and proto-oncogenes (Caput *et al.*, 1986). A role for these sequences was further suggested by the observations that mutated forms of the c-*myc* (Aghib *et al.*, 1990; Hollis *et al.*, 1988) and c-*fos* (Meijlink *et al.*, 1985) genes, with mutated AREs lead to stabilisation of their mRNAs and also renders them oncogenic. Since these findings might imply some functionality, experiments were carried out to investigate whether the AU sequences did have some role in gene expression. In their experiments Shaw and Kamen (Shaw and Kamen, 1986) found that a 51-nucleotide sequence from the 3'UTR of human GM-CSF could destabilise the normally stable rabbit β-globin mRNA. These experiments led to the identification of the AU-destabilising element which at that time was thought to be AUUUA, since this was the motif common to all of the cytokines and proto-oncogenes examined. Until recently, the notion that the AU-instability element (AUIE) is the motif AUUUA has pervaded the literature, but the functional element has now been shown to be a longer nonamer motif (Lagnado *et al.*, 1994; Zubiaga *et al.*, 1995) comprising UUAUUU(U/A)(U/A), a motif

similar to that originally suggested, but not tested, by (Caput *et al.*, 1986). Since the initial finding of Shaw and Kamen that a cis-acting sequence motif is probably responsible for the rapid turnover of cytokine and proto-oncogene mRNAs a whole field of investigation into mechanisms involved in the regulation of rapidly degraded mRNAs has evolved.

1.3 The relationship between mRNA stability and translation

Since the initial observation that the degradation process of c-*fos* mRNA was dependant on protein synthesis (Greenberg *et al.*, 1986), much evidence has accumulated to suggest an intimate relationship between mRNA stability and translation. The first line of evidence comes from the use of inhibitors of translation such as cyclohexamide, (which inhibits elongation of the poly-peptide chain) and puromycin, (which prematurely releases the ribosomes from the mRNA), both of which lead to the stabilisation of the mRNA. Two explanations may account for these observations. The first possibility is that for decay of mRNA there is a requirement for active translation, which might suggest that the location of ribonucleases involved in the decay process is within the ribosome complex. The second possibility is that a labile protein required for the decay process is itself degraded when protein synthesis is inhibited. This second possibility seems somewhat unlikely for several reasons including the fact that decay of labile mRNAs is arrested immediately after cyclohexamide treatment of cells, which would require the labile protein to be extremely unstable. Several other lines of evidence suggest that translation itself has to be actively ongoing for decay of the mRNA to occur. Savant-Bhonsale and Cleveland (Savant Bhonsale and Cleveland, 1992) observed formation of a large (>20S) complex on unstable mRNAs. When translation was inhibited by mutating the first methionine codon, if the AU element was moved into the translated region, or when the AUIEs

were disrupted, increased stability of the mRNA was observed and formation of the complex did not occur. Similar observations indicated that decay of c-*fos* (Schiavi *et al.*, 1994), c-*myc* (Herrick and Ross, 1994) and GM-CSF mRNAs (Winstall *et al.*, 1995) only occurred when the transcripts were distributed on polyribosomes. The evidence for a close relationship between efficient translation and degradation of the mRNA was further extended by the observation that inserting strong stem-loop structures into various positions in the coding region, preventing complete translation, or even into the 3'UTR, inhibited decay of the GM-CSF mRNA (Curatola *et al.*, 1995). This claim has been somewhat countered, however, by the findings of Chen *et al* (Chen *et al.*, 1995) whose insertion of a hairpin loop to inhibit translation did not impede decay of chimeric genes bearing c-*fos* or GM-CSF 3'UTRs, suggesting that mRNA decay can be uncoupled from translation. These observations may be due to differences in cell lines used, different treatment of cells and technical differences in the experimental procedures, since the bulk of evidence suggests that mRNA decay is tightly coupled to the process of translation.

1.4 The role of the poly(A) tail in mRNA degradation

The mechanism by which an mRNA is metabolised by the cell is still largely unknown but there is a growing body of evidence to suggest that the poly(A) tail plays a critical role in in this process. Binding of the poly(A) binding protein to the poly(A) tail at the 3' terminal end of the 3'UTR of most mammalian mRNAs is thought to protect the mRNA from deadenylation and subsequent degradation (Bernstein *et al.*, 1989). Histone mRNAs are the only mammalian mRNAs which do not possess a poly(A) tail and instead have a stem-loop structure (Birnsteil *et al.*, 1985) to protect the mRNA from degradation. The poly(A) tail with its associated binding protein (PABP) also plays an important role in initiation of protein synthesis (Sachs and Wahle, 1993). AU sequences have been shown to promote the rapid removal of the poly(A) tail (Wilson and

Treisman, 1988) and it is now known that shortening of the poly(A) tail precedes the degradation of many mRNAs that contain AU-rich sequences in the 3'UTR. The rate of poly(A) shortening is, in fact, directly proportional to the potency of an AUIE in directing degradation of the mRNA (Lagnado *et al.*, 1994; Zubiaga *et al.*, 1995; Shyu *et al.*, 1991). Deadenylation does not occur uniformly, but in several phases. During the first phase there is a progressive shortening of the tail (Brewer and Ross, 1988; Shyu *et al.*, 1991; Wilson and Treisman, 1988) and in yeast this is then followed by a more rapid phase (Lowell *et al.*, 1992). The body of the mRNA may then be either degraded immediately or first be completely deadenylated. The process by which the final adenosine residues are removed is called terminal deadenylation and involves the slow removal of an oligo(A) tail which is approximately 5-15 adenosine rsidues in yeast (Decker and Parker, 1993) and 25-60 residues in some mammalian transcripts (Shyu *et al.*, 1991; Chen and Shyu, 1994). Deadenylation to oligo(A) might result in the loss of the last poly(A) binding protein associated with the transcript which may trigger further decay events.

1.5 The pathway of mRNA decay

It seems clear that for many, but not all yeast mRNAs, removal of the poly(A) tail triggers removal of a protective 7-methyl guanosine 5' triphosphate (5' "cap") (Decker and Parker, 1993) present at the 5' end of the mRNA, and this precedes decay of the body of the mRNA. Yeast mRNAs may undergo deadenylation-independent decay in a number of circumstances as part of an mRNA surveillance process. This decay pathway is utilised if mRNA contains nonsense codons (Leeds *et al.*, 1992) others from intro), unspliced introns (He *et al.*, 1993) or elongated 3'UTRs (Pulak and Anderson, 1993) and ensures removal of aberrant transcripts. When the mRNA undergoes deadenylation prior to degradation, decay of the mRNA may proceed in a 5' to 3' or alternatively 3' to 5' direction, and there is evidence that 5' to 3' exonucleolytic

decay may be the predominant decay pathway in yeast (Larimer and Stevens, 1990; Muhlrad *et al.*, 1994; Muhlrad *et al.*, 1995). with 3' to 5' decay being detectable when the 5' to 3' decay pathway is blocked (Muhlrad and Parker, 1994). It seems likely that both of these pathways are used but the 5' to 3' pathway being the faster, primary route (Muhlrad *et al.*, 1995). It is not known how prevalent the 3' to 5' pathway of decay is or whether endonucleases or exonucleases are involved.

1.6 Protein factors associated with short-lived mRNAs

It is likely that trans-acting factors will be involved in mRNA decay, possibly binding to the instability element and stimulating the subsequent decay of the transcript. The proteins that are involved in the decay of eukaryotic mRNAs have not been elucidated although several candidates have been identified. Adenosine-uridine binding factor (AUBF) which binds 4 reiterations of the pentamer motif AUUUA, forming a 44kD complex in T lymphocytes (suggesting a binding factor of approximately 36kDa), was the first potential factor to be identified (Malter, 1989). A factor of 32kDa was identified in HeLa cells (Vakalopoulou *et al.*, 1991) with binding characteristics so similar to AUBF that it is likely to be the same protein. AUBF was subsequently shown to bind mRNAs from GM-CSF, IFN-γ, IL-3, c-*fos*, and v-*myc* (Gillis and Malter, 1991). Although these results showed that AUBF could bind sequences containing multiple AUIEs, the exact binding motif was not elucidated and a role in degradation was not demonstrated. A role for AUBF in protecting GM-CSF mRNA from degradation was suggested, however, by the observations that it was upregulated in PBMC stimulated with phorbol ester or calcium ionophore (Malter and Hong, 1991) under which conditions some mRNAs, including GM-CSF are stabilised. A role in protecting mRNAs from degradation was also suggested in an *in vitro* degradation system using polysomes prepared from PBMC (Rajagopalan and Malter, 1994). Subsequently, additional binding proteins have been identified. AU-A is constitutively produced by

human T lymphocytes where it binds to sequences in the 3'UTRs of TNF, IL-2, and c-*myc,* and to a sequence comprising AUUUAUUUAUUUAUUUAUUUA (5AU) from the GM-CSF 3'UTR. Based on the similar binding characterisics of AU-A and AUBF, they are likely to be the same protein. AU-B and AU-C were isolated at the same time and have qualities distinct from AU-A. (Bohjanen *et al.*, 1991) AU-B and AU-C also bind sequences in the 3' UTRs of TNF and IL-2 and the 5AU sequences, in human T lymphocytes but are distinct from AU-A in that binding was only observed when the cells were stimulated through the TCR/CD3 complex, which induces but does not stabilise these mRNAs. AU-B and AU-C, unlike AU-A, did not bind to the c-*myc* sequences and were not competed by these sequences. Furthermore, stimulation of the T cells with PMA, which stabilises the cytokine but not the c-*myc* transcripts, decreased AU-B binding and increased AU-A binding. These were important findings since they suggested a mechanism for the differential regulation observed between cytokine and c-*myc* transcripts (Schuler and Cole, 1988). The observation that AU-B is inducible in T cells following TCR/CD3 stimulation but is downregulated in lymphocytes stimulated by phorbol-ester suggests a role for this protein in mRNA metabolism, possibly targeting it for degradation. Although AU-B and AU-C have different apparent molecular masses (30 and 43 kDa, respectively) they display identical patterns of induction, sequence specificities, binding characteristics and protease cleavage patterns which suggests that they are likely to be alternatively processed or modified products of the same gene (Bohjanen *et al.*, 1992).

Several candidate factors have also been isolated using *in vitro* systems; AUF1, made up of 2 polypeptides of 37 and 40kD, (Brewer, 1991) was identified using an *in vitro* decay system. AUF1 binds c-*myc* and GM-CSF and selectively accelerates degradation of the c-*myc* transcript. Affinity purification was used to isolate AU-H, a 32kD protein was which binds $(AUUUA)_6$ (Nakagawa *et al.*, 1995) and, interestingly, this protein has intrinsic enoyl-CoA hydratase activity although the physiological significance of this observation is not understood. Although several proteins that bind to AU sequences have been identified, attribution of a definite role in regulation of mRNA stability to these proteins remains elusive.

1.7 Regulation of Cytokine mRNA stability

Constitutive expression of cytokines is very low and their mRNAs, in many cases, are undetectable. The low steady state levels observed are largely owing to their very short half-lives. In response to a variety of stimuli, such as growth factors, phorbol-esters, lectins and antigens, however, a rapid, transient burst of production occurs. For many cytokines this results from stabilisation of the mRNA (Shaw and Kamen, 1986; Ernst *et al.*, 1989; Bickel *et al.*, 1990; Thorens *et al.*, 1987; Koeffler *et al.*, 1988; Gorospe *et al.*, 1993; Le *et al.*, 1991; Akahane and Pluznik, 1992; Falkenburg *et al.*, 1991; Bagby *et al.*, 1990; Wodnar-Filipowitz and Moroni, 1990), the transcript becoming transiently stabilised to enable a brief pulse of protein production. Thus, modulation of mRNA stability plays an important role in gene expression. The mechanisms that regulate stability of cytokine mRNAs, however, are complex and poorly understood. It seems likely that mechanisms will vary between cytokines, cell types and depending on which signalling pathways are activated. In view of their role in directing rapid decay of mRNAs it would seem reasonable to predict that the AUIE would also be involved in stabilising the mRNAs. There are various lines of evidence to suggest that, in fact, the AUIE may play only a small part in this process (Iwai *et al.*, 1991; Bagby *et al.*, 1990; Akashi *et al.*, 1991), with as yet undefined *cis*-acting sequences or structures playing a predominant role. Chapter 4 of this thesis describes an investigation into mechanisms involved in regulation of GM-CSF mRNA stability.

1.8 Coordinate *versus* independent regulation of cytokine production

As part of the initial development of an inflammatory response pro-inflammatory cytokines such as IL-1 and TNF are released, which mediate a wide range of

inflammatory events including production of many other inflammatory cytokines. This network of interactions leads to a whole cascade of cytokine signalling events, resulting in a complex, self-limiting immune response. The waves of cytokine release culminate in production of anti-inflammatory cytokines such as IL-10 (Fiorentino *et al.*, 1989; Fiorentino *et al.*, 1991; de Waal Malefyt *et al.*, 1991), IL-4 (te Velde *et al.*, 1990), IL-13 (de Waal Malefyt *et al.*, 1993)and TGF-β (Espevik *et al.*, 1987), which downregulate production of inflammatory cytokines such as TNF, IL-1, G-CSF, GM-CSF and IL-8 and thus limit the imune response. Release of inflammatory cytokines would therefore be expected to be an initial event, followed by production of the anti-inflammatory cytokines. Thus, in response to specific stimulation there may be both simultaneous induction of a number of cytokines (Le *et al.*, 1987; Koeffler *et al.*, 1988; de Waal Malefyt *et al.*, 1991; Broudy *et al.*, 1986), or independent release (Clark and Kamen, 1987; Vellenga *et al.*, 1988; Hamilton, 1994). Similarly, cytokines may be produced independently by cells to promote maturation, proliferation and stimulation of certain cell lineages. To allow such a complex network of cytokine release mechanisms must exist to permit coordinate and independant cytokine production. One mechanism that could account for independent regulation of cytokine expression would be the presence of alternative instability determinants which may be present in some cytokines but not others. In Chapter 3, I observe that G-CSF and GM-CSF mRNAs are regulated independently of IL-10 mRNA. G-CSF and GM-CSF mRNAs are more rapidly induced by LPS than IL-10 mRNA and then subsequently more rapidly downregulated by IL-10, than the IL-10 transcript itself, which does suggest the presence of alternative regulatory elements in addition to the AUIEs. Iwai *et al* (Iwai *et al.*, 1991) found that a region in the GM-CSF 3'UTR 160 nucleotides upstream of the AUIE was required for response to PMA and instability elements in addition to the AUIEs have been observed in several other cytokines and proto-oncogenes. The c-*myc* mRNA (Alberta *et al.*, 1994) contains a 39 base uridine-rich domain which cooperates with the AUIE to generate a destabilising signal. A similar uridine-rich element is present in the 3'UTR of c-*fos* mRNA (Chen and Shyu, 1994) as well as an instability determinant in its protein coding region (Shyu *et al.*, 1989). Although the AU sequences in the 3'UTR of IFN γ destabilise a chimeric

mRNA, deletion of these sequences does not lead to accumulation of IFN γ mRNA (Peppel *et al.*, 1991), suggesting that this cytokine mRNA may also possess alternative instability elements.

Finally, in Chapter 5 I discuss the identification of stem-loop destabilising elements in the 3'UTR of G-CSF which are functionally distinct from the AUIEs. Additional instability determinants present in G-CSF and possibly other mRNAs may help to explain selective expression of some cytokines while others remain uninduced, thus allowing greater control of gene expression.

Chapter 2

Materials and Methods

2.1 Abbreviations

Standard abbreviations were as described for The Journal of Biological Chemistry, 1993, volume 268, pages 750-753. Non-standard abbreviations are listed below:

APS	ammonium persulphate
ATP	adenosine triphosphate
AU	absorbance units
AUBF	adenosine-uridine binding factor
AUIE	adenosine-uridine instability element
Amp	ampicillin
BEB	blunt-end buffer
bp	base pairs
BSA	bovine serum albumen
CIP	calf intestinal phosphatase
CMV	cytomegalo virus
CTP	cytosine triphophate
d	deoxy (ribonucleotide)
DEPC	diethyl pyrocarbonate
DMEM	Dulbecco's modified Eagle's Medium
DMSO	dimethylsulphoxide
DNA	deoxyribonucleic acid
DNase	deoxyribonuclease
DTT	dithiothreitol
EDTA	ethylenediaminetetra-acetic acid
EGF	epithelial growth factor
FCS	foetal calf serum
FSB	frozen storage buffer
G-CSF	granulocyte-colony stimulating factor

GH	growth hormone
GM-CSF	granulocyte macrophage-colony stimulating factor
GTP	guanosine triphosphate
HBS	hepes buffered saline
HBSS	Hank's balanced salt solution
h	hour
IFN	interferon
IL	interleukin
IRE	iron response element
LPS	lipopolysaccharide
kDa	kilodalton
mA	milliamps
M-CSF	macrophage-colony stimulating factor
MEN	MOPS EDTA sodium acetate
mins	minutes
MoAb	monoclonal antibody
mRNA	messenger RNA
NK	natural killer
nt	nucleotides
OD	optical density
PAGE	polyacrylamide gel electrophoresis
PBMC	peripheral blood monocluclear cell
PBS	phosphate buffered saline
PCR	polymerase chain reaction
PKC	protein kinase C
PMA	phorbol myristate acetate
RNA	ribonucleic acid
RNase A	ribonuclease A
rpm	revolutions per minute
SSC	saline sodium citrate

secs	seconds
SEM	standard error of the mean
SDS	sodium dodecyl sulphate
SLDE	stem-loop destabilising element
TAE	tris acetic acid EDTA
TBE	tris-boric acid EDTA
TBS	tris-buffered saline
TCA	trichloroacetic acid
TE	tris-EDTA
TEG	tris-EDTA glucose
TELT	tris-EDTA lithium chloride
TEMED	N,N,N',N'-tetramethyl-ethene-diamine
TGF	transforming growth factor
TLC	thin layer chromatography
TNF	tumour necrosis factor
TTP	thymidine triphosphate
tRNA	transfer RNA
UTP	uridine triphosphate
UTR	untranslated region
UV	ultra-violet

2.2 Chemicals, reagents and consumables

Standard chemicals were obtained from Ajax Chemicals (Auburn, NSW), BDH Chemicals (Poole, UK) and Sigma Chemical Company (St. Louis, MO)

2-Mercaptoethanol : **Ajax Chemicals, Auburn NSW.**

Urea, formamide, glycerol, triton X-100, DMSO : **BDH, Poole UK.**

TEMED, acrylamide, bis-acrylamide, SDS: **Bio-Rad, Richmond, CA.**

Actinomycin D, proteinase K, ampicillin, glycogen : **Boehringer-Mannheim, Mannheim, FRG**

LPS, yeast extract : **DIFCO laboratories, Detroit, MI.**

Guanidine thiocyanate : **Fluka, Biochemica, Buchs, Switzerland.**

Agar, caesium chloride, DMEM, foetal calf serum, G418 (Geneticin), RPMI, ammonium persulphate, low melting point agarose, peptone : **Gibco Laboratories, Glen Waverly, Victoria.**

Trypsin : **Multicell, Trace Biosciences, Aust.**

Lymphoprep: **Nycomed, Oslo, Norway.**

Tryptone: **Oxoid, Basingstoke, UK.**

deoxyribonucleotide triphosphates, ribonucleotide triphosphates, actinomycin D, BSA : **Pharmacia, Uppsala, Sweden.**

Agarose, ampicillin, BSA, chloramphenicol, DTT, EDTA, ethidium bromide, salmon sperm DNA, SDS. tetracycline,Tris base tRNA, DePeX, DEPC, lysozyme, spermidine, DEAE dextran, E-toxa clean: **Sigma Chemical Company, St. Louis, MO.**

Phenol : **WAKO Pure Chemical Industries Ltd, Osaka, Japan.**

3MM filter paper: **Whatman International Ltd. Maidstone, UK**

2.3 Radiochemicals

Reagents were obtained from the following sources:

[α-^{35}S]dATP (1,500 Ci/mmol), [α-^{32}P]UTP (3,000 Ci/mmol), [γ-^{32}P]ATP (4,000 Ci/mmol) : BRESATEC, Adelaide, S.A.

[^{3}H]thymidine (6.7 Ci/mmol) : ICN, Costa Mesa, CA.

2.4 Enzymes

All restriction enzymes were purchased from New England Biolabs (Beverly, MA.), Pharmacia (Uppsala, Sweden), Boehringer Mannheim (Mannheim, FRG.) or Amersham (Amersham, UK)

Other enzymes were purchased from the sources listed:

RNase H : **Amersham, Amersham, UK.**

Calf intestinal phosphatase : **Boehringer Mannheim, Mannheim, FRG.**

T7 Superbase Sequencing kit : **BRESATEC, Adelaide, S.A.**

T4 DNA ligase, T4 polynucleotide kinase : **New England Biolabs, Beverly, MA.**

Thermus *aquaticus* (*Taq*) DNA polymerase : **The Perkin Elmer Corporation, Norwalk, CT.**

RNasin, E. *coli* DNA polymerase I Klenow fragment, T7 DNA polymerase, T4 DNA ligase : **Pharmacia, Uppsala, Sweden.**

RQ-DNase, SP6 RNA polymerase, T7 RNA polymerase, Proteinase K, RNase A : **Promega Corporation, Madison, WI.**

Lysozyme : **Sigma Chemical Company, St. Louis, MO.**

2.5 Standard solutions

2x blunt-end buffer (BEB)	50mM Tris-HCl pH7.4, 10mM $MgCl_2$, 0.5mM spermidine, 20µg/ml BSA, 10mM DTT, 2.5mM hexamine cobalt chloride. Stored at -20°C.
10x CIP dephosphorylation buffer	10mM $ZnCl_2$, 10mM $MgCl_2$, 100mM TrisHCl pH8.3. Stored at -20°C.
10x DNase buffer	100mM Tris pH8 (DEPC), 100mM $MgCl_2$ (DEPC), 10mM DTT. Stored at -20°C.
Solution D	4M guanidinium thiocyanate, 25mM sodium citrate pH 7.0, 0.5% sarcosyl, 0.1M β-mercaptoethanol. Stored at - 20°C.
1x Denhardt's solution	0.02% (w/v) Ficoll, 0.02% (w/v) BSA, 0.02% (w/v) PVP. Stored at -20°C.
Electroporation buffer	Hepes buffered saline, above, 0.6% glucose. Made fresh.
Elutriation buffer	1x HBSS, 0.1% FCS (v/v), 0.01% EDTA (w/v), 0.1% glucose (w/v). Made fresh.
Formaldehyde sample buffer	1.2x MEN, 8.4% (v/v) formaldehyde, 64% formamide
Formamide loading buffer	95% formamide, 20mM EDTA, 0.05% bromophenol blue, 0.05% xylene cyanol FF. Stored at 4°C.
10x HBS	8.18% (w/v) NaCl, 5.94% (w/v) Hepes, 0.2% (w/v) (calcium phosphate transfection) Na_2HPO4. Filter sterilised, stored at 4°C
2x HBS	diluted 10x pH 7.12 adjusted with 1M NaOH. Stored at 4°C

10x HBSS	4.0g KCl, 0.6g KH_2PO_4, 80.0g NaCl, 3.5g $NaHCO_3$ 0.475g Na_2HPO_4 to 1L. Autoclaved, stored at 4°C
Hepes buffered saline	20mM Hepes, 137mM NaCl, 5mM KCl pH7.05, filter sterilised. Autoclaved, stored at 4°C.
Hybridisation solution (RNase protection assay)	40mM PIPES pH 6.7 (DEPC), 400mM NaCl (DEPC), 1mM EDTA (DEPC), 80% formamide. Stored at -20°C.
6x Type111 loading solution	0.25% (w/v) bromophenol blue, 0.25% xylene cyanol, 30% glycerol. Stored at 4°C.
5x Kinase buffer	250mM Tris-HCl pH7.6, 50mM $MgCl_2$, 25mM DTT, 0.5mM spermidine HCl, 0.5mM EDTA pH8.0. Stored at-20°C.
10x MEN	200mM MOPS, 10mM EDTA, 50mM sodium acetate pH 7.0
Phenol	includes 0.1% 8 hydoxyquinoline. Stored in dark at 4°C.
Qiagen P1 buffer	100µg/ml RNase A, 50mM Tris-HCl, 10mM EDTA, pH8.0. Stored at 4°C.
Qiagen P2 buffer	200mM NaOH, 1% SDS.
Qiagen P3 buffer	3.0M Potassium acetate, pH5.5. Stored at 4°C
QT buffer	750mM NaCl, 50mM MOPS, 15% ethanol, pH7.0 0.15% Triton X-100.
QC buffer	1.0M NaCl, 50mM MOPS, 15% ethanol, pH7.0
QF buffer	1.25M NaCl, 50mM Tris-HCl,15% ethanol, pH8.5.
RNase buffer	10mM Tris-HCl pH 7.5 (DEPC), 5mM EDTA (DEPC), 200mM NaCl (DEPC), 100mM LiCl (DEPC)

5x T7 RNA polymerase buffer	200mM Tris-HCl pH 7.5 (DEPC), 50mM $MgCl_2$ (DEPC), 10mM spermidine. Stored at -20°C
5x SP6 RNA polymerase buffer	200mM Tris-HCl pH 7.5 (DEPC), 30mM $MgCl_2$ (DEPC). Stored at -20°C
RNA probe Elution Buffer	500mM ammonium acetate (DEPC), 0.1 mM EDTA (DEPC), 0.1% SDS.
2x RNase H buffer	40mM Tris-HCl pH7.5, 20mM $MgCl_2$, 1mM EDTA, 70mM NaCl, 2mM DTT, 30µg/ml BSA. Stored at -20°C.
1x SSC	150mM NaCl, 15mM sodium citrate pH7.4.
10x*Taq* buffer	500mM Kcl, 100mM Tris-HCl (pH 8.3), 15mM $MgCl_2$, 0.01 % w/v gelatin.
1x TAE	40mM Tris, 20mM acetic acid, 0.9mM EDTA.
1x TBE	50mM Tris, 42mM boric acid, 1mM EDTA.
TBS: 10x Solution A	8% (w/v)NaCl, 0.38% (w/v) KCl, 0.2% (w/v) Na_2HPO_4, 3% (w/v) pH 7.5. Filter sterilised, stored at -20°C.
TBS: 100x Solution B	1.5% (w/v) $CaCl_2$ 1.0% (w/v) $MgCl_2$. Filter sterilised, stored at -20°C.
TE	10mM Tris-HCl pH7.5, 0.1mM EDTA.
TEG	25mM Tris-HCl pH8.0, 50mM glucose,10mM EDTA. Autoclaved.
TELT	50mM Tris-HCl pH7.5, 62.5mM EDTA, 0.4% Triton X-100, 2.5M LiCl.
TLC running buffer	0.8M NaH_2PO_4, ph 3.5. Autoclaved.

2.6 Bacterial Media

L-agar	L-broth, 1.5% (w/v) agar. Autoclaved
Luria broth (L-broth)	170 mM NaCl, 0.5% (w/v) yeast extract, 1.0% (w/v) tryptone or peptone. Autoclaved
FSB	100mM Kcl, 45 mM $MnCl_24H_2O$, 10 mM $CaCl_22H_2O$, 3mM $HACoCL_3$, 10 mM potassium acetate, 10% glycerol. pH6.2. filter sterilise and store at 4^oc.
SOB	2% tryptone (w/v), 0.5% yeast extract (w/v), 0.05% NaCl (w/v). Autoclaved.

2.7 Molecular weight standards

*Eco*RI digested bacteriophage SPP-1 DNA molecular weight markers were obtained from BRESATEC (Adelaide, S.A.) and used at a final concentration of 125ng/µl in 1 X Type III loading sol^n. Approximate fragment sizes in Kbp are 8.51, 7.35, 6.11, 4.84, 3.59, 2.81, 1.95, 1.86, 1.51, 1.39, 1.16, 0.98, 0.72, 0.48, 0.36.

*Hpa*II digested pUC19 DNA molecular weight markers were obtained from BRESATEC (Adelaide, S.A.). Fragment sizes in base pairs are: 501, 489, 404, 331, 242, 190, 147, 111, 110, 67, 34, 34, 26.

1Kb molecular weight markers was obtained from GIBCO/ BRL, Glen Waverly, Victoria, Aust. Fragment sizes in Kbp are 12.216, 11.198, 10.180, 9.162, 8.144, 7.126, 6.108, 5.090, 4.072, 3.054, 2.036, 1.636, 1.018, 0.506, 0.517, 0.396, 0.344, 0.298, 0.220, 0.201, 0.154, 0.134, 0.075.

2.8 Methods

2.8.1 Processing Oligonucleotides

2.8.1A Synthesis, cleavage and deprotection

Oligonucleotides were synthesised on an Applied Biosystems model 381A DNA synthesiser (Applied Biosystems, Foster City, CA) by Julie Philips, Paul Moretti, Leanne Noack, Lori Varcoe and Andrew Bert. Following trityl-off synthesis, oligonucleotides were cleaved from the support by three sequential incubations with 450-500µl ammonium hydroxide for 15 mins at room temperature. This procedure was carried out by inserting one 1ml disposable syringe on one end of the column. The ammonium hydroxide is drawn into another and this syringe is then carefully inserted onto the other end of the column and the ammonium hydroxide allowed to fill the cavity of the column. After each incubation, the ammonium hydroxide is collected in a glass screw-top vial and the pooled fractions of crude (OLD synthesis) oligonucleotide deprotected by incubation overnight at 56°C. Oligonucleotides synthesised using FOD chemistry were deprotected by incubation at 56°C for 2 hours.

The mixture containing crude oligonucleotide was thoroughly mixed with 9volumes of n-butanol and centrifuged at 3,700 in a GPR benchtop centrifuge (Beckman) at room temperature for 20'. The pelleted oligonucleotide was washed in 100% ethanol, dried and resuspended in 200µl (MilliQ) H_2O. Oligonucleotides were quantified by measuring the OD_{260nm} and assuming 1AU=38µg/ml

After July 1995 all oligonucleotides were synthesised as crude preparations by BRESATEC, Adelaide, SA obviating the need for cleavage and deprotection steps.

2.8.1B Oligonucleotide Purification by PAGE

Full-length oligonucleotides were purified from the crude synthesis mixture by polyacrylamide gel electrophoresis. Typically, gels contained 12% (w/v) acrylamide (oligonucleotides of between 40-100 in length are well resolved on gels containing this

percentage acrylamide) with an acrylamide:bis-acrylamide ratio 30:1, 8M Urea, 1xTBE and were polymerised by adding final concentrations of 0.1 % (v/v) TEMED and 0.05 % (w/v) ammonium persulphate. Gels were pre-electrophoresed at 850 Volts/29 mAmps for approximately 30 min in 1xTBE buffer. Samples of approximately 100-200 µg were dried in a speedivac (Savant, Farmingdale, NY) before being resuspended in 10µl 95% formamide (no dyes). Samples were denatured for 5 min at 95°C and loaded into 1cm wide wells of the pre-electrophoresed gel. A marker dye containing 95% formamide, 20mM EDTA, 0.05% bromophenol blue and 0.05% Xylene cyanol FF was loaded into an adjacent track. Gels were electrophoresed at 850 volts/29 mAmps until the xylene cyanol dye was approximately half-way down the gel as this dye migrates with approximately the same characteristics as an oligonucleotide 40 bases in length. The upper glass plate was then removed and the gel covered with Saran wrap. The gel was then turned over, the remaining glass plate removed and the exposed side of the gel covered with Saran wrap. Bands were then visualised by placing on a TLC plate coated with a fluorescent (254nm) indicator dye and placed under a UV lamp (254nm). Bands visualised by shadowing corresponding to full-length products were then excised and transferred into micro-centrifuge tubes. Oligonucleotides were eluted from the polyacrylamide gel in 400µl DNA oligo elution buffer overnight at room temperature in an eppendorf shaker (Eppendorf,Hamburg, FRG.). Purified oligonucleotides were pelleted, as before, by n-butanol extraction, washed in 70% ethanol, dried and resuspended in 100µl milliQ H_2O and quantified as before.

2.8.1C Phosphorylation of oligonucleotides

Oligonucleotides were 5 min phosphorylated with ATP prior to anealing with complimentary oligonucleotides for use in subsequent ligation reactions. 2µg of oligonucleotide in a 20µl reaction was incubated with 2µl 10x One for All buffer, 2µl 10mM ATP and 1µl of T4 polynucleotide kinase (30U/µl) made up to 20µl with (MilliQ) H_2O at 37°C for 30 mins.

2.8.1D Annealing oligonucleotides

Complimentary phosphorylated oligonucleotides were annealed to form double stranded fragments prior to use in ligation reactions. The 20µl of phosphorylated oligonucleotides were mixed in a microfuge tube then placed in a weighted, sealed bag and incubated in a waterbath pre-heated to 80°C and allowed to cool to room temperature overnight.

2.8.2 The polymerase chain reaction

A standard PCR protocol was used to amplify defined DNA fragments with terminal restriction sites. The typical 25µl reaction contained 2.5µl of 10x Taq buffer, 4µl of 1.25mM dATP, dGTP, dCTP and dTTP, 1µl of 100ng/ml of each purified oligonucleotide primer, 1µl of 100ng/ml template DNA, 0.5µl of 5 U/µl *Taq* DNA polymerase, 1.5µl 25mM $MgCl_2$ and 13.5µl of MilliQ H_2O. The reaction mix was overlayed with 30µl mineral oil and subjected to 25-30 cycles of PCR using a BRESATEC minicycler.

The typical PCR profile consisted of a 2 min incubation at 94°C to denature the DNA, a 1 min incubation at 45°C to anneal the primers and template followed by a 1 min incubation at 72°C for primer extension. This profile was carried out for one cycle and was followed by a further 24 cycles where the 45°C annealing incubation was replaced by incubation at 55°C.

2.8.2A A modified PCR reaction to incorporate specific point mutations into the amplified product.

A number of PCR amplification procedures using mutant primers were designed to incorporate several defined point mutations into the amplified product. To ensure successful annealing of primers to the template DNA the annealing temperature was reduced. In this protocol a single cycle of a 2 min incubation at 95°C, 1 min incubation at 37°C and 30 secs at 72°C was followed by 29 further cycles where the 37°C annealing temperature was replaced by an annealing temperature of 55°C.

2.8.3 Maintenance and transformation of E. *coli*

2.8.3A Maintenance of strains

An E. *coli,* strain, DH5α, was used during the course of the work described in this thesis. Glycerol stocks of this strain and plasmid-containing strains were prepared by mixing 500µl of fresh overnight culture with 500µl 40% (v/v) glycerol in L-broth. These were immediately plunged into liquid N_2 and stored at -70°C.

2.8.3B Preparation of competent DH5α cells

2-3 mm DH5α colonies grown at 37°C on L-agar plates were inoculated into 1ml SOB, mixed and added to 130ml SOB containing $MgSO_4$ to a final concentration of 20mM. These were incubated at 37°C with shaking, to an OD_{550nm} of 0.16. Cultures were then decanted into pre-chilled tubes and chilled on ice for 10-15 min. The cultures were pelleted by centrifugation at 2,000 rpm, at 4°C for 10 min in a JA-20 Beckman rotor. The supernatants were discarded and the pellets resuspended in a total volume of 40ml (14 ml/tube) ice-cold FSB. After gentle mixing the cells were chilled on ice for 10-15 min followed by centrifugation at 2,000 rpm for 10 min at 4°C in a JA-20 rotor. The supernatants were discarded once more and the cells resuspended in 10ml ice-cold FSB (3.3ml/tube). The cells were combined in one tube and 350µl DMSO added the cells were swirled for 5-10 secs and then chilled on ice for 5 min. A further 350µl DMSO was added, the mixture swirled, chilled on ice for 10-15 min and finally 200µl of cells dipensed into chilled microfuge tubes on ice. The cells were then snap frozen in liquid nitrogen and stored at -70°C. Competence of cells was checked using 1µl of 1ng/µl supercoiled plasmid, IL-3T 7N.

2.8.3C Transformation of DH5α E.*coli*

Competent DH5α E. *coli* were thawed on ice until just liquid, then very gently mixed, by swirling, with 20µl DNA solution and incubated on ice for 20-60 min. The mixture was then heat shocked in a 42°C waterbath for 1.5 min and then placed immediately on ice for 2 min. 0.8ml of L-broth with $MgSO_4$ and $MgCl_2$ to a final concentration of 10mM was added and the cell culture incubated at 37°C on a heating

block. The culture was then pelleted at 6,500 for 20 secs in a MSE microcentaur centrifuge, resuspended in 200µl L-broth and spread onto L-agar plates containing 100µg/ml ampicillin.

2.8.4 Isolation of plasmid DNA

2.8.4A Small scale isolation of plasmid DNA

The procedure for isolating plasmid DNA from bacteria was based on the boiling method described by Wilimzig (Wilimzig, 1985). Using suitable antibiotic selection, usually 100 µg/ml ampicillin, a single, fresh colony of E. *coli* harbouring the appropriate plasmid was inoculated into 2mls L-broth + ampicillin and incubated at 37°C, with shaking, overnight. 1.5 mls was then transferred to a microfuge tube and pelleted at 13,000 rpm in an MSE microcentaur centrifuge for 17 secs. The medium was then aspirated off and the pellet resuspended in 250µl TELT lysing buffer by vortexing vigorously. The cells were then chilled on ice for 5-10 min and then lysozyme to a final concentration of 140µg/ml was added. The tube was vortexed briefly and then plunged into a boiling waterbath for 1 min.The tubes were then returned to ice for 5-15 min and then centrifuged for 20 min at 4°C in an MSE microcentaur centrifuge. The resulting slimy pellet, present at the bottom of the tube, was removed with a sterile toothpick and 500µl 100% ethanol added to the supernatant. The DNA was then pelleted by centrifuging for 15 min at 4°C in an MSE microcentaur centrifuge. The pellet was then washed in 70% ethanol, dried and then resuspended in 50µl TE.

2.8.4B Large scale preparation of plasmid DNA

Large scale preparation of plasmid DNA used alkaline lysis followed by banding of covalently closed circular DNA in a caesium chloride gradient. Using 100µg/ml ampicillin, a single, fresh colony of E.*coli* harbouring the appropriate plasmid was inoculated into 2mls L-broth + ampicillin and incubated overnight at 37°C with shaking. The following day 1ml of the overnight culture was added to 400mls of L-broth containing 100µg/ml Amp in a 2l conical flask. The culture was incubated at 37°c with

shaking to an OD_{650nm} of 1.0 before being adjusted to a final concentration of 200µg/ml chloramphenicol and the incubation at 37°C continued overnight.

The following day the cells were pelleted by centrifugation at 4,000 rpm for 10 min at 4°C in a JA-10 rotor, vigorously resuspended in 20ml ice cold resuspension buffer, 50 mM Tris-HCl (pH 8.0), 0.1 M NaCl and repelleted by centrifugation in JA-20 tubes at 5,000 rpm for 10 min at 4°C in a JA-10 rotor. The supernatant was decanted and the pellet chilled for at least 1h at -20°C.

The pellets were thawed to room temperature, resuspended in 6ml TEG on a mechanical shaker and, freshly made, lysozyme added to a final concentration of 2mg/ml. After a 30 min incubation on ice, the cells were brought to room temperature and 12mls freshly made 0.2M NaOH, 1% SDS, was added , mixed gently and incubated on ice for 10 min. 9mls of 3M sodium acetate pH 4.7, or lower, was added mixing gently by swirling and the tubes incubated on ice for 60 min. Cellular and chromosomal debris were pelleted by centrifuging in a JA-20 rotor at 20,000 rpm for 30 min at 4°C. The supernatant was decanted into a new tube and 1/2 volume of iso-propanol was added. After a 10 min incubation at room temperature the mixture was centrifuged in a JA-20 rotor at 10,000 rpm for 15 min at room temperature. The pellet was broken up by resuspending in 6mls 2M ammonium acetate and vortexing followed by mechanical shaking and recentrifuging in a JA-20 rotor at 10,000 rpm for 15 min at room temperature. The supernatant was decanted into a new tube 3.6mls iso-propanol added and left at room temperature for 10 min. The DNA was then pelleted by centrifuging in a JA-20 rotor at 10,000 rpm for 15 min at room temperature. The supernatant was decanted and the pellet resuspended in 2.1ml TE.

2.23g optical grade caesium chloride was added as was 60µl 10mg/ml ethidium bromide and 39µl of 1% triton X-100. The solution of DNA was loaded into a Quick-seal tube, balanced, sealed and centrifuged in a TLN-100 rotor at 90,000rpm for 4 hrs at 21°C. The lower band, containing covalently closed circular plasmid DNA, was collected using a 25 guage needle, puncturing the tape-covered tube just below the band. The DNA was transferred to a 10 ml yellow-capped tube and the ethidium bromide removed by multiply extracting with 2mls sodium chloride/MilliQ H_2O-saturated iso-

propanol removing the upper, pink phase until the solution was clear. The solution was transferred to a JA-21 tube, 2.5 volumes of MilliQ H_2O added followed by 2 volumes of absolute ethanol, precipitated at -20°C for 30 min and then the DNA was pelleted by centrifugation in a JA-21 rotor at 10,000 rpm for 15 min at 4°C. The supernatant was decanted and the pellet washed with 70% (v/v) ethanol, dried and resuspended in 200µl TE. The DNA was quantified by measuring the OD_{260nm} and assuming 1AU=50µg/ml.

2.8.4C Medium scale preparation of plasmid DNA

This medium scale preparation of plasmid DNA, a modified alkaline lysis procedure, utilises a commercial resin column (Qiagen, Hilden, FRG.) which isolates the DNA. A single, fresh bacterial colony, harbouring the desired plasmid, was inoculated into 100mls of L-broth, containing ampicillin to a concentration 100µg/ml, and incubated overnight at 37°C with shaking. The cells were then pelleted by centrifuging at 4,200 rpm for 15min at 4°C in a JA-4.2 rotor. The pellet was then resuspended in 4mls of cold P1 buffer. The resuspended cells were then transferred to 50 ml centrifuge tubes and 4mls freshly made P2 buffer gently added, mixed by gentle inversion several times and incubated at room temperature for 5 min. 4mls of cold P3 buffer was added, mixing by inversion several times chilled on ice for 10 min and the cell debris and chromosomal DNA pelleted by centrifuging at 16,000 rpm for30 min at 4°C in a JA-20 rotor.

In the meantime a Qiagen column was equilibrated by passing 3mls through QT buffer. The supernatant was then applied to the column and the column washed twice with 10mls QC buffer. The DNA was then eluted with 5 mls QF buffer into a small Nalgene centrifuge tube and precipitated with 3.5 mls iso-propanol at 13,000 rpm for30 min at 4°C in a JA-21 rotor. The DNA was washed with 70% (v/v) ethanol, dried and resuspended in 200µl TE and transferred to a microfuge tube. The DNA was then re-precipitated with 20µl 3M sodium acetate and 440µl 100% ethanol chilled at -20°C for 30 min and pelleted by centrifugation for 30 min at 13,000 rpm at 4°C in an MSE microcentaur microfuge. The DNA was finally washed in 70% ethanol, dried,

resuspended in 200µl TE and quantified by measuring the OD_{260nm} and assuming 1AU=50µg/ml.

2.8.5 Preparing plasmid DNA fragments for ligation

2.8.5A Dephosphorylation of linearised plasmid DNA

1-2µg of suitably linearised plasmid DNA was incubated at 37°C for 20 min with 1µl 1U/µl CIP and 1xCIP buffer in a 20µl reaction made up with MilliQ H_2O. A further 1µl of CIP was added and the reaction mix incubated at 56°C for a further 45 min after which time the reaction was inhibited with EDTA to a final concentration of 5mM at 75°C for 10 min. The DNA was then made up to 100µl with MilliQ H_2O and extracted with an equal volume of TE saturated phenol/chloroform (1:0.8) by vortexing followed by 2 min centrifugation at 13,000rpm in an MSE microcentaur centrifuge. The DNA was precipitated by adding 10µl 3M sodium acetate and 220µl 100% ethanol and chilled for 30 min at -20°C. DNA was then pelleted by centrifuging at 13,000rpm for 30 min at 4°C in an MSE microcentaur microfuge, washed in 70% ethanol, dried and resuspended in 20µl TE.

2.8.5B End-filling linearised plasmid DNA for blunt ended-subcloning

1-2µg DNA in 20µl TE was incubated for 20 min at room temperature with dNTPs to a final concentration of 1.2mM and 1µl of 4U/µl DNA polymerase Klenow fragment. The volume was then made up to 100µl with TE, an equal volume of TE saturated phenol/chloroform (1:0.8) was added, the mix vortexed vigorously, centrifuged for 2 min and the supernatant decanted into a new microfuge tube. The DNA was then precipitated in the presence of 25µl 10M ammonium acetate and 250µl 100% ethanol and chilled at-20°C for 30 min. The DNA was pelleted by centrifuging at 13,000 rpm in an MSE microcentaur centrifuge at 4°C for 15 min, washed with 70% ethanol, dried and resuspended in TE as appropriate.

2.8.5C Ligation of DNA fragments from a low melting-point agarose gel slice.

200-600ng of prepared DNA was resuspended in 10µl MilliQ H_2O with 2µl 6x loading buffer. The DNA was then loaded onto an appropriate percentage, pre-chilled low melting-point TBE agarose gel and electrophoresed at 4°C for approximately 1hr at 80 volts in pre-chilled 1x TBE containing ethidium bromide, to a final concentration of 1µg/ml,.

A band corresponding to the correctly sized fragment was excised under UV light $_{360nm}$ and placed in a microfuge tube. The agarose gel slices of the plasmid vector and insert were then melted on a 65°C heating block for at least 5 min. 15µl of 2x BEB, 1µl of 1M potassium chloride, MilliQ H_2O to a final total volume of 30µl and 1µl of 30mM ATP were added to a microfuge tube and maintained at 37°C. When the agarose gel slices had melted volumes equivalent to approximately equal molar ratios of vector and insert were added to the pre-warmed reaction and finally 1µl of 1U/µl T4 DNA ligase was added and the reaction incubated at room temperature overnight.

2.8.6 DNA sequencing

2.8.6A Denaturation of double stranded DNA and annealing of primer

Approximately 1µg of double stranded DNA, in 8µl TE was denatured by adding sodium hydroxide to a final concentration of 400mM and incubating at room temperature for 5 min. 35 pmol of primer (7pmol/µl), 3µl of 3M sodium acetate and 75µl 100% ethanol were added and the mix chilled at -20°C for 10 min. The primer/template mix was then pelleted by centrifugationg for 15 min at 13,000 rpm in an MSE microcentaur centrifuge at 4°C, washed in 70% ethanol, dried and resuspended in 10µl of 1x annealing buffer.

2.8.6B Labelling/extending reaction

DNA was sequenced by the chain termination method originally described by (Sanger *et al.*, 1977), using a T7 Superbase kit and T7 DNA polymerase. This method was used to sequence single-stranded DNA using [α-^{35}S]dATP.

The labelling reaction contained 15.38 mM DTT, 2µl label/extend mix, 5 µCi [α-^{35}S]dATP, 1µl manganese buffer (150mM sodium iso-citrate, 100mM manganese chloride,check) and 2.5 Units of T7 polymerase was added to the annealing reaction to a final volume of 16.5 µl. This mix was incubated at room temperature for 3 min.

2.8.6C Termination reaction

The extension reaction was terminated by mixing 3.5µl of the labelling mix with 2.5µl of each of C,A,G,T termination reagent in tubes pre-warmed to 37°C. Termination reactions were incubated at 37°C for 5 min after which time the reaction was stopped by addition of 4µl stop solution, containing 95% (v/v) formamide, 20mM EDTA, 0.05% (w/v) bromophenol blue, 0.05% (w/v) xylene cyanol FF.

2.8.6D Electrophoresis of sequencing reactions

The sequencing reactions were analysed on 400mm x 400mm x 0.4mm sequencing gels. Gels contained 6% acrylamide with an acrylamide:bisacrylamide ratio of 30:1, 8M urea, 1xTBE and were polymerised by adding final concentrations 0.05% (w/v) ammonium persulphate and 0.1% TEMED. Gels were pre-electrophoresed at 58mAmps for about 45 min in 1xTBE buffer prior to loading. Samples were denatured at 95°C for 3 min, and loaded at 1-2µl per well, (depending on the comb used) and electrophoresed at 58 mAmps until the bromo-phenol blue had just run off the bottom of the gel. The gel was then fixed by triplicate 5 min washes of 300ml 10% (v/v) ethanol, 10% (v/v) acetic acid and transferred to (Whatman) filter paper, covered in cling wrap and dried under vacuum for 1hr at 80°C. Once dry the gel was autoradiographed.

2.8.7 Maintentance of mammalian cells

COS cells, NIH3T3 mouse fibroblasts and HEL (human embryonic lung) fibroblasts were maintained similarly in DMEM containing 10mM HEPES, 0.2% (w/v) sodium bicarbonate, 2mM L-glutamine, 0.012 µg/ml penecillin, 0. 16µg/ml gentamycin and 7.5% FCS. Cells were usually grown to 80% confluence in 75cm^3 canted neck flasks containing 12.5mls of medium, for routine maintenance, or 225cm^3 canted neck

flasks containing 25mls medium prior to experiments. Medium was aspirated off and cells rinsed briefly in 1x PBS before adding 1ml of 0.1% trypsin, 0.2mM EDTA to $75cm^3$ flasks and 2mls to $225cm^3$ flasks and incubating for 1 min. Cells were dislodged by "knocking", 10mls or 20mls (as appropriate) of medium was added and cells collected by centrifugation at 1,400rpm for 5 min. For routine maintenance, the cell pellet was resuspended in a small volume of medium and an appropriate fraction of the cells was then added to a new flask. Cells for transfection or further experiments were counted and resuspended in an appropriate volume of medium.

Routine maintenance of 5637 bladder carcinoma cells was slightly different. Cells were maintained in RPMI containing supplements as detailed above. Cells were usually grown to 70-80% confluence in similar flasks and washed briefly in 5mM EDTA and then rinsed in triplicate with 1xPBS shaking vigorously during each rinse. 1ml or 2mls of trypsin/EDTA, was added and the cells incubated for 6 min at 37°C. Cells were dislodged, and centrifuged.

2.8.8 Transfection of mammalian cells

2.8.8A Preparation of DNA for transfection

Typically, 20µg of plasmid DNA linearized with *Sal*1 was used for transfections. A small volume of the linearized DNA was checked for efficient digestion on a 1% agarose gel and the rest made up to 100µl with TE and extracted in an equivalent volume of phenol:chloroform (ratio 1:0.8). This was vortexed vigorously, centrifuged for 2'in an MSE microcentaur centrifuge and the aqueous, upper layer removed into a fresh microfuge tube. 10µl of 3M sodium acetate was added followed by 220µl 100% ethanol and the DNA precipitated at -20°C for 30 min. The DNA was pelleted by centrifugation at 4°C for 30 min in an MSE microcentaur centrifuge. The DNA was washed in 70% ethanol which was then removed in a laminar flow tissue culture hood and left to dry in these sterile conditions. When dry, the DNA was resuspended in 20µl of tissue-culture sterile TE.

2.8.8B Permanent transfection of NIH3T3 fibroblasts by calcium phosphate precipitation.

3-4 x10^6 cells were evenly seeded onto 14.5 cm dishes at incubated overnight at 37°C. The following day, the medium was replaced with fresh medium buffered at pH 7.2 with 1 M HEPES. The linearised, sterile DNA was made up to 750µl with sterile room temperature MilliQ H_2O and 250µl room temperature 2 M calcium chloride was then added. The DNA/calcium chloride mix was added dropwise to 1ml of room temperature 2x HBS (which had been adjusted to pH 7.12 with 1 M sodium hydroxide) in a separate 10ml clear tube, whilst air was bubbled through. This was then incubated for about 25 min until a slight, milky precipitate could be observed. The tube was then vortexed and the contents added dropwise around the dish containing the cells. After incubation for 16 h at 37°C the medium was aspirated and the cells washed with fresh medium. This was aspirated and 1ml of 15% sterile glycerol in 1x HBS was added to the cells and incubated at room temperature for 4 min. The plate was then washed with 5mls of medium which was then replaced with fresh medium. The cells were then returned to the 37°C incubator and 72 h later clones selected by addition of G418 to a final concentration of 400 µg/ml for a period of 9-12 days until all mock transfectants had been killed. After selection, clones were pooled and maintained as described above continuing selection pressure in G418 at a concentration of 200 µg/ml.

2.8.8C Permanent transfection of 5637 bladder carcinoma cells by electroporation

6x10^6-1x10^7 cells from semi-confluent 225cm^3 flasks were resuspended in 0.8ml HEPES buffered saline containing 0.2% glucose and electroporated in 4mm electroporation cuvettes. Mock transfections contained 20µl of TE substituting for 20µg linearised plasmid DNA. The mixture was electroporated at 250 volts, 500µF using a Bio-Rad Gene Pulser and capacitance extender (Richmond, CA) and left at room temperature for 10 min before adding to a 150cm^3 flask containing 20mls medium. After 72 h, G418 to a final concentration of 400µg/ml was added and clones selected for about 5 days until all mock transfectants had been killed, as described above.

Transient transfections of these cells was carried out similarly with cells from one cuvette being divided between 3 10cm culture dishes. Cells were returned to 37°C for at least 24 h prior to experiments.

2.8.8D Transient transfection of NIH3T3 fibroblasts and COS cells by electroporation.

$2x10^6$ cells were resuspended in 0.8ml electroporation buffer, added to 20µg of prepared DNA in pre-chilled 4 mm electroporation cuvettes and chilled on ice for 10 min. The mixture was then electroporated ,as described above, and then returned to ice for a further 10 min. Cells were then divided into 3 10cm tissue culture dishes and returned to 37°C for 24 h prior to experiments.

In some experiments NIH3T3 fibroblasts were stably transfected by electroporation. In this case hepes buffered saline containing 0.2% D-glucose was used as the electroporation buffer and after electroporation, cells were added to $150cm^3$ flasks containing 20mls HDMEM complete medium. After 72 h G418 at a final concentration of 400µg/ml was added and clones selected described in section 2.8.2B above.

2.8.8E Transient transfection of HEL fibroblasts by DEAE Dextran.

$1x10^6$ cells were seeded into 10cm tissue culture dishes and incubated at 37°C for 1-2 days until 70% confluent and then the medium was removed and replaced with fresh medium just before transfection of the cells. 10µg of prepared DNA, resuspended in 80µl sterile TBS, was added to sterile DEAE Dextran at a final concentration of 400µg/ml (inTBS) which had been previously aliquoted into microfuge tubes and maintained at 37°c. The DNA/DEAE Dextran mix was flicked to mix the contents and added dropwise around the dish of cells. After gently rotating the dish to evenly disperse the contents the cells were returned to 37°C for 2-4 h.

Medium was then aspirated from the cells and replaced with 5ml pre-warmed 10% DMSO in 1xPBS. After incubation for 1 min at room temperature the DMSO was removed and the cells washed briefly with 1x PBS, which was then replaced with fresh,

warm medium and the cells returned to 37°C. The cells were then incubated for 24 h at 37°C for 24 h prior to experiments.

2.8.9 Purification of human monocytes from peripheral blood

A fresh blood pack, containing 500 mls of packed cells, was collected from the Red Cross Blood Transfusion Service (Pirie street, Adelaide). This was then diluted 1:1 with 1x Hanks balanced salt solution (HBSS) in 500ml capped, plastic pot. This was mixed thoroughly, by inversion, and left to stand for several minutes. 30 ml aliquots of diluted blood were dispensed into sterile polypropylene tubes (Falcon) and underlayed with 15mls, room temperature, lymphoprep. This was carried out by attaching a 10ml disposable syringes to sterile canulas and allowing the lymphoprep to pass down the syringes into the blood by gravity.

The blood was separated into a series of layers by centrifuging in a J-6 Beckman centrifuge at 1,800 rpm for 25 min at room temperature. The acceleration speed was set to 4 and the deceleration to 5 to avoid unneccesary vibration which may disturb the layers. The fuzzy buffy-layer, above the packed red blood cells, was collected using a 20ml plastic syringe with a cut off pastic transfer pipette attached to facilitate sucking up the cells. The interfaces were pooled and washed with an equal volume of 1xHBSS and pelleted by centrifuging at 1,500 for 10 min in a benchtop GPR centrifuge at room temperature with normal acceleration and deceleration. Cells were then resuspended and pooled in one tube, made up to 45 mls with 1xHBSS, and pelleted at 1,000 rpm for 8 min as described above.

While preparing the mononuclear layer the elutriation chamber of the elutriator (Beckman J6-E) was assembled and thoroughly washed. All glassware for use in this procedure was soaked overnight in "E-toxa clean" detergent, thoroughly rinsed in freshly made MilliQ H_2O, and baked for 4 h at 250°C and maintained in sterile conditions. After assembly the elutriator was cleaned by passing through 200 mls 1:10 Beckman detergent, then 200 mls 70% ethanol and finally 1L freshly produced MilliQ H_2O. Just before use the chamber was washed with elutriation buffer, the rotor speed set to 2050 rpm and the pump speed set to 12 mls/minute. The mononuclear cells were

resuspended in 10 mls elutriation buffer and slowly allowed to enter the elutriation chamber. For full details on operation refer to manufacturers protocol.

After 30 min, centrifuged monocytes form a band owing to differential sedimentation, and can be collected by turning the pump speed to maximum and switching off the centrifuge, into a sterile 50ml falcon tube. Monocytes were washed carefully, in complete RPMI, and counted. Purity of the monocyte preparation was assessed by diluting the cells to $1x10^6$/100µl and centrifuging onto a glass slide at 500rpm for 5 min in a cytospin centrifuge with 100µl FCS. The slide was air dried, fixed and giemsa stained (courtesy of DSL I.M.V.S.). Cells were then differentially counted under DEPEX mounting fluid to assess the percentage of monocytes.

Monocytes were then maintained in RPMI in 6cm or 10 cm tissue culture dishes incubated at 37°C and used immediately for experiments.

2.8.10 Checking actinomycin D for inhibition of transcription

All cell types where actinomycin D was used, were initally checked to determine efficiency of transcriptional inhibition. $1x10^6$ cells were seeded on 5 cm dishes and grown to near confluence. 15 min prior to starting the assay, 50µlof medium containing 4µl [^{3}H] uridine was added to each plate. Actinomycin D at a final concentration of 50 µg/ml was then added to a series of dishes which were incubated at 37°C for increasing times. To harvest the cells, duplicate 1x PBS washes were followed by quadruplicate washes with ice-cold 5% TCA. The cells were then fixed with duplicate 100% ethanol washes and were allowed to air dry. Cells were then lysed with 1ml 0.3M sodium hydroxide, transferred to scintillation vials and 0.1ml 1.5M hydrochloric acid was added as was 6 mls of scintillation fluid. Scintillations were then counted on the ^{3}H channel of a scintillation counter to assess uptake of ^{3}H uridine in the presence of the transcription inhibitor, actinomycin D.

2.8.11 Preparing mammalian cells for storage in liquid nitrogen

Near confluent cells were harvested, counted, their concentration adjusted to 2-$5x10^6$ cells /700µl and added to a labelled, pre-chilled freezing vial on ice. 200µl of

FCS was added to the vial and finally 100µl of DMSO was very slowly dropped into the vial. The contents were mixed very gently, placed in a freezing chamber, which rests in the vapour phase of a liquid nitrogen storage tank and left undisturbed for at least 2 h. After this time the frozen cells were placed in the liquid nitrogen-containing part of a storage tank, until required.

2.8.12 Thawing mammalian cells from liquid nitrogen storage.

Cells were rapidly brought to room temperature by thawing quickly in a 37°C waterbath and when still icy added to 20mls cold medium and allowed to warm to room temperature for 10 min. The cells were then centrifuged in a Beckman GPR benchtop centrifuge at 1,000rpm for 5 min at room temperature resuspended in medium and seeded into a 150cm flask.

2.8.13 Induction of transcription from the c-*fos* promoter

Cells transfected with plasmids containing the serum-inducible fos promoter were treated so that transcription was induced. $1x10^6$ NIH3T3 cells or $2x10^6$ 5637 cells were plated onto 10cm tissue culture dishes in DMEM or RPMI, respectively, containing 7% FCS and incubated overnight at 37°C. The next day the cells were carefully washed twice with warm 1x PBS and fresh medium containing 0.5% FCS was added. After 16-24 h the low serum-containing medium was replaced with fresh, warm medium containing 15% FCS which induced transcription from the c-*fos* promoter. RNA was then isolated at time points thereafter.

2.8.14 Stimulation of cells with activating agents

Cells were plated out and serum starved as described above (section 2.8.13). Transcription from the fos promoter was induced when the low serum-containing medium was then replaced with warm medium containing 15% FCS. This medium was freshly supplemented with TNFα (50ng/ml) or PMA (200ng/ml) or IL-1β (100U/ml) or the calcium ionophore A21387 (2µM). RNA was then isolated at time points thereafter.

2.8.15 Preparing total RNA from a monolayer of cells.

Cells were harvested by aspirating medium, washed with ice-cold 1x PBS and RNA was extracted, by vigorous pipetting, with 3 mls of solution D, containing 4M guanidinium thiocyanate, 25mM sodium citrate at pH7.0, 0.5% sarcosyl and supplemented with β-mercaptoethanol at a final concentration of 0.1M. The lysates were then frozen at -20°C until required.

The lysates were thawed and 266µl of 3M sodium acetate, 4mls water-saturated phenol and 800µl of chloroform/iso-amyl alcohol at a ratio of 49:1 were added. These were mixed vigorously, chilled on ice for 5-15 min and the aqueous phase was separated from the phenol phase by centrifuging at 3,750 rpm for 15 min at 4°C in a Beckman GPR benchtop centrifuge. The aqueous phase was carefully removed, avoiding the interface, into a new tube containing 4 mls isopropanol and the RNA solutions were precipitated for 1 h at -20°C. The RNA was pelleted by centrifuging in a J-6 Beckman centrifuge at 4,200rpm for 40 min at 4°C.

The supernatants were carefully removed and 600µl of solution D +βmercaptoethanol, as described above, was added to the tube. The pellet was dissolved in this and transferred to a microfuge tube containing 600µl iso-propanol. The RNA was precipitated for 15 min at -20°C, pelleted by centrifuging at 13,000rpm for 10 min at 4°C, thoroughly washed in 70% ethanol and dried on a 37°C block until just dry. The RNA was then resuspended in 100µl DEPC-treated MilliQ H_2O containing 0.1mM EDTA, which required heating to 65°C for approximately 1 h with intermittent vortexing, and quantified by measuring the OD_{260nm} and assuming 1AU=40µg/ml.

For samples from cells transiently tranfected with plasmids, DNase treatment was required to remove plasmid DNA. In this case the RNA was resuspended in 52.5µl DEPC-treated (MilliQ) H_2O containing 1mM EDTA and incubated for 30 min at 37°C with 6µl 10x DNase buffer, 0.5µl 10U/µl RNasin and 1µl of 1U/µl RQ-DNase. The mix was then made up to 100µl with DEPC-treated TE and an equal volume of TE-saturated phenol/chloroform (1:0.8), vortexed thoroughly and centrifuged for 2 min in an MSE microcentaur microfuge. The upper, aqueous layer was then removed to a fresh RNase-free microfuge tube containing 16µl 3M DEPC-treated pH 4.5 sodium acetate and 440µl

100% ethanol. The RNA was then precipitated at -20°C for 15 min and pelleted by centrifuging at 13,000rpm for 15 min in an MSE microcentaur centrifuge at 4°C. The RNA was washed thoroughly with 70% ethanol, dried briefly as described above and resuspended in 100µl MilliQ H_2O containing 0.1mM EDTA. The RNA was then quantified as described above.

2.8.15A Modified procedure for preparing RNA from human monocytes

Owing to the relatively low number of monocytes in 500mls blood a slightly modified procedure for preparing RNA was used. The volumes of solution D and β-mercaptoethanol were reduced by 2/3 as were the subsequent phenol extraction and 1st iso-propanol precipitation steps; the subsequent iso-propanol precipitation step, and steps thereafter, remained unchanged. At the phenol extraction step and first iso-propanol precipitation steps 10 µg/ml of tRNA was used as a carrier. For this reason these RNAs were not quantified and the entire sample was used for experiments.

2.8.16 Formaldehyde agarose gel for checking the fidelity of prepared RNA

2.8.16A Preparation of formaldehyde agarose gel

1g of electrophoresis grade agarose was melted in 10mls of 10x MEN and 72mls MilliQ H_2O using a microwave oven. The agarose was cooled to 55°C, and formaldehyde was added to 28.7mls of agarose to a final concentration of 6.7 % (v/v). The gel was then cast, in a fumehood, using a medium-sized tray and comb.

2.8.16B Preparation of RNA samples for electrophoresis

5µg of total RNA was dried and resuspended in 2.2µl MilliQ H_2O and 7.8µl formaldehyde sample buffer. Samples were then heated for 5 min at 68°C and 2µl 6xType III loading buffer. Samples were then loaded into the wells and the gel run in 1x MEN at 90 volts for about 1-1.5 h until the bromophenol blue dye had migrated 2/3 down the gel.

2.8.16C Visualising the RNA

After completion, the gel was removed from the tank and stained with 1x MEN containing ethidium bromide at a final concentration of 10µg/ml for 10 min. The gel was then destained with 3x 200ml MilliQ H_2O washes and a photograph taken under UV light at a wavelength of 254_{nm}.

2.8.17 *in vitro* transcription of probes labelled with [α-^{32}P]UTP

2.8.17A Preparation of plasmid template

2-4 µg of plasmid DNA, harbouring the desired template sequence, was digested with an appropriate restriction enzyme to create a fragment of an appropriate size that could be resolved on a 6% poly-acrylamide gel. This was checked for efficient digestion by running 1µl on an agarose, gel and then was made up to 100µl with TE and extracted with an equivalent volume of TE-saturated phenol/chloroform (ratio 1.0.8). After vigorous vortexing and separation of the aqueous and phenol phases by centrifugation at 13,000rpm for 2 min in an MSE microcentaur centrifuge, the aqueous phase was removed to a fresh RNase-free microfuge tube containing 10µl DEPC-treated 3M sodium acetate and 220µl of 100% ethanol. After a 30 min precipitation step at -20°C and pelleting by centrifuging for 30 min at 13,000 rpm in an MSE microcentaur centrifuge at 4°C, the DNA template was washed in DEPC-treated 70% ethanol, dried briefly and resuspended in 30-40µl DEPC-treated TE, the exact volume depending on the abundance of the DNA.

2.8.17B The *in vitro* transcription reaction

Depending on which RNA polymerase transcription promoter was present, 2µl of T7 or SP6 5x buffer was added to the bottom of an RNase-free microfuge tube. To this was added 0.5µl 500mM of DTT; 0.5µl of 100µM UTP; 2.0µl of 2.5mM CTP, ATP and GTP; 0.5µl 40U/µl RNasin, 2µl of 3000Ci/mmol [α-^{32}P]UTP, 0.5µl of 2.55mg/ml BSA and 0.5µl of T7 or SP6 RNA polymerase, as appropriate. All of these solutions were either made up with DEPC-treated MilliQ H_2O or were commercial reagents assumed to be RNase-free. These reagents were mixed with a pipette tip and finally

1.5µl of the RNase-free template was added. The reaction was then incubated at 37°C for 1h, after which time any remaining DNA was digested with RQ-DNase by incubating at 37°C for a further 15 min.

This was a typical reaction mix which was modified to increase or decrease specific activity of the probe as required. A typical example of a probe that was reduced in activity for routine use was that of glyceraldehyde phosphate dehydrogenase (GAPDH). This was routinely made at 1/4 specific activity, by maintaining the volume of [α-^{32}P]UTP but increasing the concentration of "cold" UTP from 100µM to 400µM and maintaining the final volume. Another typical modification to the standard protocol was to increase the reaction mix by 2-4 fold depending on the number of samples requiring the probe. When these modifications were carried out the subsequent precipitation step was altered accordingly.

2.8.17C Purification of the probes by PAGE

After RQ-DNase digestion of remaining DNA the probe was precipitated by adding100µl DEPC-treated TE, 1µl of 10mg/ml tRNA, 67µl of 5M DEPC-treated ammonium acetate and 420µl 100% ethanol and chilled at -20°C for a minimum of 20 min. The probe was then pelleted by centrifuging in an MSE microcentaur centrifuge at 13,000 rpm for 25 min at 4°C.

In the meantime a 6% polyacrylamide gel was prepared as described (2.8.1b) using a comb containing 1cm slots, which was pre-electrophoresed for 30 min at 29mAmps in 1xTBE running buffer. The pelleted probe was washed with 70% ethanol, dried very briefly on a 37°C heating block and resuspended in 5µl formamide loading buffer. The probe was denatured for 3 min at 95°C and loaded onto the pre-electrophoresed gel which was run for about 30 min until the bromo-phenol blue dye had just run off the end of the gel.

2.8.17D Eluting the probes from the acrylamide gel

The upper glass plate was removed and the gel covered in cling-wrap. Activated fluorescent markers were attached to the cling-wrap to facilitate orientation of bands

corresponding to probe. The gel was then exposed to X-ray film for 90 seconds, which was then developed. Cuts above and below each band were made on the X-ray film and the film was then orientated by aligning the fluorescent markers with those attached to the gel. Corresponding cuts were made on the gel and the film was removed to allow the probes to be excised. The gel fragment was placed in an RNase-free microfuge tube centrifuged briefly to pellet the fragment and the gel fragment was then mashed with a previously prepared blunt-ended (by bunsen burner) pipette tip until homogeneous. The probe was then eluted by adding 300µl DEPC-treated elution buffer and shaking for 2 h at room temperature.

2.8.17E Precipitating the purified probe

The eluted probe was then separated from the acrylamide fragment by centrifuging for 5 min at 13,000rpm in an MSE microcentaur centrifuge. The upper, 200µl probe phase, was then removed to a fresh RNase-free microfuge tube containing 84µl 5M DEPC-treated ammonium acetate, 1µl of 10mg/ml tRNA and 696µl 100% ethanol and the probe precipitated by chilling for 20 min at -20°C followed by pelleting by centrifuging for 20 min at 13,000rpm in an MSE microcentaur centrifuge at 4°C. The probe was then washed with 70% ethanol, dried very briefly and resuspended in 100µl of RNase protection assay hybridising solution. 5µl of the probe was then counted using a Bioscan QC 2000 β counter (Bioscan Inc. Washington D.C.) to determine activity of the probe.

2.8.17F Hybridising the probe with RNA

30,000-100,000 cpm of probe, depending on the probe yield and expression of RNA, in 10µl of hybridising solution, was added to, typically, 10-20 µg dry RNA. This ensured that probe was in excess over RNA to facilitate hybridisation of RNA and probe. The probe/RNA mixture was denatured at 80°C for 5 min and then hybridised for at least 16 h in a 45°C incubator. RNA prepared from monocytes was hybridised for 2 nights to ensure maximal hybridisation of RNA and probe.

2.8.18 Analysing mRNA abundance by RNase A protection assay

2.8.18A Digestion with RNase A

Single-stranded RNA was removed (from samples from section 2.8.17) by digestion for 40 min at 26°C with 100µl RNase A at a concentration suitable for efficient removal of single-stranded RNA without clipping double-stranded probe/RNA hybrids. This was achieved for each new probe by initial titration experiments using RNase-A at increasing concentrations, typically, 2.5; 10; 20; 30 and 40µg/ml in RNase-A buffer and determining the most suitable concentration for each probe. Where 2 or more probes were used simultaneously a compromise was reached. For efficient digestion, RNase-A at a concentration of 10µg/ml was used for the majority of probes.

After digestion, the reaction was inhibited by the addition of SDS at a final concentration of 0.17% (v/v) and proteinase-K at a final concentration of 261µg/ml,the reaction mix was briefly vortexed and centrifuged to bring the reaction to the bottom of the tube which was then incubated at 37°C for 15 min. 110µl was then transferred to a fresh RNase-free tube containing 1µl of 10mg/ml tRNA and 100µl of TE-saturated phenol/chloroform (ratio 1:0.8).

2.8.18B Precipitation of RNase protection assay samples

The reaction was thoroughly vortexed and then centrifuged for 2 min in an MSE microcentaur centrifuge, to separate aqueous from phenol phases and the aqueous phase removed to a fresh RNase-free microfuge tube containing 250µl RNase-free 100% ethanol. The RNA was precipitated by chilling at -20°C for 15 min and pelleted by centrifuging for 30 min at 13,000 rpm in an MSE microcentaur centrifuge at 4°C. The supernatant was then very carefully removed, the pellet washed with 70% ethanol and the pellet dried in a speedivac. The pellet was then resusended in 4µl formamide load buffer.

2.8.18C Electrophoresis of RNase-A protection assay samples

In the meantime a 6% polyacrylamide gel was prepared in essentially the same way that the sequencing gel was prepared previously (2.8.6D), however, instead of

sequencing combs wider combs with 4mm teeth were used. The gel was pre-electrophoresed for 30-45 min at 58 mAmps, the samples were then denatured for 5 min at 95°C and loaded into the wells. The gel was run for about 45 min until the xylene cyanol dye had migrated 10 cm. The gel was then fixed in 3 changes of 10% (v/v) ethanol, 10% (v/v) acetic acid as described previously, and dried for 50 min at 80°C on a Bio-Rad gel drier. The dried gel was then exposed to either autoradiographic film for 2 nights at -20°C or overnight to a phosphor-image screen. Gels exposed to a phosphor-image screen were then scanned using a phosphor-imager (Molecular Dynamics, Sunnyvale CA.) and relative intensity of bands corresponding to protected mRNA fragments quantitated.

2.8.19 Northern blot Assay using radio-labelled oligonucleotide probe

2.8.19A Cleavage of RNA samples by RNase H digestion

20 µg of total RNA was dried and resuspended in 23µl DEPC-treated MilliQ H_2O and incubated for 15 min at 65°C with intermittent shaking to dissolve the RNA. 1µl of appropriate cleaveage oligo, at a concentration of 450ng/µl, was added to the RNA and to 1 sample 500ng of oligo dT, at a concentration of 500ng/µl was added, to provide a Poly(A)- sample. The reactions were mixed, denatured at 95°C for 5 min and then allowed to cool for approximately 15 min. 25µl of 2x RNase H buffer and 1µl (2U) of RNase H enzyme, diluted in 1x RNase H buffer, were added and the 50µl reaction incubated for 15 min at 37°C. The reaction was then made up to 200µl with DEPC-treated TE and extracted in an equivalent volume of TE-saturated phenol/chloroform (ratio 1:0.8). After vigorous vortexing and centrifuging for 2 min at 13,000rpm in an MSE microcentaur centrifuge the upper, aqueous phase was removed to a fresh, RNase-free microfuge tube containing 19µl 3M DEPC-treated pH 4.5 sodium acetate and 522.5µl 100% ethanol. The RNA was then precipitated at -20°C for 15 min and pelleted by centrifuging at 13,000 rpm for 30 min in an MSE microcentaur centrifuge at 4°C. The pellet was then washed with 70% ethanol, dried in a speed vac and resuspended in 10µl formamide load.

2.8.19B PAGE of RNA samples for electroblotting

A 4.5 % denaturing polyacrylamide gel was prepared using (18x15cm) glass plates as described in section 2.8.6D, modified slightly by using 0.75 mm spacers and a 4 mm wide comb. A rectangle of 15.5 cm x 10 cm was marked on the glass plates to facilitate location of samples. The gel was pre-electrophoresed in 1x TBE buffer for approximately 30 min at 40 mAmps, the samples denatured at 95°C for 3 min, loaded and run for about 30 min until the bromophenol had just migrated of the end of the gel. The upper glass plate was then removed and the 15.5cm x 10cm rectangle excised with a scalpel.

2.8.19C Electro-transfer of RNA from a polyacrylamide gel to a nylon membrane

The gel was then floated into a tray containing 0.1x TAE buffer and soaked 3 times for 20 min. The gel was slid onto cling-wrap and orientated onto a piece of Whatman 3MM filter paper. The TE 70 semi dry electroblotting apparatus (Hoefer Scientific Instruments, San Francisco, CA) was assembled. 5 sheets of Whatman 3MM filter paper were cut to size, soaked, briefly, in 0.1x TAE buffer and placed in the bottom of the apparatus. expelling all bubbles between successive sheets of filter paper before the next one was applied. A piece of Hybond N+ (Amersham, Amersham, UK.) membrane was cut to size, soaked in MilliQ H_2O for 5 min and then soaked 3 times for 10 min each in 0.1x TAE buffer. This was then placed on top of the pieces of filter paper and once more bubbles were expelled. The equilibrated gel was carefully aligned with the Hybond N+ membrane and placed on top removing all bubbles. 5 further sheets of pre-soaked Whatman 3MM filter were placed on top of the gel and the assembly lid attached. The electro-transfer was carried out at 4°C at a constant current of 0.85 mAmps x gel area (cm^2) for 2 h. After the transfer was complete the apparatus was then dismantled, the membrane removed and washed briefly in 8x SSC, to reduce background interference, and then baked between 2 pieces of filter paper for 2 h at 80°C.

2.8.19D 5' end labelling of synthetic oligonucleotide probes by phosphorylation

An appropriate oligonucleotide was 5'-end labelled by incubating 10 pmols of oligonucleotide in 1µl, with 4µl of 5x kinase buffer; 6 µl [γ-^{32}P]ATP; 8µl MilliQ H_2O and 1µl of bacteriophage T4 polynucleotide kinase at 37°C for 40 min. The probe was then precipitated by the addition of 132 µl TE, EDTA to a final concentration of 0.83mM, tRNA to a final concentration of 33.3µg/ml and 400ml of 100% ethanol and chilled at -20°C for 1 h. The probe was pelleted by centrifuging for 30 min at 13,000rpm in an MSE microcentaur centrifuge at 4°C, washed in 70% ethanol, dried and resuspended in 50µl of TE.

2.8.19E Assessing efficiency of [γ-^{32}P]ATP incorporation into the probe.

Efficiency of the labelling reaction was determined by dipping a pipette tip in to the probe sample and spotting a small amount at a pencil line drawn 1cm from the bottom of a PEI TLC strip. This was then placed in a beaker containing a small volume of TLC running buffer and allowed to migrate 2/3 of the way up the strip. The PEI strip was then cut just above the pencil line and the 2 pieces were counted using a Geiger counter to assess approximate percentage of incorporated *vs* unincorporated probe.

2.8.19F Purification of the probe by passing through a chromatography column

The G25 sephadex chromatography column (Bio-rad, Richmond, CA.) was prepared by removing the bottom end and centrifuging in a Beckman GPR benchtop centrifuge at 2,000 rpm for 4 min to remove the suspension solution. The probe (50µl) was then applied to the column and passed through the column into a microfuge tube by centrifuging at 4,000 rpm for 4-6 min in a Beckman GPR benchtop centrifuge. The collected probe was then counted in an Bioscan bench top counter.

2.8.19G Pre-hybridisation of RNA

The membrane was placed in a large 20 cm petri-dish with pre-hybridising solution containing a final concentration of 25% (v/v) formamide; 5x (v/v) SSC; 5x (v/v) Denhardts solution; 1%(v/v) SDS; 0.05%(w/v) NaPPi, 200µg/ml sheared salmon sperm (S/S) DNA and 32ml of MilliQ H_2O. The S/S DNA was boiled for 5 min before adding and thesolution was filtered before adding to the membrane. The membrane was incubated with this pre-hybridising solution for 4 h at 36°C.

2.8.19H Hybridising the RNA with the 5'-end labelled probe

The entire probe was added to the pre-hybridisation mix and the reaction incubated overnight at 36°C.

2.8.19I Washing the filter

The following day the filter was washed twice for 30 min at 60°C in 1% SDS and 1x SSC, sealed in a plastic bag and exposed to a phosphor-image screen for 2 nights. The screen was then scanned and the image recorded.

2.8.20 Development of a model system to study mRNA decay

In order to study regulation of cytokine mRNA stability a system designed to allow observation of mRNA decay was essential. The approach we took was to construct a chimeric gene encoding an mRNA which is usually very stable (human growth hormone) and inserting various sequences, into the 3'UTR of this gene, to investigate their effect on the stability of the mRNA (2.8.20A). The development of this apparently simple system was in fact not trivial.

Initially, transcription of the gene was driven by the constitutively active CMV promoter. Using this promoter I did not observe rapid decay of a chimeric gene bearing the AU-rich region of human GM-CSF in transiently transfected COS cells (Fig 2.8.1). Transient transfection of HEL fibroblasts resulted in very poor expression of the mRNAs.

Figure 2.8.1. Stability of CMVGH-GM mRNA in NIH3T3 cells

NIH3T3 fibroblasts ($1x10^6$ cells) transiently expressing the CMVGH-GM transcript were treated with Actinomycin D (5 μg/ml) to inhibit transcription and RNA was isolated at times indicated. 20μg of total RNA was then hybridised with *in vitro* synthesised complimentary RNA probes (see sections 2.8.15, 2.8.17 and 2.8.18).

The CMVGH-GM mRNA was detected by RNase protection assay using a probe complimentary to a 230 nt fragment of the of the CMVGH-GM mRNA, synthesised from *Dra*I digested pCMVGH-GM plasmid (see Table I: Appendix) using SP6 RNA polymerase and 400Ci/mmol [α^{32}P]-UTP.

The GAPDH mRNA was detected by using a probe complimentary to a 120bp internal fragment the mouse GAPDH mRNA, synthesised from *Dde*I-digested plasmid pGAPM (see Table I: Appendix) using T7 RNA polymerase and 100Ci/mmol [α^{32}P]-UTP. Abundance of mRNA was determined by RNase protection assay.

Panel A) Phosphorimage of RNase protection gel

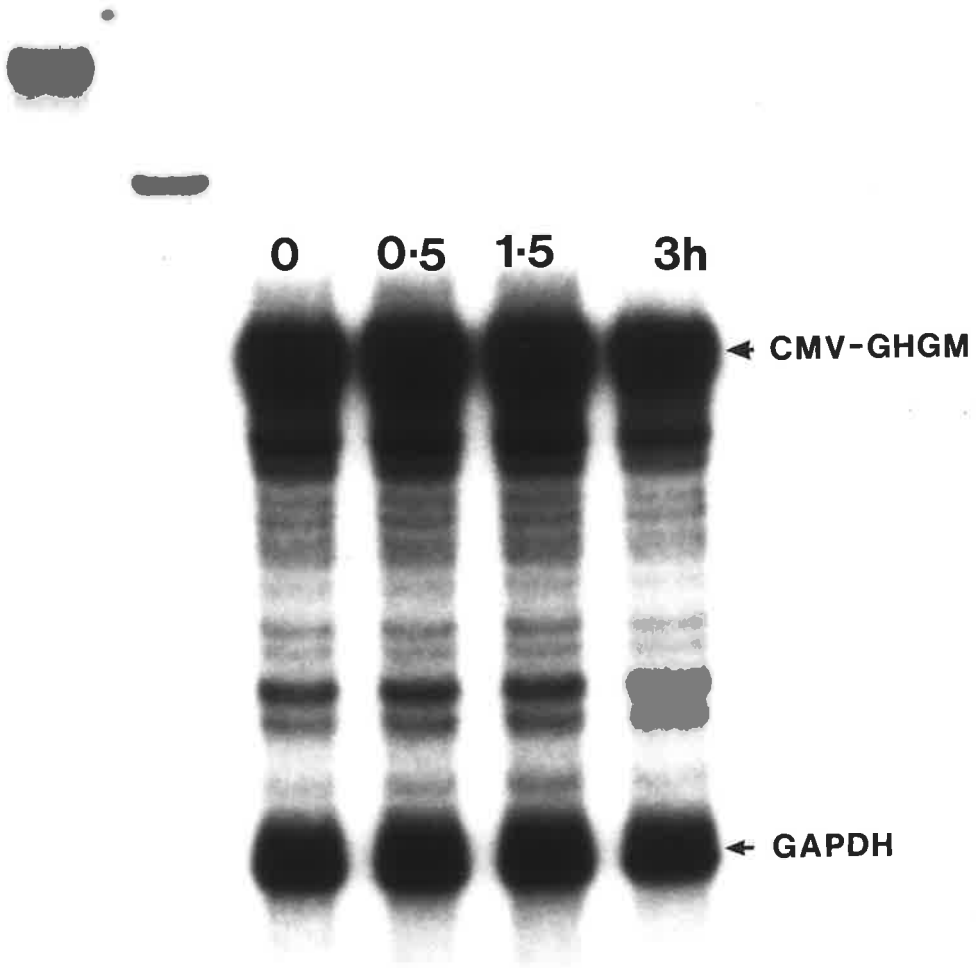
0
0·5
1·5
3h
CMV-GHGM
GAPDH

The CMV promoter was replaced by the serum inducible chicken c-*fos* promoter to investigate whether the presence of a constitutive promoter was preventing either degradation of the mRNAs or observation of degradation. The c-*fos* promoter has very low constitutive activity but after transfected cells are incubated in medium containing low (0.5%) concentrations of serum for at least 16 h, a brief pulse of transcription is induced by stimulation with medium containing 15% FCS (Shyu *et al.*, 1989). This pulse of transcription lasts less than 1 h and allows measurement of mRNA decay rates. The advantage of using a serum inducible promoter is that it obviates the need for transcription inhibitors which have been observed to unnaturally prolong the apparent half-life of an mRNA (Ahern *et al.*, 1993).

Using this promoter I still observed poor mRNA expression in Hel fibroblasts and constitutively stable mRNAs in Cos cells. Expression in Cos cells was constitutively stable, I found out, owing to the ability of these plasmids to replicate in Cos cells by the presence in Cos cells of the large T Antigen. In stably, or transiently, transfected NIH3T3 mouse fibroblasts, however, rapid decay of mRNAs bearing destabilising AUIEs was observed (see Figures in subsequent chapters). Subsequently, stably transfected NIH3T3 cells were routinely used to investigate aspects of regulation of cytokine mRNA stability.

2.8.20A Construction of the pfGH plasmid.

Plasmid pfGH (Fig 2.8.2) was prepared in multiple steps. Plasmid pRcCMV (Invitrogen) was digested with *Eco*RI and *Kpn*I, blunt ended, and ligated shut to generate pRcCMVΔ2. Plasmid pG4BGH was prepared by inserting a 241bp *Pvu*II-*Bcl*I fragment of pRcCMV, containing the bovine growth hormone 3'UTR and polyadenylation signals, into the *Eco*RI site of pGEM4Z (Promega). Plasmid pG4HGHBGH was prepared by inserting a 660bp *Nco*I-*Sma*I fragment from plasmid pHGH (kindly provided by A. Robins, Bresatec Pty. Ltd., Adelaide, South Australia, Australia), containing the coding region of human growth hormone, into the *Sma*I site of pG4BGH. Plasmid pCMVGH was prepared by insertion of a 1,081bp *Pvu*I-*Bam*HI fragment from pG4HGHBGH (containing the human growth hormone coding region,

Figure. 2.8.2. Schematic representation of the dfGH gene.

The boxes represent segments of the gene that were derived from the chicken c-*fos* gene (c-fos), human growth hormone cDNA (GH), indicated by shading, and bovine growth hormone 3'UTR (bGH); plasmid derived sequences are indicated by a line. The transcription start site and polyadenylation site are indicated by arrows. Also shown are the relative location of the SP6 promoter, used to make probes for RNase protection assays, and the neomycin resistance gene.

fGH

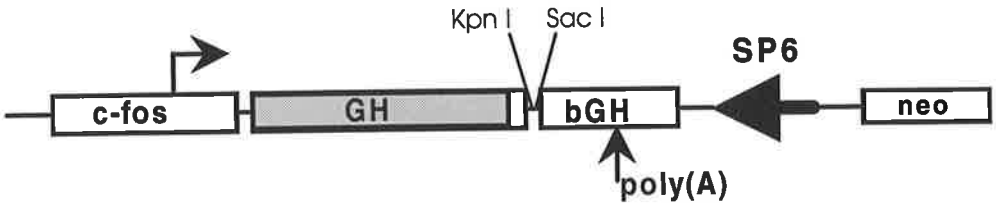

bovine growth hormone polyadenylation sequence and SP6 promoter) into the *Eco*RI site of pRcCMV (these manipulations were carried out by G. Goodall and C. Lagnado). The cytomegalovirus promoter was removed by digestion with *Nru*I and *Hind*III, and was replaced with a 700bp *Eco*RI-*Hind*III fragment of plasmid pfos3CAT (kindly provided by H. Iba and D. Cohen), containing the chicken c-*fos* promoter to produce plasmid fGH.

Chapter 3

Differential regulation of the stability of AUIE-containing cytokine mRNAs in LPS-activated human blood monocytes in response to IL-10

3.1 Introduction

In response to activation by many stimuli, but particularly microbial antigens, monocytes produce a number of cytokines, including G-CSF, GM-CSF, IL-1, TNFα IL-8 MIP-1α and IL-6 (de Waal Malefyt *et al.*, 1991) which play a vital role in orchestrating immune and inflammatory responses. The stability of their mRNAs plays an important part in determining the duration and level of expression of these cytokines. On the other hand negative regulation of these cellular responses plays an essential role in limiting the magnitude and duration of these responses. Several cytokines induce cytokine production but relatively few, most notably, IL-10 (Fiorentino *et al.*, 1991; Moore *et al.*, 1993), IL-4 (te Velde *et al.*, 1990), IL-13 (de Waal Malefyt *et al.*, 1993) and TGF β (Espevik *et al.*, 1987) have been found to act as negative regulators.

IL-10 acts on a wide range of cell types including B-cells (Rousset *et al.*, 1992; Go *et al.*, 1990), mast cells (Thompson Snipes *et al.*, 1991), neutrophils (Kasama *et al.*, 1994; Cassatella *et al.*, 1994; Howard *et al.*, 1982), T-cells (Fiorentino *et al.*, 1989; Horowitz *et al.*, 1986), NK cells (Tripp *et al.*, 1993; Hsu *et al.*, 1992), macrophages (Fiorentino *et al.*, 1991; Bogdan *et al.*, 1991) and monocytes (de Waal Malefyt *et al.*, 1991). It has pleiotropic activities, exerting both stimulatory and suppressive effects. It can serve as a stimulatory factor for B cells (Rousset *et al.*, 1992; Go *et al.*, 1990) and mast cells (Thompson Snipes *et al.*, 1991) but its most well documented effects are its inhibitory activities. IL-10 inhibits proliferation of and reduces cytokine production from T-cells (Fiorentino *et al.*, 1989), particularly affecting IFN-γ and IL-2 production. IL-10, IL-4, IL-13 and TGF-β are considered to be the most important macrophage deactivating factors reducing their synthesis of IL-1, IL-6 and TNFα (Fiorentino *et al.*, 1991) following stimulation with LPS. Although unlike IL-10 and TGF-β, which act as downmodulators of many phagocytic functions (Bogdan *et al.*, 1991; Bogdan *et al.*, 1992), IL-4 and IL-13 have a more complex mode of function (D'Andrea *et al.*, 1995). IL-10 reduces synthesis of IL-8, MIP-1α, MIP-1β (Kasama *et al.*, 1994), IL-1 and TNFα (Cassatella *et al.*, 1994) in neutrophils stimulated with LPS. In polymorphonuclear

leukocytes IL-10, IL-13 and IL-4 upregulate production of IL-1 receptor antagonist, a potent anti-inflammatory agent which is a competitive inhibitor of IL-1α and IL-1β and acts by binding to type I and type II IL-1 receptors without activating them. IL-10 inhibits LPS-induced survival of eosinophils and their synthesis of GM-CSF, TNFα and IL-8 (Takanaski *et al.*, 1994) and in monocytes activated with LPS IL-10 reduces synthesis of IL-1α, IL-1β, IL-6, IL-8, TNFα , GM-CSF and G-CSF (de Waal Malefyt *et al.*, 1991).

IL-4, originally designated B cell stimulatory factor-1, was initially described as a T-cell derived factor that led to DNA synthesis in resting B lymphocytes (Howard *et al.*, 1982). More recently the nature of its pleiotropic effects has become apparent. In B-cells it acts as a proliferation and differentiation factor, induces class II major histocompatibility antigens on resting B-cells (Noelle *et al.*, 1984; Roehm *et al.*, 1984), regulates switching to IgG_1 and IgE secretion by activated B-cells (Vitetta *et al.*, 1985), and regulates expression of Fc_ε receptors (CD23) and its own receptors on B-cells. (Conrad *et al.*, 1987; Defrance *et al.*, 1987; Hudak *et al.*, 1987; Snapper and Paul, 1987; Ohara and Paul, 1988). Its effects are not restricted to cells of the B lymphoid lineage however. IL-4 activities on cells of the myeloid lineage are complex and may appear contradictory; IL-4 suppresses the IL-3 supported proliferation but enhances the G-CSF-supported granulocytic colony formation, whereas in monocytes it suppresses the endotoxin and IL-1-induced expression of G-CSF, TNF, and IL-1 (Dokter *et al.*, 1993), LPS and IFNγ-induced production of TNF, IL-1β, PGE_2 (Hart *et al.*, 1989), and IL-6 (te Velde *et al.*, 1990), LPS induced production of TNF-α , IL-10, IL-1β and IL-12 (D'Andrea *et al.*, 1995) and Anti-CD45 induced expression of M-CSF (Gruber *et al.*, 1994). Thus, both IL-10 and IL-4 can be regarded as anti-inflammatory cytokines with some distinct and some overlapping properties.

Since the production of many cytokines is induced at least in part by stabilisation of the mRNAs that encode them in this chapter I have investigated the possibility that downregulation induced by both IL-10 and IL-4 involves abrogation of this stabilisation event, causing mRNAs to revert to the unstable state. IL-4 and IL-10 share some anti-inflammatory properties acting synergistically to inhibit macrophage cytotoxic activity

(Oswald *et al.*, 1992) and cell mediated immunity *in vivo* (Powrie *et al.*, 1993). Thus, I also examined the possibility that since both of these cytokines downregulate cytokine expression in monocytes that they act additively to further destabilise the mRNAs and hence deactivate monocytes.

IL-10 is currently the only cytokine known to downregulate its own production (de Waal Malefyt *et al.*, 1991) obviously by a negative feedback mechanism. The stability of IL-10 was not known before these studies but the 3'UTR of IL-10 does contain multiple copies of the AUIE, suggesting its mRNA may be unstable and that it may be regulated at the level of mRNA stability. I therefore investigated the possibility that its own expression is also downregulated by decreasing the stability of its mRNA. G-CSF and GM-CSF are released as part of the primary inflammatory response in monocytes and are quickly downregulated to limit the duration of the response. In contrast, IL-10 is released slightly later in an immune response and acts on the monocytes to deactivate them and somewhat later in the response its own expression is inhibited. Since its role in the inflammatory response is different from that of G-CSF and GM-CSF mRNAs I also wished to investigate whether IL-10 downregulates its own expression by a mechanism different from that for G-CSF and GM-CSF.

3.2 Methods

3.2.1 Reagents

Human IL-10 and anti-IL-10 mAb19F1 were generous gifts from Dr. Anne O'Garra and Dr. Rene de Waal Malefyt (DNAX Research Institute Palo-Alto California USA) and were used at a concentration of 100U/ml and 5mg/ml respectively. IL-4 (kindly provided by J. Gamble, Human Imunology Hanson Centre for Cancer Research, Adelaide, Sth. Australia) was used at a concentration of 10ng/ml. LPS was used at a concentration of 1mg/ml and actinomycin D was used at 5mg/ml.

3.2.2 Isolation and Culture of Human Monocytes

All experiments were performed using freshly isolated cells. Human peripheral blood monocytes were isolated from 500ml of blood from normal donors (gift from Red Cross Transfusion Service, Adelaide). Mononuclear cellswere isolated on lymphoprep density gradients followed by fractionation into lymphocytes and monocytes by centrifugal elutriation. The monocyte fraction ($7x10^7$- $2x10^8$ cells) was collected and judged 94-99% pure by Giemsa staining of cytocentrifuged preparations. Monocytes were cultured in RPMI 1640 (endotoxin free) supplemented 200mM L-Glutamine, penicillin/gentamycin, 10% FCS and 7.5% sodium bicarbonate in 60mm tissue culture dishes at a concentration of 4-8 $x10^6$/ml (see 2.8.9 for details).

3.3 Results

3.3.1 IL-10 acts rapidly to inhibit the accumulation of GM-CSF and G-CSF mRNAs

In unstimulated freshly isolated monocytes GM-CSF and G-CSF mRNAs are undetectable. Therefore, in order to establish conditions under which the influence of IL-10 on GM-CSF and G-CSF mRNA stability could be measured I first determined the timecourse of GM-CSF mRNA expression in response to LPS. GM-CSF mRNA accumulated for at least 8 hr following stimulation with LPS but by 24hr post-stimulation the level of GM-CSF mRNA had declined to be almost undetectable (Fig 3.3.1). When monocytes were incubated with LPS in the presence of 100U/ml IL-10, GM-CSF mRNA was not detected at any of the timepoints, indicating that IL-10 prevents accumulation of GM-CSF mRNA. Since monocytes can themselves produce IL-10 in response to LPS, activated monocytes were also incubated in the presence of anti-IL-10 monoclonal antibody 19F1. This IL-10 neutralizing mAb has previously been shown to enhance the production of GM-CSF protein by LPS-activated human monocytes (de Waal Malefyt *et al.*, 1991). By 8 h post-stimulation, much higher (5-fold) levels of GM-CSF mRNA had accumulated than in cells incubated with LPS alone, suggesting that endogenously synthesised IL-10 was capable of downregulating GM-CSF mRNA.

These first experiments indicated that when added simultaneously with LPS, IL-10 entirely prevented accumulation of GM-CSF which meant that it was not possible to determine the effect of IL-10 on the turnover rate. I therefore next investigated whether IL-10 could inhibit G-CSF and GM-CSF mRNA accumulation if added some time after stimulation by LPS when significant levels of G-CSF and GM-CSF mRNA had already accumulated. IL-10 was added to the culture medium of monocytes 2 h or 3.5 h after stimulation of monocytes with LPS and the level of G-CSF and GM-CSF mRNAs measured by RNase protection assay at various times thereafter. At either time of addition IL-10 rapidly blocked subsequent accumulation of both G-CSF and GM-CSF

Figure. 3.3.1 Accumulation of GM-CSF mRNA in response to IL-10 in LPS-activated human monocytes.

Human monocytes (2-5 x 10^6) were activated with LPS (1 μg/ml) alone (■) or in the presence of either IL-10 (100 U/ml) (●) or neutralising IL-10 mAb 19F1 (5 μg/ml) (▲). Total RNA was isolated at 0, 4, 8 and 24 h after addition of LPS. GM-CSF and IL-10 mRNAs were detected by RNase protection analysis using *in vitro* synthesised complimentary RNA probes (see sections, 2.8.15, 2.8.17 and 2.8.18).

The GM-CSF mRNA was detected using a probe complimentary to a 207bp fragment of the GM-CSF mRNA, synthesised from *Nco*I digested pfGH-GM3C plasmid using SP6 RNA polymerase and 400Ci/mmol [α^{32}P]-UTP.

The IL-10 mRNA was detected using a probe complimentary to a 246bp fragment of the IL-10 mRNA, synthesised from *Hind*III digested pfGH-IL10 plasmid using SP6 RNA polymerase and 400Ci/mmol [α^{32}P]-UTP.

The GAPDH mRNA was detected by using a probe complimentary to a 120bp internal fragment the mouse GAPDH mRNA, synthesised from *Dde*I-digested plasmid pGAPM using T7 RNA polymerase and 100Ci/mmol [α^{32}P]-UTP. Abundance of mRNA was determined by RNase protection assay.

Panel A) Phosphorimage of RNase protection gel showing duplicate samples.

Panel B) GM-CSF mRNA levels were quantitated by phosphorimaging and plotted as mean +/- SEM (n=2) relative to the GAPDH internal standard.

A

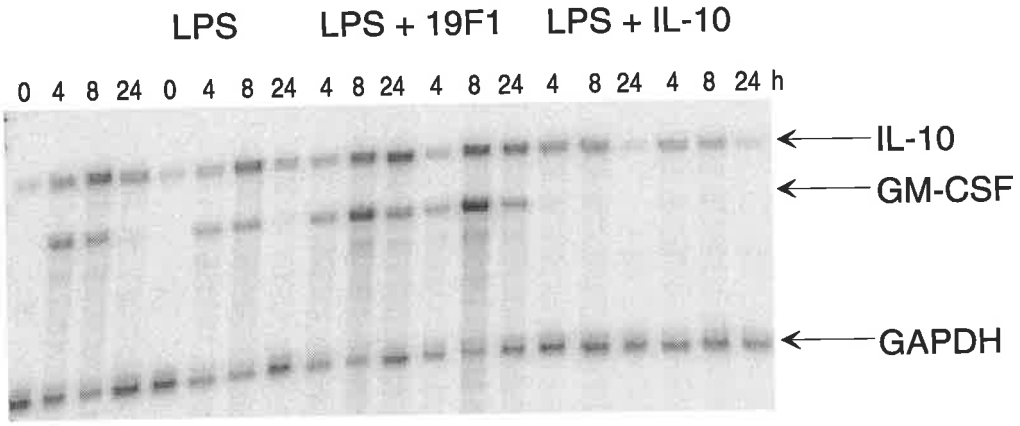
LPS
LPS + 19F1
LPS + IL-10
0 4 8 24 0 4 8 24 4 8 24 4 8 24 4 8 24 4 8 24 h
IL-10
GM-CSF
GAPDH

B

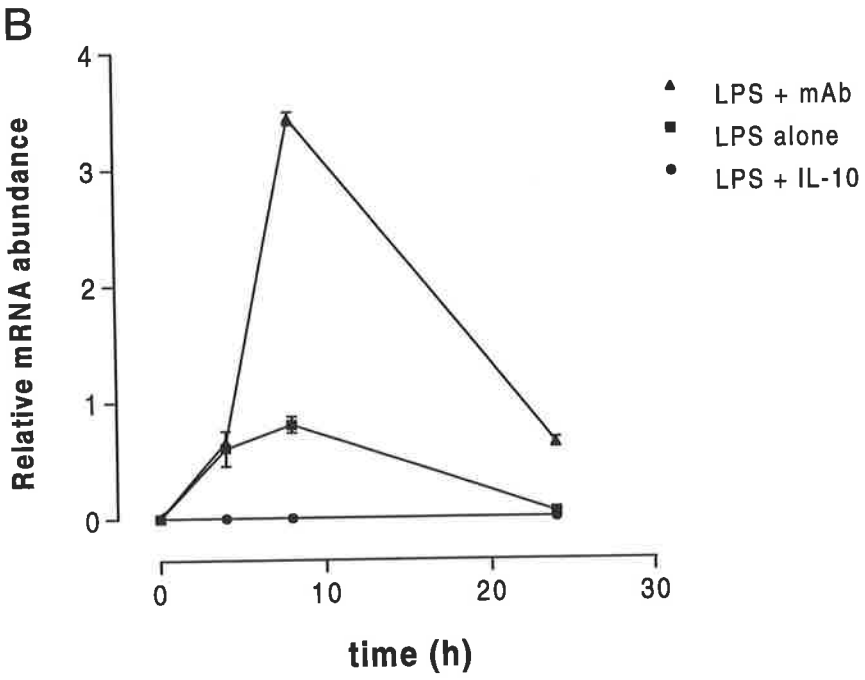
Relative mRNA abundance
4
3
2
1
0
0
10
20
30
time (h)
LPS + mAb
LPS alone
LPS + IL-10

Figure. 3.3.2 Decreased accumulation of G-CSF and GM-CSF mRNA in response to IL-10 added at 2 or 3.5 h after LPS-activation of human monocytes.

Human monocytes (2-5 x 10^6) were activated with LPS (1 μg/ml) with either no addition of IL-10 (■), or addition of 100 U/ml IL-10 at 2 h (▲) or 3.5 h (●) after addition of LPS. RNA was isolated at times indicated and G-CSF and GM-CSF mRNAs were detected by RNase protection analysis using *in vitro* synthesised complimentary RNA probes (see section, 2.8.15, 2.8.17 and 2.8.18)

The GM-CSF mRNA was detected using a probe complimentary to a 207bp fragment of GM-CSF mRNA, synthesised from *Nco*I digested pfGH-GM3C plasmid using SP6 RNA polymerase and 400Ci/mmol [α^{32}P]-UTP.

The G-CSF mRNA was detected using a probe complimentary to a 278bp fragment of G-CSF mRNA, synthesised from *Mlu*I digested pfGH-G plasmid using SP6 RNA polymerase and 400Ci/mmol [α^{32}P]-UTP.

The GAPDH mRNA was detected by using a probe complimentary to a 120bp internal fragment the mouse GAPDH mRNA, synthesised from *Dde*I-digested plasmid pGAPM using T7 RNA polymerase and 100Ci/mmol [α^{32}P]-UTP. Abundance of mRNA was determined by RNase protection assay.

Panel A) Phosphorimage of RNase protection gel showing duplicate samples

Panel B) G-CSF mRNA levels were quantitated by phosphorimaging and plotted as mean ± SEM (n=2) relative to the GAPDH internal standard.

Panel C) GM-CSF mRNA levels were quantitated by phosphorimaging and plotted as mean ± SEM (n=2) relative to the GAPDH internal standard.

A

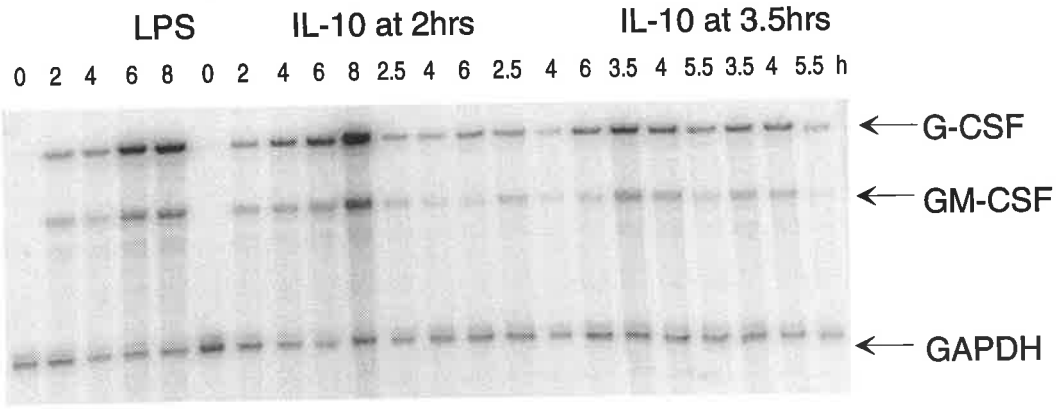
LPS
IL-10 at 2hrs
IL-10 at 3.5hrs
0 2 4 6 8 0 2 4 6 8 2.5 4 6 2.5 4 6 3.5 4 5.5 3.5 4 5.5 h
G-CSF
GM-CSF
GAPDH

B

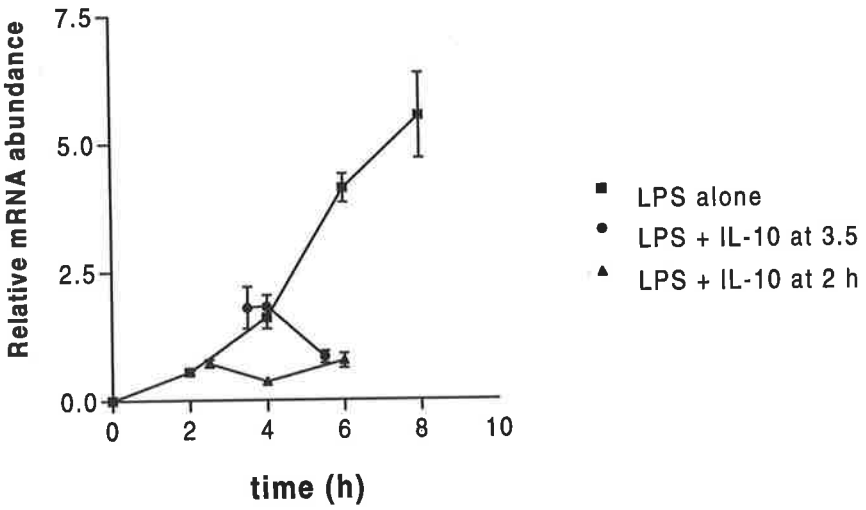
Relative mRNA abundance
7.5
5.0
2.5
0.0
0 2 4 6 8 10
time (h)
LPS alone
LPS + IL-10 at 3.5
LPS + IL-10 at 2 h

C

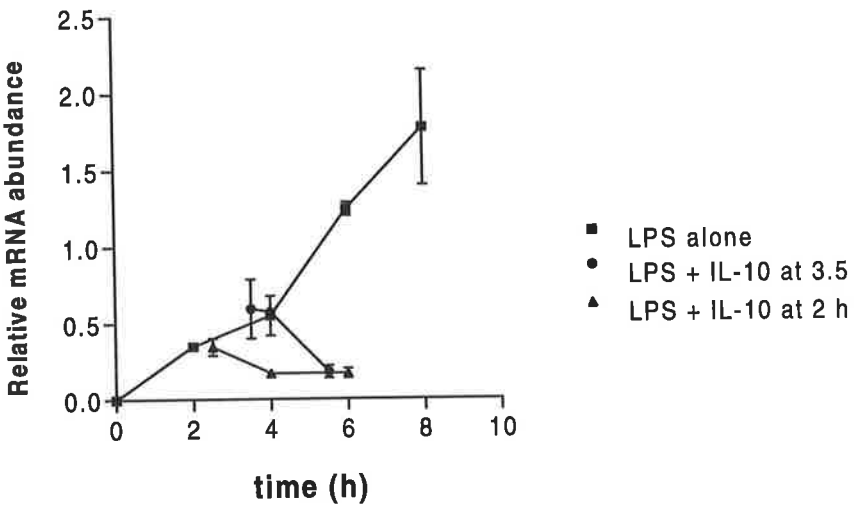
Relative mRNA abundance
2.5
2.0
1.5
1.0
0.5
0.0
0 2 4 6 8 10
time (h)
LPS alone
LPS + IL-10 at 3.5
LPS + IL-10 at 2 h

mRNAs (Fig 3.3.2) between 0.5 and 2 h after addition of IL-10. Thus activated monocytes respond rapidly to IL-10 by switching from G-CSF and GM-CSF mRNA accumulation to G-CSF and GM-CSF mRNA depletion. In the case of addition of IL-10 at 3.5 h, the mRNA levels actually declined rapidly, indicating the mRNAs were unstable. I chose this time of addition to measure the influence of IL-10 on mRNA stability.

3.3.2 IL-10 reduces the Stability of G-CSF and GM-CSF mRNAs in LPS-activated Monocytes

The degradation rates of the G-CSF and GM-CSF mRNAs were measured 4 h after incubation in the presence of LPS, at which time actinomycin D was added to inhibit transcription. To determine whether IL-10 increases the degradation rates, the experiment was performed with and without the addition of IL-10 0.5 h prior to the addition of the actinomycin D and RNA was isolated at this and subsequent times. Exposure to actinomycin D was limited to no more than 2.5 h to minimise secondary effects that can result from actinomycin D treatment. In initial experiments I found that the effects of IL-10 on G-CSF and GM-CSF mRNA degradation were dose dependent, and were maximal at IL-10 concentrations greater than 25 U/ml (Fig. 3.3.3). IL-10 was used at 100 U/ml in all subsequent experiments. I found that both G-CSF and GM-CSF mRNAs were very stable in cells treated with LPS alone, with no loss over 2 h, whereas in IL-10 treated cells both mRNAs were unstable (Fig. 3.3.4). In experiments with monocytes from 6 different donors, I consistently found no significant degradation of GM-CSF or G-CSF mRNAs in the absence of IL-10, whereas in the presence of IL-10 both mRNAs were consistently unstable, with mean half-lives of 1.8 +/- 0.4 h (n=6) and 2.5 +/- 0.4 h (n=6), respectively (see Table II Appendix).

3.3.3 IL-10 negatively regulates its own mRNA in LPS-activated monocytes

The IL-10 mRNA contains several perfect or near-perfect copies of the AUIE in the 3'UTR, suggesting that the IL-10 mRNA could be unstable. Furthermore, since IL-

Figure. 3.3.3 The stability of G-CSF and GM-CSF mRNAs in response to increasing concentrations of IL-10 in LPS-activated monocytes.

Human monocytes (1.5×10^6) were activated with LPS (1 μg/ml) for 3.5 h and then for a further 30 min in the presence of increasing concentrations of IL-10 (concentration as indicated). Actinomycin D (5μg/ml) was then added to inhibit transcription and RNA was isolated either immediately or 3 h after addition of actinomycin D. G-CSF and GM-CSF mRNAs were detected by RNase protection analysis using *in vitro* synthesised complimentary RNA probes (see sections 2.8.15, 2.8.17 and 2.8.18).

The GM-CSF mRNA was detected using a probe complimentary to a 207bp fragment of GM-CSF mRNA, synthesised from *Nco*I digested pfGH-GM3C plasmid using SP6 RNA polymerase and 400Ci/mmol [α^{32}P]-UTP.

The G-CSF mRNA was detected using a probe complimentary to a 278bp fragment of G-CSF mRNA, synthesised from *Mlu*I digested pfGH-G plasmid using SP6 RNA polymerase and 400Ci/mmol [α^{32}P]-UTP.

The GAPDH mRNA was detected by using a probe complimentary to a 120bp internal fragment the mouse GAPDH mRNA, synthesised from *Dde*I-digested plasmid pGAPM using T7 RNA polymerase and 100Ci/mmol [α^{32}P]-UTP. Abundance of mRNA was determined by RNase protection assay.

Panel A) Phosphorimage of RNase protection gel showing duplicate samples

Panel B) The abundance of G-CSF and GM-CSF mRNAs remaining after 3 h exposure to actinomycin D was quantitated for each concentration of IL-10 and plotted relative to the GAPDH internal control. Data are the means of duplicate samples ± SEM from single representative experiments.

A

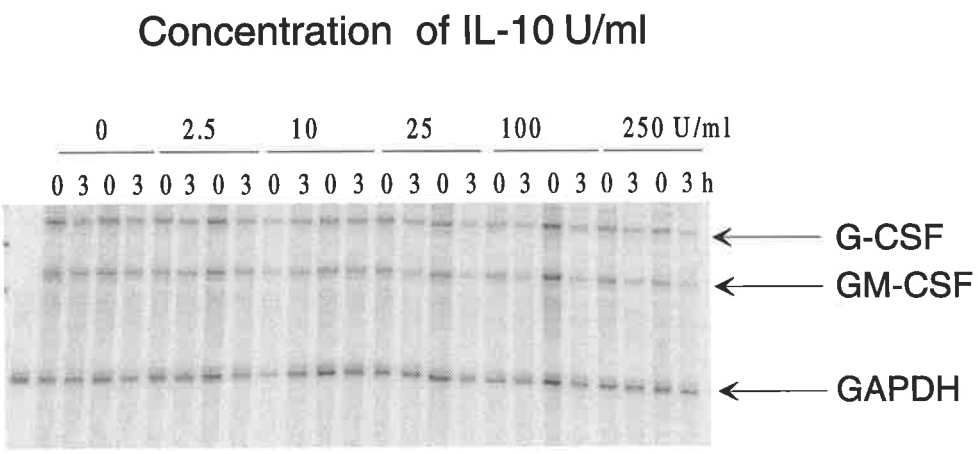
Concentration of IL-10 U/ml
0
2.5
10
25
100
250 U/ml
0 3 0 3 0 3 0 3 0 3 0 3 0 3 0 3 0 3 0 3 0 3 h
G-CSF
GM-CSF
GAPDH

B

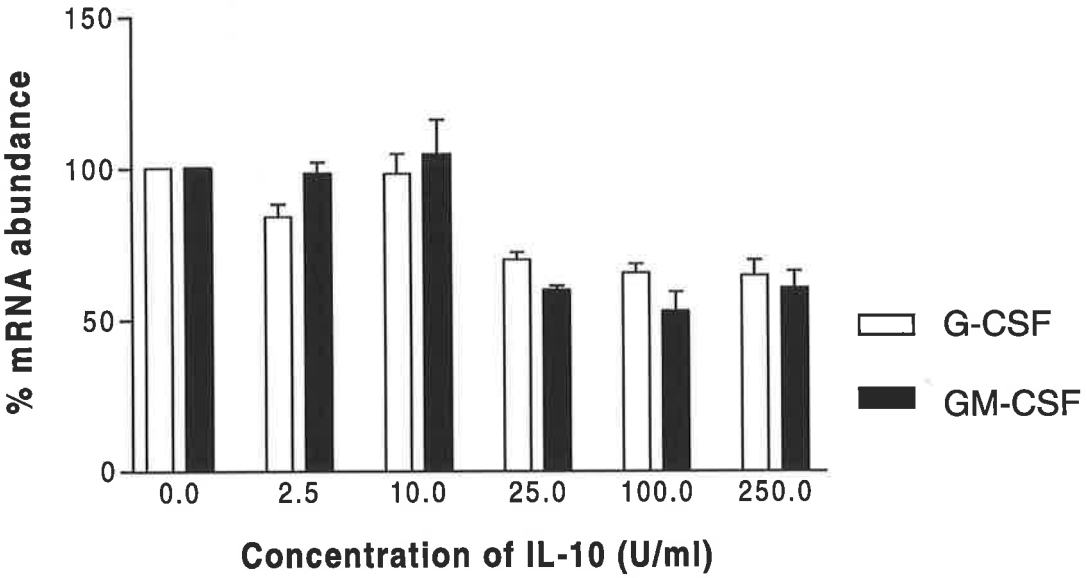
% mRNA abundance
150
100
50
0
0.0
2.5
10.0
25.0
100.0
250.0
Concentration of IL-10 (U/ml)
G-CSF
GM-CSF

Figure. 3.3.4. The stability of G-CSF and GM-CSF mRNAs in LPS-activated monocytes treated with IL-10 for 30 mins.

Monocytes (2-5 x 10^6) were activated with LPS (1μg/ml) for 3.5 h and then for a further 30 mins in the presence (■) or absence (●) of 100 U/ml IL-10. Actinomycin D (5 μg/ml) was then added to inhibit transcription and RNA was isolated at the times shown. G-CSF and GM-CSF mRNAs were detected by RNase protection analysis using *in vitro* synthesised complimentary RNA probes (see sections 2.8.15, 2.8.17 and 2.8.18).

The GM-CSF mRNA was detected using a probe complimentary to a 207bp fragment of GM-CSF mRNA, synthesised from *Nco*I digested pfGH-GM3C plasmid using SP6 RNA polymerase and 400Ci/mmol [α^{32}P]-UTP.

The G-CSF mRNA was detected using a probe complimentary to a 278bp fragment of G-CSF mRNA, synthesised from *Mlu*I digested pfGH-G plasmid using SP6 RNA polymerase and 400Ci/mmol [α^{32}P]-UTP.

The GAPDH mRNA was detected by using a probe complimentary to a 120bp internal fragment the mouse GAPDH mRNA, synthesised from *Dde*I-digested plasmid pGAPM using T7 RNA polymerase and 100Ci/mmol [α^{32}P]-UTP. Abundance of mRNA was determined by RNase protection assay.

Panel A) Phosphorimage of RNase protection gel.

Panel B) The abundance of G-CSF and GM-CSF mRNAs remaining from cells activated for 3.5 h and then for a further 30 mins in the presence (■) or absence (●) of IL-10 (100 U/ml) and exposed to actinomycin D (5μg/ml) was quantitated and plotted relative to the GAPDH internal control. Data are the means of duplicate samples ± SEM from single representative experiments.

A

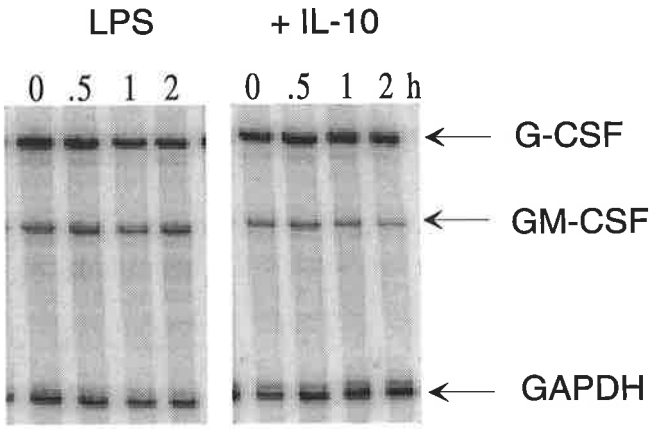
LPS
+ IL-10
0 .5 1 2
0 .5 1 2 h
G-CSF
GM-CSF
GAPDH

B

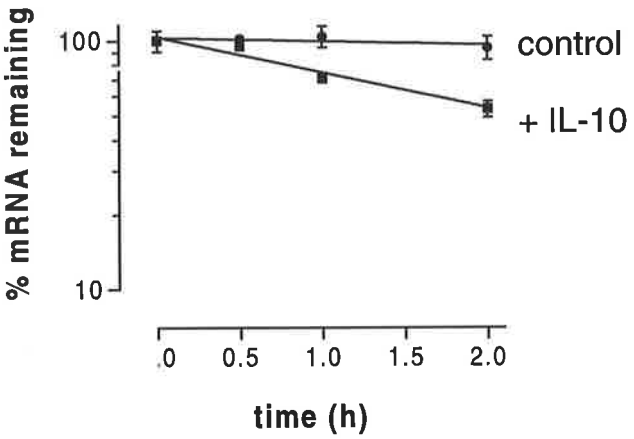
% mRNA remaining
100
10
control
+ IL-10
.0 0.5 1.0 1.5 2.0
time (h)

C

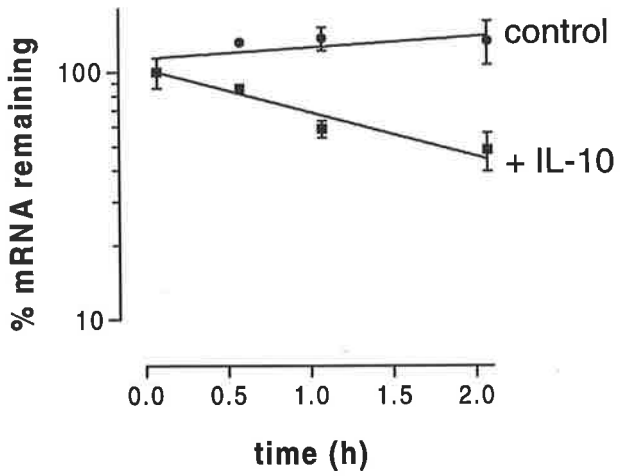
% mRNA remaining
100
10
control
+ IL-10
0.0 0.5 1.0 1.5 2.0
time (h)

10 destabilises the mRNAs for G-CSF and GM-CSF, it is also possible that IL-10 may influence the stability of its own mRNA. To investigate these possibilities I first measured IL-10 mRNA levels in monocytes following activation by LPS, either alone or in the presence of exogenously added IL-10 or anti-IL-10 mAb.

In LPS-activated monocytes the level of IL-10 mRNA increased for at least 8 h but had substantially declined by 24 h (Fig. 3.3.5). When IL-10 was added to the culture medium simultaneously with the LPS there was no effect after 4 h, but the amount of IL-10 mRNA at 8 h and 24 h post-stimulation was markedly reduced. Addition of anti-IL-10 mAb with the LPS resulted in modest enhancement of the IL-10 mRNA level at 8 h and a much slower rate of decline in mRNA level subsequently. Thus activated monocytes respond to both exogenously added and endogenous IL-10 by downregulating IL-10 mRNA. However, the influence on IL-10 mRNA was delayed, compared with the effects on G-CSF and GM-CSF mRNAs (compare Figs 3.3.1 and 3.3.5). For example, addition of IL-10 at the time of exposure to LPS completely eliminated accumulation of GM-CSF, but inhibition of IL-10 accumulation was not seen until the 8 h time point. The delay was also evident when the downregulation due to endogenously synthesised IL-10 was monitored using anti-IL-10 monoclonal antibody. There was a large effect of the monoclonal antibody on GM-CSFmRNA accumulation within 8 h, whereas the effect on IL-10 mRNA levels was slight at 8 h but large at 24 h, indicating that the endogenously synthesised IL-10 was affecting GM-CSF mRNA levels several hours earlier than it was affecting IL-10 mRNA.

3.3.4 IL-10 acts late to destabilise its own mRNA.

To investigate whether IL-10 affects the stability of its own mRNA I initially used the same conditions that revealed a destabilisation of the G-CSF and GM-CSF mRNAs; I added IL-10 to monocytes 3.5 h after stimulation with LPS and inhibited transcription with actinomycin D 0.5 h later. Under these conditions I found no effect on the stability of the IL-10 mRNA (Fig 3.3.6), consistent with the observation that there is a lag before seeing an inhibition of accumulation of IL-10 mRNA (Fig 3.3.5). I therefore chose to expose cells to IL-10 for a longer period before measuring IL-10 mRNA

Figure. 3.3.5. Accumulation of IL-10 mRNA in response to IL-10 in LPS-activated human monocytes.

Human monocytes (2-5 x 10^6) were activated with LPS (1 μg/ml) alone (■) or in the presence of either IL-10 (100 U/ml) (●) or neutralising IL-10 mAb 19F1 (5 μg/ml) (▲). Total RNA was isolated at 0, 4, 8 and 24 h after addition of LPS. IL-10 mRNA was detected by RNase protection analysis using *in vitro* synthesised complimentary RNA probes (see sections 2.8.15, 2.8.17 and 2.8.18).

The IL-10 mRNA was detected using a probe complimentary to a 246bp fragment of the IL-10 mRNA, synthesised from *Hind*III digested pfGH-IL10 plasmid using SP6 RNA polymerase and 400Ci/mmol [α^{32}P]-UTP.

The GAPDH mRNA was detected by using a probe complimentary to a 120bp internal fragment the mouse GAPDH mRNA, synthesised from *Dde*I-digested plasmid pGAPM using T7 RNA polymerase and 100Ci/mmol [α^{32}P]-UTP. Abundance of mRNA was determined by RNase protection assay. See Fig. 3.3.1 for RNase protection assay gel.

Figure IL-10 mRNA levels were quantitated by phosphorimaging and plotted as mean +/- SEM (n=2) relative to the GAPDH internal standard.

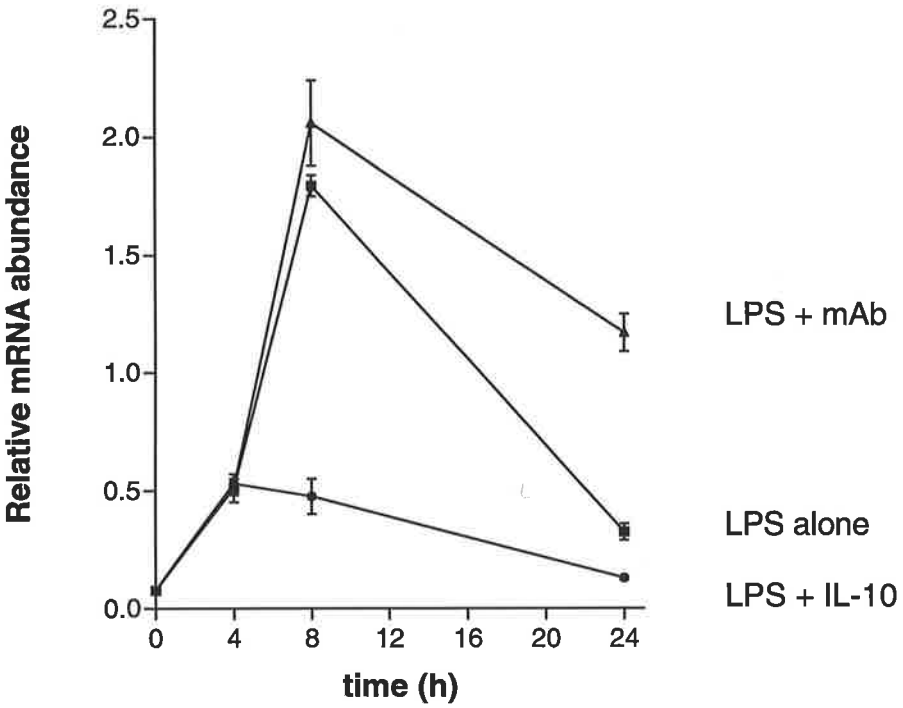
Relative mRNA abundance
2.5
2.0
1.5
1.0
0.5
0.0
0
4
8
12
16
20
24
time (h)
LPS + mAb
LPS alone
LPS + IL-10

Figure. 3.3.6. The stability of IL-10 mRNA in LPS-activated monocytes treated with IL-10 for 30 mins.

Monocytes (2-5 x 10^6) were activated with LPS (1µg/ml) for 3.5 h and then for a further 30 mins in the presence (■) or absence (●) of 100 U/ml IL-10. Actinomycin D (5 µg/ml) was then added to inhibit transcription and RNA was isolated at the times shown. IL-10 mRNA was detected by RNase protection analysis using *in vitro* synthesised complimentary RNA probes (see sections 2.8.15, 2.8.17 and 2.8.18).

The IL-10 mRNA was detected using a probe complimentary to a 246bp fragment of the IL-10 mRNA, synthesised from *Hind*III digested pfGH-IL10 plasmid using SP6 RNA polymerase and 400Ci/mmol [α^{32}P]-UTP.

The GAPDH mRNA was detected by using a probe complimentary to a 120bp internal fragment the mouse GAPDH mRNA, synthesised from *Dde*I-digested plasmid pGAPM using T7 RNA polymerase and 100Ci/mmol [α^{32}P]-UTP. Abundance of mRNA was determined by RNase protection assay.

Panel A) Phosphorimage of RNase protection gel.

Panel B) The abundance of IL-10 mRNA remaining from cells activated for 3.5 h with LPS and then for a further 30 mins in the presence (■) or absence (●) of IL-10 (100 U/ml) and exposed to actinomycin D (5µg/ml) was quantitated and plotted relative to the GAPDH internal control. Data are the means of duplicate samples +/- SEM from single representative experiments.

A

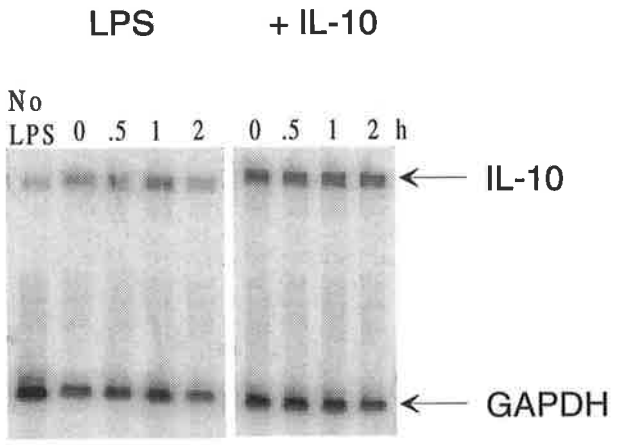
LPS
+ IL-10
No LPS
0 .5 1 2 0 .5 1 2 h
IL-10
GAPDH

B

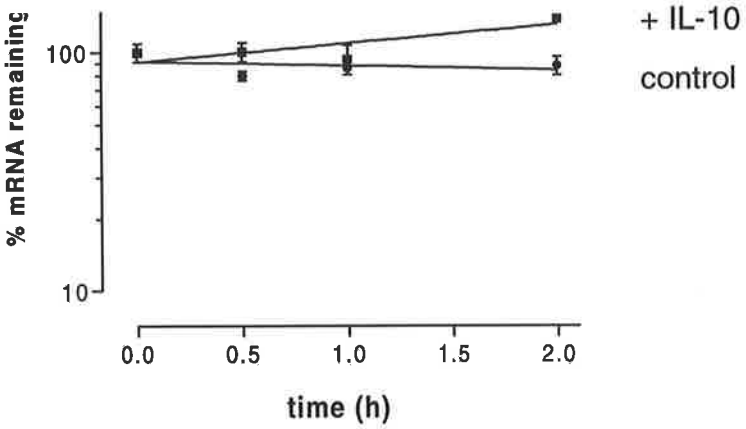
% mRNA remaining
100
10
0.0
0.5
1.0
1.5
2.0
time (h)
+ IL-10
control

Figure. 3.3.7 The stability of IL-10 mRNA in LPS-activated monocytes treated with IL-10 for 4 h

---

Monocytes (2-5 x 10^6) were activated with LPS (1μg/ml) for 2 h and then for a further 4 h in the presence (■) or absence (●) of 100 U/ml IL-10. Actinomycin D (5 μg/ml) was then added to inhibit transcription and RNA was isolated at the times shown. IL-10 mRNA was detected by RNase protection analysis using *in vitro* synthesised complimentary RNA probes (see sections 2.8.15, 2.8.17 and 2.8.18).

The IL-10 mRNA was detected using a probe complimentary to a 246bp fragment of the IL-10 mRNA, synthesised from *Hind*III digested pfGH-IL10 plasmid using SP6 RNA polymerase and 400Ci/mmol [α^{32}P]-UTP.

The GAPDH mRNA was detected by using a probe complimentary to a 120bp internal fragment the mouse GAPDH mRNA, synthesised from *Dde*I-digested plasmid pGAPM using T7 RNA polymerase and 100Ci/mmol [α^{32}P]-UTP. Abundance of mRNA was determined by RNase protection assay.

Panel A) Phosphorimage of RNase protection gel.

Panel B) The abundance of IL-10 mRNA remaining from cells activated for 2 h with LPS and then for a further 4 h in the presence (■) or absence (●) of IL-10 (100 U/ml) and exposed to actinomycin D (5μg/ml) was quantitated and plotted relative to the GAPDH internal control. Data are the means of duplicate samples +/- SEM from single representative experiments.

A

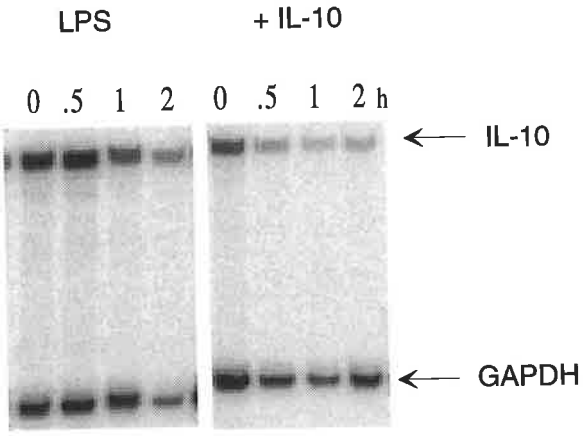
LPS
+ IL-10
0 .5 1 2 0 .5 1 2 h
IL-10
GAPDH

B

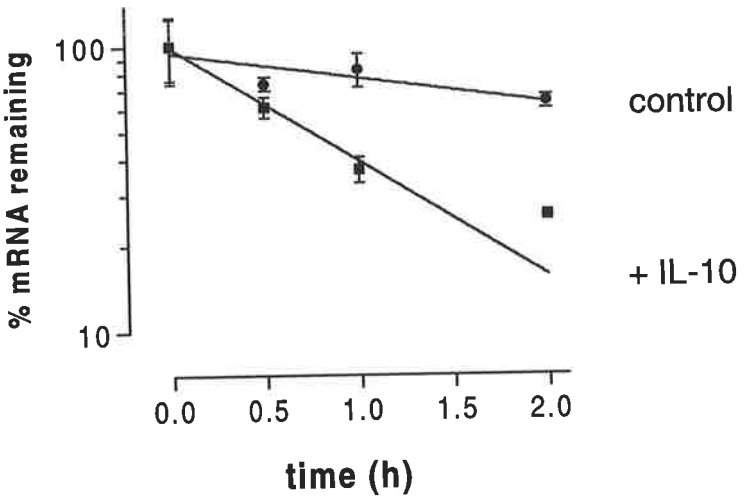
% mRNA remaining
100
10
0.0
0.5
1.0
1.5
2.0
time (h)
control
+ IL-10

degradation rates. Freshly isolated monocytes were incubated with LPS for 2 h, after which IL-10 was added to the culture medium for a further 4 h. Actinomycin D was then added and RNA harvested at intervals thereafter. With this longer incubation in the presence of IL-10 there was significant effect on the IL-10 mRNA stability (Fig 3.3.7 and Table III appendix). Thus the stability of the IL-10 mRNA is regulated, but not contemporaneously with the G-CSF and GM-CSF mRNAs.

3.3.5 Stabilities of G-CSF and GM-CSF mRNAs in IL-4 treated monocytes

Since IL-4 is known to downregulate cytokine production from a number of cell types (Akahane and Pluznik, 1992), including monocytes (Donnelly et al., 1991; Wang et al., 1995; te Velde et al., 1990; de Waal Malefyt et al., 1993; Hart et al., 1989), I investigated the possibility that downregulation of G-CSF and GM-CSF in monocytes by IL-4 was by increasing the turnover rate of their mRNAs.

Initially, I investigated whether conditions that revealed destabilisation of G-CSF and GM-CSF mRNAs by IL-10 would also result in destabilisation of these mRNAs by IL-4. Thus, IL-4 was added to monocytes 3.5 h after stimulation with LPS and transcription inhibited with actinomycin D 0.5 h later. Under these conditions, however, I did not observe any significant degradation of G-CSF and GM-CSF mRNAs (Fig 3.3.8). In previous studies (Donnelly et al., 1991) incubation of monocytes with LPS in the presence of IL-4 for 4 h resulted in reduced production of IL-1β. Based on these observations in subsequent experiments degradation rates of G-CSF and GM-CSF mRNAs were measured 4 h after incubation of monocytes with LPS (1mg/ml) in the presence or absence of IL-4 (10ng/ml) at which time actinomycin D was added to inhibit transcription and RNA isolated at this and subsequent times.

Results from experiments to determine the optimal IL-4 concentration to use for these studies suggested that the stabilities of GM-CSF and to a lesser extent G-CSF mRNAs were reduced in response to incubation of cells with IL-4 and that these effects were dose dependant being maximal at IL-4 concentrations of 10ng/ml or greater (Fig 3.3.9). IL-4 was used at a concentration of 10ng/ml in experiments thereafter. Further

Figure. 3.3.8 The stability of G-CSF and GM-CSF mRNAs in LPS-activated monocytes treated with IL-4 for 30 mins.

Monocytes (2-5 x 10^6) were activated with LPS (1μg/ml) for 3.5 h and then for a further 30 mins in the presence (■) or absence (●) of 10 ng/ml IL-4. Actinomycin D (5 μg/ml) was then added to inhibit transcription and RNA was isolated at the times shown. G-CSF and GM-CSF mRNAs were detected by RNase protection analysis using *in vitro* synthesised complimentary RNA probes (see sections 2.8.15, 2.8.17 and 2.8.18).

The GM-CSF mRNA was detected using a probe complimentary to a 207bp fragment of GM-CSF mRNA, synthesised from *Nco*I-digested pfGH-GM3C plasmid using SP6 RNA polymerase and 400Ci/mmol [α^{32}P]-UTP.

The G-CSF mRNA was detected using a probe complimentary to a 278bp fragment of G-CSF mRNA, synthesised from *Mlu*I digested pfGH-G plasmid using SP6 RNA polymerase and 400Ci/mmol [α^{32}P]-UTP.

The GAPDH mRNA was detected by using a probe complimentary to a 120bp internal fragment the mouse GAPDH mRNA, synthesised from *Dde*I-digested plasmid pGAPM using T7 RNA polymerase and 100Ci/mmol [α^{32}P]-UTP. Abundance of mRNA was determined by RNase protection assay.

Panel A) Phosphorimage of RNase protection gel.

Panel B) The abundance of G-CSF and GM-CSF mRNAs remaining from cells activated for 3.5 h and then for a further 30 mins in the presence (■) or absence (●) of IL-4 (10 ng/ml) and exposed to actinomycin D (5μg/ml) was quantitated and plotted relative to the GAPDH internal control. Data are the means of duplicate samples +/- SEM from single representative experiments.

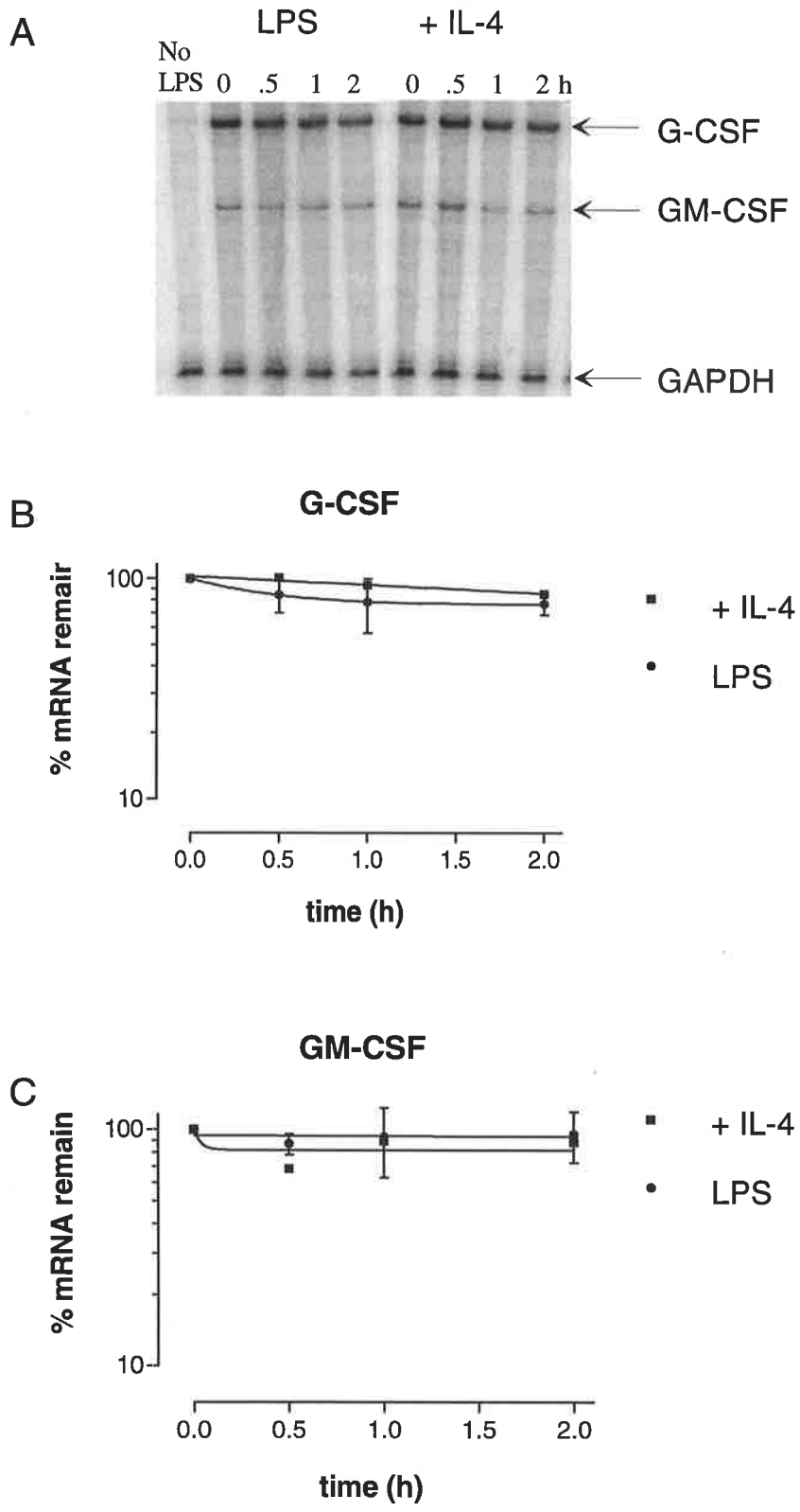
A
LPS
+ IL-4
No LPS
0 .5 1 2 0 .5 1 2 h
G-CSF
GM-CSF
GAPDH
B
G-CSF
% mRNA remair
100
10
0.0 0.5 1.0 1.5 2.0
time (h)
+ IL-4
LPS
C
GM-CSF
% mRNA remain
100
10
0.0 0.5 1.0 1.5 2.0
time (h)
+ IL-4
LPS

Figure. 3.3.9 The stability of G-CSF and GM-CSF mRNAs in response to increasing concentrations of IL-4 in LPS-activated monocytes.

Human monocytes (1.5×10^6) were activated with LPS (1 μg/ml) for 4 h in the absence or presence of increasing concentrations of IL-4 (concentration as indicated). Actinomycin D (5μg/ml) was then added to inhibit transcription and RNA was isolated immediately and 3 h after addition of actinomycin D. G-CSF and GM-CSF mRNAs were detected by RNase protection analysis using *in vitro* synthesised complimentary RNA probes (see sections 2.8.15, 2.8.17 and 2.8.18).

The GM-CSF mRNA was detected using a probe complimentary to a 207bp fragment of GM-CSF mRNA, synthesised from *Nco*I digested pfGH-GM3C plasmid using SP6 RNA polymerase and 400Ci/mmol [α^{32}P]-UTP.

The G-CSF mRNA was detected using a probe complimentary to a 278bp fragment of G-CSF mRNA, synthesised from *Mlu*I-digested pfGH-G plasmid using SP6 RNA polymerase and 400Ci/mmol [α^{32}P]-UTP.

The GAPDH mRNA was detected by using a probe complimentary to a 120bp internal fragment the mouse GAPDH mRNA, synthesised from *Dde*I-digested plasmid pGAPM using T7 RNA polymerase and 100Ci/mmol [α^{32}P]-UTP. Abundance of mRNA was determined by RNase protection assay.

Panel A) Phosphorimage of RNase protection gel showing duplicate samples.

Panel B) The abundance of G-CSF and GM-CSF mRNAs remaining after 3 h exposure to actinomycin D was quantitated for each concentration of IL-4 and plotted relative to the GAPDH internal control. Data are the means of duplicate samples ± SEM from single representative experiments.

A

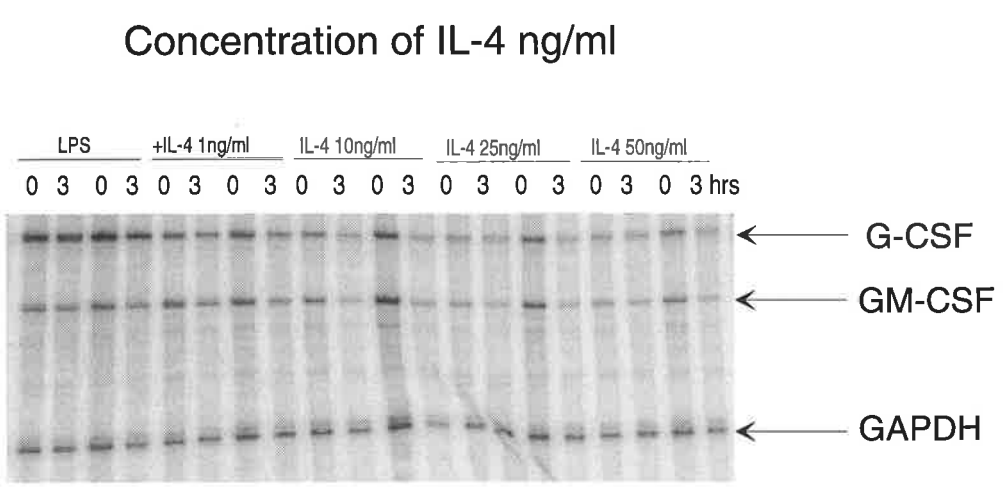
Concentration of IL-4 ng/ml
LPS
+IL-4 1ng/ml
IL-4 10ng/ml
IL-4 25ng/ml
IL-4 50ng/ml
0 3 0 3 0 3 0 3 0 3 0 3 0 3 0 3 0 3 0 3 hrs
G-CSF
GM-CSF
GAPDH

B

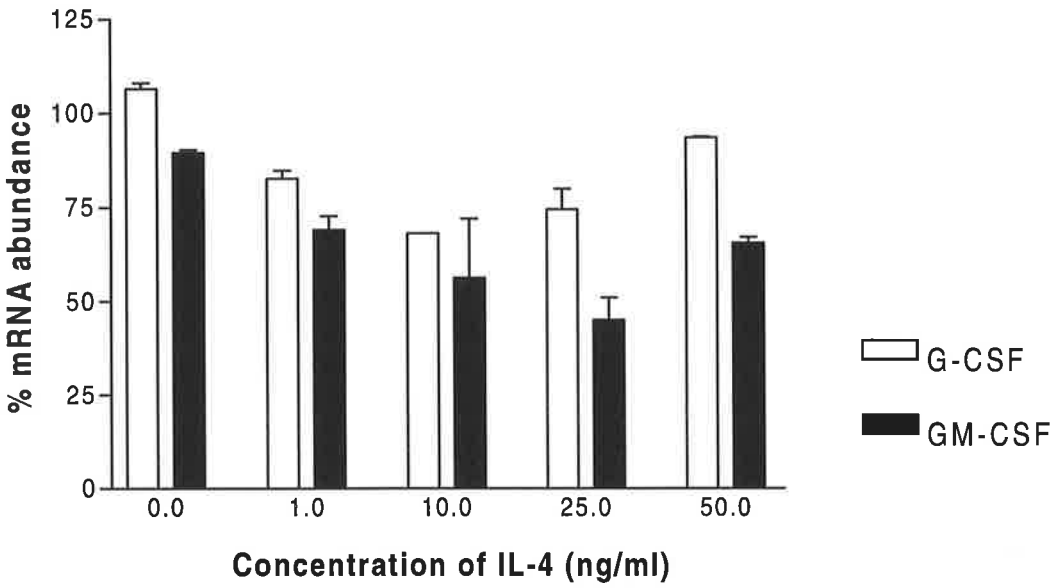
% mRNA abundance
125
100
75
50
25
0
0.0
1.0
10.0
25.0
50.0
Concentration of IL-4 (ng/ml)
G-CSF
GM-CSF

Figure. 3.3.10 The stability of G-CSF and GM-CSF mRNAs in LPS-activated monocytes treated with IL-4 for 4 h.

Monocytes (2-5 x 10^6) were activated with LPS (1μg/ml) for 4 h in the presence (■) or absence (●) of 10 ng/ml IL-4. Actinomycin D (5 μg/ml) was then added to inhibit transcription and RNA was isolated at the times shown. G-CSF and GM-CSF mRNAs were detected by RNase protection analysis using *in vitro* synthesised complimentary RNA probes (see sections 2.8.15, 2.8.17and 2.8.18).

The GM-CSF mRNA was detected using a probe complimentary to a 207bp fragment of GM-CSF mRNA, synthesised from *Nco*I digested pfGH-GM3C plasmid using SP6 RNA polymerase and 400Ci/mmol [α^{32}P]-UTP.

The G-CSF mRNA was detected using a probe complimentary to a 278 nt fragment of G-CSF mRNA, synthesised from *Mlu*I digested pfGH-G plasmid using SP6 RNA polymerase and 400Ci/mmol [α^{32}P]-UTP.

The GAPDH mRNA was detected by using a probe complimentary to a 120bp internal fragment the mouse GAPDH mRNA, synthesised from *Dde*I-digested plasmid pGAPM using T7 RNA polymerase and 100Ci/mmol [α^{32}P]-UTP. Abundance of mRNA was determined by RNase protection assay.

Plots A and B) The abundance of G-CSF(plot A) and GM-CSF (plot B) mRNAs remaining from cells activated with LPS for 4 h in the presence (■) or absence (●) of IL-4 (10 ng/ml) and exposed to actinomycin D (5μg/ml) was quantitated and plotted relative to the GAPDH internal control. Data are the means of duplicate samples +/- SEM from single representative experiments.

A

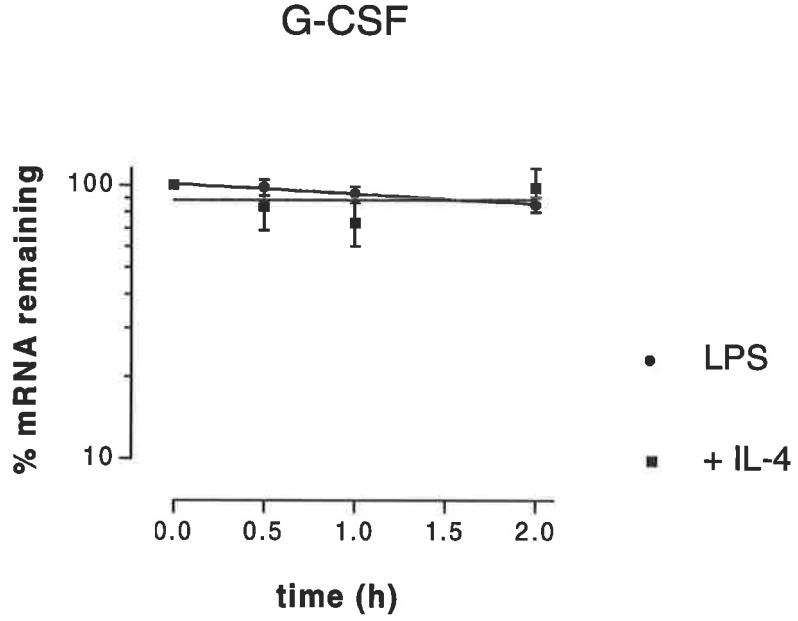
G-CSF
% mRNA remaining
100
10
0.0
0.5
1.0
1.5
2.0
time (h)
LPS
+ IL-4

B

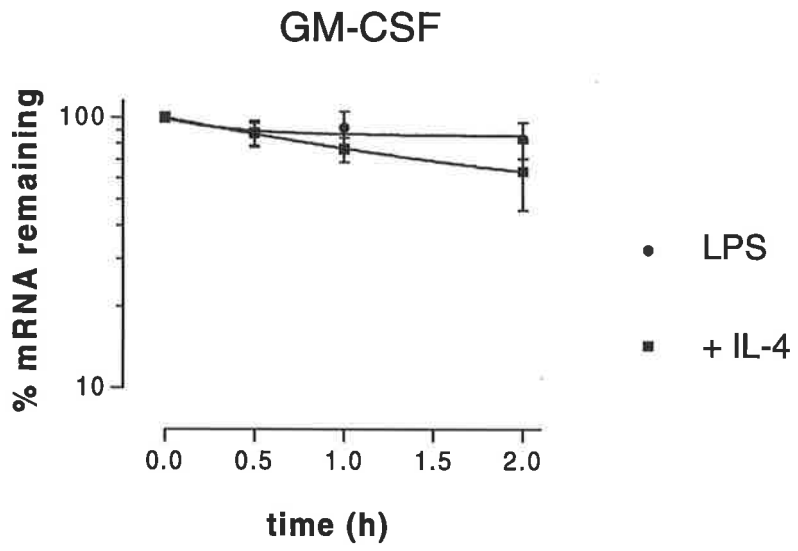
GM-CSF
% mRNA remaining
100
10
0.0
0.5
1.0
1.5
2.0
time (h)
LPS
+ IL-4

experiments, however, revealed variable effects and pooled data suggested that the effect of IL-4 on the stabilities of G-CSF and GM-CSF (Fig 3.3.10) was not significant. Further experiments designed to optimise incubation times of monocytes with IL-4 may help to address some of the unanswered questions but owing to time constraints these investigations were not pursued.

3.4 Discussion

I have found that IL-10 causes destabilisation of the G-CSF, GM-CSF and IL-10 mRNAs and inhibits their accumulation in LPS-activated monocytes. However, whereas IL-10 acts rapidly to destabilise G-CSF and GM-CSF mRNAs, being effective within half an hour of exposure of cells to IL-10, the action of IL-10 on its own mRNA is delayed, not being evident until after several hours of exposure. The rapidity of the effect on the stability of G-CSF and GM-CSF mRNAs suggests that this is a direct effect; the IL-10 receptor activates signalling pathways that influence the degradation of the G-CSF and GM-CSF mRNAs. On the other hand, the lack of a similar response in the degradation of IL-10 mRNA indicates that different or additional signalling pathways control the degradation of IL-10 mRNA. The fact that IL-10 responds after a delay of several hours suggests that the effect is indirect. The IL-10 could be inducing the synthesis of a factor that promotes IL-10 mRNA degradation, or it could be inhibiting the production of a factor that causes stabilisation of the IL-10 mRNA. If the latter were the case the putative stabilising factor, whether intracellular or secreted, would have to be labile, since the medium in which the cells were incubated was not changed during these experiments.

Many types of cell, especially those of the immune system, can produce multiple cytokines that contain AUIE, and are subject to regulation of mRNA stability. An implication of these findings is that the stability of these cytokine mRNAs can be independently regulated. This suggests there may be regulatory elements in these mRNAs in addition to the AUIE. The possibility that sequences in addition to the AUIEs participate in the regulation of cytokine mRNA stability is also suggested by the observation that a region of the GM-CSF 3'UTR about 160 bases upstream of the AU-rich region is required for regulation in response to PMA (Iwai *et al.*, 1991). In the case of IL-11 mRNA, which also contains AUIEs in the 3'UTR, sequences outside of the 3'UTR appear to be necessary for stabilisation in response to IL-1 (Yang and Yang,

1994). Additionally, in chapter 5 I describe identification of a novel stem-loop instability element in the G-CSF mRNA.

Monocytes play a crucial role in defense responses to infection and trauma, releasing a variety of products including a number of cytokines, some of which act as pro-inflammatory mediators. Their uncontrolled activation, however, is a major contributing factor to chronic inflammatory diseases.Negative regulators of monocyte activation therefore play an essential part in moderating and inhibiting an inflammatory response. The delayed downregulation of IL-10 compared to G-CSF and GM-CSF mRNAs may be an important factor in the generation and control of inflammatory responses. The delay this imposes before IL-10 downregulation takes effect may be to ensure deactivation of the monocytes occurs before its own synthesis is downregulated. This presumably allows the initial development of inflammatory responses, and the recruitment of a first wave of leukocytes to the site of inflammation, but then dampens the response unless cells at the inflammatory site are further stimulated, for example by antigen mediated activation. The low but detectable level of IL-10 mRNA in freshly isolated monocytes may indicate a low level constitutive production of IL-10 by resting monocytes. This might help *in vivo* to suppress synthesis of activating cytokines such as G-CSF and GM-CSF and ensure that monocytes remain unactivated in the absence of exogenous stimulation.

An individuals response to various stimuli will naturally vary and additionally the medical history of the donors was unknown, which inevitably meant that there was some variation between results in these experiments. This problem was overcome by carrying out multiple experiments as indicated in figure legends. It may have been possible to use cell lines rather than primary cells for these experiments but there appears to be no cell line that bears many of the surface markers found on primary monocytes. One of the better monocyte cell lines is the Monomac 6 (Ziegler-Heitbrock *et al.*, 1988) but this does not possess all monocyte characteristics and so I decided to pursue experiments with primary monocytes

Although I find that IL-10 downregulates expression of G-CSF, GM-CSF and IL-10 mRNAs by increasing the turnover rate of their mRNAs this does not preclude the

possibility that other mechanisms such as modulation of transcription or translation may contribute to the regulation of production of these cytokines. IL-10 has been shown to regulate other cytokines in various ways. For example, Wang *et al* (Wang *et al.*, 1995) found that in human PBMCs IL-10 appeared to downregulate TNFα and IL-1β by transcriptional mechanisms alone, whereas IL-6 was downregulated both transcriptionally and through enhanced mRNA degradation. Similarly in PMNs IL-8, (Wang *et al.*, 1994), MIP-1α, and MIP-1β (Kasama *et al.*, 1994) were regulated by IL-10 at both the transcriptional and post-transcriptional level. In murine macrophages IL-10 is proposed to downregulate IL-1 and TNFα by promoting the rapid decay of their mRNAs, whereas TGF-β, another macrophage deactivator may suppress TNFα production by predominantly translational mechanisms (Bogdan *et al.*, 1992).

IL-4 downregulates production of several cytokines as well as tissue factor (Ramani *et al.*, 1993) by various cells and there is evidence that several mechanisms play a role in this process. In IL-1α-stimulated murine B-lymphocytes, IL-4 inhibits GM-CSF gene expression by intranuclear destabilisation of the primary transcript (Akahane and Pluznik, 1992). In contrast, tissue factor in LPS-or PMA-stimulated monocytes may be downregulated by decreasing transcription (Ramani *et al.*, 1993) as is M-CSF mRNA in anti-CD45 stimulated monocytes (Gruber *et al.*, 1994), treated with either IL-4 or IL-10. Wang *et al* found that IL-4 decreases the expression of IL-1β, IL-6, IL-8 and TNFα mRNAs solely by decreasing their stabilities in LPS-activated monocytes (Wang *et al.*, 1995) although Donnelly *et al*, found that IL-1β,was downregulated at both the level of decreased transcription and decreased mRNA stability (Donnelly *et al.*, 1991). These last, somewhat conflicting, findings may suggest that either incubation times of LPS-activated monocytes with IL-4 or some other system differences are important in determining how a cytokine mRNA is downregulated. Donnelly *et al* found that 4 h treatment with IL-4 was necessary for significant inhibition of IL-1 mRNA expression, whereas Wang *et al* carried out their studies using monocytes activated with LPS and treated with IL-4 for just 2 h. My own results suggested that either more studies were required in order to optimise treatment times

with IL-4 or that IL-4 does not downregulate G-CSF and GM-CSF expression by destabilising their mRNAs but perhaps by some other mechanism.

Chapter 4

Regulation of cytokine mRNA stability

4.1 Introduction

In resting cells, production of many cytokines and proto-oncogenes is very low, and their mRNAs may be undetectable. The half-lives of these mRNAs is very short, often less than one hour, but upon induction by a variety of stimuli expression of the mRNAs is substantially increased. An increase in the rate of transcription contributes to the accumulation of many mRNAs but there is now a great deal of evidence to suggest that modulation of mRNA stability also plays an important role in regulating cytokine expression.

Stabilisation of cytokine mRNAs has been observed in response to a variety of different stimuli including TPA, (Shaw and Kamen, 1986; Ernst *et al.*, 1989; Bickel *et al.*, 1990), LPS, cyclohexamide (Thorens *et al.*, 1987; Ernst *et al.*, 1989), TNF, (Koeffler *et al.*, 1988; Gorospe *et al.*, 1993), EGF, TGFα (Le *et al.*, 1991), IL-1 (Akahane and Pluznik, 1992; Falkenburg *et al.*, 1991; Bagby *et al.*, 1990) and calcium ionophore (Wodnar-Filipowitz and Moroni, 1990). Stabilisation of cyokine mRNAs has also been observed in some tumour cells (Schuler and Cole, 1988; Baumbach *et al.*, 1987), *ras* transformed cells (Hahn *et al.*, 1991) and in virus-infected cells (Lieberman *et al.*, 1990).

In many cell types, several cytokines may be simultaneously produced after activation (Koeffler *et al.*, 1988; Sieff *et al.*, 1988; Broudy *et al.*, 1986) but in some cases selective expression of cytokines has been observed (Clark and Kamen, 1987; Chan *et al.*, 1986; Hahn *et al.*, 1991). Different mechanisms must exist to allow induction of cytokine genes which can lead to either selective or co-ordinate production. This may occur by differentially regulating transcription, stability, subsequent translation of the mRNA, or combinations of these, although the mechanisms have not yet been fully elucidated. Sometimes, even co-ordinate expression of cytokines may involve differential or multiple regulatory mechanisms. For example, Falkenburg *et al* (Falkenburg *et al.*, 1991) found that in murine fibroblasts IL-1 induction of G-CSF mRNA was mainly post-transcriptional whereas GM-CSF induction was controlled at

the level of transcription and stability. Thorens *et al* (Thorens *et al.*, 1987) similarly observed that GM-CSF was induced primarily by modulation of transcript stability in macrophages stimulated with LPS or LPS and interferong, while TNFα was transcriptionally upregulated under these conditions. Bickel *et al* (Bickel *et al.*, 1990) observed differential regulation of IL-2 and GM-CSF mRNAs; IL-2 was predominantly regulated at the level of transcription while GM-CSF was regulated primarily by modulating mRNA stability. In contrast, Koeffler *et al* (Koeffler *et al.*, 1988) found that increased transcription and mRNA stabilisation acted coordinately to modulate levels of G-CSF and GM-CSF transcripts in murine fibroblasts (WI38). In the case of TNF, however, response to endotoxin is mediated by modulation of translational efficiency (Han and Beutler, 1990).

Many cytokines and proto-oncogenes whose expression is regulated at the level of mRNA stability contain AU-rich sequences in their 3'UTRs. Since these sequences are an important determinant of mRNA instability, and there are no other obviously conserved sequences in cytokine mRNAs, it seemed likely that AU sequences may also mediate stabilisation in response to cellular activation. In support of this hypothesis, Schuler and Cole (Schuler and Cole, 1988) found that the mRNA for a chimeric gene containing the 3'UTR of GM-CSF was stabilised in tumour cells. Although these results implicated 3'UTRs in regulating stability of cytokine mRNAs the AUIE of GM-CSF was insufficient to mediate responsiveness to PMA (Iwai *et al.*, 1991), TNF-α (Akashi *et al.*, 1991) or IL-1α (Bagby *et al.*, 1990) suggesting that other elements either in the 3'UTR or elsewhere in the gene may be involved.

These conflicting reports highlighted the paucity of knowledge about the exact mechanisms involved in stabilisation of cytokine mRNAs in response to stimuli. I wanted to elucidate the requirements for stabilisation of mRNAs by examining various regions of the gene and defining the elements that may play a role. Thus, in this chapter I describe an investigation into the regions of the GM-CSF gene that are required to allow stabilisation of the mRNA in NIH3T3 mouse fibroblasts, in response to physiological inducers of cytokine synthesis such as IL-1 and TNF, and in response to activation of PKC. My initial hypothesis was that these elements would reside within

the 3'UTR of GM-CSF, but the investigation was extended to include the entire mRNA when my results suggested that other regions of the gene may be required.

4.1.1 GM-CSF

GM-CSF is a member of the family of haemopoietic growth factors which are essential for the differentiation, proliferation and maturation of haemopoietic cells. GM-CSF specifically stimulates differentiation and proliferation of the common progenitor cell of the neutrophil, eosinophil and monocyte and is also involved in the proliferation of the erythrocyte and megakaryocyte progenitors. In unactivated cells, although constitutively transcribed (Yamato *et al.*, 1989), GM-CSF mRNA does not accumulate owing to its short half-life. Upon activation by IL-1, TNF, antigens, lectins and phorbol-esters, GM-CSF mRNA accumulates rapidly in fibroblasts, endothelial cells, mononuclear phagocytes, mesothial cells and bone marrow stromal cells.

4.2 Methods

4.2.1 Construction of Plasmids Containing Human GM-CSF 3'UTR Sequences

Oligonucleotides

#72/25U 5 CTGGTACCTGAGACGGGCCAGATGA

#73/30L 5'CGTGAGCTCAGAAGCATATTTTTAATAATA

Plasmid fGH-GM This plasmid was generated in a multi-step process initally inserting the human GM-CSF cDNA (kindly provided by Dr. F. Shannon) into *Pst*1-*Sma*1 sites of plasmid pGEM-1. A *Sac*I- *Mbo*II fragment of the GM-CSF cDNA was then inserted into plasmid pCMV-GH (see section 2.8.20A) to create pCMVGH-GM (kindly prepared by Ms. C. Lagnado). The CMV promoter was then removed by *Nru*I and *Hind*III digests and replaced with a 700bp *EcoR*I-*Hind*111fragment containing the chicken -fos promoter to create fGH-GM.

Plasmid dfGH-GM3C This plasmid was prepared by inserting the human GM-CSF 3'UTR (bp 440-756bp) into *Kpn*1-*Sac*1 sites of plasmid dfGH (see section 2.8.20A). The 3'UTR of GM-CSF was generated by PCR amplification incorporating 5' *Kpn*I and 3'*Sac*I restriction sites (oligonucleotides #72/25 and #73/30) from a plasmid pG4-GM which contains the human GM-CSF cDNA (kindly provided by Dr. F. Shannon). Plasmid pG4-GM was generated by inserting the human GM-CSF cDNA into *Pst*1-*Sma*1 sites of plasmid pGEM4Z.

Plasmid fGH-7,2 This plasmid was prepared by inserting a chemically synthesised oligonucleotide comprising 4 AUIEs [(GGUCCAUUUAUUUAUUUAUUUAUUU ACUCAGCUGCAGUUUAUUUAUUUAUUUAUUUCUCGAGCUC (named 7,2)] into *Kpn*1-*Sac*1 sites of the pCMV-GH plasmid to create pCMV-GH7,2 (constructed by Ms. C. Lagnado). The CMV promoter was then removed by *Nru*I and *Hind*III digests

and replaced with a 700bp *EcoR*I-*Hind*111fragment containing the chicken *-fos* promoter to create fGH-7,2.

4.2.2 Construction of plasmids containing murine GM-CSF sequences

Plasmid dfGH3'muGM (dfGHGM-1) This plasmid was constructed by inserting the 3'UTR of murine GM-CSF, from bases 3190-3560, into the *Sac*I site of pfGH. The 3'UTR of mouse GM-CSF was generated by PCR amplification (oligonucleotides #125/41 and #139/63) from a murine GM-CSF genomic clone (pAOGM) (kindly provided by Tom Gonda) incorporating 5' and 3' *Sac*I restriction sites. For directional screening a *Cla*I restriction site was incorporated immediately upstream of the 3'*Sac*I site.This 3' PCR primer also included sequences corresponding to the T7 RNA polymerase promoter to enable transcription of a suitable RNase protection assay probe. Owing to the nature of these constructs the existing SP6 RNA polymerase promoter would result in probes too large to be useful. To eliminate any possible influence of the bovine growth hormone Poly-A signal on regulation of mRNA turnover this fragment includes the Poly-A signal and a further 66 bases (hence the use of the genomic clone) of GM-CSF 3'UTR. The 3' PCR primer also incorporated 3 further GT pairs to extend the GT rich region after the Poly-A signal to ensure that Polyadenylation occurs at this location and not at the bovine growth hormone poly-A signal. (Fig 4.2.1).

Plasmid df5'muGMGH3'muGM (dfGHGM-2) This plasmid contains the 3'UTR of murine GM-CSF and also contains the 5'UTR of murine GM-CSF (Fig 4.2.2). This plasmid was generated by inserting chemically synthesised oligonucleotides (#125/41 and #126/41) spanning nt 1132-1170 of the murine GM-CSF gene and adding 5' *Hind*III and 3'*Nco*I restriction sites for sub-cloning into *Hind*III and *Nco*I sites of plasmid pdfGHGM-1DXhoI. Construction of plasmids dfGHGM-2 and dfGM4 was complicated by the presence of multiple *Nco*I sites in the plasmid pdfGHGM-1. To overcome this an intermediate plasmid named dfGHGM1DXhoI was constructed in which an *Xho*I digest removed a fragment of 1,947bp between bases 1319-3266 thus removing the 2 *Nco*I

Figure. 4.2.1 Schematic representation of the dfGHGM-1 gene.

Panel A The boxes represent segments of the gene that were derived from the chicken c-*fos* gene (c-fos), human growth hormone cDNA (GH), indicated by shading, and mouse GM-CSF 3'UTR (mu GM); plasmid derived sequences are indicated by a line. The transcription start site and polyadenylation site are indicated by arrows. Also shown are the relative location of the T7 promoter, used to make probes for RNase protection assays and the neomycin resistance gene.

Panel B Sequence of oligonucleotides used for PCR amplification of the 3' UTR of mouse GM-CSF incorporating 5' and 3' *Sac*I sites.

A

dfGHGM-1

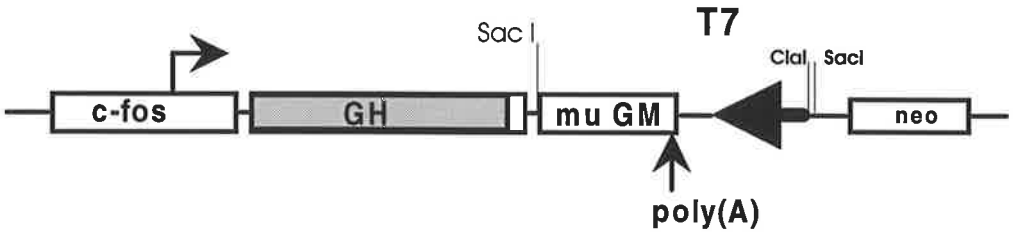

B **oligonucleotides**

Sac I 3190

#129/27U 5' GAGCTCGGAAGCCCAGGCCAGCTC

Sac I Cla I

#139/63L 5' CGCGAGCTCATCGATTAATACGACTCACT

ATAGGGAGACACACACCTATGCCCAAATTTTTCC

3560

Figure. 4.2.2 Schematic representation of the dfGHGM-2 gene.

Panel A The boxes represent segments of the gene that were derived from the chicken c-*fos* gene (c-fos), human growth hormone cDNA (GH), indicated by shading, mouse GM-CSF 5'UTR (5'UTR mu GM-CSF) and mouse GM-CSF 3'UTR (mu GM); plasmid derived sequences are indicated by a line. The transcription start site and polyadenylation site are indicated by arrows. Also shown is the relative location of the T7 promoter, used to make probes for RNase protection assays.

Panel B Sequence of the oligonucleotides representing the upper and lower strands of the 5'UTR of mouse GM-CSF incorporating 5' *Hind*III and 3' *Nco*I sites.

dfGHGM-2

A

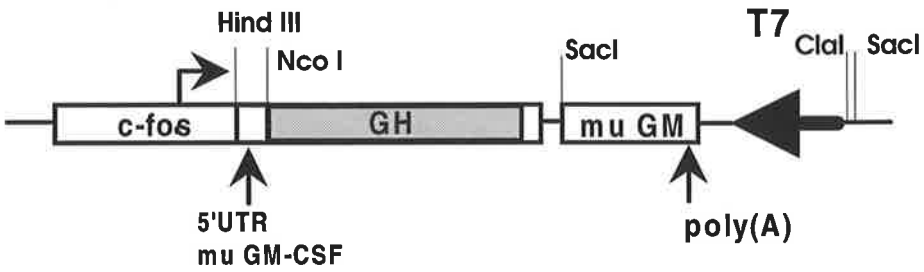

B **Oligonucleotides**

#125/41U↓1133
5' AGCTTAGTACTCAGAGAGAAAGGCTAAGGTCCTGA
GGAGGC 3'

#126/41L
5' CATGGCCTCCTCAGGACCTTAGCCTTTCTCTCTGAG
TACTA 3'

Figure. 4.2.3 Schematic representation of the dfGHGM-4 gene.

Panel A The boxes represent segments of the gene that were derived from the chicken c-*fos* gene (c-fos), mouse GM-CSF cDNA (muGM) translated region is indicated by shading, mouse GM-CSF 5'UTR (5'UTR mu GM-CSF) and mouse GM-CSF 3'UTR (mu GM); plasmid derived sequences are indicated by a line. The. The transcription start site and polyadenylation site are indicated by arrows. Also shown is the relative location of the T7 promoter, used to make probes for RNase protection assays.

Panel B Sequence of oligonucleotides used for PCR amplification of the translated region of mouse GM-CSF incorporating 5'*Nco*I and 3' *Kpn*I sites.

A

dfGM-4

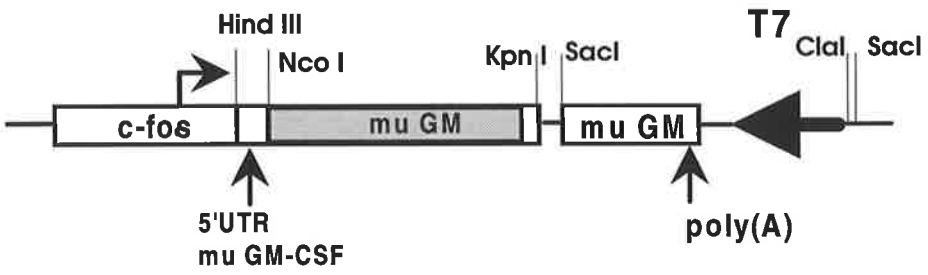

B

Oligonucleotides

#127/33U ↓174
5' CTGAGGCCATGGTGCTGCAGAATTTAC TTTTCC 3'
Nco I

#128/31L
5' CGTGGTACCTCATTTTTGGACTGGTTTTTTG
Kpn I ↑599

restriction sites contained within this fragment. Unfortunately, this digest also removed the neomycin resistance gene necessitating cotransfection with a resistence marker plasmid for generation of stable cell lines.

Plasmid df5' mu GMmuGM3'muGM (df-GM4). This plasmid contains the 5'UTR, the coding region and the 3'UTR of mouse GM-CSF with a 6nt region retained of the parent plasmid between the coding region and the 3'UTR (Fig 4.2.3). This is to ensure that subsequent RNase A digestion during an RNase protection assay will distinguish between endogenous and transfected GM-CSF mRNAs by cleaving the endogenous transcript at this point owing to mismatched nucleotides. This construct was generated by removing the growth hormone coding region of dfGH-GM2 with *Nco*I/*Kpn*I digests and inserting the murine GM-CSF coding region. The mouse GM-CSF coding region was generated by PCR amplification (oligonucleotides #127/33 and #128/31) from a plasmid containing the murine GM-CSF cDNA (pGMG) (kindly provided by T.Gonda) spanning 174-599bp a fragment of 428 bp and incorporating 5'*Nco*I and 3' *Kpn*I restriction sites into 5' and 3' PCR primers respectively. The incorporation of an *Nco*I site at the start codon (nt 174) changes nt 177 from a T to a G substituting a tryptophan for a glycine. In order to maintain a hydrophobic amino acid at this position a mutation was introduced at position nt 178 substituting the G for a T thus creating a valine at this position.

4.3 Results

4.3.1 AU instability elements are sufficient for stabilisation in response to calcium ionophore

I wished to determine which region of the GM-CSF gene was required to confer responsiveness to calcium ionophore. To address this NIH3T3 cells stably transfected with dfGH-GM3C, a plasmid containing the complete 3'UTR of GM-CSF, were stimulated with medium containing 15% FCS and the calcium ionophore A23187 to a final concentration of 2mm. I found that the stability of fGH-GM3C was significantly enhanced (Fig 4.3.1) compared with mRNAs from cells stimulated with 15% FCS alone, indicating that the 3'UTR of GM-CSF contains elements that confer responsiveness to calcium ionphore.

Having shown that the 3'UTR of human GM-CSF mRNA contains elements that mediate responsiveness to calcium ionophore I wished to define further the location of this responsive element. I found that in cells transfected with a plasmid containing the AU-rich region from GM-CSF (fGH-GM) treatment with A23187 resulted in mRNAs also being significantly stabilised compared with mRNAs from cells stimulated with 15% FCS alone (Fig 4.3.2). These results suggested that the elements responsive to A23187 in NIH3T3 mouse fibroblasts reside within the AU rich region.

The previous experiments showed that the AU-rich region of GM-CSF contains elements that allow stabilisation of the mRNA in response to A23187, but these results did not show whether the element was the AUIE alone or some other component of the AU-rich region. To address this I examined the stability of mRNAs from NIH3T3 cells transfected with fGH-7,2 which contains a synthetic sequence comprising 4 reiterated AUIEs. I found that fGH-7,2 mRNA from cells treated with A23187 was significantly stabilised compared with mRNA from cells stimulated with 15% serum alone (Fig. 4.3.3). These results indicate that the AUIE alone is sufficient for stabilisation in response to calcium ionophore in stably transfected NIH3T3 fibroblasts.

Figure 4.3.1 Stability of dfGH-GM3C mRNA in NIH3T3 cells stimulated with 15% FCS in the presence and absence of calcium ionophore (A231387)

NIH3T3 fibroblasts ($1x10^6$ cells) stably expressing the dfGH-GM3C transcript were stimulated with 15% FCS in the presence or absence of A23187 to a final concentration of 2μM and RNA was isolated at times indicated (see sections 2.8.15, 2.8.17 and 2.8.18). 20μg of total RNA was then hybridised with *in vitro* synthesised complimentary RNA probes.

The dfGH-GM3C mRNA was detected by RNase protection assay using a probe complimentary to a 338bp internal fragment of the growth hormone region of the dfGHGM3C mRNA, synthesised from *Pvu*II digested pG-5'hGH plasmid (see Table I: Appendix) using SP6 RNA polymerase and 400Ci/mmol [α^{32}P]-UTP.

The GAPDH mRNA was detected by using a probe complimentary to a 120bp internal fragment of the mouse GAPDH mRNA, synthesised from *Dde*I-digested plasmid pGAPM (see Table I: Appendix) using T7 RNA polymerase and 100Ci/mmol [α^{32}P]-UTP. Abundance of mRNA was determined by RNase protection assay.

Panel A) Phosphorimage of RNase protection gel

Panel B) Phosphorimager quantitation of dfGH-GM3C mRNA levels relative to GAPDH mRNA from NIH3T3 cells stimulated with 15% FCS in the presence (●) or absence (■) of 2μM A23187. Data are plotted as the mean ± SEM from 3 experiments.

A

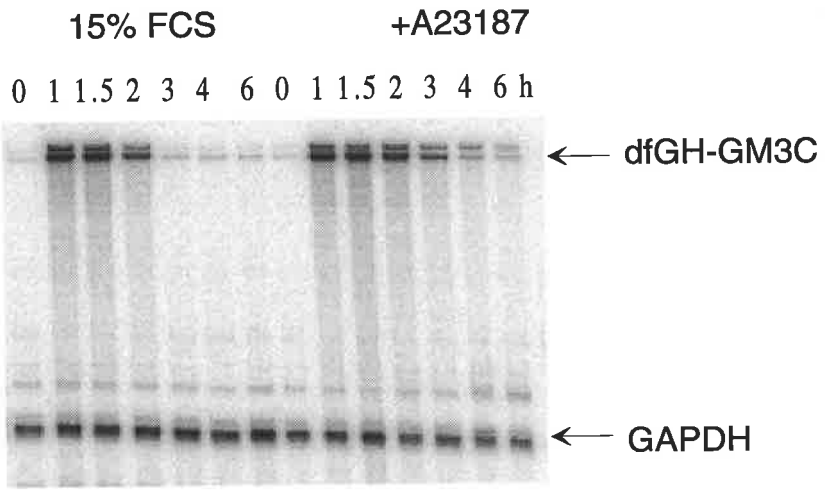
15% FCS
+A23187
0 1 1.5 2 3 4 6 0 1 1.5 2 3 4 6 h
dfGH-GM3C
GAPDH

B

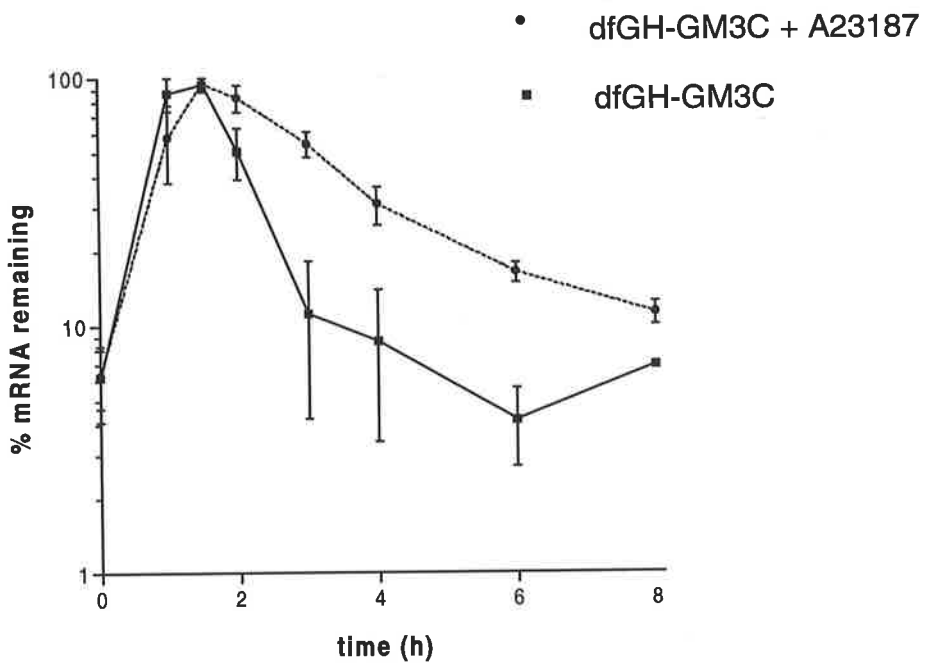
dfGH-GM3C + A23187
dfGH-GM3C
% mRNA remaining
100
10
1
0
2
4
6
8
time (h)

Figure 4.3.2 Stability of dfGH-GM mRNA in NIH3T3 cells stimulated with 15% FCS in the presence or absence of calcium ionophore (A231387)

NIH3T3 fibroblasts ($1x10^6$ cells) stably expressing the dfGH-GM transcript were stimulated with 15% FCS in the presence or absence of A23187 to a final concentration of 2μM and RNA was isolated at times indicated. 20μg of total RNA was then hybridised with *in vitro* synthesised complimentary RNA probes (see sections 2.8.15, 2.8.17 and 2.8.18.)

The dfGH-GM mRNA was detected by Rnase protection assay using a probe complimentary to a 338bp internal fragment of the growth hormone region of the dfGHGM mRNA, synthesised from *Pvu*II digested pG-5'hGH plasmid (see Table I: Appendix) using SP6 RNA polymerase and 400Ci/mmol [α^{32}P]-UTP.

The GAPDH mRNA was detected by using a probe complimentary to a 120bp internal fragment of the mouse GAPDH mRNA, synthesised from *Dde*I-digested plasmid pGAPM (see Table I: Appendix) using T7 RNA polymerase and 100Ci/mmol [α^{32}P]-UTP. Abundance of mRNA was determined by RNase protection assay.

Panel A) Phosphorimage of RNase protection gel

Panel B) Phosphorimager quantitation of dfGH-GM mRNA levels relative to GAPDH mRNA from NIH3T3 cells stimulated with 15% FCS in the presence (●) or absence (■) of 2μM A23187. Data are plotted as the mean +/- SEM from 3 experiments.

A

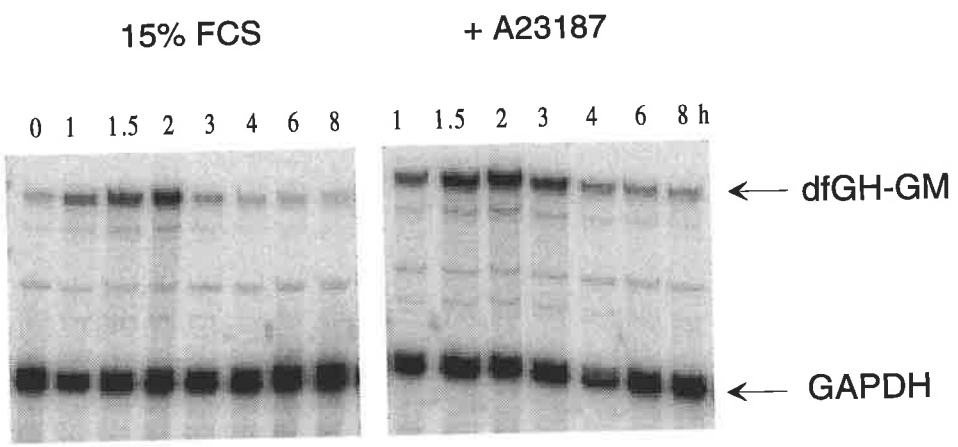
15% FCS
+ A23187
0 1 1.5 2 3 4 6 8
1 1.5 2 3 4 6 8 h
dfGH-GM
GAPDH

B

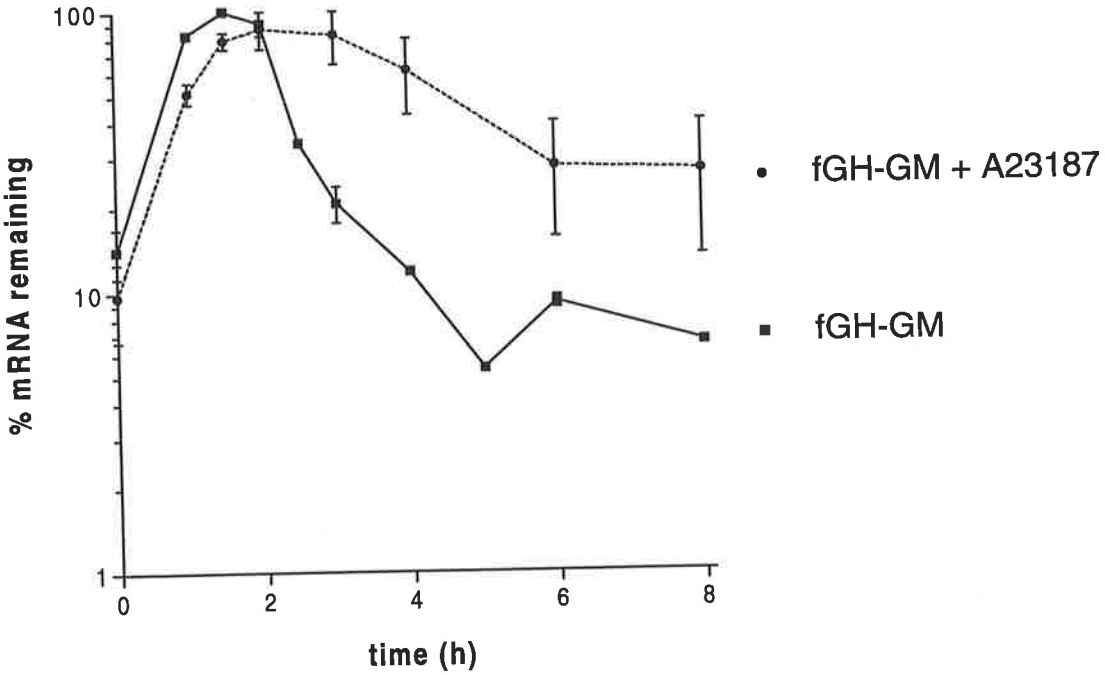
100
10
1
% mRNA remaining
0
2
4
6
8
time (h)
fGH-GM + A23187
fGH-GM

Figure 4.3.3 Stability of fGH-7,2 mRNA in NIH3T3 cells stimulated with 15% FCS in the presence or absence of calcium ionophore (A231387)

NIH3T3 fibroblasts ($1x10^6$ cells) stably expressing the fGH-7,2 transcript were stimulated with 15% FCS in the presence or absence of A23187 to a final concentration of 2μM and RNA was isolated at times indicated (see Materials and Methods section). 20μg of total RNA (see sections 2.8.15, 2.8.17 and 2.8.18) was then hybridised with *in vitro* synthesised complimentary RNA probes.

The fGH-7,2 mRNA was detected by RNase protection assay using a probe complimentary to a 338bp internal fragment of the growth hormone region of the fGH-7,2 mRNA, synthesised from *Pvu*II digested pG-5'hGH plasmid (see Table I: Appendix) using SP6 RNA polymerase and 400Ci/mmol [α^{32}P]-UTP.

The GAPDH mRNA was detected by using a probe complimentary to a 120bp internal fragment of the mouse GAPDH mRNA, synthesised from *Dde*I-digested plasmid pGAPM (see Table I: Appendix) using T7 RNA polymerase and 100Ci/mmol [α^{32}P]-UTP. Abundance of mRNA was determined by RNase protection assay.

Panel A) Phosphorimage of RNase protection gel

Panel B) Phosphorimager quantitation of fGH-7,2 mRNA levels relative to GAPDH mRNA from NIH3T3 cells stimulated with 15% FCS in the presence (▲) or absence (■) of 2μM A23187. Data are plotted as the mean ± SEM from 3 experiments.

A

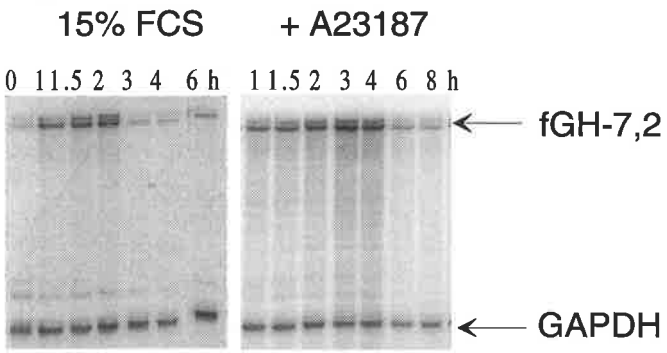
15% FCS
+ A23187
0 1 1.5 2 3 4 6 h
1 1.5 2 3 4 6 8 h
fGH-7,2
GAPDH

B

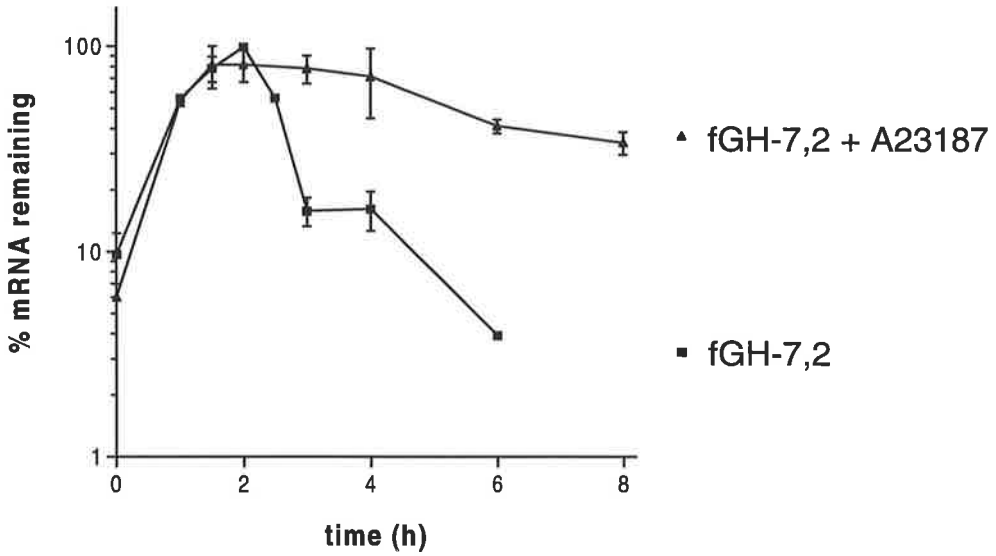
% mRNA remaining
100
10
1
0
2
4
6
8
time (h)
fGH-7,2 + A23187
fGH-7,2

Although these experiments show that reiterated AUIEs confer responsiveness to calcium ionophore it is interesting to note that mRNAs from chimeric genes containing the AU-rich region of GM-CSF (dfGH-GM) or repeated AUIEs (fGH-7,2) were stabilised to a greater degree than mRNA from the gene containing the complete 3'UTR (dfGH-GM3C). I observed that there was little discernable degradation of the fGH-GM mRNA over 4 hrs compared with the mRNA for dfGH-GM3C whose levels were reduced to approximately 40% of maximal levels by this time (compare Figs 4.3.2 and 4.3.1). This suggests that the AUIE may be sufficient for responsiveness to A23187 but elements elsewhere in the 3'UTR may partially inhibit or mask this responsiveness in dfGH-GM3C.

4.3.2 The 3'UTR of Human GM-CSF Does Not Confer Responsiveness to TNFα or PMA in NIH3T3 mouse Fibroblasts.

Although the signalling pathways activated by TNF are not fully elucidated, it seemed reasonable to propose that since the AU elements alone confer responsiveness to calcium ionophore, they may also be sufficient for regulation of stability by TNF. The elements required for response to PMA had also not been defined and again it seemed reasonable to investigate the role of the AUIE in this process. I therefore carried out experiments using chimeric genes containing the AU-rich region of GM-CSF (dfGH-GM) or repeated AUIEs (fGH-7,2). When NIH3T3 cells stably transfected with these chimeric genes were stimulated with 15% FCS in the presence or absence of TNFα (50 ng/ml) or PMA (200ng/ml), however, there was no difference in the decay of fGH-7,2 and dfGH-GM mRNAs in cells which had been treated with either of these stimuli compared with the decay of the mRNAs in cells which had been stimulated with 15% FCS alone (Figs 4.3.4 and Fig 4.3.5).These results indicated that the AUIE or the AU-rich region of GM-CSF mRNA are not sufficient to confer responsiveness to these stimuli.

Since the AU-rich region did not contain elements responsive to TNFα or PMA I next examined the complete 3'UTR of GM-CSF (dfGH-GM3C) to investigate whether

Figure 4.3.4 Stability of fGH-7,2 mRNA in NIH3T3 cells stimulated with 15% FCS alone or in the presence of PMA or TNFα

NIH3T3 fibroblasts ($1x10^6$ cells) stably expressing the fGH-7,2 transcript were stimulated with 15% FCS in the presence or absence of PMA to a final concentration of 200ng/ml or TNFα to a final concentration of 50ng/ml and RNA was isolated at times indicated (see sections 2.8.15, 2.8.17 and 2.8.18). 20μg of total RNA was then hybridised with *in vitro* synthesised complimentary RNA probes.

The fGH-7,2 mRNA was detected by RNase protection assay using a probe complimentary to a 338bp internal fragment of the growth hormone region of the fGH-7,2 mRNA, synthesised from *Pvu*II digested pG-5'hGH plasmid (see Table I: Appendix) using SP6 RNA polymerase and 400Ci/mmol [α^{32}P]-UTP.

The GAPDH mRNA was detected by using a probe complimentary to a 120bp internal fragment of the mouse GAPDH mRNA, synthesised from *Dde*I-digested plasmid pGAPM (see Table I: Appendix) using T7 RNA polymerase and 100Ci/mmol [α^{32}P]-UTP. Abundance of mRNA was determined by RNase protection assay.

Panel A) Phosphorimage of RNase protection gel

Panel B) Phosphorimager quantitation of fGH-7,2 mRNA levels relative to GAPDH mRNA from NIH3T3 cells stimulated with 15% FCS in the absence (■) or presence of 200ng/ml PMA (◆)or 50ng/ml TNFα (●). Data are plotted as the mean +/- SEM from 2 experiments.

A

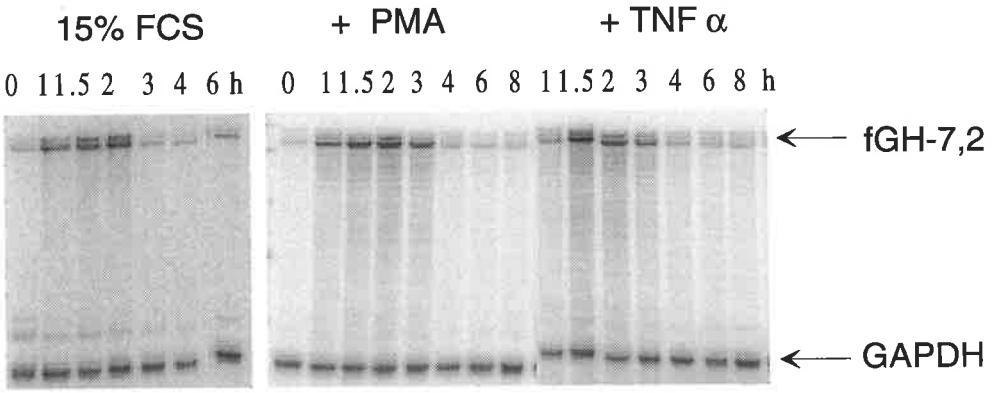
15% FCS
+ PMA
+ TNF α
0 1 1.5 2 3 4 6 h
0 1 1.5 2 3 4 6 8
1 1.5 2 3 4 6 8 h
fGH-7,2
GAPDH

B

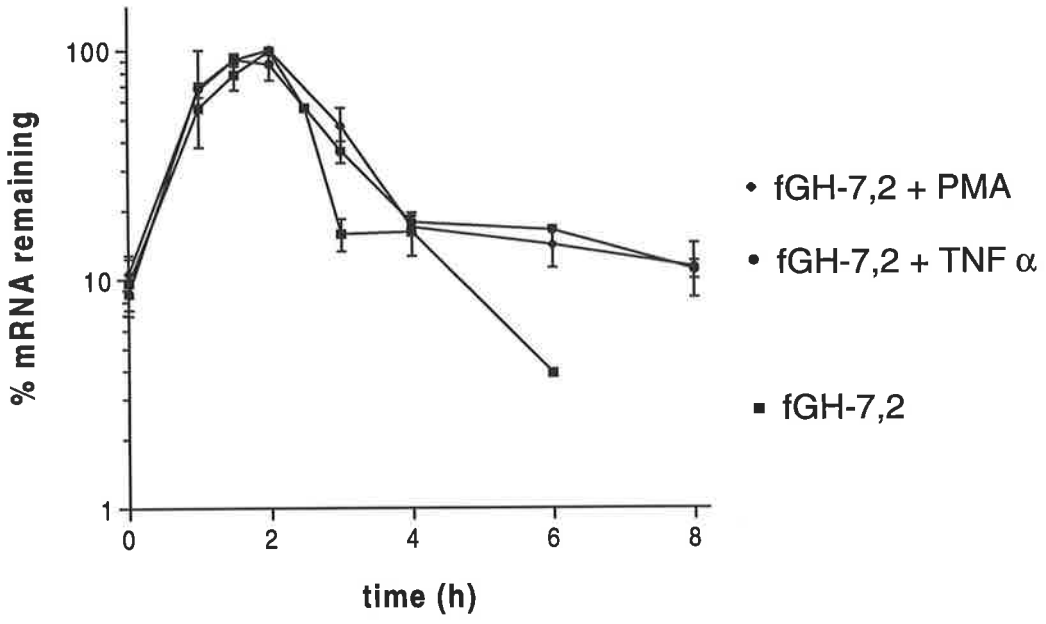
% mRNA remaining
100
10
1
0
2
4
6
8
time (h)
• fGH-7,2 + PMA
• fGH-7,2 + TNF α
▪ fGH-7,2

Figure 4.3.5 Stability of dfGH-GM mRNA in NIH3T3 cells stimulated with 15% FCS alone or in the presence of PMA or TNFα

NIH3T3 fibroblasts ($1x10^6$ cells) stably expressing the dfGH-GM transcript were stimulated with 15% FCS in the presence or absence of PMA to a final concentration of 200ng/ml or TNFα to a final concentration of 50ng/ml and RNA was isolated at times indicated (see sections 2.8.15, 2.8.17 and 2.8.18). 20μg of total RNA was then hybridised with *in vitro* synthesised complimentary RNA probes.

The dfGH-GM mRNA was detected by RNase protection assay using a probe complimentary to a 338bp internal fragment of the growth hormone region of the dfGH-GM mRNA, synthesised from *Pvu*II digested pG-5'hGH plasmid (see Table I: Appendix) using SP6 RNA polymerase and 400Ci/mmol [α^{32}P]-UTP.

The GAPDH mRNA was detected by using a probe complimentary to a 120bp internal fragment of the mouse GAPDH mRNA, synthesised from *Dde*I-digested plasmid pGAPM (see Table I: Appendix) using T7 RNA polymerase and 100Ci/mmol [α^{32}P]-UTP. Abundance of mRNA was determined by RNase protection assay.

Panel A) Phosphorimage of RNase protection gel

Panel B) Phosphorimager quantitation of dfGH-GM mRNA levels relative to GAPDH mRNA from NIH3T3 cells stimulated with 15% FCS in the absence (■) or presence of 200ng/ml PMA (●)or 50ng/ml TNFα (▼). Data are plotted as the mean +/- SEM from 3 experiments and 2 experiments for cells stimulated with 15% FCS alone or in the presence of PMA respectively and from a single representative experiment for cells stimulated in the presence of TNFα.

A

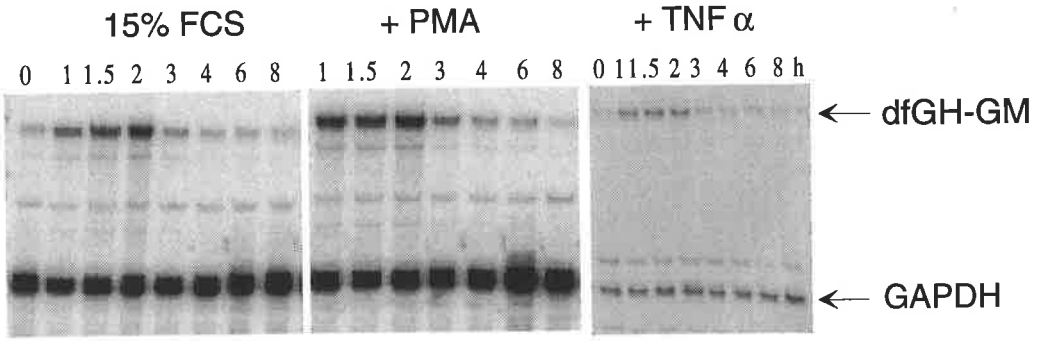
15% FCS
+ PMA
+ TNF α
0 1 1.5 2 3 4 6 8
1 1.5 2 3 4 6 8
0 1 1.5 2 3 4 6 8 h
dfGH-GM
GAPDH

B

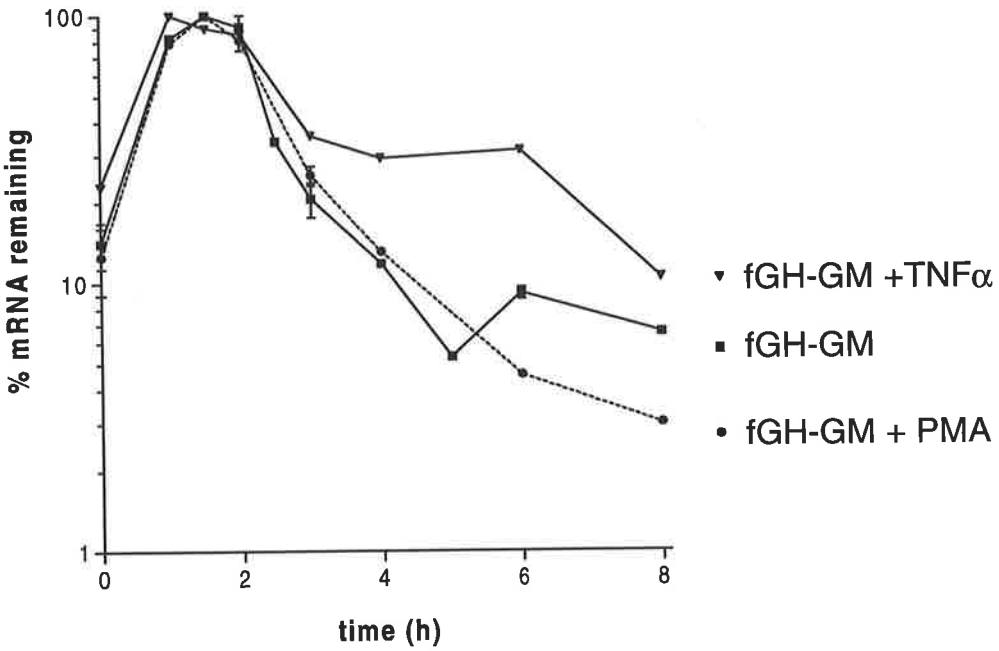
100
10
1
% mRNA remaining
0
2
4
6
8
time (h)
fGH-GM +TNFα
fGH-GM
fGH-GM + PMA

Figure 4.3.6 Stability of dfGH-GM3C mRNA in NIH3T3 cells stimulated with 15% FCS alone or in the presence of PMA or TNFα

NIH3T3 fibroblasts ($1x10^6$ cells) stably expressing the dfGH-GM3C transcript were stimulated with 15% FCS in the presence or absence of PMA to a final concentration of 200ng/ml or TNFα to a final concentration of 50ng/ml and RNA was isolated at times indicated (see sections 2.8.15, 2.8.17 and 2.8.18). 20μg of total RNA was then hybridised with *in vitro* synthesised complimentary RNA probes.

The dfGH-GM3C mRNA was detected by RNase protection assay using a probe complimentary to a 338bp internal fragment of the growth hormone region of the dfGH-GM3C mRNA, synthesised from *Pvu*II digested pG-5'hGH plasmid (see Table I: Appendix) using SP6 RNA polymerase and 400Ci/mmol [α^{32}P]UTP.

The GAPDH mRNA was detected by using a probe complimentary to a 120bp internal fragment of the mouse GAPDH mRNA, synthesised from *Dde*I-digested plasmid pGAPM (see Table I: Appendix) using T7 RNA polymerase and 100Ci/mmol [α^{32}P]-UTP. Abundance of mRNA was determined by RNase protection assay.

Panel A) Phosphorimage of RNase protection gel

Panel B) Phosphorimager quantitation of dfGH-GM3C mRNA levels relative to GAPDH mRNA from NIH3T3 cells stimulated with 15% FCS in the absence (■) or presence of 200ng/ml PMA (●) or 50ng/ml TNFα (▼). Data are plotted as the mean +/- SEM from 2 experiments for cells stimulated with 15% FCS alone or in the presence of PMA and from 1 representative experiment for cells stimulated with 15% FCS in the presence of TNFα.

A

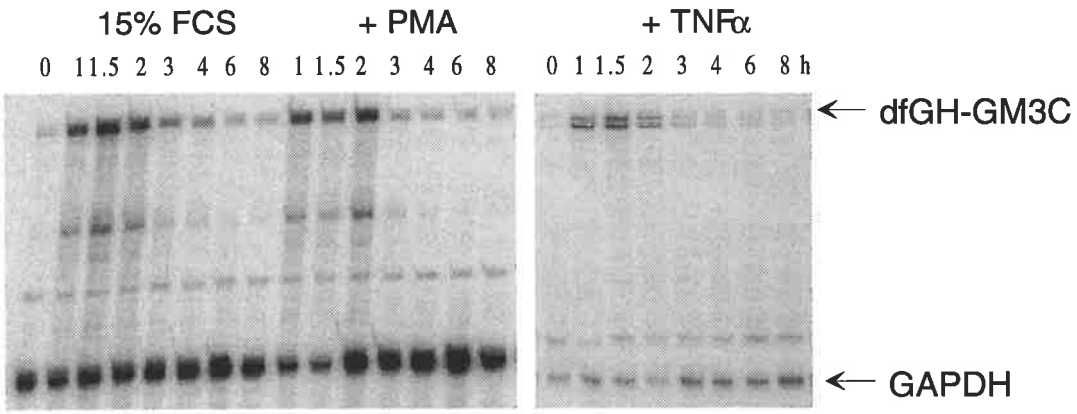
15% FCS
+ PMA
+ TNFα
0 1 1.5 2 3 4 6 8 1 1.5 2 3 4 6 8
0 1 1.5 2 3 4 6 8 h
dfGH-GM3C
GAPDH

B

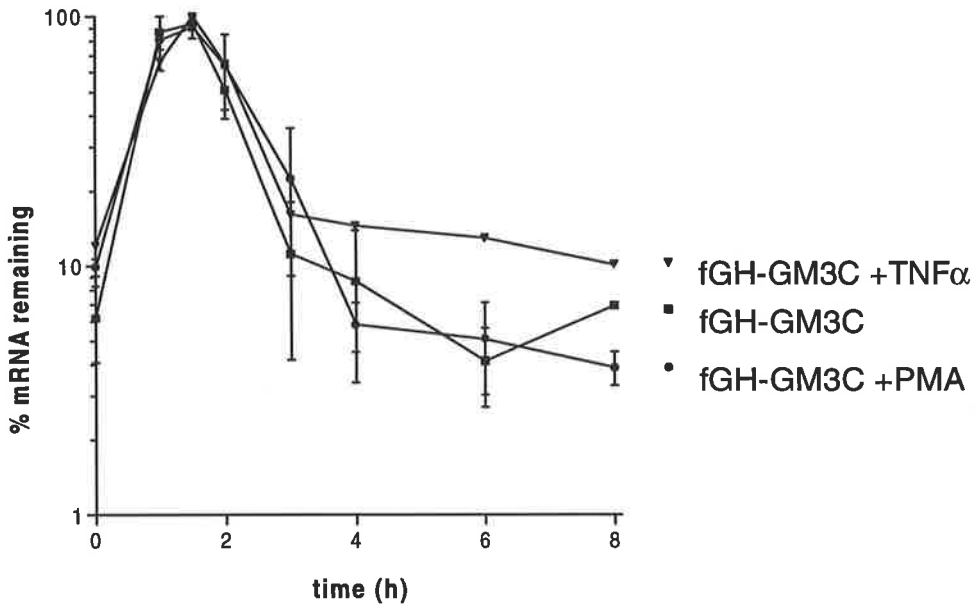
100
10
1
% mRNA remaining
0
2
4
6
8
time (h)
fGH-GM3C +TNFα
fGH-GM3C
fGH-GM3C +PMA

regulation resides within this region. The stability of dfGH-GM3C mRNA (containing the entire 3'UTR of GM-CSF) was not altered by treatment of cells with PMA or TNFα (Fig 4.3.6). These results indicate that neither the AUIEs nor the entire 3'UTR confer response to PMA or TNFα in NIH3T3 mouse fibroblasts.

4.3.3 Possible reasons for the absence of regulation by TNFα or PMA of mRNAs from chimeric genes in NIH3T3 fibroblasts

There may be several possible reasons why our chimeric genes do not respond to TNFα or PMA. It is possible that NIH3T3 fibroblasts, do not respond to PMA or TNFα because they do not express receptors for TNFα or have defective signalling pathways which prevent the transduction of signals from the cell surface to the effectors in the interior of the cell. It is also possible that the NIH3T3 cells neither produce produce GM-CSF (Iwai *et al.*, 1991) nor possess the machinery necessary for regulating GM-CSF production. If either of these possibilities were correct alternative cells would need to be used. Another possibility is that the human GM-CSF mRNA sequences transcribed from our chimeric gene are not be recognised by regulatory factors in mouse cells, in which case mouse sequences should be used instead of the human GM-CSF sequences. It is quite conceivable that regulatory regions do not reside within the 3'UTR, which would then require examination of other regions of the gene. These possibilities are addressed in the following experiments.

4.3.4 NIH3T3 fibroblasts are responsive to TNFα , PMA and IL-1β

To establish whether NIH3T3 cells are responsive to TNFα, IL-1β or PMA I measured the expression of endogenous c-*fos* and GM-CSF mRNAs. Cells were treated with TNFα , IL-1β, PMA or calcium ionophore and then RNA was collected after 30 mins to detect expression of fos mRNA (an early response gene which is only transiently expressed) and after 6 hr to detect expression of endogenous GM-CSF mRNA. RNA

Figure 4.3.7 Induction of endogenous GM-CSF and c-*fos* mRNAs in NIH3T3 cells stimulated with IL-1β, or TNFα, or PMA or A23187

NIH3T3 fibroblasts ($1x10^6$ cells) were stimulated with 15% FCS alone or in the presence of IL-1β to a final concentration of 100 U/ml, or TNFα to a final concentration of 50ng/ml or PMA to a final concentration of 200ng/ml or A23187 to a final concentration of 2μM and RNA was isolated after 30mins and 6 h and also after 6 h from cells that had not been serum starved and subsequently stimulated with 15% FCS. 20μg of total RNA was then hybridised with *in vitro* synthesised complimentary RNA probes (see sections 2.8.15, 2.8.17 and 2.8.18).

The endogenous GM-CSF mRNA was detected by RNase protection assay using a probe complimentary to a 160bp fragment of the mouse GM-CSF mRNA, synthesised from *Xmn*I digested pG-musGM plasmid (see Table I: Appendix) using T7 RNA polymerase and 400Ci/mmol [α^{32}P]-UTP.

Endogenous c-*fos* mRNA was detected using a probe complimentary to a 70bp fragment of the mouse c-*fos* mRNA, synthesised from *Stu*I digested pG-fos plasmid (see Table I: Appendix) using SP6 RNA polymerase and 400Ci/mmol [α^{32}P]-UTP.

The GAPDH mRNA was detected by using a probe complimentary to a 120bp internal fragment of the mouse GAPDH mRNA, synthesised from *Dde*I-digested plasmid pGAPM (see Table I: Appendix) using T7 RNA polymerase and 100Ci/mmol [α^{32}P]-UTP. Abundance of mRNA was determined by RNase protection assay.

Phosphorimage of RNase protection gel. With each treatment, the 2nd 6 h sample was isolated from cells which had not been serum starved or subsequently stimulated with 15% FCS.

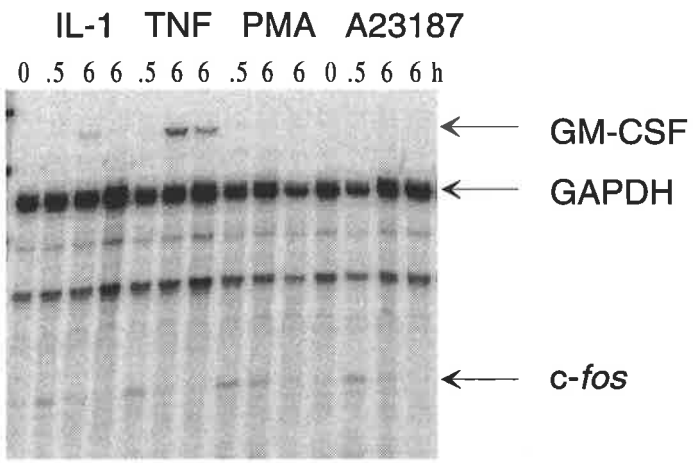
IL-1 TNF PMA A23187
0 .5 6 6 .5 6 6 .5 6 6 0 .5 6 6 h
GM-CSF
GAPDH
c-fos

Figure 4.3.8 Stability of endogenous GM-CSF mRNA in NIH3T3 cells stimulated with IL-1β or TNFα

NIH3T3 fibroblasts ($1x10^6$ cells) were stimulated with 15% FCS alone or in the presence of TNFα to a final concentration of 50ng/ml for 6 h. Actinomycin D (5 μg/ml) was then added to inhibit transcription and total RNA was isolated at the times indicated. 20μg of RNA was then hybridised with *in vitro* synthesised complimentary RNA probes (see sections 2.8.15, 2.8.17 and 2.8.18).

The endogenous GM-CSF mRNA was detected by RNase protection assay using a probe complimentary to a 160bp fragment of the mouse GM-CSF mRNA, synthesised from *Xmn*I digested pG-musGM plasmid (see Table I: Appendix) using T7 RNA polymerase and 400Ci/mmol [α^{32}P]-UTP.

The GAPDH mRNA was detected by using a probe complimentary to a 120bp internal fragment of the mouse GAPDH mRNA, synthesised from *Dde*I-digested plasmid pGAPM (see Table I: Appendix) using T7 RNA polymerase and 100Ci/mmol [α^{32}P]-UTP. Abundance of mRNA was determined by RNase protection assay.

Panel A) Phosphorimage of RNase protection gel.

Panel B) Phosphorimager quantitation of endogenous GM-CSF mRNA levels relative to GAPDH mRNA from NIH3T3 cells stimulated with 15% FCS in the presence of or 50ng/ml TNFα. Data are plotted from a single representative experiment.

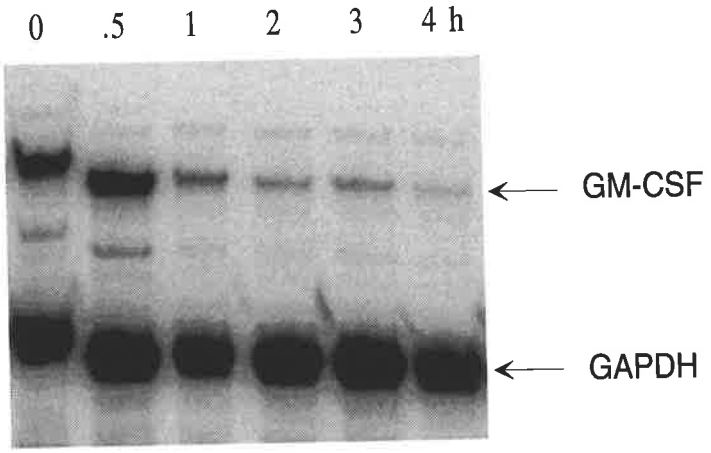
0
.5
1
2
3
4 h
GM-CSF
GAPDH

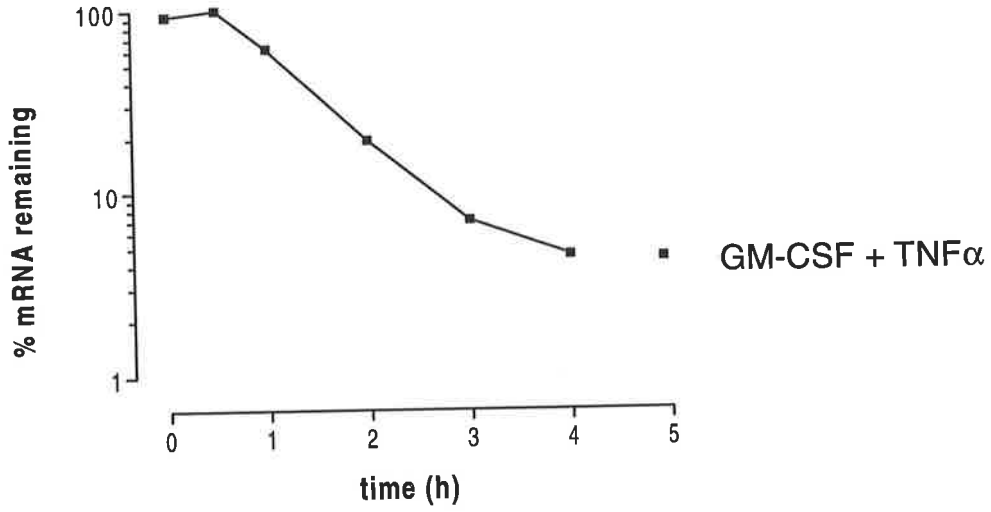
100
10
1
% mRNA remaining
0
1
2
3
4
5
time (h)
GM-CSF + TNFα

was also collected after 6hr from treated cells that had been serum starved to investigate whether serum starvation of cells actually alters their responsiveness to further stimulation. Endogenous c-*fos* was induced by all 3 agents within 30 minutes (Fig 4.3.7) indicating that NIH3T3 cells are responsive to these cellular activators. Endogenous GM-CSF mRNA accumulated in response to TNF-α (Fig 4.3.7) and a subsequent experiment showed that it had a half-life of approximately 1.25 h (Fig 4.3.8). Endogenous GM-CSF mRNA also accumulated in response to IL-1β treatment but did not accumulate in response to PMA or A23187. Interestingly, GM-CSF was induced to a greater extent in cells that had been serum starved and subsequently stimulated with 15% FCS in addition to the activating agent. These results show that NIH3T3 cells can respond to TNFα , IL-1β, PMA and A23187 and are capable of producing GM-CSF.

4.3.5 Overcoming a possible species problem and examination of other regions of the GM-CSF gene

My results show that although NIH3T3 cells are responsive to all of the cellular activators tried, regulation of mRNA stability using chimeric genes containing the 3'UTR of human GM-CSF was only achieved with A23187. This suggests that either other regions of the gene may be required for regulation by the other agents or alternatively that human sequences are not recognised by the mouse regulatory machinery. To address both of these issues new chimeric genes were constructed containing various regions of the mouse GM-CSF mRNA substituted into the fGH reporter gene.

All genes in this series (shown schematically in Figs 4.2.1, 4.2.2 and 4.2.3) contained the mouse GM-CSF 3'UTR since it is very likely this region, which contains the AU-destabilising elements, is necessary for stability regulation. In the dfGH-GM1 gene the 3'UTR alone was inserted (4.2.1). In the dfGH-GM2 gene the 5'UTR of mouse GM-CSF was also inserted (4.2.2) to examine whether this region was important for regulation. To investigate whether regulation of stability requires the coding region of the mouse GM-CSF cDNA, in the dfGM4 gene the human growth hormone coding region was replaced with the entire cDNA of mouse GM-CSF(Fig 4.2.3). These

Figure 4.3.9 Stability of dfGHGM-1, dfGHGM-2 and dfGM-4 mRNAs in NIH3T3 cells stimulated with 15% FCS

NIH3T3 fibroblasts ($1x10^6$ cells) stably expressing the dfGHGM-1, dfGHGM-2 or dfGM-4 transcripts were stimulated with 15% FCS and RNA was isolated at times indicated. 20µg of total RNA was used to detect the transcripts by RNase protection analysis using *in vitro* synthesised complimentary RNA probes (see sections 2.8.15, 2.8.17 and 2.8.18).

The dfGHGM-1 and dfGHGM-2 mRNAs were detected using a probe complimentary to a 338bp internal fragment of the growth hormone region of the dfGHGM-1 and dfGHGM-2 mRNAs, synthesised from *Pvu*II digested pG-5'hGH plasmid (see Table I: Appendix) using SP6 RNA polymerase and 400Ci/mmol [α^{32}P]-UTP.

The dfGM-4 mRNA was detected by RNase protection assay using a probe complimentary to a 410bp fragment of the dfGM-4 mRNA, synthesised from *Msp*I digested pdfGM-4 plasmid (see Table I: Appendix) using T7 RNA polymerase and 400Ci/mmol [α^{32}P]-UTP. dfGM-4 mRNA could be distinguished from endogenous GM-CSF mRNA since the region of endogenous GM-CSF mRNA complimentary to the dfGM-4 probe was only 310bp, 100bp smaller than the complimentary region of the dfGM-4 mRNA. The difference in size of the regions complimentary to dfGM-4 probe was generated during the construction of the dfGM-4 plasmid. Although the dfGM-4 plasmid contains the entire mouse GM-CSF cDNA, the plasmid was constructed in stages to retain a 5bp section of the growth hormone 3'UTR between the mouse GM-CSF coding region and the mouse GM-CSF 3'UTR (see Fig. 4.2.3). During the RNase A digestion step, endogenous GM-CSF mRNA hybridised to the probe will be clipped at this region which is non-complimentary to the probe.

The GAPDH mRNA was detected by using a probe complimentary to a 120bp internal fragment of the mouse GAPDH mRNA, synthesised from *Dde*I-digested plasmid pGAPM (see Table I: Appendix) using T7 RNA polymerase and 100Ci/mmol [α^{32}P]-UTP. Abundance of GAPDH mRNA was determined by RNase protection assay.

Panel A) Phosphorimage of RNase protection gel

Panel B) Phosphorimager quantitation of dfGHGM-1 (■), dfGHGM-2 (●) and dfGM-4 (▼) mRNA levels relative to GAPDH mRNA from NIH3T3 cells stimulated with 15% FCS. Data are plotted from a single representative experiment.

A

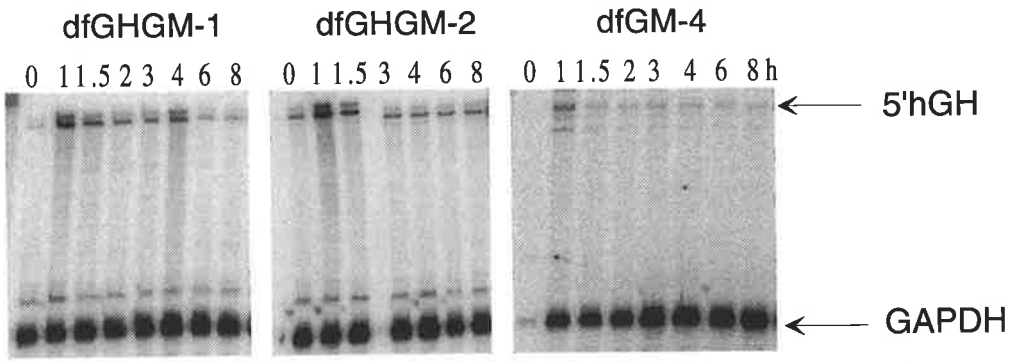
dfGHGM-1
dfGHGM-2
dfGM-4
0 1 1.5 2 3 4 6 8
0 1 1.5 3 4 6 8
0 1 1.5 2 3 4 6 8 h
5'hGH
GAPDH

B

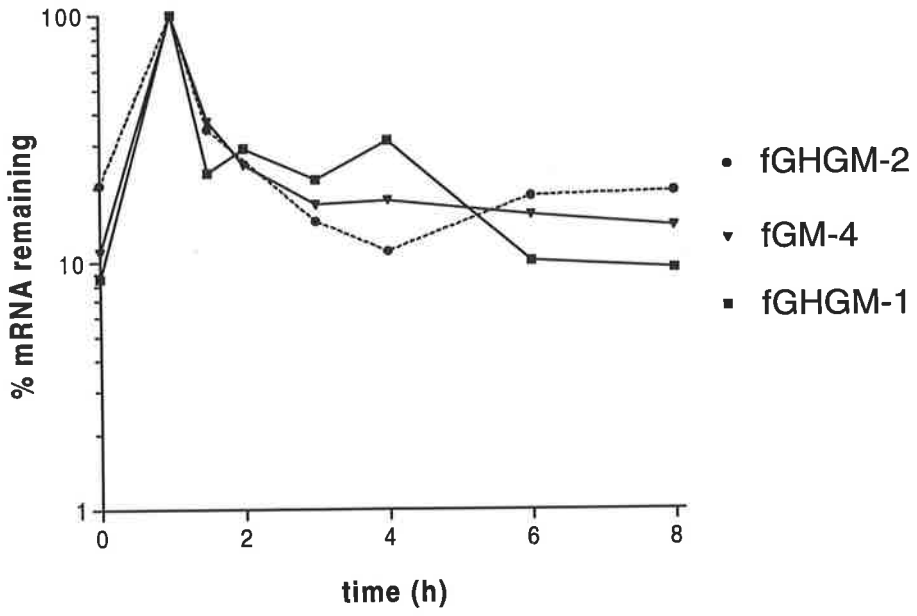
100
10
1
% mRNA remaining
0
2
4
6
8
time (h)
fGHGM-2
fGM-4
fGHGM-1

Figure 4.3.10 Stability of dfGHGM-1 mRNA in NIH3T3 cells stimulated with 15% FCS in the presence or absence of TNFα or IL-1β

NIH3T3 fibroblasts ($1x10^6$ cells) stably expressing the dfGHGM-1 transcripts were stimulated with 15% FCS alone, or in the presence of TNFα (50ng/ml) or IL-1-β (100 U/ml) and RNA was isolated at times indicated. 20μg of total RNA was used to detect the transcripts by RNase protection analysis using *in vitro* synthesised complimentary RNA probes (see sections 2.8.15, 2.8.17 and 2.8.18).

The dfGHGM-1 mRNA was detected using a probe complimentary to a 338bp internal fragment of the growth hormone region of the dfGHGM-1 mRNA, synthesised from *Pvu*II digested pG-5'hGH plasmid (see Table I: Appendix) using SP6 RNA polymerase and 400Ci/mmol [α^{32}P]-UTP.

The GAPDH mRNA was detected by using a probe complimentary to a 120nt internal fragment of the mouse GAPDH mRNA, synthesised from *Dde*I-digested plasmid pGAPM (see Table I: Appendix) using T7 RNA polymerase and 100Ci/mmol [α^{32}P]-UTP. Abundance of mRNA was determined by RNase protection assay.

Panel A) Phosphorimage of RNase protection gel

Panel B) Phosphorimager quantitation of dfGHGM-1 mRNA levels relative to GAPDH mRNA from NIH3T3 cells stimulated with 15% FCS alone (■), or in the presence of TNFα (50ng/ml) (●) or IL-1β (100 U/ml) (▼). Data are plotted from a single representative experiment.

A

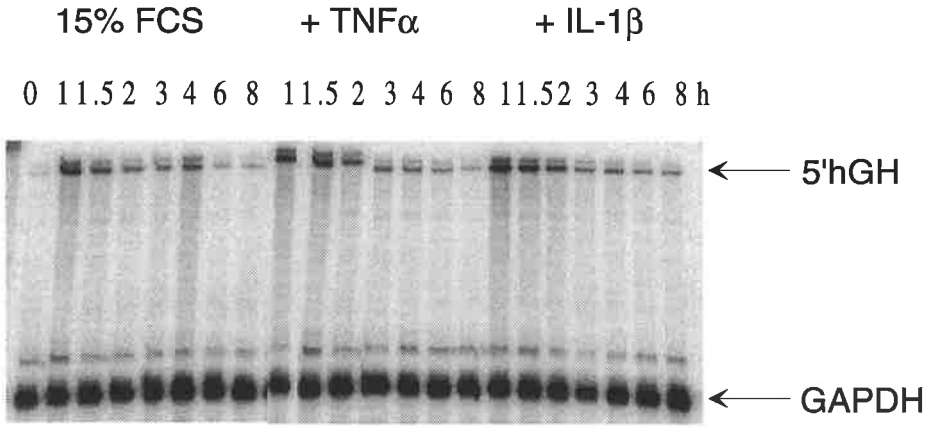
15% FCS
+ TNFα
+ IL-1β
0 1 1.5 2 3 4 6 8 1 1.5 2 3 4 6 8 1 1.5 2 3 4 6 8 h
5'hGH
GAPDH

B

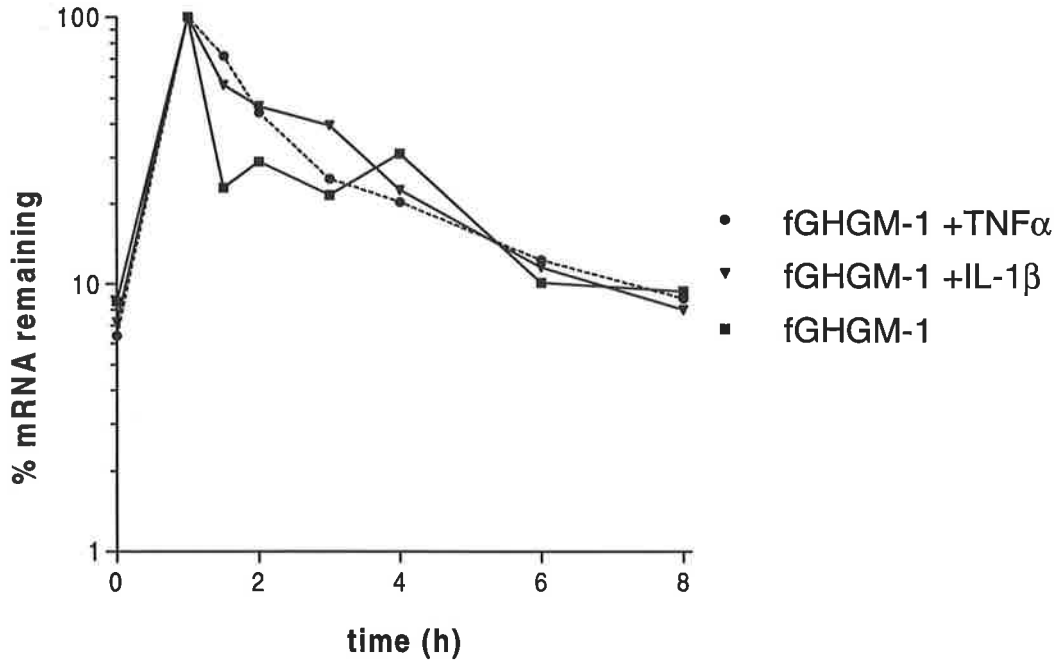
100
10
1
% mRNA remaining
0
2
4
6
8
time (h)
fGHGM-1 +TNFα
fGHGM-1 +IL-1β
fGHGM-1

constructs were stably transfected into NIH3T3 cells and as expected, produced unstable mRNAs in cells stimulated with serum alone (Fig 4.3.9).

4.3.6 The cDNA of murine GM-CSF does not confer response to TNFα or IL-1β.

Having established that the 3'UTR of mouse GM-CSF is able to destabilise the otherwise stable fGH plasmid I sought to determine whether this region accounts for the responsiveness of GM-CSF to TNFα and IL-1β. I found that treatment with TNFα or IL-1β did not stabilise mRNA from a chimeric gene containing the 3'UTR of murine GM-CSF [dfGHGM-1 (Fig 4.3.10)]. These results suggest that the 3'UTR was not sufficient for mediating response to TNFα or IL-1β.

I next examined whether inclusion of the GM-CSF 5'UTR along with the 3'UTR (dfGHGM-2) or the entire GM-CSF cDNA (dfGM-4), allowed stabilisation in response to IL-1β or TNFα. The dfGM-4 chimeric gene, containing the entire GM-CSF cDNA, would also reveal whether multiple components are required for regulation of mRNA stability. I not only found that the presence of the 5'UTR made no difference (Fig 4.3.11) but even the enitire GM-CSF cDNA did not allow responsiveness to TNFα or IL-1β (Fig 4.3.12). These results indicated that no regulation of mRNA stability was observed using a chimeric gene containing the mouse GM-CSF cDNA in NIH3T3 cells.

Figure 4.3.11 Stability of dfGHGM-2 mRNA in NIH3T3 cells stimulated with 15% FCS in the presence or absence of TNFα or IL-1β

NIH3T3 fibroblasts ($1x10^6$ cells) stably expressing the dfGHGM-2 transcripts were stimulated with 15% FCS alone, or in the presence of TNFα (50ng/ml) or IL-1-β (100 U/ml) and RNA was isolated at times indicated (see Materials and Methods section). 20μg of total RNA was used to detect the transcripts by RNase protection analysis using *in vitro* synthesised complimentary RNA probes (see sections 2.8.15, 2.8.17 and 2.8.18).

The dfGHGM-2 mRNA was detected using a probe complimentary to a 338bp internal fragment of the growth hormone region of the dfGHGM-2 mRNA, synthesised from *Pvu*II digested pG-5'hGH plasmid (see Table I: Appendix) using SP6 RNA polymerase and 400Ci/mmol [α^{32}P]-UTP.

The GAPDH mRNA was detected by using a probe complimentary to a 120bp internal fragment of the mouse GAPDH mRNA, synthesised from *Dde*I-digested plasmid pGAPM (see Table I: Appendix) using T7 RNA polymerase and 100Ci/mmol [α^{32}P]-UTP. Abundance of mRNA was determined by RNase protection assay.

Panel A) Phosphorimage of RNase protection gel

Panel B) Phosphorimager quantitation of dfGHGM-2 mRNA levels relative to GAPDH mRNA from NIH3T3 cells stimulated with 15% FCS alone (■), or in the presence of TNFα (50ng/ml) (●) or IL-1β (100 U/ml) (▼). Data are plotted from a single representative experiment.

A

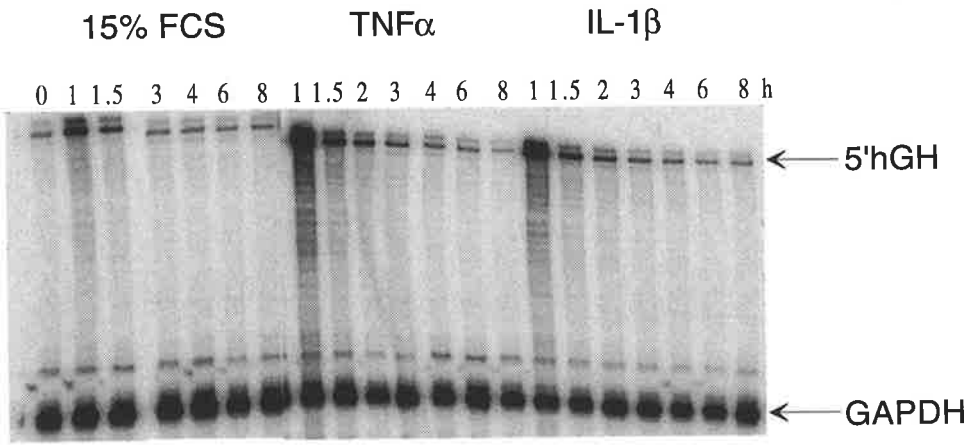
15% FCS
TNFα
IL-1β
0 1 1.5 3 4 6 8 1 1.5 2 3 4 6 8 1 1.5 2 3 4 6 8 h
5'hGH
GAPDH

B

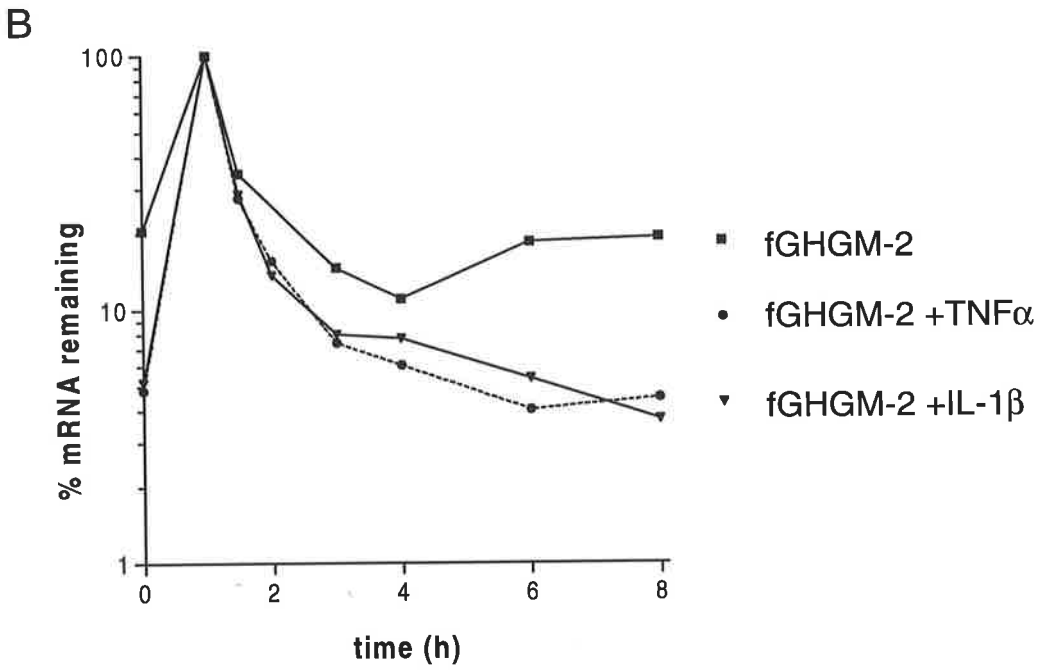
100
10
1
% mRNA remaining
0
2
4
6
8
time (h)
fGHGM-2
fGHGM-2 +TNFα
fGHGM-2 +IL-1β

Figure 4.3.12 Stability of dfGHGM-4 mRNA in NIH3T3 cells stimulated with 15% FCS in the presence or absence of TNFα or IL-1β

NIH3T3 fibroblasts ($1x10^6$ cells) stably expressing the dfGHGM-4 transcripts were stimulated with 15% FCS alone, or in the presence of TNFα (50ng/ml) or IL-1-β (100 U/ml) and RNA was isolated at times indicated. 20μg of total RNA was used to detect the transcripts by RNase protection analysis using *in vitro* synthesised complimentary RNA probes (see sections 2.8.15, 2.8.17 and 2.8.17).

The dfGM-4 mRNA was detected using a probe complimentary to a 410bp fragment of the dfGM-4 mRNA, synthesised from *Msp*I digested pdfGM-4 plasmid (see Table I: Appendix) using T7 RNA polymerase and 400Ci/mmol [α^{32}P]-UTP. dfGM-4 mRNA could be distinguished from endogenous GM-CSF mRNA since the region of endogenous GM-CSF mRNA complimentary to the dfGM-4 probe was only 310bp, 100bp smaller than the complimentary region of the dfGM-4 mRNA. The difference in size of the regions complimentary to dfGM-4 probe was generated during the construction of the dfGM-4 plasmid. Although the dfGM-4 plasmid contains the entire mouse GM-CSF cDNA, the plasmid was constructed in stages to retain a 5bp section of the growth hormone 3'UTR between the mouse GM-CSF coding region and the mouse GM-CSF 3'UTR (see Fig. 4.2.3). During the RNase A digestion step, endogenous GM-CSF mRNA hybridised to the probe will be clipped at this region which is non-complimentary to the probe.

The GAPDH mRNA was detected by using a probe complimentary to a 120bp internal fragment of the mouse GAPDH mRNA, synthesised from *Dde*I-digested plasmid pGAPM (see Table I: Appendix) using T7 RNA polymerase and 100Ci/mmol [α^{32}P]-UTP. Abundance of mRNA was determined by RNase protection assay.

Panel A) Phosphorimage of RNase protection gel

Panel B) Phosphorimager quantitation of dfGHGM-4 mRNA levels relative to GAPDH mRNA from NIH3T3 cells stimulated with 15% FCS alone (■), or in the presence of TNFα (50ng/ml) (●) or IL-1β (100 U/ml) (▼). Data are plotted from single samples.

A

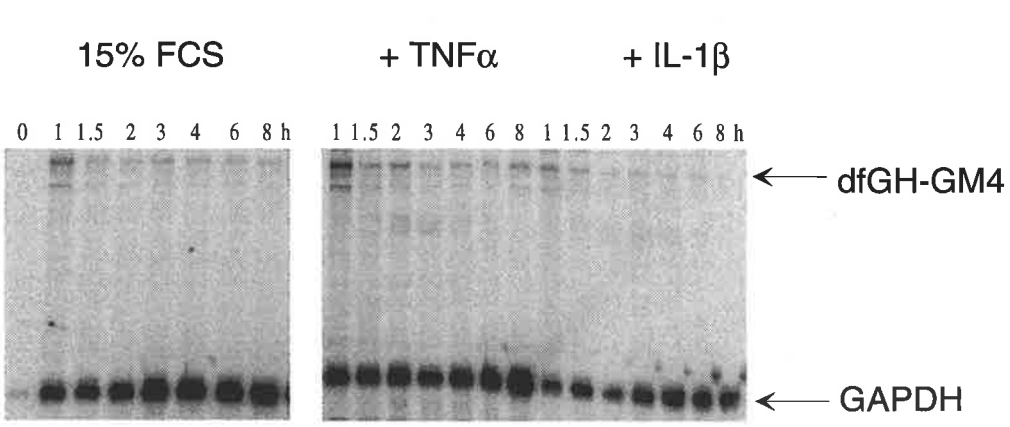
15% FCS
+ TNFα
+ IL-1β
0 1 1.5 2 3 4 6 8 h
1 1.5 2 3 4 6 8 1 1.5 2 3 4 6 8 h
dfGH-GM4
GAPDH

B

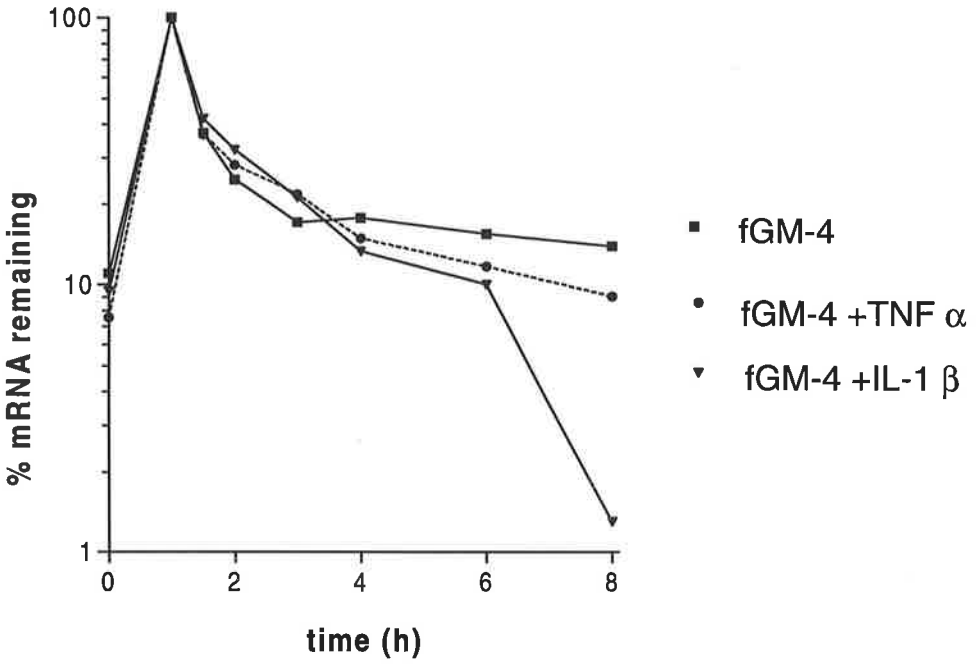
100
10
1
% mRNA remaining
0
2
4
6
8
time (h)
fGM-4
fGM-4 +TNF α
fGM-4 +IL-1 β

4.4 Discussion

Cellular activation by calcium ionophore mimics intracellular signal transduction pathways involving calcium fluxes, which play an important role in activation of various types of cell. I have shown that regulation of mRNA stability by A23187 is mediated by interaction with the AUIE although the exact mechanism is not yet known. Recently, Iwai *et al* (Iwai *et al.*, 1993) has also observed that the AU rich regions of mouse GM-CSF mRNA respond to A23187 in thymoma EL4 cells but with some contribution from sequences elsewhere in the 3'UTR. Interestingly, I observed that there was little discernable degradation of the dfGH-GM mRNA (containing the AU-rich region of GM-CSF) over 4 h compared with the mRNA for the gene containing the complete 3'UTR of GM-CSF (dfGH-GM3C) whose levels were reduced to approximately 40% by this time. This suggests that elements elsewhere in the 3'UTR may partially override or inhibit the stabilisation by calcium ionophore stimulation. This, however, is in contrast of the findings of Iwai *et al* (Iwai *et al.*, 1993) who observe that elements upstream of the AU-rich region actually enhance responsiveness to A23187. This apparent contradiction may reflect a system difference since different cells and GM-CSF species were studied by the two approaches. Iwai *et al* (Iwai *et al.*, 1993) do, however, observe that endogenous GM-CSF mRNA is stabilised to a much lesser extent than their chimeric gene containing the GM-CSF 3'UTR, which suggests that the difference in magnitude of stabilisation may arise from regulatory elements elsewhere in the gene.

Since the AU-rich sequences are an important determinant of mRNA instability and they are found in many mRNAs whose expression is regulated at the level of stability, it seemed likely that they would be involved in stabilisation of the mRNA. In support of this hypothesis I found that the AUIEs were sufficient for stabilisation in response to A23187 and therefore I speculated that the regulatory elements which mediate responsive to IL-1β, TNFα and PMA might also reside in the 3'UTR and could be the AUIEs. Surprisingly this did not appear to be the case. mRNA from genes containing the AU-rich region of human GM-CSF 3'UTR or synthetic AUIEs were not

sufficient to mediate response to PMA, consistent with the findings of Akashi *et al* (Akashi *et al.*, 1994) and Iwai *et al* (Iwai *et al.*, 1991) who found that a region in the 3'UTR 160 nucleotides upstream of the AUIE in murine GM-CSF was required for PMA-mediated responsiveness in thymoma EL-4 cells. In contrast, AU-motifs ligated to ICAM-1 coding region did confer responsiveness to PMA (Ohh *et al.*, 1994) although they were not sufficient for regulation by IFNγ. I found that the entire 3'UTR of murine or human GM-CSF still did not allow stabilisation in response to PMA, however, contrasting with the findings of Iwai *et al* (Iwai *et al.*, 1993). My results were consistent with similar findings of Yang and Yang (Yang and Yang, 1994) who likewise observed that the 3'UTR of IL-11 in a chimeric gene was insufficient to respond to IL-1 although the endogenous IL-11 mRNA was stabilised in primate bone marrow stromal cells stimulated with IL-1. Although TNFα induces GM-CSF mRNA by enhancing its stability (Koeffler *et al.*, 1988) it failed to stabilise mRNA from a chimeric gene bearing the 58bp region of the 3'UTR of GM-CSF wwhich contains 4 AUIEs (Akashi *et al.*, 1991), or in my experiments, the 3'UTR of murine or human GM-CSF mRNA. Since these experiments used both murine and human GM-CSF sequences this ruled out the possibility that the lack of responsiveness resulted from a failure of the regulatory machinery of these mouse cells to recognise the human GM-CSF sequences.

Little is known about the immediate postreceptor events that constitute early signals of IL-1 and TNF action although both activate mitogen-activated protein (MAP) kinase (Bird *et al.*, 1991; Vietor *et al.*, 1993; Bird *et al.*, 1994) and TNF is known to act independently of calcium flux (Yamato *et al.*, 1989). Protein kinase C (PKC) activation may account for part of the signalling events in IL-1 and TNF signal transduction (Gorospe *et al.*, 1993) although it may not be a predominant event (Mukaida *et al.*, 1987). PMA, a tumour promoter, also activates PKC although unlike IL-1 and TNF, PMA activates PKC directly and probably uses no other signalling pathways (Nishizuka, 1984). PMA possibly intercalates into the cell membrane and interacts with PKC at this location (Castagna *et al.*, 1982). In contrast, calcium ionophore directly enters the cell, changing intracellular calcium levels by releasing stored calcium which then initiates a cascade of signalling events including activation of protein kinase C (Nishizuka, 1984).

If some of these pathways are deficient in NIH3T3 cells the different signalling pathways these activators elaborate may account for the lack of regulation observed. At least some components of the signalling pathways must be intact since I found that endogenous GM-CSF and c-*fos* mRNAs were induced by IL-1β and TNFα, and c-*fos* was also induced by PMA and A23187. Induction of endogenous GM-CSF mRNA was not observed following treatment of cells with A23187 and PMA, possibly reflecting a requirement for a second activating event to initiate transcription of the cytokine. Nevertheless, these results show that NIH3T3 fibroblasts are innately responsive to several cellular activators and that GM-CSF mRNA can be induced in these cells, suggesting that NIH3T3 cells should be capable of regulating GM-CSF mRNA metabolism.

My initial results, and the findings of others investigating different cytokines (Yang and Yang, 1994) suggested that other regions of the gene confer response to TNF, IL-1 and PMA. However, experiments carried out to investigate this revealed that the mRNA from a chimeric gene containing the entire cDNA from murine GM-CSF also remained unstable in response to these agents. These results have led me to speculate on possible reasons for the lack of responsiveness by these mRNAs in NIH3T3 cells.

Although the cells may be responsive to a variety of cellular activators, some of the downstream effectors in the cell may be disrupted, which may affect production, or activation of proteins involved in regulating turnover of the mRNAs. This may not be unlikely given that NIH3T3 cells must have undergone several changes to allow culture of them for so long without senescence occuring. In an attempt to overcome possible problems with the NIH3T3 cells use of other cell lines for these experiments was investigated. I tried to establish stably transfected clones from several human fibroblast cell lines; human foreskin fibroblasts (HFF) and two strains of human embryonic lung fibroblasts, WI38 and HEL and also an endothelial cell line, C11. These proved difficult to establish, by electroporation and calcium phosphate precipitation transfection procedures. In transiently transiently transfected HEL fibroblasts I observed poor expression of plasmid mRNAs, but further studies could be pursued to optimise transient tranfection conditions in these cell lines since they might prove useful for these

studies. Unfortunately, time constraints have limited these investigations. I also felt that cellular processing of stably transfected plasmids, compared with transiently transfected plasmids, was more likely to be similar to that occuring naturally.

Although my chimeric gene contains the entire cDNA of GM-CSF there are c-*fos* 5'UTR sequences still present in the plasmid which may exert an inhibitory effect on stabilisation Another possible explanation for the lack of stabilisation of chimeric GM-CSF mRNAs may be that this chimeric gene has to be transfected into the NIH3T3 cells. The half-life of endogenous GM-CSF induced by TNFα was approximately 1.25 h which may be a fourfold increase in stability compared with an estimate of 20 mins in untreated cells (Akashi *et al.*, 1989). It cannot be assumed that a chimeric, transfected gene will be spliced, transported from the nucleus and modified in the same way as an endogenous gene and therefore that the regulation observed for endogenous GM-CSF mRNA will be reflected by similar regulation of a transfected chimeric gene. The full GM-CSF gene contains several introns and it is possible that regulatory elements might reside within these. Our chimeric gene contains no such introns and so this could explain why the stability of our mRNAs are not regulated. There are no examples, in cytokines, of introns containing regulatory information but it is always a possibility.

Another possibility is that the problems have arisen as a result of using the c-*fos* promoter for these experiments. The c-*fos* promoter is very powerful and may lead to overexpression of the transfected GM-CSF mRNA resulting in unregulated gene expression. Half-lives of mRNAs have been shown to increase when 20μg of test plasmid was used to transiently transfect NIH3T3 fibroblasts compared with using 5μg (Shyu *et al.*, 1989) suggesting that saturation of the degradation machinery may occur. I observe that mRNAs are not stabilised in response to various stimuli, but instead remain unstable. Although this explanation apparently contradicts the findings of Shyu *et al* who observe more stable mRNA when plasmids are overexpressed, it seems quite conceivable that stably transfected plasmids may be subject to different processing compared with transiently transfected plasmids resulting in different aberrations of regulation.

Cellular activation of many cell types leads to concomitant production of a number of different cytokines. Cytokines are involved at many levels in an immensely complex communication network leading to heterogeneous biological activities. Little information exists concerning the precise mechanisms by which regulation is achieved, as discussed in the introduction to this chapter, but it is likely that regulation may vary in mechanism between cytokines, between cell types and depending on the stimulus applied. I have attempted to address this question with a single cytokine, GM-CSF, in one cell type using several cellular activators. The conclusions I have reached indicate that even this has proven to be more complex than first imagined.

Chapter 5

A novel cytokine destabilising element with functional properties distinct from AU instability elements

5.1 Introduction

Several independent observations have led us, and others, to speculate that there may be regulatory elements in cytokine mRNAs in addition to the AUIEs. Findings in chapter 3 indicated that the stabilities of G-CSF and GM-CSF mRNAs may be regulated independently of IL-10 mRNA. The possibility that sequences in addition to the AUIEs participate in the regulation of cytokine mRNA stability is also suggested by the observations the AU sequences are not sufficient to confer responsiveness to PMA or IL-1 (Akashi *et al.*, 1994; Bagby *et al.*, 1990) respectively, and that in fact a region of the GM-CSF 3'UTR about 160 bases upstream of the AU-rich region is required for regulation by PMA (Iwai *et al.*, 1991). In the case of IL-11 mRNA, which also contains AUIEs in the 3'UTR, sequences outside the 3'UTR appear to be necessary for stabilisation in response to IL-1 (Yang and Yang, 1994).

In some mRNAs other mechanisms exist for regulating stability of the mRNA. Turnover of the transferrin receptor (Tfr) mRNA is tightly linked to intracellular iron levels. Upon iron deprivation, the iron regulatory protein (IRP) stabilizes Tfr mRNA by binding to stem-loop structures in the 3'UTR, whereas increased iron levels result in inactivation of the mRNA-binding protein and rapid degradation of Tfr mRNA.(Mullner and Kuhn, 1988; Casey *et al.*, 1989; Rouault *et al.*, 1988) Histone mRNAs are the only class of mammalian mRNAs that lack a poly(A) tail. Instead a highly conserved stem-loop structure is present which is necessary and sufficient for regulating the half-life of the histone mRNA (Pandey and Marzluff, 1987).

In some cases instability elements in addition to AUIEs participate in mediating the rapid decay of some mRNAs. The 3'UTR of urokinase-type plasminogen activator mRNA contains a stem loop instability determinant, located downstream of the poly-(A) consensus sequence, as well as AUIEs (Nanbu *et al.*, 1994), which contributes to the high turnover rate of this mRNA. Stability of ribonucleotide reductase R1 mRNA is likewise regulated by an element that does not contain AUIEs but is instead a 49 base domain located in 3'UTR (Chen *et al.*, 1993). Uridine-rich domains that cooperate with

the AUIEs occur in c-*myc* (Alberta *et al.*, 1994) and c-*fos* (Chen and Shyu, 1994), and c-*fos* also contains an instability determinant in its coding region (Shyu *et al.*, 1989). There is also a suggestion that IFN-γ contains non-AU instability determinants in its 3'UTR since deletion of the AU-rich region does not increase the half-life of this mRNA (Peppel *et al.*, 1991).

In cytokines, the AUIE has been intensely studied but, although inferred, little is known about the existence of any other instability or regulatory elements. In chapter 4, I referred to an early observation that mRNA from chimeric genes containing the 3'UTR of G-CSF appeared to be regulated quite differently from mRNAs from chimeric genes containing the 3'UTR of GM-CSF in NIH3T3 fibroblasts activated by calcium ionophore. I followed up these early puzzling observations and in this chapter I describe the identification and characterisation of stem-loop structures in the 3'UTR of G-CSF mRNA which act as a destabilising element , and further, which are regulated independently of the AUIE.

5.1.1 G-CSF

Like GM-CSF, G-CSF is a member of the family of haemopoietic growth factors which are essential for differentiation, proliferation, maturation and function of haemopoietic cells. G-CSF particularly stimulates maturation of neutrophilic granulocytes and also plays an important role in a variety of inflammatory responses. In unactivated cells G-CSF mRNA does not accumulate owing to its short half-life but upon activation by various cellular activators, including antigens, IL-1, TNF, phorbol-esters, lectins and calcium ionophores G-CSF mRNA accumulates in a variety of cell types.

5.2 Methods

5.2.1 Construction of plasmids containing the 3'UTRs of various cytokines

Oligonucleotides

#51/27U 5'GCTGGTACCTGAGCCAAGCCCTCCCCA

#52/28L 5'CGTGAGCTCGGAGGCAAACACTTTATTA

#60/28L 5'CGTGAGCTCTGTCTTTAAATATGAGGCT

#54/27U 5'GCTGGTACCTGATAATTAAGTGCTTCC

#55/26L 5'CGTGAGCTCAAATTTATTAAATAGTT

#56/27U 5'GCTGGTACCTAGCATGGGCACCTCAGA

#57/29L 5'CGTGAGCTCTTGGTATAAAAACCATTTAT

Plasmid dfGH-G. This plasmid was constructed by inserting the full 3'UTR of human G-CSF from bases 653-1508 into the *Kpn*I and *Sac*I sites of pfGH (see section 2.8.20A). The 3'UTR of human G-CSF was generated by PCR amplification (oligonucleotides 5'#51/27 and 3'#52/28) from a plasmid containing human G-CSF cDNA sequences. The plasmid containing the G-CSF cDNA sequences, pGEM-G, was prepared by a 2-step process (kindly prepared by Ms Cathy Lagnado). Firstly, a 1.8kb *Xho*I G-CSF cDNA fragment was inserted into the vector pXM (kindly prepared by Dr. F Shannon) and subsequently a 900 bp *Xho*I-*Pst*I fragment, between bases 604-1508 of G-CSF, from this vector was inserted between the *Sal*I and *Pst*I sites of pGEM-1 to create pGEM-G.

Plasmid dfGH-G70. This plasmid was constructed by inserting the sequence shown (in fig)into the *Kpn*I and *Sac*I sites of pfGH (see section 2.8.20A). The G70 sequence was generated by PCR amplification (oligonucleotides 5'#51/27 and 3'#60/28) from plasmid

pGEM-G containing human G-CSF cDNA sequences,. The construction of pGEM-G is described above.

Plasmid dfGH-IL-2. This plasmid was constructed by inserting the 3'UTR of IL-2, from bases 507-780, into the *Kpn*I and *Sac*I sites of pfGH (see section 2.8.20A). The 3'UTR of human IL-2 was generated by PCR ampification (oligonucleotides 5'#54/27 and 3'#55/27) from a plasmid containing the IL-2 cDNA. The plasmid containing the IL-2 cDNA, pGEM-IL2, was prepared (by Ms C Lagnado) by inserting a 520bp *BamH*I-*Xba*I fragment from plasmid pAT153-IL2 (kindly provided by Dr W.Fiers Laboratorium voor Moleculaire Biologie, Gent, Belgium) between *BamH*I and *Xba*I sites of pGEM-1.

Plasmid dfGH-IL6. This plasmid was constructed by inserting the 3'UTR of IL-6, from bases 700-1107, into the *Kpn*I and *Sac*I sites of pfGH (see section 2.8.20A). The 3'UTR of human IL-6 was generated by PCR amplification (oligonucleotides 5'#56/27 and 3'#57/29) from a plasmid containing IL-6 cDNA sequences, pGEM-IL6. pGEM-IL6 was prepared (by Dr G. Goodall) by inserting a 1,100bp *Sma*I-*BamH*I from plasmid pBSF2.3.8.1 (kindly provided by Dr.T. Hirano, Osaka University Medical School, Japan) which contains the entire IL-6 cDNA into pGEM-1 (Promega).

Plasmid pGAPM, containing a portion of the coding region of the human GAPDH cDNA, was prepared by inserting a 400bp *Sac*II-*Hind*III fragment of plasmid pHcGAP (ATCC 57090) between the *Hinc*II and *Hind*III sites of plasmid pGEM-1 (Promega Corporation Madison, WI.)

5.2.2 Construction of plasmids designed to investigate the stem-loop region of G-CSF 3'UTR

Oligonucleotides

#107/35U 5'GCTGAGCTCAAGCTTATAGGTAAATACCAAGTAT

#108/27L 5'CGTGAGCTCGGGGAACACTGCTGTTTA

#109/42U 5'GCTGAGCTCAAGCTTATAGGTAGATACCAAGTATCTATTACT

#110/42L 5'CGTGAGCTCGGGGAACACTGCTGTTTGAATATCAAACAGGGA

#111/41U 5'GCTGAGCTCAAGCTTATAGGTTTCGACCAAGTATTTATTAC

#112/49L 5'CGTGAGCTCGGGGAACACTGCTGTTTAAATATTCTTGAGGGA TTTCTTG

#132/63U 5'CATAGGTAGATACCAAGTATCTATTACTATCGATTCCCTGTTT GATATTCAAACAGCAGAGCT

#133/63L 5'CTGCTGTTTGAATATCAAACAGGGAATCGATAGTAATAGATAC TTGGTATCTACCTATGGTAC

#134/36U 5'GCTGGTACCATAGGTAGATACGCGGTATCTATTACT

#135/41L 5'CGTGAGCTCCTGCTGTTTGATGTTCAAACAGGGATTTCTTG

#143/46U 5'GCTGGTACCATAGGTTTCGACCAAGTCGAAATTACTATGA CTGCTC

#144/51L 5'GCTCAGCTCGGGGAACACTGCTCAAGGAATATCCTTGAGG GATTTCTTGTCTC

#145/39U 5'CATCGATAAATCCCTGTTTGATATTCAAACAGCAGAGCT

#146/39L 5'CTGCTGTTTGAATATCAAACAGGGATTTATCGATGGTAC

Plasmid dfGH-SL1. This plasmid was prepared by inserting a 183bp region of the human G-CSF 3'UTR between bases 850-1033 (SL-1) into the *Sac*I site of pfGH. This region was generated by PCR amplification from the plasmid dfGH-G (described in section 5.2.1 above) using PCR primers 5' #107/33 and 3'#108/27 (Fig 5.2.1). 5' and 3' *Sac*I sites were incorporated into these primers for sub-cloning. To screen for orientation

Fig. 5.2.1 Sequence and computer-modeled secondary structure of stem-loops fGH-SL1, fGH-SL2 and fGH-SL3

RNA sequence and computer-modelled secondary structure of a 183nt region of the G-CSF 3'UTR (850-1033nt) using the RNA folding programme of Zuker. The 2 predicted stem-loop structures (called stem-loop A and stem-loop B respectively) conserved between human and mouse are shown and the intervening (124nt) region indicated. Mutations are indicated by arrows with replacement bases shown. These constructs were inserted into the *Sac*I site of the fGH plasmid.

fGH-SL1 The 2 conserved stem-loop structures, A and B including 2 potential AUIEs.

fGH-SL2 The 2 conserved stem-loop structures, A and B have compensated point mutations to each of the AUIEs of each stem-loop, to abolish function of the AUIEs but to maintain the potential for stem-loop formation.

fGH-SL3 The conserved stem-loop structures, A and B have 4 uncompensated mutations to each stem, to disrupt stem-loop formation but leaving the potential AUIEs intact.

fGH-SL1

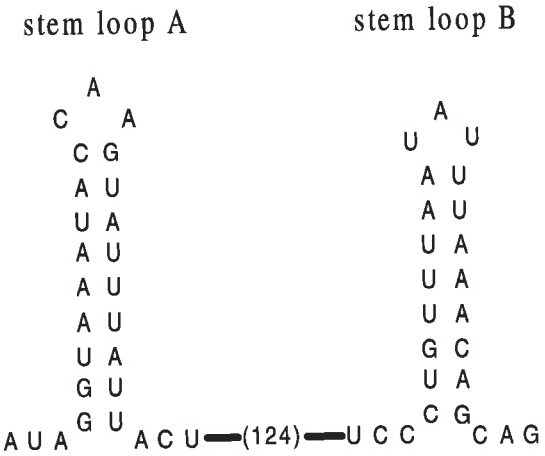

fGH-SL2

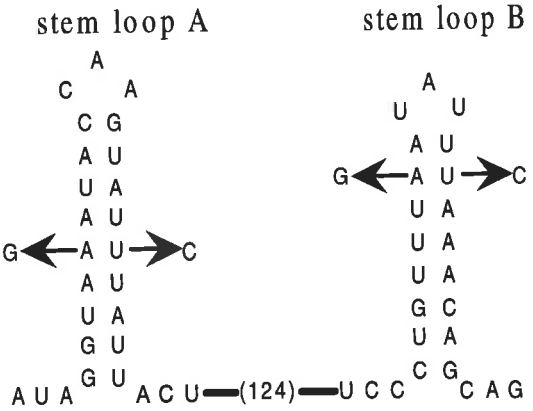

fGH-SL3

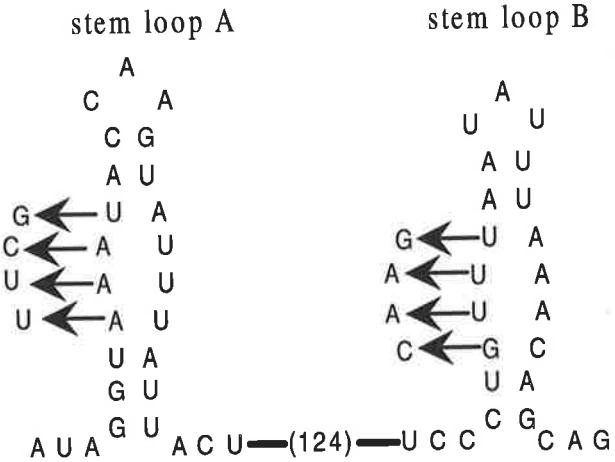

a Hind III site was included in the 5' PCR primer immediately 3' to the *Sac*I site. Thus, Hind III digests can distinguish between plasmids bearing inserts in either orientation.

Plasmid dfGH-SL2. This plasmid was prepared by inserting a 183bp region of the human G-CSF 3'UTR between bases 850-1033 introducing 4 point mutations into this region (SL-2) (Fig 5.2.1) into the *Sac*I site of pfGH. This region was generated by PCR amplification from the plasmid dfGH-G using PCR primers 5' #109/42 and 3' #110/42. As described for SL-1, above, as well as incorporation of 5' and 3' *Sac*I sites for sub-cloning, a Hind III site was included in the 5' PCR primer immediately 3' of the *Sac*I site to screen for orientation.

Plasmid dfGH-G70SL2. This plasmid was prepared by inserting the SL-2 G-CSF fragment, described above, into the *Sac*I site of plasmid dfGH-G70 (described in section 5.2.1).

Plasmid dfGH-SL3. This plasmid was prepared by inserting a 183bp region of the human G-CSF 3'UTR between bases 850-1033 introducing 8 mutations into this region (SL-3) (Fig 5.2.1) into the *Sac*I site of plasmid dfGH. This fragment was generated by PCR amplification from the plasmid dfGH-G using PCR primers 5' #111/44 and 3' #112/49. These PCR primers each introduce 4 mutations into the amplified product (Fig 5.2.1). As described for SL-1 and SL-2, above, as well as incorporation of 5' and 3' *Sac*I sites for sub-cloning a single Hind III site was included in the 5' PCR primer.

Plasmid dfGH-G70SL3. This plasmid was prepared by inserting the SL-3 G-CSF fragment, described above, into the *Sac*I site of dfGH-G70 (described in section 5.2.1 above).

Plasmid dfGH-SL4. This plasmid was prepared by inserting annealed, chemically synthesised oligonucleotides (#132/63 and #133/63) into the *Kpn*I and *Sac*I sites of plasmid dfGH-G. These oligonucleotides span a region of the human G-CSF 3'UTR

Fig. 5.2.2 Sequence and computer-modeled secondary structure of stem-loop fGH-SL5

RNA Sequence and computer-modelled secondary structure of a 183nt region of the G-CSF 3'UTR (850-1033nt) using the RNA folding programme of Zuker. The 2 predicted stem-loop structures (called stem-loop A and stem-loop B respectively) conserved between human and mouse are shown and the intervening (124nt) region indicated. Mutations are indicated by arrows with replacement bases shown. This construct was inserted into the *Sac*I and *Kpn*I site of the fGH plasmid.

fGH-SL5 The conserved stem-loop structures, A and B have compensated point mutations to each of the AUIEs of each stem-loop, to abolish function of the AUIEs but to maintain the potential for stem-loop formation. Additionally, each base of each loop has been changed to a sequence which maintains potential for stem-loop formation.

fGH-SL5

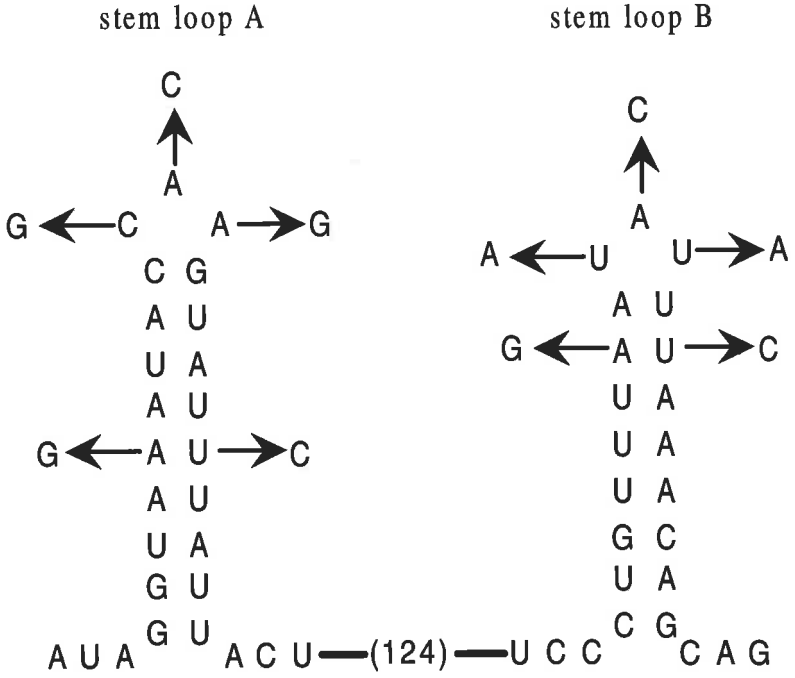
stem loop A
stem loop B
C
A
G C A G
C G
A U
U A
A U
G A U C
A U
U A
G U
G U
A U A
A C U
(124)
U C C
C A G
C
A
A U U A
A U
G A U C
U A
U A
U A
G C
U A
C G

between bases 850-1025 (Fig. 5.2.3), introducing 4 point mutations but deleting a region between bases 876-1000, creating a 63 base fragment. 5' *Kpn*I and 3' *Sac*I restriction sites were included in these oligonucleotides as was a *Cla*I site located in the middle of the oligonucleotide for subsequent screening purposes.

Plasmid dfGH-SL5. This plasmid was prepared by inserting a 183bp region of the human G-CSF 3'UTR between bases 850-1033 introducing 10 mutations into this region (SL-5) (Fig. 5.2.2) into the *Kpn*I and *Sac*I sites of plasmid dfGH. This SL-5 fragment was generated by PCR amplification from the plasmid dfGH-G using PCR primers 5' #134/36 and 3' #135/41 These PCR primers each introduce 5 mutations into the amplified product. 5' *Kpn*I and 3' *Sac* I restriction sites were incorporated for sub-cloning.

Plasmid dfGH-SL6. This plasmid was prepared by inserting a 183bp region of the human G-CSF 3'UTR between bases 850-1033, introducing 6 mutations into this region (SL-6) (Fig 5.2.3), into the *Sac*I site of plasmid dfGH. This SL-6 fragment was generated by PCR amplification from the plasmid dfGH-G (described in the section above) using PCR primers 5' #111/41 and 3' #110/42 as described above. The 5' PCR primer introduces 4 mutations and the 3'PCR primer introduces 2 mutations and each of these primers incorporate terminal *Sac*I sites for sub-cloning.

Plasmid dfGH-SL7. This plasmid was prepared by inserting a 183bp region of the human G-CSF 3'UTR between bases 850-1033, introducing 6 mutations into this region (SL-7) (Fig. 5.2.3), into the *Sac*I site of plasmid dfGH. This SL-7 fragment was generated by PCR amplification from the plasmid dfGH-G (described in the section above) using PCR primers 5' #109/42 and 3' #112/49 described above. The 5' PCR primer introduces 2 mutations and the 3'PCR primer introduces 4 mutations and each of these primers incorporate terminal *Sac*I sites for sub-cloning.

Fig. 5.2.3 Sequence and computer-modeled secondary structure of stem-loops fGH-SL4, fGH-SL6 and fGH-SL7

RNA Sequence and computer-modelled secondary structure of a 183nt region of the G-CSF 3'UTR (850-1033nt) using the RNA folding programme of Zuker. The 2 predicted stem-loop structures (called stem-loop A and stem-loop B respectively) conserved between human and mouse are shown and the intervening region indicated. Mutations are indicated by arrows with replacement bases shown. fGH-SL4 was inserted into *Sac*I and *Hind*III sites of the fGH plasmid,and fGH-SL6 and fGH-SL7 were inserted into the *Sac*I site of the fGH plasmid.

fGH-SL4 The 2 conserved stem-loop structures, A and B have compensated point mutations to each of the AUIEs of each stem-loop, to abolish function of the AUIEs but to maintain the potential for stem-loop formation. Additionally, the 124nt region between stem-loop A and stem-loop B has been replaced by a *Cla*I site.

fGH-SL6 Stem-loop A has 4 uncompensated mutations to the stem, to disrupt stem-loop formation but leaving the potential AUIE intact. Stem-loop B has compensated point mutations to the AUIE, to abolish function of the AUIE but to maintain the potential for stem-loop formation.

fGH-SL7 Stem-loop A has compensated point mutations to the AUIE, to abolish function of the AUIE but to maintain the potential for stem-loop formation. Stem-loop B has 4 uncompensated mutations to the stem, to disrupt stem-loop formation but leaving the potential AUIE intact.

fGH-SL4

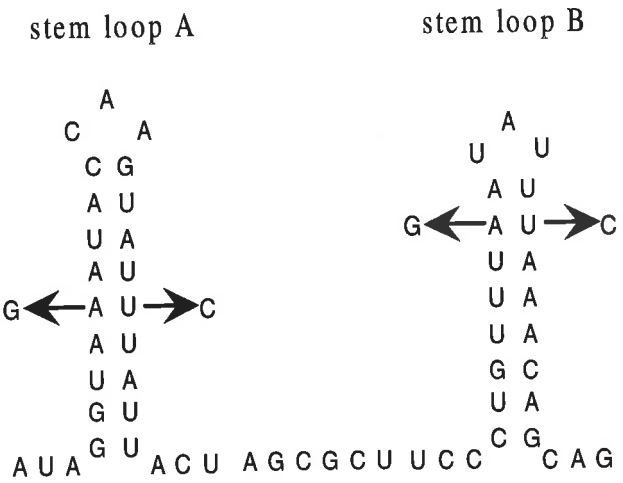

fGH-SL6

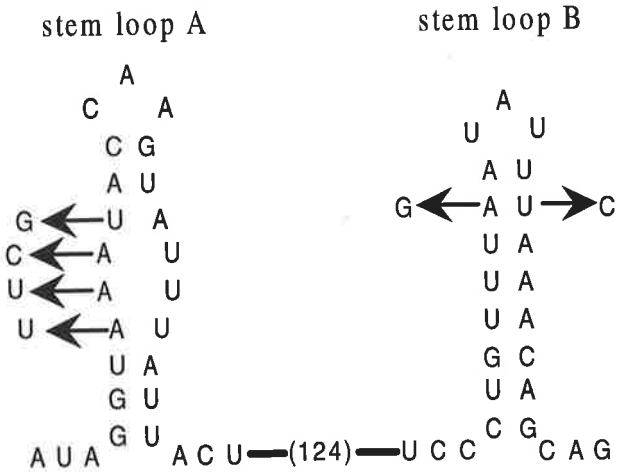

fGH-SL7

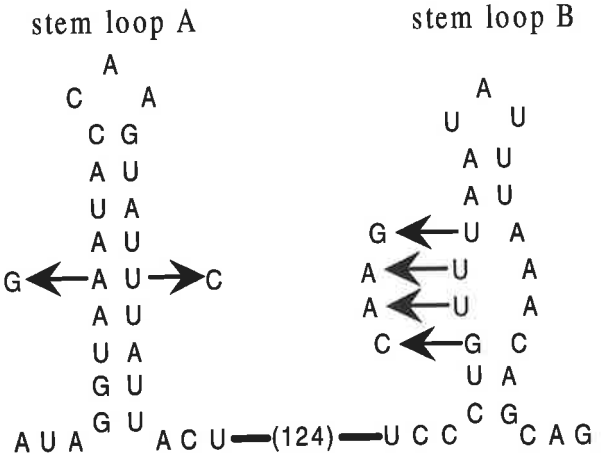

Plasmid dfGH-SL8. This plasmid was prepared by inserting a 183bp region of the human G-CSF 3'UTR between bases 850-1033, introducing 18 mutations into this region (SL-8) (Fig. 5.2.4) oligos and stem-loop structures), into the *Sac*I and *Kpn*I sites of plasmid dfGH. This SL-8 fragment was generated by PCR amplification from the plasmid dfGH-G (described in the section above) using PCR primers 5' #143/46 and 3' #144/51. The 5' PCR primer introduces 8 mutations and a 5' terminal *Kpn*I site and the 3'PCR primer introduces 10 mutations and a terminal *Sac*I site.

Plasmid dfGH-SL9. This plasmid was prepared by inserting chemically synthesised, annealed oligonucleotides (#145/39 and #146/39) into the *Kpn*I and *Sac*I sites of dfGH. This fragment (SL-9) spans a region of human G-CSF 3'UTR between bases 998-1026, and introduces 2 point mutations (Fig. 5.2.4). 5' *Kpn*I and 3' *Sac*I were incorporated for sub-cloning as was a *Cla*1 site immediately following the *Kpn*I site for subsequent screening purposes.

Fig. 5.2.4 Sequence and computer-modeled secondary structure of stem-loops fGH-SL8 and fGH-SL9

RNA Sequence and computer-modelled secondary structure of a 183nt region of the G-CSF 3'UTR (850-1033nt) using the RNA folding programme of Zuker. The 2 predicted stem-loop structures (called stem-loop A and stem-loop B respectively) conserved between human and mouse are shown and the intervening region indicated. Mutations are indicated by arrows with replacement bases shown. These fGH-SL8 and fGH-SL9 constructs were inserted into *Sac*I and *Hind*III sites of the fGH plasmid.

fGH-SL8 The 2 conserved stem-loop structures, A and B have mutations to each side of each stem to compensate for those of fGH-SL3 where stem structures had been disrupted. Each stem-loop has compensated point mutations to the AUIE, to abolish function of the AUIE.

fGH-SL9 The conserved stem-loop B alone is present and has compensated point mutations to the AUIE, to abolish function of the AUIE but to maintain the potential for stem-loop formation.

fGH-SL8

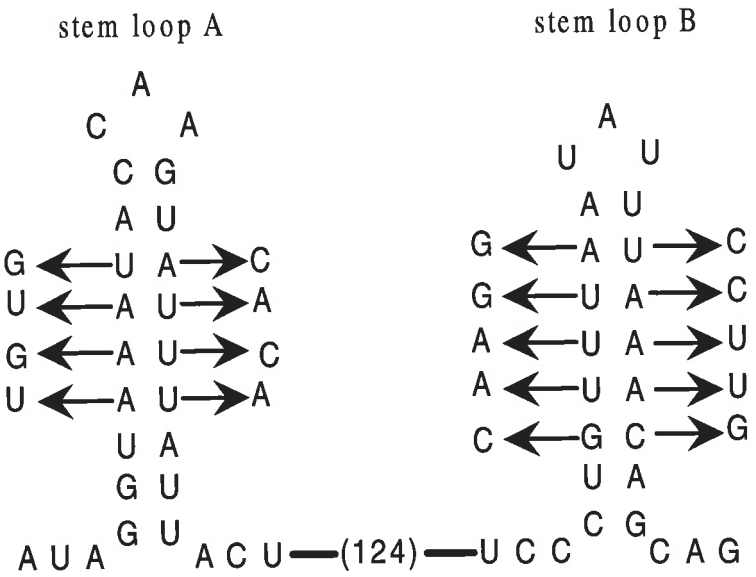

fGH-SL9

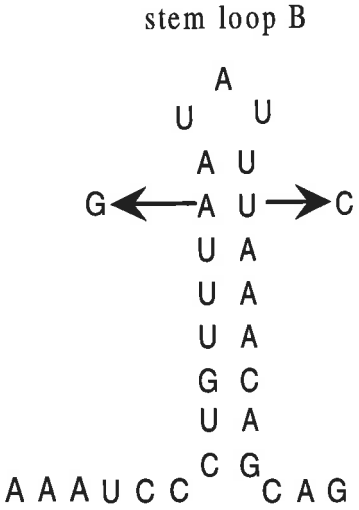

5.3 Results

5.3.1 Regulation of G-CSF mRNA stability by calcium ionophore

In the previous chapter I reported my search for sequence elements that confer regulation in response to IL-1β, TNFα, PMA and the calcium ionophore A23187. Initially, I used the G-CSF 3'UTR as a model for these studies and found that when the AU-rich region of G-CSF 3'UTR was inserted into the dfGH gene (dfGH-G70) the resulting mRNA was rapidly degraded (Fig. 5.3.1). This mRNA was stabilised several-fold upon treatment of these cells with the calcium ionophore A23187 (Fig 5.3.1). However, when I included the entire G-CSF 3'UTR the resulting dfGH-G mRNA was not only unstable in untreated NIH3T3 cells but also in NIH3T3 cells treated with calcium ionophore (Fig 5.3.2).

5.3.2 Regulation of G-CSF mRNA stability in 5637 human bladder carcinoma cells

5637 bladder carcinoma cells constitutively produce a number of cytokines owing to the contitutive stability of their mRNAs (Ross *et al.*, 1991). When 5637 cells were stably transfected, I found that AU-rich sequences (dfGH-G70) or repeated AUIEs (fGH7,2) were not functional in these cells since the mRNAs were very stable (Figs. 5.3.3 and 5.3.4 respectively) However, the mRNA for a chimeric gene containing the entire 3'UTR of G-CSF (dfGH-G) remained relatively unstable (Fig. 5.3.5). Since I had already shown that the AUIE does not function in the presence of calcium ionophore these combined results suggested that some other instability element was exerting itself.

5.3.3 Conserved stem-loop structures in the G-CSF 3'UTR

Since these results suggested that there might be some other element elsewhere in the 3'UTR of G-CSF mRNA that regulates stability of this mRNA, I decided to investigate further. Sequence alignments were carried out in an attempt to find some

Figure 5.3.1 Stability of dfGH-G70 mRNA in NIH3T3 cells stimulated with 15% FCS in the presence and absence of calcium ionophore (A231387)

NIH3T3 fibroblasts ($1x10^6$ cells) stably expressing the dfGH-G70 transcript were stimulated with 15% FCS in the presence or absence of A23187 to a final concentration of 2μM and RNA was isolated at times indicated. 20μg of total RNA was then hybridised with *in vitro* synthesised complimentary RNA probes (see sections 2.8.15, 2.8.17 and 2.8.18).

The dfGH-G70 mRNA was detected by RNase protection assay using a probe complimentary to a 338bp internal fragment of the growth hormone region of the dfGH-G70 mRNA, synthesised from *Pvu*II digested pG-5'hGH plasmid (see Table I: Appendix) using SP6 RNA polymerase and 400Ci/mmol [α^{32}P]-UTP.

The GAPDH mRNA was detected by using a probe complimentary to a 120bp internal fragment of the mouse GAPDH mRNA, synthesised from *Dde*I-digested plasmid pGAPM (see Table I: Appendix) using T7 RNA polymerase and 100Ci/mmol [α^{32}P]-UTP.

Panel A) Phosphorimage of RNase protection gel

Panel B) Phosphorimager quantitation of dfGH-G70 mRNA levels relative to GAPDH mRNA from NIH3T3 cells stimulated with 15% FCS alone (■) or in the presence of 2μM A23187 (▲). Data plotted are the mean ± SEM from 2 experiments.

A

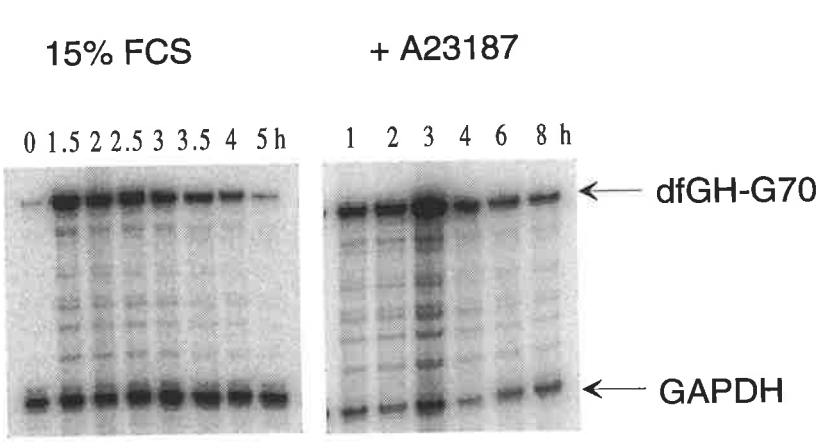
15% FCS
+ A23187
0 1.5 2 2.5 3 3.5 4 5 h
1 2 3 4 6 8 h
dfGH-G70
GAPDH

B

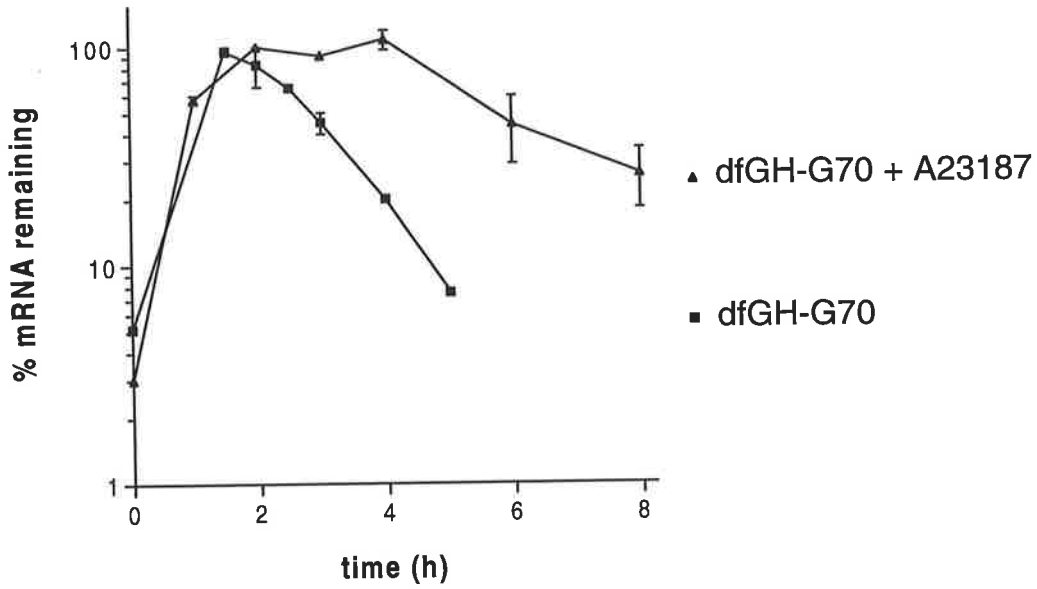
% mRNA remaining
100
10
1
0
2
4
6
8
time (h)
dfGH-G70 + A23187
dfGH-G70

Figure 5.3.2 Stability of dfGH-G mRNA in NIH3T3 cells stimulated with 15% FCS in the presence and absence of calcium ionophore (A231387)

NIH3T3 fibroblasts ($1x10^6$ cells) stably expressing the dfGH-G transcript were stimulated with 15% FCS in the presence or absence of A23187 to a final concentration of 2μM and RNA was isolated at times indicated. 20μg of total RNA was then hybridised with *in vitro* synthesised complimentary RNA probes (see sections 2.8.15, 2.8.17 and 2.8.18).

The dfGH-G mRNA was detected by RNase protection assay using a probe complimentary to a 338bp internal fragment of the growth hormone region of the dfGH-G mRNA, synthesised from *Pvu*II digested pG-5'hGH plasmid (see Table I: Appendix) using SP6 RNA polymerase and 400Ci/mmol [α^{32}P]-UTP.

The GAPDH mRNA was detected by RNase protection assay using a probe complimentary to a 120bp internal fragment of the mouse GAPDH mRNA, synthesised from *Dde*I-digested plasmid pGAPM (see Table I: Appendix) using T7 RNA polymerase and 100Ci/mmol [α^{32}P]-UTP.

Panel A) Phosphorimage of RNase protection gel

Panel B) Phosphorimager quantitation of dfGH-G mRNA levels relative to GAPDH mRNA from NIH3T3 cells stimulated with 15% FCS alone (■) or in the presence of 2μM A23187 (▲). Individual points are the mean ± SEM of 3 experiments from cells stimulated with 15% FCS alone and from 2 experiments from cells stimulated with 15% FCS in the presence of A23187.

A

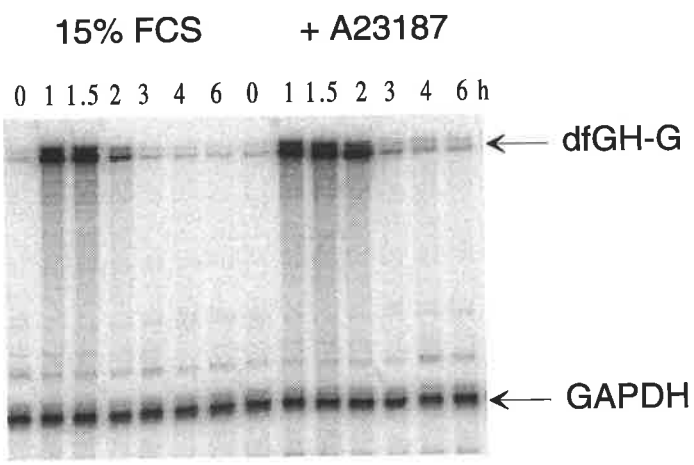
15% FCS
+ A23187
0 1 1.5 2 3 4 6 0 1 1.5 2 3 4 6 h
dfGH-G
GAPDH

B

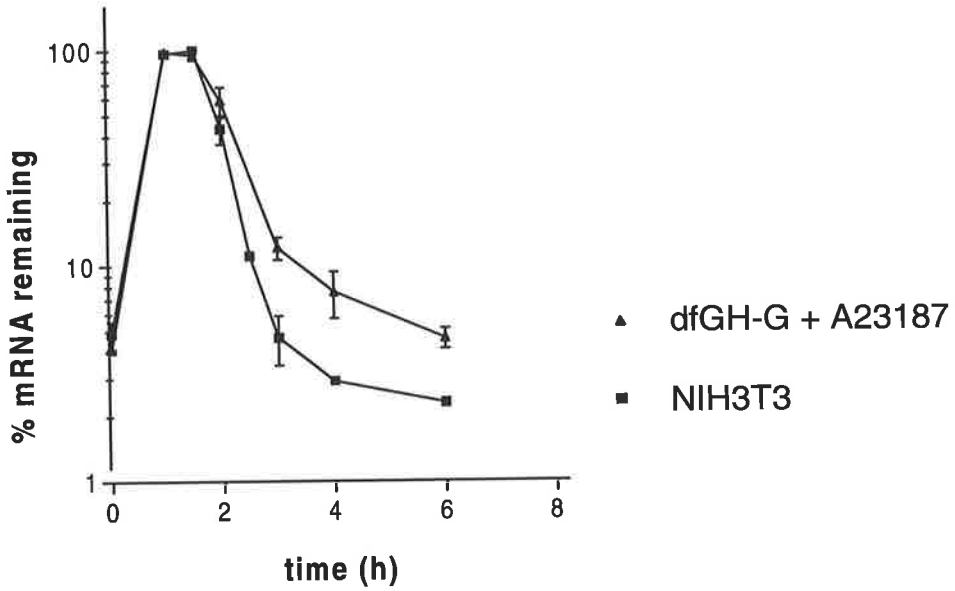
100
10
1
% mRNA remaining
0
2
4
6
8
time (h)
dfGH-G + A23187
NIH3T3

Figure 5.3.3 Stability of dfGH-G70 mRNA in 5637 bladder carcimoma cells compared with NIH3T3 cells

---

NIH3T3 fibroblasts ($1x10^6$ cells) and 5637 cells ($2x\ 10^6$ cells) stably expressing the dfGH-G70 transcript were stimulated with 15% FCS and RNA was isolated at times indicated. 20μg of total RNA was then hybridised with *in vitro* synthesised complimentary RNA probes and specific mRNAs detected by RNase protection assay (see sections 2.8.15, 2.8.17 and 2.8.18).

The dfGH-G70 mRNA was detected using a probe complimentary to a 225bp fragment of the dfGH-G70 mRNA, synthesised from *Pvu*II digested pdfGH-G70 plasmid (see Table I: Appendix) using SP6 RNA polymerase and 400Ci/mmol [α^{32}P]-UTP.

The GAPDH mRNA was detected by using a probe complimentary to a 120bp internal fragment of the mouse GAPDH mRNA, synthesised from *Dde*I-digested plasmid pGAPM (see Table I: Appendix) using T7 RNA polymerase and 100Ci/mmol [α^{32}P]-UTP. Abundance of mRNA was determined by RNase protection assay.

Panel A) Phosphorimage of RNase protection gels.

Panel B) Phosphorimager quantitation of dfGH-G70 mRNA levels relative to GAPDH mRNA from NIH3T3 cells (■) and 5637 cells (▲) stimulated with 15% FCS. Plotted data from NIH3T3 cells are the mean ± SEM from 3 experiments and from 5637 cells the mean ± SEM from 2 experiments.

A

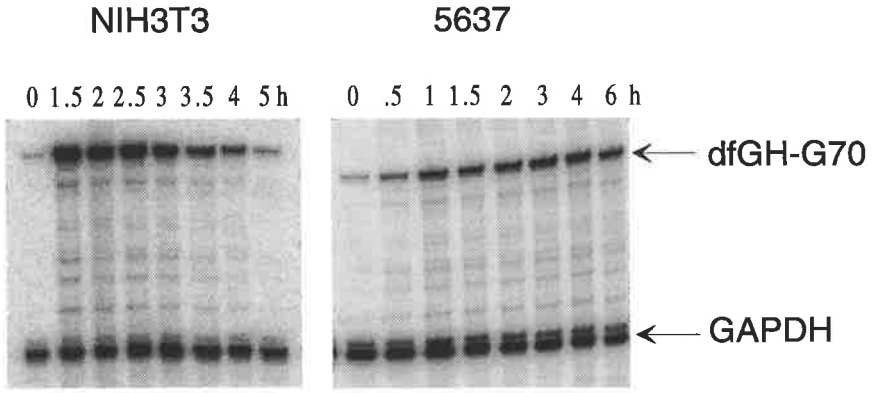
NIH3T3
5637
0 1.5 2 2.5 3 3.5 4 5 h
0 .5 1 1.5 2 3 4 6 h
dfGH-G70
GAPDH

B

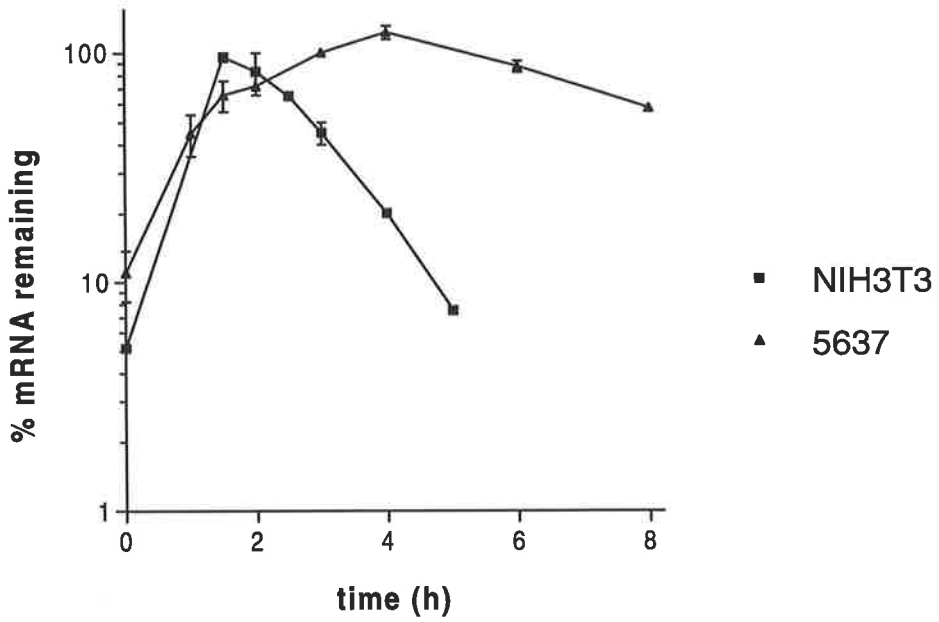
% mRNA remaining
100
10
1
0
2
4
6
8
time (h)
NIH3T3
5637

Figure 5.3.4 Stability of fGH-7,2 mRNA in 5637 bladder carcimoma cells compared with NIH3T3 cells

NIH3T3 fibroblasts ($1x10^6$ cells) and 5637 cells ($2x\ 10^6$ cells) stably expressing the fGH-7,2 transcript were stimulated with 15% FCS and RNA was isolated at times indicated. 20μg of total RNA was then hybridised with *in vitro* synthesised complimentary RNA probes and specific mRNAs detected by RNase protection assay (see sections 2.8.15, 2.8.17 and 2.8.18).

The fGH-7,2 mRNA was detected using a probe complimentary to a 190 bp fragment of the dfGH-7,2 mRNA, synthesised from *Pvu*II digested pfGH-7,2 plasmid (see Table I: Appendix) using SP6 RNA polymerase and 400Ci/mmol [α^{32}P]-UTP.

The GAPDH mRNA was detected by using a probe complimentary to a 120bp internal fragment of the mouse GAPDH mRNA, synthesised from *Dde*I-digested plasmid pGAPM (see Table I: Appendix) using T7 RNA polymerase and 100Ci/mmol [α^{32}P]-UTP.

Panel A) Phosphorimage of RNase protection gels.

Panel B) Phosphorimager quantitation of dfGH-7,2 mRNA levels relative to GAPDH mRNA from NIH3T3 cells (■) and 5637 cells (◆) stimulated with 15% FCS. Data are plotted from single representative experiments. Individual points are the mean ± SEM from 3 experiments.

A

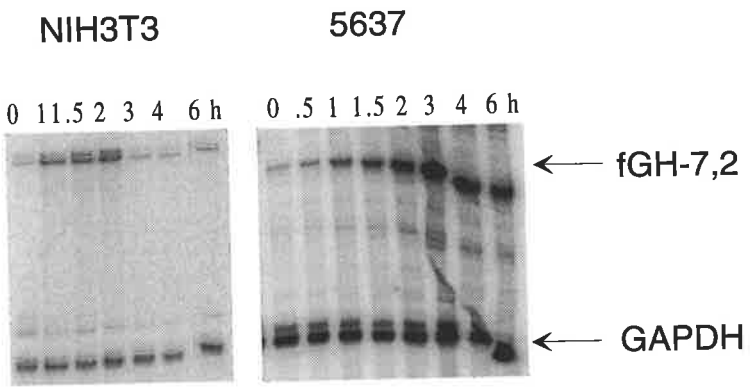
NIH3T3
5637
0 1 1.5 2 3 4 6 h
0 .5 1 1.5 2 3 4 6 h
fGH-7,2
GAPDH

B

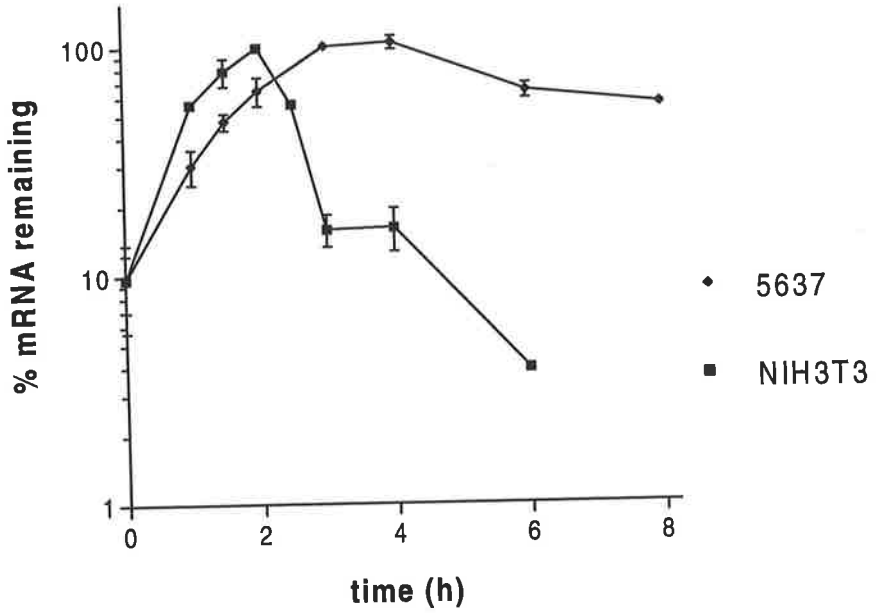
% mRNA remaining
100
10
1
0
2
4
6
8
time (h)
5637
NIH3T3

Figure 5.3.5 Stability of dfGH-G mRNA in 5637 bladder carcimoma cells compared with NIH3T3 cells

NIH3T3 fibroblasts ($1x10^6$ cells) and 5637 cells ($2x\ 10^6$ cells) stably expressing the dfGH-G transcript were stimulated with 15% FCS and RNA was isolated at times indicated. 20μg of total RNA was then hybridised with *in vitro* synthesised complimentary RNA probes and specific mRNA detected by RNase protection assay (see sections 2.8.15, 2.8.17 and 2.8.18).

The fGH-G mRNA was detected using a probe complimentary to a 338bp internal fragment of the growth hormone region of the dfGH-G mRNA, synthesised from *Pvu*II digested pG-5'hGH plasmid (see Table I: Appendix) using SP6 RNA polymerase and 400Ci/mmol [α^{32}P]-UTP.

The GAPDH mRNA was detected by using a probe complimentary to a 120bp internal fragment of the mouse GAPDH mRNA, synthesised from *Dde*I-digested plasmid pGAPM (see Table I: Appendix) using T7 RNA polymerase and 100Ci/mmol [α^{32}P]-UTP.

Panel A) Phosphorimage of RNase protection gels.

Panel B) Phosphorimager quantitation of dfGH-G mRNA levels relative to GAPDH mRNA from NIH3T3 cells (■) stimulated with 15% FCS. Data plotted are means ± SEM from 3 experiments.

Panel C) Phosphorimager quantitation of dfGH-G mRNA levels relative to GAPDH mRNA from 5637 cells (□) stimulated with 15% FCS. Data plotted are means ± SEM from 3 experiments.

A

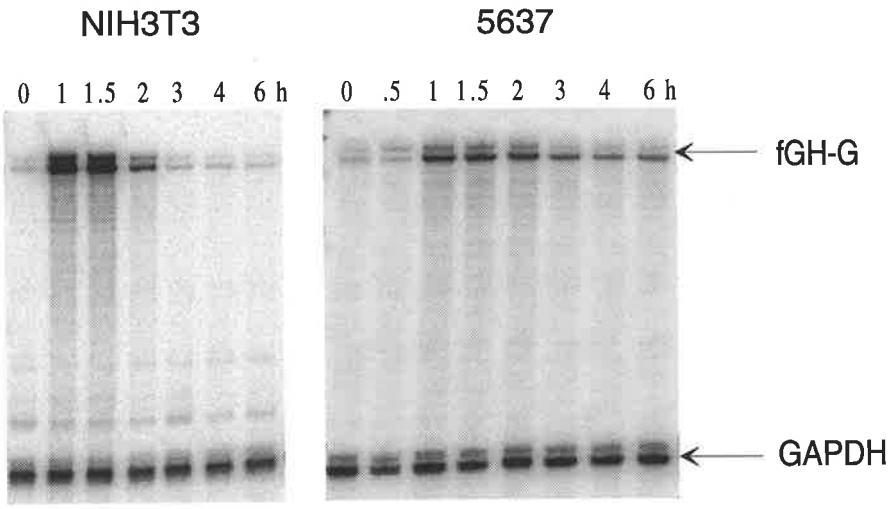
NIH3T3
5637
0 1 1.5 2 3 4 6 h
0 .5 1 1.5 2 3 4 6 h
fGH-G
GAPDH

B

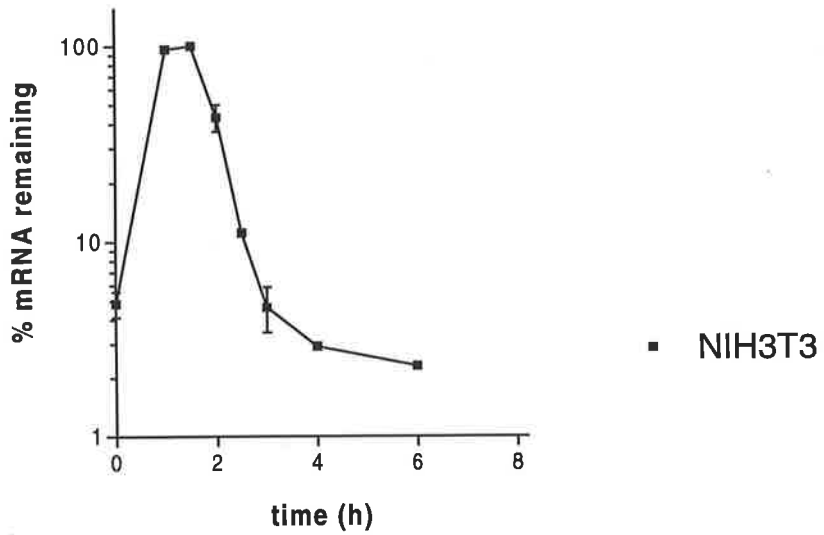
% mRNA remaining
100
10
1
0 2 4 6 8
time (h)
NIH3T3

C

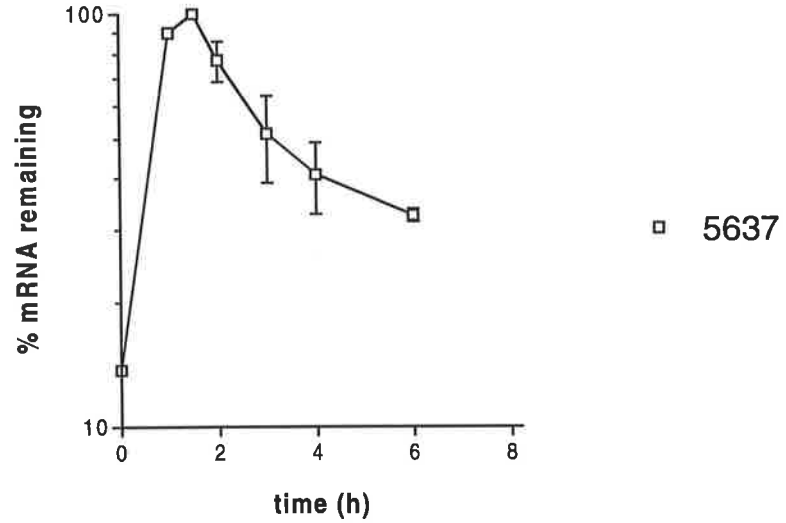
% mRNA remaining
100
10
0 2 4 6 8
time (h)
5637

element that might be conserved between species, which might indicate a region of some importance. These sequence alignments revealed that the 3'UTRs of mouse and human G-CSF were quite dissimilar except for 3 regions of 50, 40 and 20 nt (Fig. 5.3.6). The 50 nt segment contains the AU-rich region which was used to make dfGH-G70.

The 183 nt segment containing the conserved 40 nt and 20 nt regions, which appeared by eye to form stem-loop structures, was analysed by the Zuker RNA folding programme. Using an algorithm this programme calculates the most stable secondary structure likely to form. This RNA folding programme predicted that the conserved 40 nt and 20 nt sections each contained a region capable of forming a stem-loop structure. Based on these predictions constructs were designed to investigate whether these 2 stem-loop structures played a role in regulating stability of G-CSF mRNA.

5.3.4 The G-CSF 3'UTR contains a destabilising element which is distinct from the AUIE and is likely to involve stem-loops.

A series of constructs was made to investigate whether the 2 conserved stem-loops (called stem-loops A and B respectively) present in this 183nt region were destabilising elements. I inserted the 183 nt segment encompassing both the 40 nt and 20 nt conserved sequences to create dfGH-SL1 (Fig 5.2.1). This mRNA was unstable in NIH3T3 cells (Fig 5.3.7) suggesting that this region does in fact contain an instability element.

Interpretation of these results was slightly complicated by the presence of 2 sequences that almost match the UUAUUUA(U/A)(U/A) instability element, one in the putative stem of stem-loop A, the other in the stem and loop of stem-loop B (Fig. 5.2.1). I therefore made point mutations to ensure these potential AUIEs were not functional (Zubiaga *et al.*, 1995), creating dfGH-SL2 (Fig. 5.2.1). To maintain the potential for stem-loop formation in dfGH-SL2 I simultaneously introduced complementary changes to maintain base pairing in the stems. The dfGH-SL2 mRNA was at least as unstable as dfGH-SL1 indicating that the instability element was still intact (Fig. 5.3.7).

Fig. 5.3.6 Alignment of human and mouse G-CSF 3'UTRs

Alignments of the 3'UTRs of human and mouse G-CSF indicate areas conserved between the 2 species. A conserved region of 50bp contains the AU-rich region and is shaded as are 2 conserved regions of 40bp and 20bp.

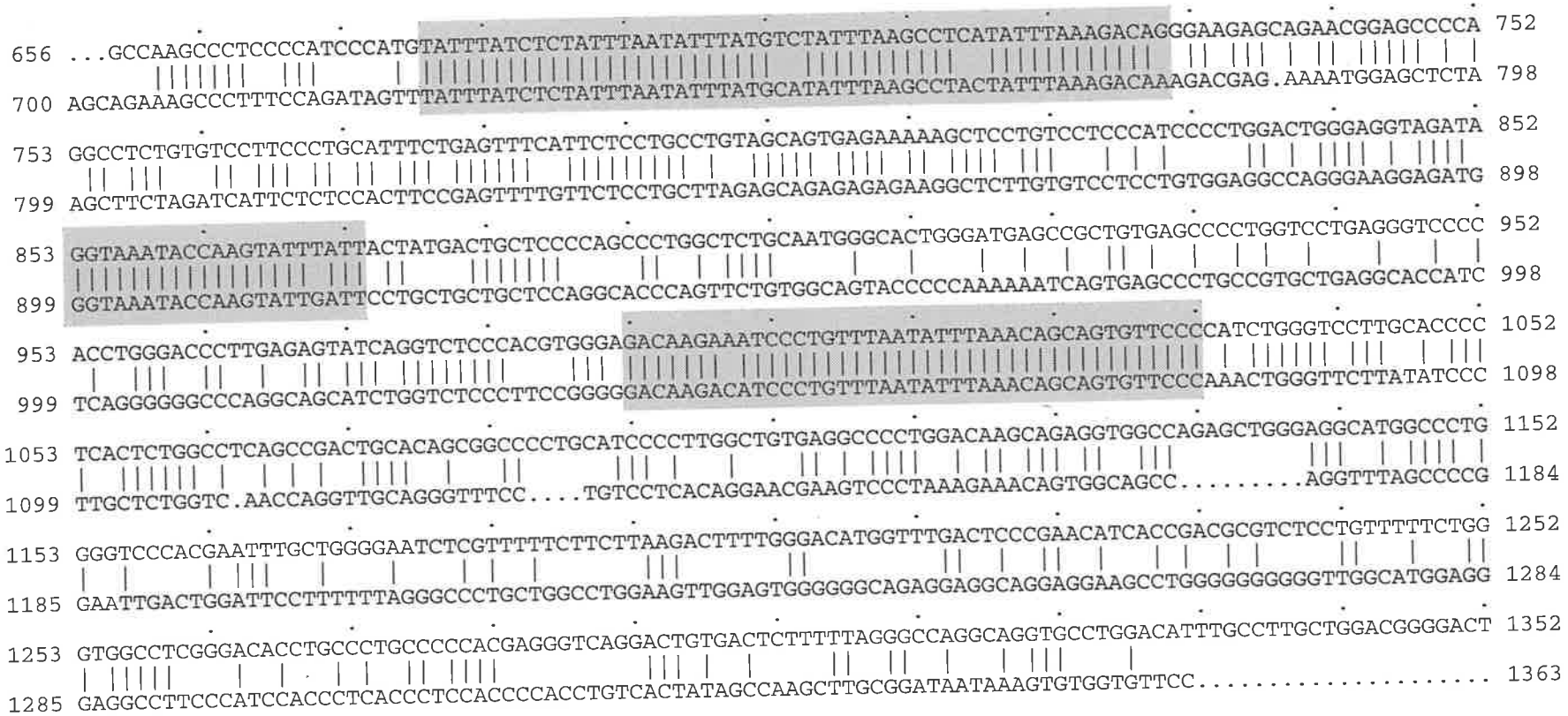
656 ...GCCAAGCCCTCCCCATCCCATGTATTTATCTCTATTTAATATTTATGTCTATTTAAGCCTCATATTTAAAGACAGGGAAGAGCAGAACGGAGCCCCA 752
700 AGCAGAAAGCCCTTTCCAGATAGTTTATTTATCTCTATTTAATATTTATGCATATTTAAGCCTACTATTTAAAGACAAAGACGAG.AAAATGGAGCTCTA 798
753 GGCCTCTGTGTCCTTCCCTGCATTTCTGAGTTTCATTCTCCTGCCTGTAGCAGTGAGAAAAAGCTCCTGTCCTCCCATCCCCTGGACTGGGAGGTAGATA 852
799 AGCTTCTAGATCATTCTCTCCACTTCCGAGTTTTGTTCTCCTGCTTAGAGCAGAGAGAGAAGGCTCTTGTGTCCTCCTGTGGAGGCCAGGGAAGGAGATG 898
853 GGTAAATACCAAGTATTTATTACTATGACTGCTCCCCAGCCCTGGCTCTGCAATGGGCACTGGGATGAGCCGCTGTGAGCCCCTGGTCCTGAGGGTCCCC 952
899 GGTAAATACCAAGTATTGATTCCTGCTGCTGCTCCAGGCACCCAGTTCTGTGGCAGTACCCCCAAAAAATCAGTGAGCCCTGCCGTGCTGAGGCACCATC 998
953 ACCTGGGACCCTTGAGAGTATCAGGTCTCCCACGTGGGAGACAAGAAATCCCTGTTTAATATTTAAACAGCAGTGTTCCCCATCTGGGTCCTTGCACCCC 1052
999 TCAGGGGGGCCCAGGCAGCATCTGGTCTCCCTTCCGGGGGACAAGACATCCCTGTTTAATATTTAAACAGCAGTGTTCCCAAACTGGGTTCTTATATCCC 1098
1053 TCACTCTGGCCTCAGCCGACTGCACAGCGGCCCCTGCATCCCCTTGGCTGTGAGGCCCCTGGACAAGCAGAGGTGGCCAGAGCTGGGAGGCATGGCCCTG 1152
1099 TTGCTCTGGTC.AACCAGGTTGCAGGGTTTCC....TGTCCTCACAGGAACGAAGTCCCTAAAGAAACAGTGGCAGCC.....AGGTTTAGCCCCG 1184
1153 GGGTCCCACGAATTTGCTGGGGAATCTCGTTTTTCTTCTTAAGACTTTTGGGACATGGTTTGACTCCCGAACATCACCGACGCGTCTCCTGTTTTTCTGG 1252
1185 GAATTGACTGGATTCCTTTTTTTAGGGCCCTGCTGGCCTGGAAGTTGGAGTGGGGGGCAGAGGAGGCAGGAGGAAGCCTGGGGGGGGGGGTTGGCATGGAGG 1284
1253 GTGGCCTCGGGACACCTGCCCTGCCCCCACGAGGGTCAGGACTGTGACTCTTTTTAGGGCCAGGCAGGTGCCTGGACATTTGCCTTGCTGGACGGGGACT 1352
1285 GAGGCCTTCCCATCCACCCTCACCCTCCACCCCACCTGTCACTATAGCCAAGCTTGCGGATAATAAAGTGTGGTGTTCC..... 1363

Figure 5.3.7 Stability of dfGHSL-1, dfGHSL-2 and dfGHSL-3 mRNAs in NIH3T3 cells

NIH3T3 fibroblasts ($1x10^6$ cells) stably expressing the dfGH-SL1, dfGH-SL2 and dfGH-SL3 transcripts were stimulated with 15% FCS and RNA was isolated at times indicated. 20μg of total RNA was then hybridised with *in vitro* synthesised complimentary RNA probes and specific mRNAs detected by RNase protection assay (see sections 2.8.15, 2.8.17 and 2.8.18).

The dfGH-SL1, dfGH-SL2 and dfGH-SL3 mRNAs were detected using a probe complimentary to a 338bp internal fragment of the growth hormone region of the dfGH-SL mRNAs, synthesised from *Pvu*II digested pG-5'hGH plasmid (see Table I: Appendix) using SP6 RNA polymerase and 400Ci/mmol [α^{32}P]-UTP.

The GAPDH mRNA was detected by using a probe complimentary to a 120bp internal fragment of the mouse GAPDH mRNA, synthesised from *Dde*I-digested plasmid pGAPM (see Table I: Appendix) using T7 RNA polymerase and 100Ci/mmol [α^{32}P]-UTP.

Panel A) Phosphorimage of RNase protection gels.

Panel B) Phosphorimager quantitation of dfGH-SL1 (■), dfGH-SL2 (●) and dfGH-SL3 (▼) mRNA levels relative to GAPDH mRNA from NIH3T3 cells stimulated with 15% FCS. Data are representative of at least 2 experiments.

A

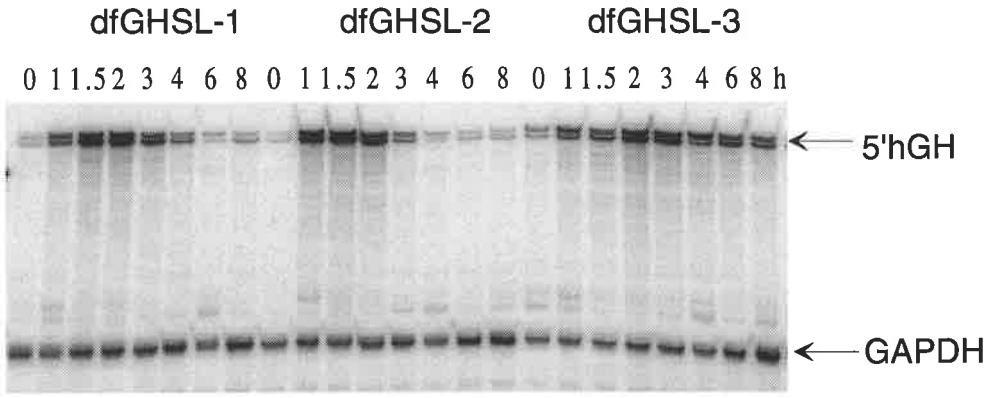
dfGHSL-1
dfGHSL-2
dfGHSL-3
0 1 1.5 2 3 4 6 8 0 1 1.5 2 3 4 6 8 0 1 1.5 2 3 4 6 8 h
5'hGH
GAPDH

B

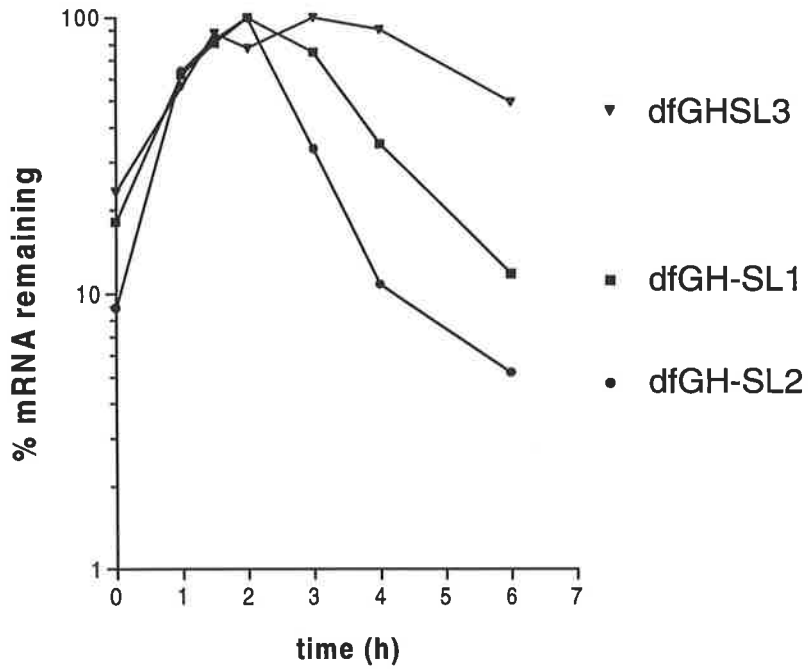
100
10
1
% mRNA remaining
0 1 2 3 4 5 6 7
time (h)
dfGHSL3
dfGH-SL1
dfGH-SL2

I next investigated whether disrupting the putative stem-loop structures but maintaining the potential AUIEs would alter the destabilising function of this region. To address this I introduced uncompensated mutations in each stem but maintained the AU sequences to create dfGH-SL3 (Fig 5.2.1). These mutations removed the destabilising effect indicating that the presence of one or both stem-loops, (from hereon called the stem-loop destabilising element (SLDE)) but not the AUIEs was necessary for the destabilising effect of this region (Fig. 5.3.7).

5.3.5 The sequence of the loops is important for instability function

To determine whether a particular loop sequence was important for the destabilising function. I changed each of the loop nucleotides of each stem-loop (Fig. 5.2.2). These mutations abolished the destabilising function (Fig 5.3.8) demonstrating that at least some part of the loop sequences was important.

5.3.6 The stem-loop destabilising element (SLDE) is not responsive to calcium ionophore.

To determine whether the SLDE was responsible for the absence of ionophore response by the G-CSF 3'UTR, NIH3T3 cells transfected with dfGH-SL2 were treated with A23187. This mRNA remained unstable (Fig 5.3.9) indicating that the SLDE is not regulated by calcium ionophore. The region containing the SLDE with point mutations in the potential AUIEs (SL2) and the SLDE containing the mutated stems (SL3) were inserted into dfGH-G70, creating dfGH-G70SL2 and dfGH-G70SL3 respectively. mRNA from dfGH-G70SL2 remained unstable (Fig. 5.3.10) in NIH3T3 cells treated with A23187 suggesting that the presence of the SLDE abolishes the responsiveness of dfGH-G70 mRNA to calcium ionophore. As expected, mRNA for dfGH-G70SL3 is stabilised in response to A23187 treament of cells (Fig. 5.3.10).

Figure 5.3.8 Stability of dfGHSL-5 mRNA compared with dfGHSL-2 mRNA in NIH3T3 cells

NIH3T3 fibroblasts ($1x10^6$ cells) stably expressing the dfGH-SL2 and dfGH-SL5 transcripts were stimulated with 15% FCS and RNA was isolated at times indicated. 20µg of total RNA was then hybridised with *in vitro* synthesised complimentary RNA probes and specific mRNAs detected by RNase protection assay (see sections 2.8.15, 2.8.17 and 2.8.18).

The dfGH-SL2 and dfGH-SL5 mRNAs were detected using a probe complimentary to a 338bp internal fragment of the growth hormone region of the dfGH-SL mRNAs, synthesised from *Pvu*II digested pG-5'hGH plasmid (see Table I: Appendix) using SP6 RNA polymerase and 400Ci/mmol [α^{32}P]-UTP.

The GAPDH mRNA was detected by using a probe complimentary to a 120bp internal fragment of the mouse GAPDH mRNA, synthesised from *Dde*I-digested plasmid pGAPM (see Table I: Appendix) using T7 RNA polymerase and 100Ci/mmol [α^{32}P]-UTP.

Panel A) Phosphorimage of RNase protection gels.

Panel B) Phosphorimager quantitation of dfGH-SL2 (●) and dfGH-SL5 (▼) mRNA levels relative to GAPDH mRNA from NIH3T3 cells stimulated with 15% FCS. Data are representative of at least 2 experiments.

A

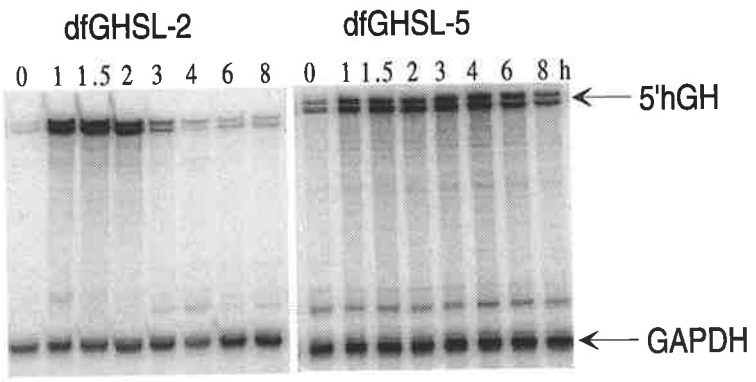
dfGHSL-2
dfGHSL-5
0 1 1.5 2 3 4 6 8
0 1 1.5 2 3 4 6 8 h
5'hGH
GAPDH

B

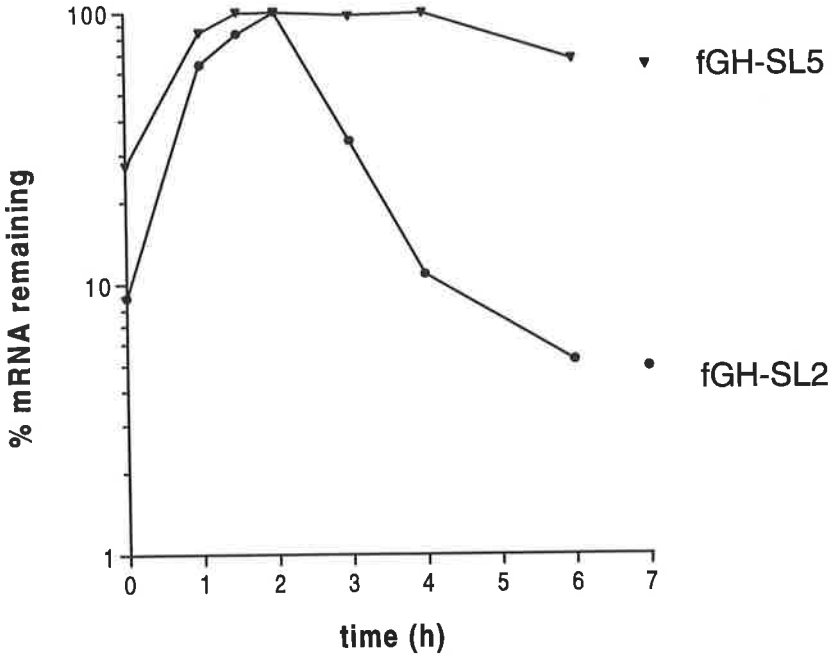
100
10
1
% mRNA remaining
0 1 2 3 4 5 6 7
time (h)
fGH-SL5
fGH-SL2

Figure 5.3.9 Stability of dfGH-SL2 mRNA in NIH3T3 cells stimulated with 15% FCS in the presence and absence of A23187

NIH3T3 fibroblasts ($1x10^6$ cells) stably expressing the dfGH-SL2 transcript were stimulated with 15% FCS alone or in the presence of A23187 to a final concentration of 2μM and RNA was isolated at times indicated. 20μg of total RNA was then hybridised with *in vitro* synthesised complimentary RNA probes and specific mRNAs detected by RNase protection assay (see sections 2.8.15, 2.8.17 and 2.8.18).

The dfGH-SL2 mRNA was detected using a probe complimentary to a 338bp internal fragment of the growth hormone region of the dfGH-SL2 mRNAs, synthesised from *Pvu*II digested pG-5'hGH plasmid (see Table I: Appendix) using SP6 RNA polymerase and 400Ci/mmol [α^{32}P]-UTP.

The GAPDH mRNA was detected by using a probe complimentary to a 120bp internal fragment of the mouse GAPDH mRNA, synthesised from *Dde*I-digested plasmid pGAPM (see Table I: Appendix) using T7 RNA polymerase and 100Ci/mmol [α^{32}P]-UTP.

Panel A) Phosphorimage of RNase protection gels.

Panel B) Phosphorimager quantitation of dfGH-SL2 mRNA levels relative to GAPDH mRNA from NIH3T3 cells stimulated with 15% FCS alone (●) or in the presence of A23187 (2μM) (▼). Data are representative of 2 experiments.

A

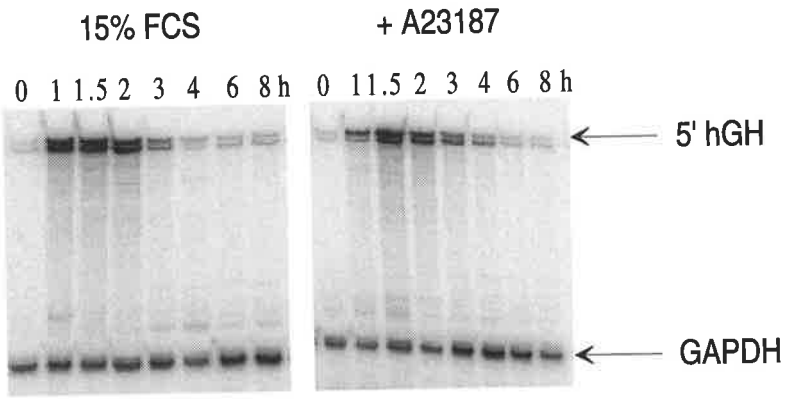
15% FCS
+ A23187
0 1 1.5 2 3 4 6 8 h
0 1 1.5 2 3 4 6 8 h
5' hGH
GAPDH

B

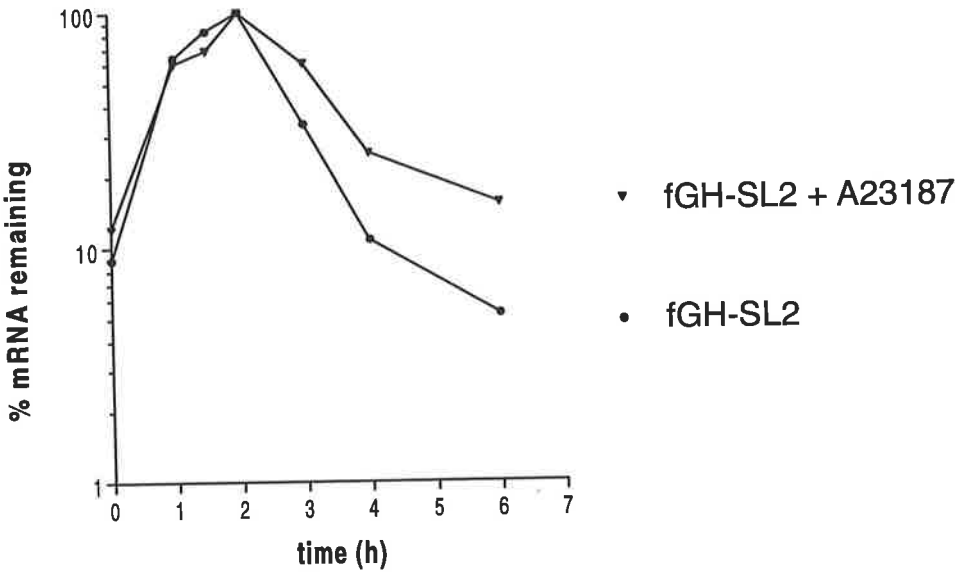
% mRNA remaining
100
10
1
0 1 2 3 4 5 6 7
time (h)
fGH-SL2 + A23187
fGH-SL2

Figure 5.3.10 Stability of dfGH-G70SL2 and dfGH-G70SL3 mRNAs in NIH3T3 cells stimulated with 15% FCS in the presence and absence of A23187

NIH3T3 fibroblasts ($1x10^6$ cells) stably expressing the dfGH-G70SL2 and dfGH-G70SL3 transcripts were stimulated with 15% FCS in the presence of A23187 to a final concentration of 2μM and RNA was isolated at times indicated. 20μg of total RNA was then hybridised with *in vitro* synthesised complimentary RNA probes and specific mRNAs were detected by RNase protection assay (see sections 2.8.15, 2.8.17 and 2.8.18).

The dfGH-G70SL2 and dfGH-G70SL3 mRNAs were detected using a probe complimentary to a 338bp internal fragment of the growth hormone region of the dfGHSL mRNAs, synthesised from *Pvu*II digested pG-5'hGH plasmid (see Table I: Appendix) using SP6 RNA polymerase and 400Ci/mmol [α^{32}P]-UTP.

The GAPDH mRNA was detected by using a probe complimentary to a 120bp internal fragment of the mouse GAPDH mRNA, synthesised from *Dde*I-digested plasmid pGAPM (see Table I: Appendix) using T7 RNA polymerase and 100Ci/mmol [α^{32}P]-UTP.

Panel A) Phosphorimage of RNase protection gels.

Panel B) Phosphorimager quantitation of dfGH-G70SL2 (▼) and dfGH-G70SL3 (●) mRNA levels relative to GAPDH mRNA from NIH3T3 cells stimulated with 15% FCS in the presence of A23187 (2μM).

A

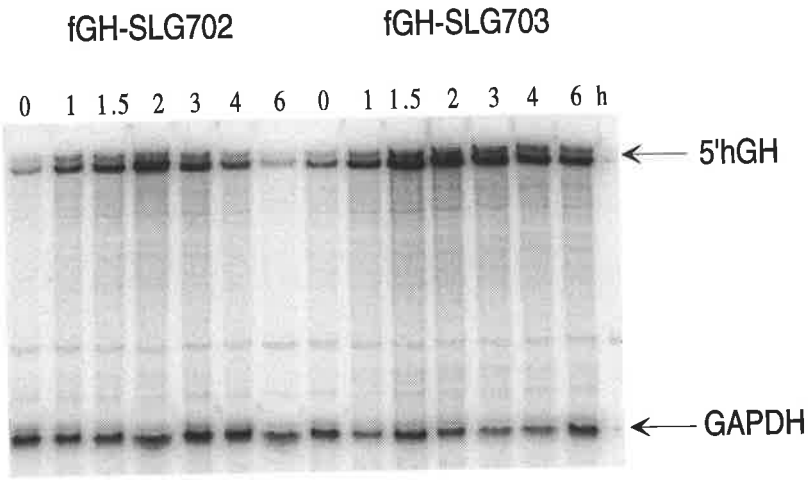
fGH-SLG702
fGH-SLG703
0 1 1.5 2 3 4 6 0 1 1.5 2 3 4 6 h
5'hGH
GAPDH

B

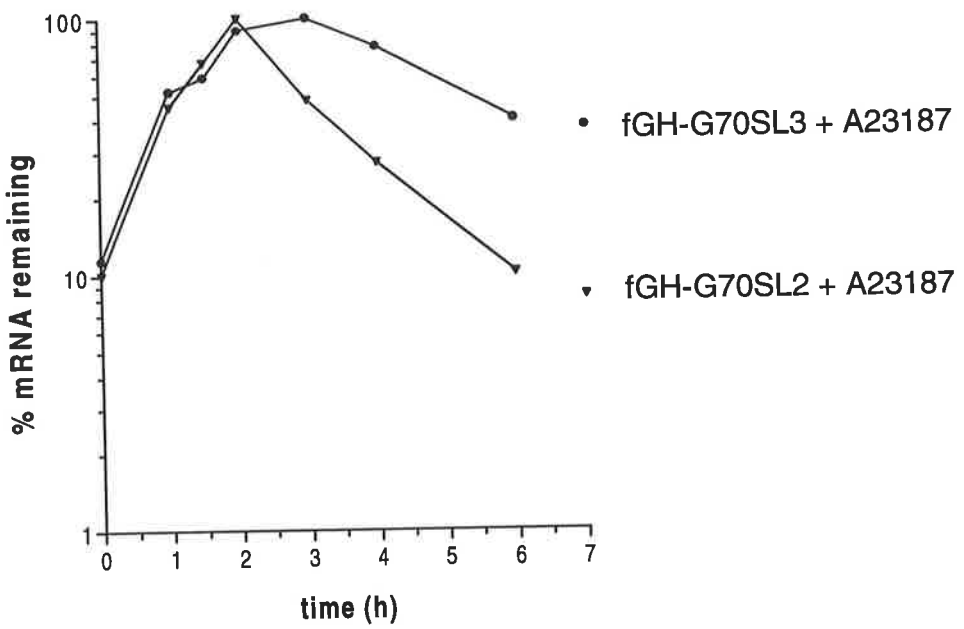
100
10
1
% mRNA remaining
0 1 2 3 4 5 6 7
time (h)
fGH-G70SL3 + A23187
fGH-G70SL2 + A23187

5.3.7 Stem-loop B is the predominant destabilising element.

To determine whether one or both of the conserved stem-loops are required for destabilisation, I made dfGH-SL6 and dfGH-SL7, in which mutations were made to disrupt stem A and stem B, respectively (Fig. 5.2.3). The dfGH-SL6 mRNA, with stem A disrupted, was unstable (Fig 5.3.11), indicating that stem-loop A is not necessary for destabilisation. The dfGH-SL6 mRNA was not as unstable as dfGH-SL1 mRNA, however, suggesting that there may be a small contribution from stem A. However, disruption of stem B caused a marked increase in the stability of the mRNA dfGH-SL7 (Fig. 5.3.11), indicating that stem-loop B is essential for the instability function.

To test whether the region between the conserved stem-loops contributed to the destabilising function I made dfGH-SL4 (Fig. 5.2.3), in which the 121 nt interloop region was replaced by just 12nt, ensuring first that the stem-loops were still predicted to form. The dfGH-SL4 mRNA was fairly stable (Fig. 5.3.11) indicating that their may be a requirement for some part of the interloop region for the destabilising function.

5.3.8 Compensating mutations to disrupted stem-loops A and B do not restore destabilising function.

I next wished to confirm that stem-loop structures define these instability elements and not some sequence therein. To address this, mutations were introduced into each side of each stem, to compensate for those of dfGH-SL3, where stem structures had been disrupted, thus restoring the folding potential of the stem-loop structures [dfGH-SL8 (Fig. 5.2.4)]. These mutations, if they were to restore the destabilising effect would provide very strong evidence that stem-loop structures were the destabilising element. These mRNAs, however, remained stable (Fig. 5.3.12) suggesting perhaps that although folding predictions suggested the stem-loops would form as before, this may not have been the case. An alternative explanation could be that the instability element identified is not a stem-loop structure but a sequence element. If the instability element is comprised of stem-loops such radical changes to the stems may prevent binding of proteins. This may occur if the stems form part of a protein

Figure 5.3.11 Stability of dfGH-SL4, dfGH-SL6 and dfGH-SL7 mRNAs in NIH3T3 cells

---

NIH3T3 fibroblasts ($1x10^6$ cells) stably expressing the dfGH-SL4, dfGH-SL6 and dfGH-SL7 transcripts were stimulated with 15% FCS in the presence of A23187 to a final concentration of 2μM and RNA was isolated at times indicated. 20μg of total RNA was then hybridised with *in vitro* synthesised complimentary RNA probes and specific mRNAs were detected by RNase protection assay (see sections 2.8.15, 2.8.17 and 2.8.18).

The dfGH-SL4, dfGH-SL6 and dfGH-SL7 mRNAs were detected using a probe complimentary to a 338bp internal fragment of the growth hormone region of the dfGHSL mRNAs, synthesised from *Pvu*II digested pG-5'hGH plasmid (see Table I: Appendix) using SP6 RNA polymerase and 400Ci/mmol [α^{32}P]-UTP.

The GAPDH mRNA was detected by using a probe complimentary to a 120bp internal fragment of the mouse GAPDH mRNA, synthesised from *Dde*I-digested plasmid pGAPM (see Table I: Appendix) using T7 RNA polymerase and 100Ci/mmol [α^{32}P]-UTP.

Panel A) Phosphorimage of RNase protection gels.

Panel B) Phosphorimager quantitation of dfGH-SL4 (■), dfGH-SL6 (▼) and dfGH-SL7 (◆) mRNA levels relative to GAPDH mRNA from NIH3T3 cells stimulated with 15% FCS. Data are representative of at least 2 experiments.

A

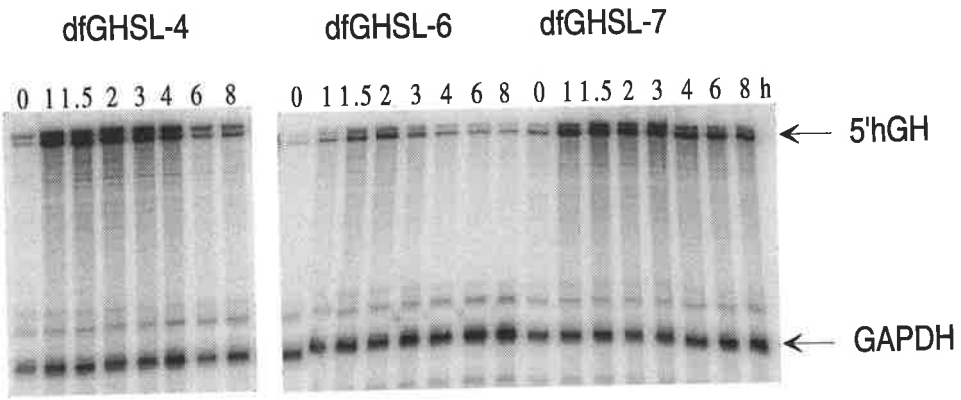
dfGHSL-4
dfGHSL-6
dfGHSL-7
0 1 1.5 2 3 4 6 8
0 1 1.5 2 3 4 6 8
0 1 1.5 2 3 4 6 8 h
5'hGH
GAPDH

B

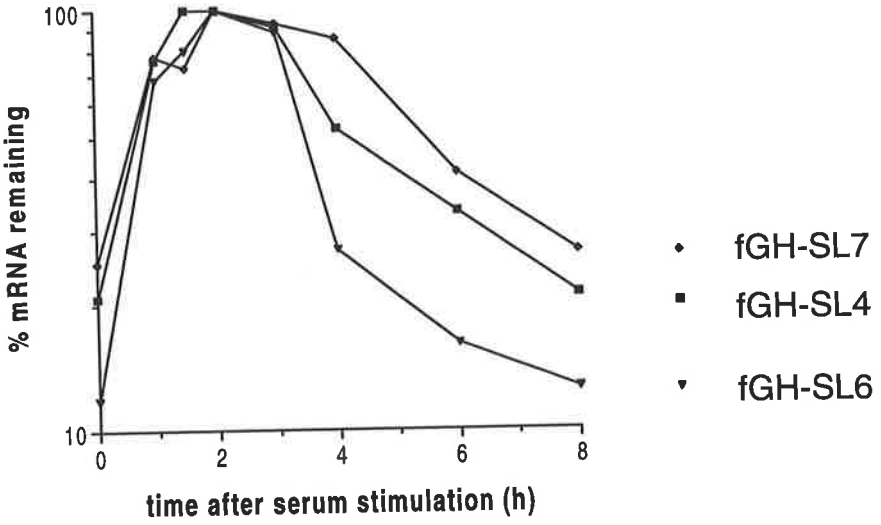
100
10
% mRNA remaining
0
2
4
6
8
time after serum stimulation (h)
fGH-SL7
fGH-SL4
fGH-SL6

recognition site. It would be very interesting to pursue this further but time constraints have prevented this.

5.3.9 Stem-loop B alone is unable to act as a destabilising element.

Having shown that stem-loop B is a necessary part of the SLDE (Figs 5.3.11) I next wished to determine whether stem-loop B alone was sufficient to act as a destabilising element. mRNA for dfGH-SL9, which comprises stem-loop B with 5 bases flanking the 5' end of stem and 3 bases flanking the 3' end (Fig 5.2.4), remained stable (Fig. 5.3.12), suggesting that in this minimal form stem-loop B was insufficient to destabilise. Although folding predictions indicated that the stem-loop would form, it may have not been a very stable structure without anchoring sequences. Alternatively, it is possible that the structure may have formed but that further flanking sequences form part of the protein recognition site without which the destabilising element cannot function.

5.3.10 The stem-loop instability element may not be confined to G-CSF.

To investigate whether cytokines in addition to G-CSF may contain similar non-AU instability elements, I made a series of chimeric genes in which the entire 3'UTRs of several AUIE-containing cytokines were inserted into dfGH. I then compared the stabilities of these mRNAs in NIH3T3 cells in the presence and absence of calcium ionophore. mRNA from chimeric genes containing the 3'UTR of human IL-4 (dfGH-IL4) or human GM-CSF (dfGH-GM3C) were unstable in NIH3T3 cells but were stabilised by treatment with A23187 (Figs 5.3.13 and 5.3.14 respectively), suggesting that for these mRNAs instability is primarily owing to AU-rich regions. In contrast, the dfGH-IL2 and dfGH-IL6 mRNAs remained fairly unstable in the presence of calcium ionophore (Figs. 5.3.15 and 5.3.16 respectively). Thus the IL-2 and IL-6 3'UTRs appear to contain instability elements with functional properties similar to the stem-loop element of G-CSF.

Figure 5.3.12 Stability of dfGH-SL8 and dfGH-SL9 mRNAs in NIH3T3 cells

NIH3T3 fibroblasts ($1x10^6$ cells) stably expressing the dfGH-SL8 and dfGH-SL9 transcripts were stimulated with 15% FCS and RNA was isolated at times indicated. 20μg of total RNA was then hybridised with *in vitro* synthesised complimentary RNA probes and specific mRNAs were detected by RNase protection assay (see sections 2.8.15, 2.8.17 and 2.8.18).

The dfGH-SL8 and dfGH-SL9 mRNAs were detected using a probe complimentary to a 338bp internal fragment of the growth hormone region of the dfGHSL mRNAs, synthesised from *Pvu*II digested pG-5'hGH plasmid (see Table I: Appendix) using SP6 RNA polymerase and 400Ci/mmol [α^{32}P]-UTP.

The GAPDH mRNA was detected by using a probe complimentary to a 120bp internal fragment of the mouse GAPDH mRNA, synthesised from *Dde*I-digested plasmid pGAPM (see Table I: Appendix) using T7 RNA polymerase and 100Ci/mmol [α^{32}P]-UTP.

Panel A) Phosphorimage of RNase protection gel.

Panel B) Phosphorimager quantitation of dfGH-SL8 (●) and dfGH-SL9 (▼) mRNA levels relative to GAPDH mRNA from NIH3T3 cells stimulated with 15% FCS. Data are representative of 2 experiments.

A

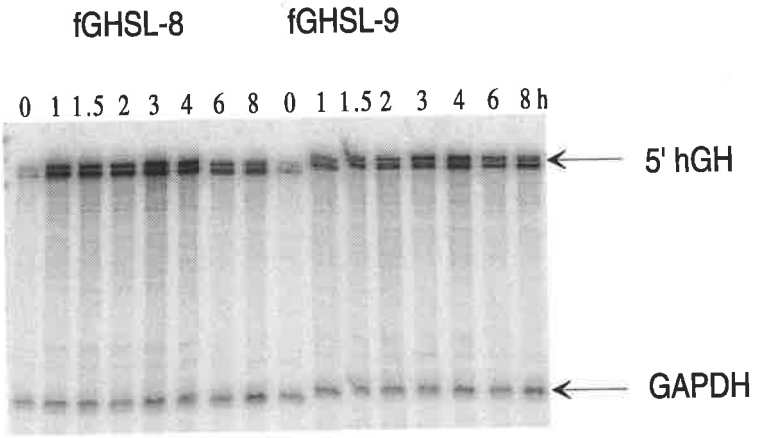
fGHSL-8
fGHSL-9
0 1 1.5 2 3 4 6 8 0 1 1.5 2 3 4 6 8 h
5' hGH
GAPDH

B

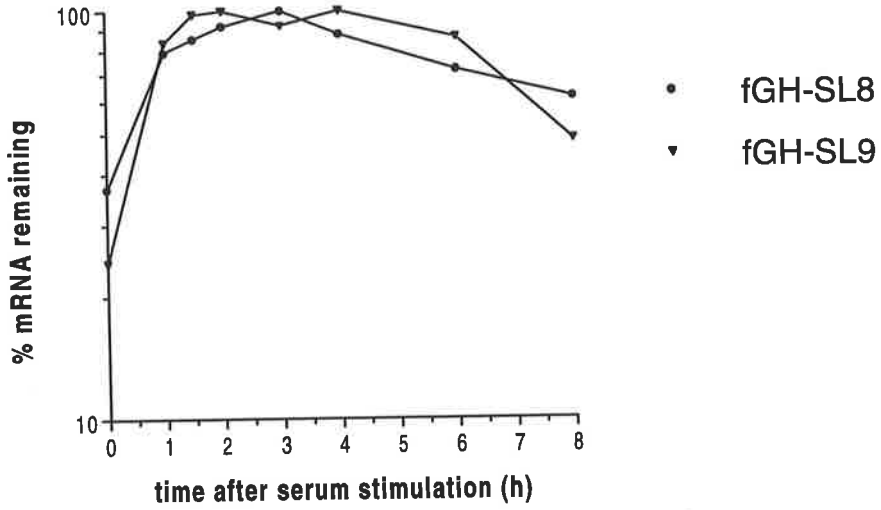
100
10
% mRNA remaining
0 1 2 3 4 5 6 7 8
time after serum stimulation (h)
fGH-SL8
fGH-SL9

Figure 5.3.13 Stability of dfGH-IL4 mRNA in NIH3T3 cells stimulated with 15% FCS in the presence and absence of A23187

NIH3T3 fibroblasts ($1x10^6$ cells) stably expressing the dfGH-IL4 transcript were stimulated with 15% FCS alone or in the presence of A23187 to a final concentration of 2μM and RNA was isolated at times indicated. 20μg of total RNA was then hybridised with *in vitro* synthesised complimentary RNA probes and specific mRNAs were detected by RNase protection assay (see sections 5.3.13).

The dfGH-IL4 mRNA was detected using a probe complimentary to a 338bp internal fragment of the growth hormone region of the dfGH-IL4 mRNA, synthesised from *Pvu*II digested pG-5'hGH plasmid (see Table I: Appendix) using SP6 RNA polymerase and 400Ci/mmol [α^{32}P]-UTP.

The GAPDH mRNA was detected by using a probe complimentary to a 120bp internal fragment of the mouse GAPDH mRNA, synthesised from *Dde*I-digested plasmid pGAPM (see Table I: Appendix) using T7 RNA polymerase and 100Ci/mmol [α^{32}P]-UTP.

Panel A) Phosphorimage of RNase protection gel.

Panel B) Phosphorimager quantitation of dfGH-IL4 mRNA levels relative to GAPDH mRNA from NIH3T3 cells stimulated with 15% FCS alone (●) or in the presence of A23187 (2μM) (▼). Data from cells stimulated with 15% FCS are plotted as means ± SEM from 2 experiments and from 3 experiments for cells stimulated with 15% FCS in the presence of A23187.

A

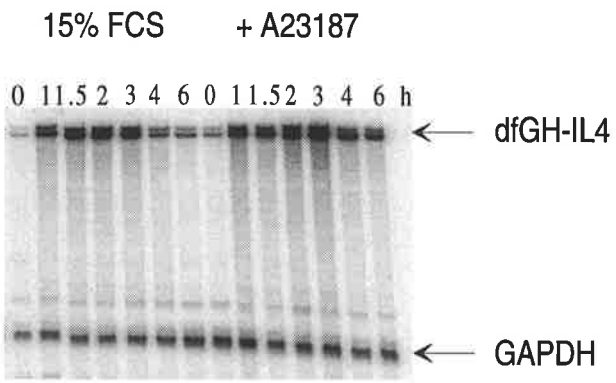
15% FCS
+ A23187
0 1 1.5 2 3 4 6 0 1 1.5 2 3 4 6 h
dfGH-IL4
GAPDH

B

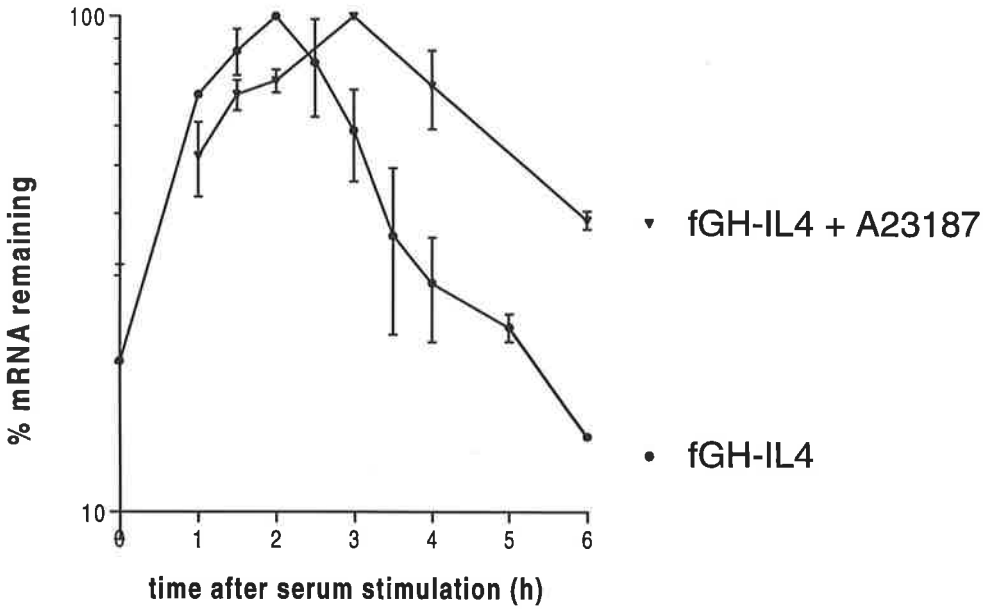
100
10
% mRNA remaining
0 1 2 3 4 5 6
time after serum stimulation (h)
fGH-IL4 + A23187
fGH-IL4

Figure 5.3.14 Stability of dfGH-GM3C mRNA in NIH3T3 cells stimulated with 15% FCS in the presence and absence of A23187

NIH3T3 fibroblasts ($1x10^6$ cells) stably expressing the dfGH-GM3C transcript were stimulated with 15% FCS alone or in the presence of A23187 to a final concentration of 2μM and RNA was isolated at times indicated. 20μg of total RNA was then hybridised with *in vitro* synthesised complimentary RNA probes and specific mRNAs were detected by RNase protection assay (see sections 2.8.15, 2.8.17 and 2.8.18).

The dfGH-GM3C mRNA was detected using a probe complimentary to a 338bp internal fragment of the growth hormone region of the dfGH-GM3C mRNA, synthesised from *Pvu*II digested pG-5'hGH plasmid (see Table I: Appendix) using SP6 RNA polymerase and 400Ci/mmol [α^{32}P]-UTP.

The GAPDH mRNA was detected by using a probe complimentary to a 120bp internal fragment of the mouse GAPDH mRNA, synthesised from *Dde*I-digested plasmid pGAPM (see Table I: Appendix) using T7 RNA polymerase and 100Ci/mmol [α^{32}P]-UTP.

Panel A) Phosphorimage of RNase protection gel.

Panel B) Phosphorimager quantitation of dfGH-GM3C mRNA levels relative to GAPDH mRNA from NIH3T3 cells stimulated with 15% FCS alone (■) or in the presence of A23187 (2μM) (●). Data plotted from cells stimulated with 15% FCS alone are the mean ± SEM from 2 experiments and from cells stimulated with 15% FCS in the presence of A23187 data are plotted as the mean ± SEM from 3 experiments.

A

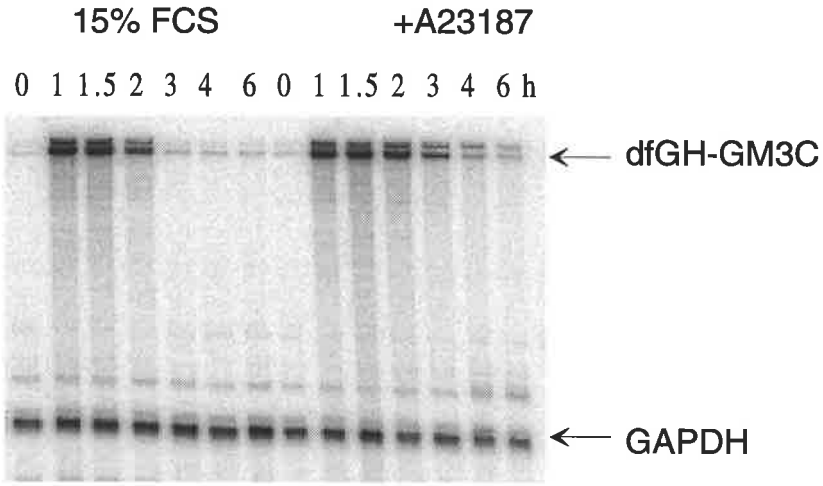
15% FCS
+A23187
0 1 1.5 2 3 4 6 0 1 1.5 2 3 4 6 h
dfGH-GM3C
GAPDH

B

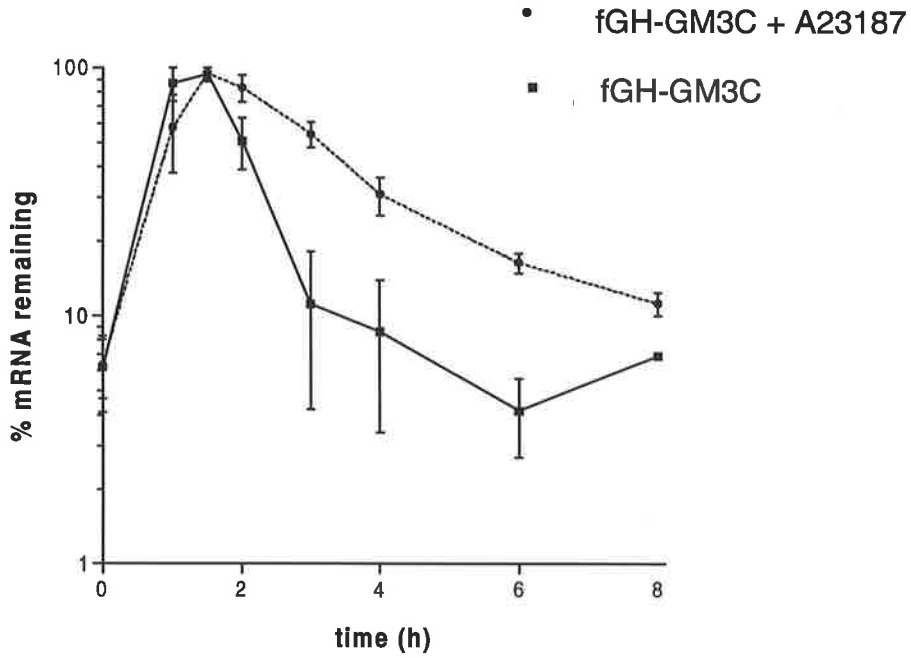
fGH-GM3C + A23187
fGH-GM3C
% mRNA remaining
100
10
1
0
2
4
6
8
time (h)

Figure 5.3.15 Stability of dfGH-IL2 mRNA in NIH3T3 cells stimulated with 15% FCS in the presence and absence of A23187

NIH3T3 fibroblasts ($1x10^6$ cells) stably expressing the dfGH-IL2 transcript were stimulated with 15% FCS alone or in the presence of A23187 to a final concentration of 2μM and RNA was isolated at times indicated. 20μg of total RNA was then hybridised with *in vitro* synthesised complimentary RNA probes and specific mRNAs were detected by RNase protection assay (see sections 2.8.15, 2.8.17 and 2.8.18).

The dfGH-IL2 mRNA was detected using a probe complimentary to a 338bp internal fragment of the growth hormone region of the dfGH-IL2 mRNA, synthesised from *Pvu*II digested pG-5'hGH plasmid (see Table I: Appendix) using SP6 RNA polymerase and 400Ci/mmol [α^{32}P]-UTP.

The GAPDH mRNA was detected by using a probe complimentary to a 120bp internal fragment of the mouse GAPDH mRNA, synthesised from *Dde*I-digested plasmid pGAPM (see Table I: Appendix) using T7 RNA polymerase and 100Ci/mmol [α^{32}P]-UTP.

Panel A) Phosphorimage of RNase protection gel.

Panel B) Phosphorimager quantitation of dfGH-IL2 mRNA levels relative to GAPDH mRNA from NIH3T3 cells stimulated with 15% FCS alone (●) or in the presence of A23187 (2μM) (▼). Data from cells stimulated with 15% FCS are plotted as means ± SEM from 2 experiments and for cells stimulated with 15% FCS in the presence of A23187 as means ± SEM from 3 experiments.

A

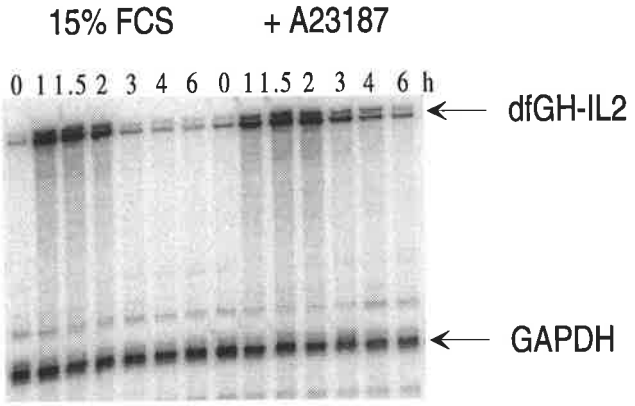
15% FCS
+ A23187
0 1 1.5 2 3 4 6 0 1 1.5 2 3 4 6 h
dfGH-IL2
GAPDH

B

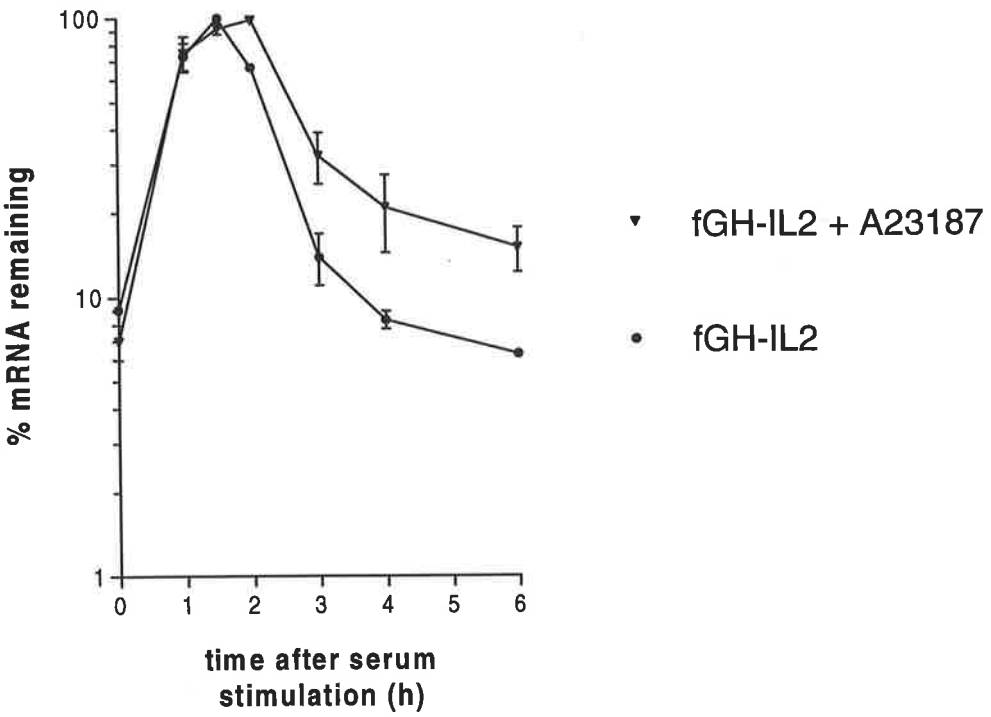
100
10
1
% mRNA remaining
0 1 2 3 4 5 6
time after serum stimulation (h)
fGH-IL2 + A23187
fGH-IL2

Figure 5.3.16 Stability of dfGH-IL6 mRNA in NIH3T3 cells stimulated with 15% FCS in the presence and absence of A23187

NIH3T3 fibroblasts ($1x10^6$ cells) stably expressing the dfGH-IL6 transcript were stimulated with 15% FCS alone or in the presence of A23187 to a final concentration of 2μM and RNA was isolated at times indicated. 20μg of total RNA was then hybridised with *in vitro* synthesised complimentary RNA probes and specific mRNAs were detected by RNase protection assay (see sections 2.8.15, 2.8.17 and 2.8.18).

The dfGH-IL6 mRNA was detected using a probe complimentary to a 338bp internal fragment of the growth hormone region of the dfGH-IL6 mRNA, synthesised from *Pvu*II digested pG-5'hGH plasmid (see Table I: Appendix) using SP6 RNA polymerase and 400Ci/mmol [α^{32}P]-UTP.

The GAPDH mRNA was detected by using a probe complimentary to a 120bp internal fragment of the mouse GAPDH mRNA, synthesised from *Dde*I-digested plasmid pGAPM (see Table I: Appendix) using T7 RNA polymerase and 100Ci/mmol [α^{32}P]-UTP.

Panel A) Phosphorimage of RNase protection gel.

Panel B) Phosphorimager quantitation of dfGH-IL6 mRNA levels relative to GAPDH mRNA from NIH3T3 cells stimulated with 15% FCS alone (●) or in the presence of A23187 (2μM) (▼). Data are plotted as means ± SEM from 2 experiments.

A

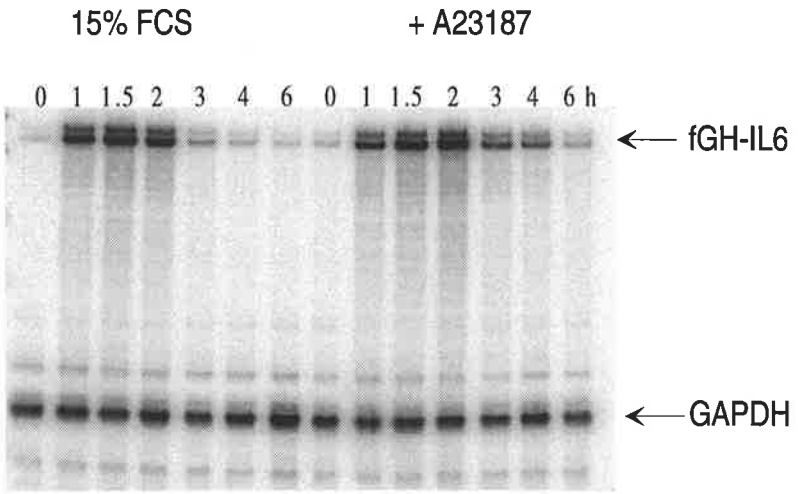
15% FCS
+ A23187
0 1 1.5 2 3 4 6 0 1 1.5 2 3 4 6 h
fGH-IL6
GAPDH

B

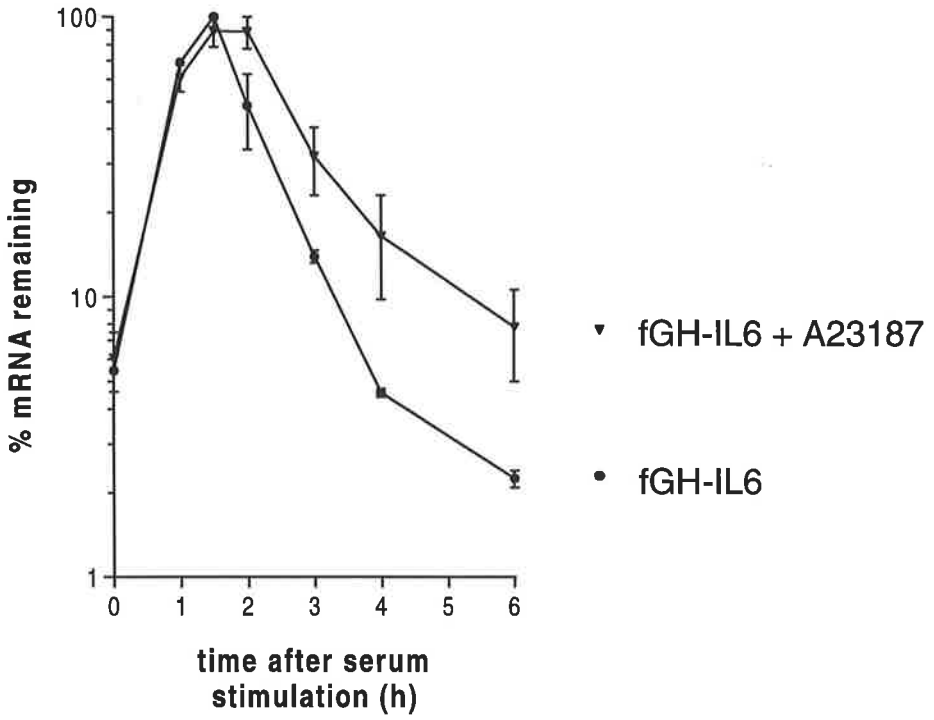
100
10
1
% mRNA remaining
0 1 2 3 4 5 6
time after serum stimulation (h)
fGH-IL6 + A23187
fGH-IL6

5.3.11 Stability of mRNAs containing the SLDE in 5637 bladder carcinoma cells

I wished to investigate whether the stem-loop instability element, which abolishes dfGH-G responsiveness to calcium ionophore, is responsible for the difference in stability between dfGH-G70 mRNA, containing the AU-rich region of the G-CSF 3'UTR, and dfGH-G, containing the full 3'UTR observed in 5637 bladder carcinoma cells. AUIEs are not functional in 5637 cells and as a consequence mRNAs such as fGH-G70 are stable (Fig. 5.3.1). In contrast, mRNA for dfGH-G (containing the entire 3'UTR) remains relatively unstable (Fig. 5.3.2) suggesting the presence of other instability elements which still function in 5637 cells. mRNA for dfGH-SL2, containing the SLDE, is relatively unstable in 5637 cells (Fig.5.3.17) indicating that the stem-loop instability element functions in these cells. This mRNA does not decay as rapidly as it does in NIH3T3 cells treated with calcium ionophore suggesting that the stem-loop instability element is only partially functional in 5637 cells.

5.3.12 Degradation of mRNAs containing the SLDE is probably dependent on prior removal of the poly(A) tail and is therefore the same as for AUIE-containing mRNAs.

In short-lived cytokine mRNAs, that contain AUIEs, removal of the poly(A) tail is the first, and rate limiting, step in the decay of the mRNA. It appears that removal of the poly(A) tail precedes degradation of the body of the mRNA. I wished to determine whether the pathway of degradation for mRNAs containing stem-loops similarly involves prior removal of the poly(A) tail or whether other mechanisms, such as endonucleolytic cleavage, are involved. To address this, Poly(A) tail shortening experiments were carried out by transferring cleaved RNAs onto nylon membrane and detecting mRNAs with a [γ-^{32}P] probe. These preliminary experiments suggested that while the poly(A) tail of a stable mRNA (fGH) was hardly shortened over a 4 h period and was still evident at 8 h, the poly(A) tails of mRNAs containing either repeated AUIEs (fGH7,2) or stem-loop instability elements (dfGH-SL2) were removed within 3 h

(Fig. 5.3.18). Poly(A) shortening appeared to precede degradation of the SLDE-containing mRNA (dfGH-SL2) as well as the AUIE-containing mRNA (fGH7,2).

Figure 5.3.17 Stability of dfGH-SL2 mRNA in 5637 bladder carcinoma cells compared with NIH3T3 cells

---

NIH3T3 fibroblasts ($1x10^6$ cells) and 5637 cells ($2x\ 10^6$ cells) stably expressing the dfGH-SL2 transcript were stimulated with 15% FCS and RNA was isolated at times indicated. 20μg of total RNA was then hybridised with *in vitro* synthesised complimentary RNA probes and specific mRNAs were detected by RNase protection assay (see sections 2.8.15, 2.8.17 and 2.8.18).

The dfGH-SL2 mRNA was detected using a probe complimentary to a 338bp internal fragment of the growth hormone region of the dfGH-SL2 mRNA, synthesised from *Pvu*II digested pG-5'hGH plasmid (see Table I: Appendix) using SP6 RNA polymerase and 400Ci/mmol [α^{32}P]-UTP.

The GAPDH mRNA was detected by using a probe complimentary to a 120bp internal fragment of the mouse GAPDH mRNA, synthesised from *Dde*I-digested plasmid pGAPM (see Table I: Appendix) using T7 RNA polymerase and 100Ci/mmol [α^{32}P]-UTP.

Panel A). Phosphorimager quantitation of dfGH-SL2 mRNA levels relative to GAPDH mRNA from NIH3T3 cells stimulated with 15% FCS. Data are representative of 2 experiments.

Panel B) Phosphorimager quantitation of dfGH-SL2 mRNA levels relative to GAPDH mRNA from 5637 cells stimulated with 15% FCS. Data are representative of 2 experiments.

A

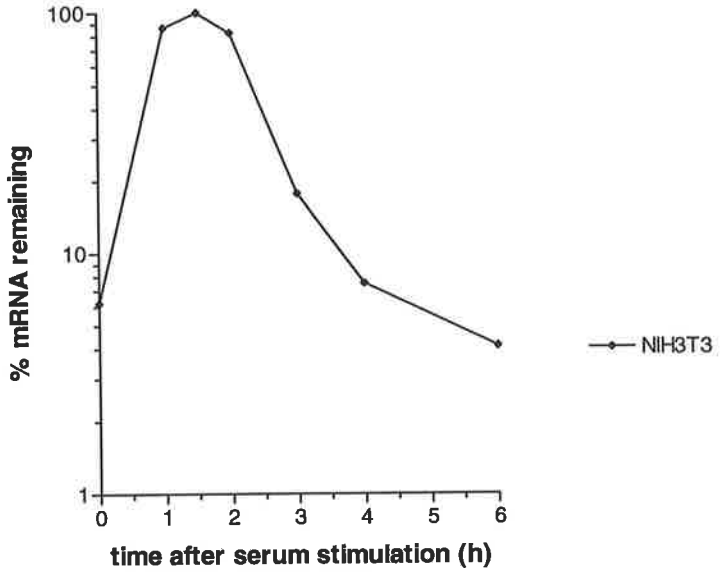
100
10
1
% mRNA remaining
0 1 2 3 4 5 6
time after serum stimulation (h)
NIH3T3

B

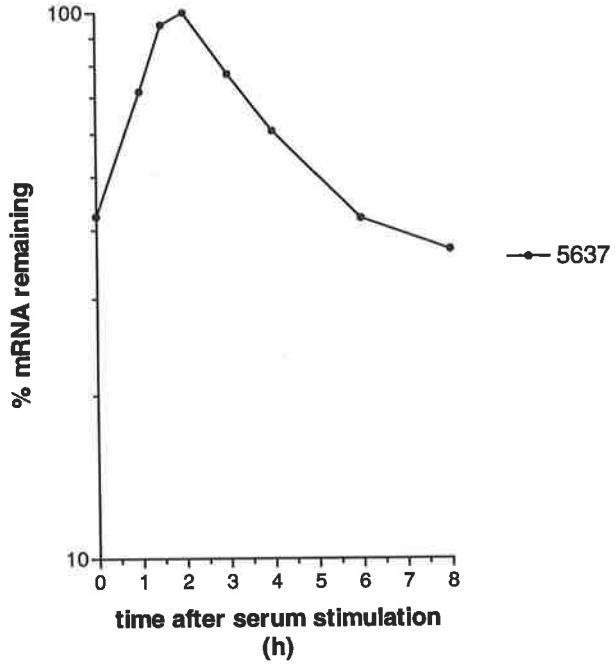
100
10
% mRNA remaining
0 1 2 3 4 5 6 7 8
time after serum stimulation (h)
5637

Fig 5.3.18 Poly(A) tail shortening of fGH, fGH-7,2 and dfGH-SL2 mRNAs in NIH3T3 cells

---

NIH3T3 fibroblasts ($1x10^6$ cells) stably expressing the fGH, fGH-7,2 and dfGH-SL2 transcripts were stimulated with 15% FCS and RNA was isolated at times indicated. 20µg of total RNA (see sections 2.8.15 and 2.8.19) was hybridised with a cleavage oligo (GTCTGCTTGAAGATCTG) and subjected to RNase H digestion (2U). RNA samples were electrophoresed and transferred to Hybond N^+ nylon membrane.

The fGH, fGH-7,2 and dfGH-SL2 mRNAs were detected using an oligonucleotide probe (GGACAGTGGGAGTGGCACCTTCCAGGGTCA) labelled at its 5' end with [γ-^{32}P] ATP.

Panel A) Phosphorimage of northen blot for fGH mRNA

Panel B) Phosphorimage of northern blot for fGH-7,2 and dfGH-SL2 mRNAs.

A

fhGH

0 1 1.5 2 3 4 6 8hr

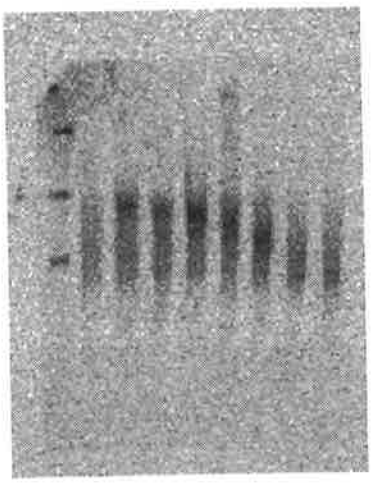

B

fhGH-7,2 fhGH-SL2

0 1 1.5 2 3 4 6 8 0 1 1.5 2 3 4 6 8 h

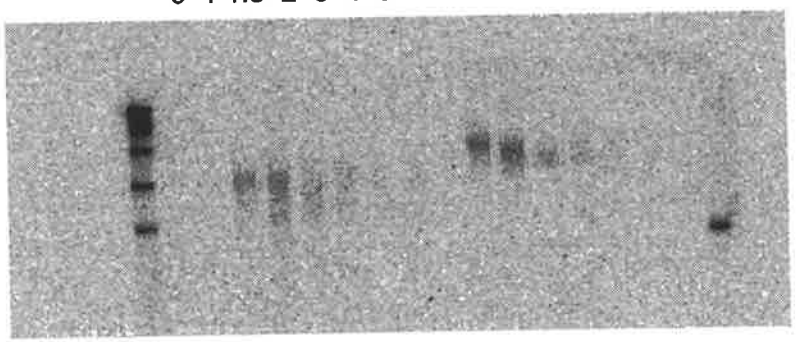

5.4 Discussion

In Chapter 4 I described some curious observations which suggested that there may be differential regulation of mRNA stability between G-CSF and GM-CSF. Whereas chimeric genes containing the full 3'UTR of GM-CSF were regulated by calcium ionophore similar genes containing the 3'UTR of G-CSF were not.

In this chapter I describe the identification and characterisation of stem-loop instability determinants present in the 3'UTR of G-CSF. Stem-loop A comprises a 9 base-pair stem, all but one nucleotide of which is conserved between mouse and human, although this non-conserved nucleotide does maintain base pairing in the stem, and a 3-nucleotide conserved loop. Interestingly, the one non-conserved nucleotide, a uridine, is part of a potential AUIE which, given the highly conserved nature of AUIEs, suggests that this is probably a non-functional AUIE. Stem-loop B comprises an 8 base pair stem conserved between human and mouse and a 3-nucleotide conserved loop. Three nucleotides flanking the 5'stem of this stem-loop are also conserved.

Stem-loop structures that regulate gene expression are not unknown. A single iron response element (IRE) in the 5'UTR is responsible for the iron-dependant translational control of the ferritin mRNA (Hentze *et al.*, 1987), while 5 of these IREs present in the 3'UTR of transferrin receptor regulate stability of this mRNA in response to intracellular iron concentrations (Casey *et al.*, 1988; Casey *et al.*, 1989). When iron is scarce the mRNA is protected from degradation by the binding of iron regulatory proteins (IRP) to the IREs and conversely when the cell is iron replete the IRP is in a [4Fe-4S] state, has low affinity for IREs and thus the mRNA is not protected from degradation. IREs present in the 5'UTR of human erythroid 5-aminolevulinate synthase (eALAS) mRNA exert iron-dependant translational control of this mRNA in erythroid cells (Cox *et al.*, 1991; Dandekar *et al.*, 1991).An IRE-like motif is present in mitochondrial aconitase although its function has yet to be determined (Dandekar *et al.*, 1991). Histone mRNAs are the only class of metazoan mRNAs that contain a highly conserved terminal stem-loop instead of a poly (A) tail (Birnsteil *et al.*, 1985). This

stem-loop is required for histone RNA processing (Gick *et al.*, 1986), efficient export of the mRNA into the cytoplasm (Eckner *et al.*, 1991) and is also necessary and sufficient for regulation of histone mRNA stability (Pandey and Marzluff, 1987). A putative stem-loop structure in the 3'UTR of urokinase-type plasminogen activator mRNA contributes to the regulation of stability of this mRNA (Nanbu *et al.*, 1994).

The G-CSF stem-loops described in this chapter confer instability on the heterologous mRNA which is abolished when the stem structures are disrupted (SL-3 Fig. 5.3.7). The destabilising function is not owing to the presence of potential AUIEs, one of which is present in stem A and the other in the stem and loop of stem loop B, since compensating changes that disrupted the AUIEs had no effect (SL-2 Fig.5.3.7). When compensating mutations were introduced to restore base pairing of stems disrupted by mutations introduced in SL-3, to create SL-8, the destabilising function was not restored (Fig.5.3.12). This may be owing to a loss of stem-loops due to alternative folding than that predicted by the RNA folding prediction programme applied (Zuker). It is also possible that if the stem is part of a protein recognition site such mutations to the stem may not be tolerated. Most commonly the loop is required for the high affinity interactions with binding factors (Mullner and Kuhn, 1988; Rouault *et al.*, 1988; Klausner *et al.*, 1993) while the stem provides structural stability. Mutations to loops in the transferrin receptor, ferritin and eALAS IREs (Mullner and Kuhn, 1988; Casey *et al.*, 1989; Rouault *et al.*, 1988; Cox *et al.*, 1991; Bhasker *et al.*, 1993) respectively result in loss of iron-dependant regulation as do mutations to a cytosine bulge (Kikinis *et al.*, 1995). The primary sequence of the upper and lower IRE stem, however, which has not been conserved is less important than is the ability to base pair. It seems likely, therefore, that the 6 highly conserved nucleotides of the loop and the cytosine bulge are the primary determinants of binding specificity and potential sites for RNA-protein interaction. Similarly, replication of the human immunodeficiency virus requires binding of the viral TAT protein to its RNA target sequence TAR at a tri-nucleotide bulge consisting of a cytosine and 2 uridine residues (Weeks and Crothers, 1991)

As with the IREs, mutation of histone loop sequences results in abolished expression of histone but in contrast, a number of mutations to the stem including

reversing the stem sequences, reversing the two base pairs at the base of the stem or destroying the UA base at the top of the stem, also abolished expression (Pandey *et al.*, 1994) indicating that the sequence of the stem is as critical as that of the loop. These results suggest that for histone mRNA a larger site for specific interactions is probably required. These results are more in keeping with my findings that mutations to the stem, which maintain the base pairing potential, result in loss of the destabilising effect. Thus, it is concievable that the stems of the G-CSF stem-loops contribute to a potential protein binding site.

In keeping with IREs and the histone stem-loop, the loop sequences of the G-CSF stem-loops are probably part of a protein recognition site since changing all 3 nucleotides of the loop completely abolished the destabilising function. It would be interesting to pursue this investigation to ascertain which, if any, of the loop nucleotides are redundant. In the case of the IREs 5 of the 6 nucleotides of the loop are highly conserved and the 6th is variable but usually a pyrimidine.

I find that stem-loop B is the predominant destabilising element since abolishing the structure of stem A (SL-6), but maintaining stem B, does not ablate the destabilising function (Fig. 5.3.11), while abolishing the structure of stem B, but not stem A (SL-7), does markedly reduce the destabilising function of this mRNA (Fig. 5.3.11). There is some reduction in destabilising function of SL-6 compared with SL-2 in which both stem-loops are intact which may reflect some requirement for stem-loop A perhaps to attract binding proteins to the stem-loop region.

Although I find that stem-loop B is the predominant destabilising element, this stem-loop does not function in isolation (SL-9 Fig. 5.3.12) nor does it function without some sequences in the inter-loop region. Removal of this intervening region (SL-4 Fig. 5.3.11) severely diminishes the destabilising function indicating that a component of this region may be required function of the instability element. Williams and Marzluff (Williams and Marzluff, 1995) found that for high affinity binding of the histone stem-loop binding protein, the 5' and 3' regions flanking the stem-loop were critical since changes to these sequences markedly reduced efficiency of binding. It is possible, therefore, that sequences flanking the stems of the G-CSF SLDE may play a role in

specific RNA-protein interactions and removal of these nucleotides may result in partial loss of the protein recognition site. I find that not only does introduction of compensating mutations to the stems that maintain base pairing abolish the destabilising function of the stem-loops, but that also a minimal stem-loop B, which appears to be the predominant destabilising element, also does not function. These results suggest the possibility that, like the histone stem-loop and unlike the IREs, the sequence of the stems and the flanking sequences may be important for the instability function of the G-CSF stem-loops.

Possibly the most important finding of this work is that the stem-loops promote different regulation of the mRNA. Whereas mRNAs from chimeric genes containing multiple AUIEs are stabilised in response to calcium ionophore (Fig. 5.3.2), SLDE-containing mRNAs remain unstable (Fig 5.3.9). As well as not being responsive to calcium ionophore, the presence of SLDEs also prevents the responsiveness of mRNAs containing AUIEs to ionophore (Figs. 5.3.2 and 5.3.10). This result not only indicates that the SLDE promotes different regulation but that it also inhibits regulation of AUIE-containing mRNAs by ionophore. How it prevents regulation is not known, it may counteract the stabilising effect of the ionophore by imposing a stronger destabilising effect or, alternatively, the SLDE may actively prevent the interaction of binding proteins with mRNA in ionophore-treated cells. The presence of proteins binding to the SLDE may prevent AU-binding protein activities by direct stearic hindrance or by imposing conformational changes within the secondary structure of the mRNA which may mask AU-binding sites or which reduce recognition by binding factors. It would be very interesting to pursue these investigations but time constraints have prevented this.

In many mRNAs degradation is initiated by removal of the poly(A) tail followed by removal of a 5" cap" (Beelman and Parker, 1995). This is not always the case, however, premature translational termination in yeast can trigger deadenylation-independent decapping (Muhlrad and Parker, 1994; Hagan *et al.*, 1995). This nonsense-mediated mRNA decay pathway is part of an mRNA surveillance process which ensures the rapid removal of aberrant transcripts. These aberrant mRNAs may contain early nonsense codons (Leeds *et al.*, 1992; Losson and Lacroute, 1979; Peltz *et al.*, 1993),

unspliced introns (He *et al.*, 1993) or elongated 3'UTRs (Pulak and Anderson, 1993). In each of these examples deadenylation-independent decay occurs as a means of removing aberrant transcripts but is not the usual decay pathway. Deadenylation-independent decay also occurs as the normal pathway of degradation of IGF2 and transferrin receptor mRNAs degradation is initiated by endonucleolytic cleavage (Nielsen and Christiansen, 1992; Binder *et al.*, 1994). The idea that degradation of the mRNA can occur independently of deadenylation prompted me to investigate whether the mRNA for the chimeric genes containing the SLDE of G-CSF would undergo poly(A) tail removal prior to decay of the mRNA as for AUIE-containing mRNAs, or deadenylation-independant decay as observed in IGF2 and transferrin receptor mRNAs. I observed that removal of the poly(A) tail preceded degradation (Fig. 5.3.18), suggesting that the pathway of decay in the SLDE-containing mRNAs was essentially as observed for AUIE-containing mRNAs.

The presence of these stem-loops suggests a mechanism for differential expression of different cytokines. IL-2 and IL-6 also appear to contain alternative instability elements which prevent regulation by calcium ionophore (Figs. 5.3.15 and 5.3.16 respectively) thus making control of their expression complex.These results suggest that non-AU instability elements are not confined to G-CSF but may represent a more widespread mechanism for regulation of mRNA stability. When cells of the immune system are activated there is often differential expression of these and other cytokines and it seems quite reasonable, therefore, that the presence of alternative regulatory elements in various cytokines will help differentially regulate their expression. Mechanisms which differentially limit the expression of cytokines such as the presence of alternative instability elements may help the fine tuning of cytokine expression in response to a variety of stimuli in a variety of cell types.

It is interesting that while the AUIEs do not function in 5637 human bladder carcinoma cells, which constitutively produce a number of cytokines (Ross *et al.*, 1991), the stem-loops of G-CSF, so that the mRNAs remain unstable. This suggests that degradation mechanisms for the AUIEs and stem-loops may be different. The lack of AUIE-mediated degradation suggests loss, or alternatively, constitutive activation of

second messenger signalling, while signalling for the stem-loop mediated degradation remains largely intact. This interesting observation may provide a useful tool in the investigation of cancer cell lesions which lead to constitutive cytokine expression and may provide information on tumour progression.

Chapter 6

General conclusions

The aim of the work described in this thesis was to study some aspects of the complex subject of regulation of cytokine mRNA stability. This is an important mechanism by which levels of cytokine gene expression can be controlled. Although much has been elucidated over the past decade there is still very little known about the exact mechanisms involved in regulating mRNA stability. An important element involved in mediating the rapid decay of mRNAs, the AUIE, has been identified, (Shaw and Kamen, 1986; Lagnado *et al.*, 1994; Zubiaga *et al.*, 1995) but how its presence directs decay of the mRNA is still unknown. It is very likely that protein factors will bind to the AUIEs and trigger the process of degradation. A number of proteins that bind AU sequences with some selectivity have been identified (Malter, 1989; Bohjanen *et al.*, 1991; Brewer, 1991; Nakagawa *et al.*, 1995) although there has been no direct evidence of their involvement in the decay process.

Cytokine half-lives are typically very short (Shaw and Kamen, 1986; Raj and Pitha, 1981) but upon induction by a variety of stimuli they become transiently stabilised to allow protein production. Stabilisation of the cytokine transcript is only short-lived to prevent overexpression which can potentially lead to malignant transformation (Schuler and Cole, 1988). Mechanisms therefore exist to allow both stabilisation of the transcript and the subsequent return to an unstable state. I, and others (Iwai *et al.*, 1993) have shown that AUIEs mediate stabilisation of GM-CSF mRNA in response to stimulation with A23187, but there is still very little known about how stabilisation in response to other stimuli is mediated. There is evidence from my own data and that of others to suggest that the AUIEs are not responsible for stabilisation in response to TNFα (Akashi *et al.*, 1991) and PMA (Iwai *et al.*, 1991). Using entire 3'UTRs I and others have been unable to elicit response to IL-1 (Yang and Yang, 1994), PMA and TNFα. Even the entire GM-CSF cDNA did not stimulate response to these agents, suggesting the possibility of either some fundamental system problem or the presence of regulatory elements in introns. These results have yielded little useful information regarding mechanisms of decay although they have highlighted some of the problems associated with carrying out these sorts of experiments.

It seems increasingly likely that the AUIEs are not the only element involved in regulating stability of cytokine mRNAs. The differential regulation of G-CSF and GM-CSF mRNAs compared with IL-10 mRNA observed in monocytes stimulated with LPS and treated with IL-10 also suggests the presence of other regulatory elements. In addition to this indirect evidence I have identified a novel non-AU instability element in the 3'UTR of G-CSF which is not responsive to A23187, suggesting a mechanism to explain the differential production of cytokines observed in certain cell types. My work has also suggested the presence of these non-AU instability elements, which mediate ionophore independent regulation, in at least 2 other cytokines. These observations indicate that regulation of stability involves more than simply induction and suppression of AU-binding protein activities. Although there have been indications that some AU-binding proteins play a role in either stabilisation of the mRNA (Malter and Hong, 1991), or in mediating cytokine specific decay (Bohjanen *et al.*, 1991) when cells are activated with certain stimuli again there is no direct evidence. Although cytokines exhibit some functional overlap, they also have discrete roles in haemopoiesis. To account for this there must be differential, as well as co-ordinate, production of cytokines. This is essential for correct inter-cellular signalling and it is therefore simplistic to assume that the AUIEs and associated binding factors can account for the complex differential regulation which must take place. It seems more likely that there will be interactions between different types of binding protein factors which differentially bind to different regulatory elements. These differential binding activities may depend on the cell type, the stimulus applied and the role of the cytokine induced.

The mechanisms involved in this must inevitably be complex but will be exciting to pursue. The presence of alternative instability elements which may mediate response to some stimuli, but not others, suggests that they can somehow prevent stabilisation in response to specific stimuli. I observe that not only do the stem-loop instability elements in the 3'UTR of G-CSF not respond to ionophore, they prevent response by AUIE-containing mRNAs (Figs. 5.3.9 and 5.3.10). This suggests that they may somehow impede the action of AU-binding factors. It is not yet known whether mRNA stabilisation involves induction of a binding activity to protect the mRNA from

degradation or, conversely, the suppression of a binding activity which promotes degradation of the mRNA. The presence of proteins binding to a stem-loop structure may prevent AU-binding protein activities by direct stearic hindrance. This seems a little implausible, however, given the great distance between the AUIEs and the stem-loops. It is possible that binding to stem-loop structures induces conformational changes within the secondary structure of the mRNA which could either mask the AU binding sites or which are not recognised by binding proteins. An alternative suggestion might be that the destabilising activity of the stem-loops is sufficient to counteract the stabilising effect of the stimulus applied.

One of the interesting findings of this part of my work is the observation that the stem-loop instability element appears to be a more potent destabilising element than the AUIEs. The evidence for this comes from my observation that the 2 stem-loops destabilise an mRNA significantly moreso than does the AU-rich region of G-CSF (Fig. 5.3.7 compared with Fig. 5.3.1). This result suggests that the stem-loop instability element may be of more importance in G-CSF than the AUIEs. If this is the case then it is worth reconsidering the significance of AUIEs in other cytokines. If the stem-loops are more important than the AUIEs in G-CSF then why are the AUIEs still conserved between species? Conservation usually implies functionality therefore it is reasonable to speculate that the AUIEs and stem-loops both contribute to destabilising the mRNA but may confer response to different stimuli. We know that the AUIEs can confer response to at least ionophore so maybe the stem-loops are responsive to other stimuli and there may be other elements that respond to still other stimuli. In this way, depending on which signalling pathways are activated, and what regulatory elements are present in a gene, a cell may be able to independently produce certain cytokines even though genes for all cytokines are present and perhaps transcribed.

In chapter 3 I demonstrate a mechanism by which IL-10 downregulates expression of G-CSF, GM-CSF and IL-10. G-CSF and GM-CSF both play an important role in the inflammatory phase of an immune response. IL-10 is very interesting in that not only is it one of few cytokines that downregulate production of many inflammatory cytokines and thus limits an immune response, it is the first example of a cytokine

downregulating its own production. Cytokines released as part of the inflammatory response are produced early and then are subsequently inhibited in order to limit the response, whereas IL-10, whose function is to subdue the primary inflammatory response, is released somewhat later and then negatively regulates its own production. Given the role of IL-10, autoregulation must involve a different mechanism from its suppression of pro-inflammatory cytokine production. The delay I observed in the destabilisation of its own mRNA compared with that for G-CSF and GM-CSF mRNAs (Fig. 3.37 compared with Fig. 3.3.4) indicates that differential regulation exists in the regulation of these cytokines. The effect of IL-10 on its own production may be indirect, involving stimulation or suppression of other signalling pathways, whereas the rapidity of its effect on the destabilisation of G-CSF and GM-CSF mRNAs suggests a direct effect. How IL-10 abolishes the stabilising effect of LPS, however, is not known. It would be interesting to conduct experiments using chimeric genes containing AUIEs to see whether its effect is via these regulatory elements. It might activate signalling pathways which stimulate binding activity of AU binding factors involved in triggering decay of the mRNAs. Conversely, it might suppress activity of signalling pathways which induce activities of binding factors which protect the mRNAs from degradation. Alternatively it may work through other regulatory elements which inhibit or mask the effects of the stabilising stimuli.

The work presented in this thesis indicates how complex even this relatively small area of control of gene expression is. I have presented data to suggest that downregulation of cytokines, including IL-10 itself, by IL-10 is through destabilisation of their transcripts but it is not yet known how this is achieved. IL-10 downregulates its own expression differentially from that of G-CSF and GM-CSF, but again how this is achieved is not known, although the results suggest the presence of additional instability elements. I have identified a novel destabilising element in the 3'UTR of G-CSF which is functionally different from the AU destabilising elements, but there is much more characterisation to be carried out. It would be interesting to determine the minimal SLDE, which could then facilitate identification of binding proteins. It would also be interesting to identify the ionophore-independant elements in the 3'UTR's of IL-2 and

IL-6 and determine if other cytokines contain these. Also worth pursuing is the notion that although these elements still function in the presence of ionophore, they may not function in response to other stimulating agents thus facilitating the search for regions of the gene which respond to inducing stimuli.

Appendices

Appendix

Table I

RNase Protection Assay Probes

Target mRNA	Plasmid	Restriction Digest	Protected Fragment Size (bp)	RNA polymerase	RNaseA conc µg/ml
hGH	pG-hGH5'	*Pvu*II	338	SP6	10
GAPDH	pG-GAPM	*Dde*I	120	T7	10
hu G-CSF	pfGH-G	*Mlu*I	278	SP6	10
hu GM-CSF	pfGH-GM3C	*Nco*I	207	SP6	10
mouse GM-CSF	pG-musGM	*Xmn*I	160	T7	10
hu IL-10	pfGH-IL10	*Hind*III	246	SP6	10
fGH-G70	pfGH-G70	*Pvu*II	225	SP6	10
fGH-7,2	pfGH-7,2	*Pvu*II	190	SP6	10
c-*fos*	pG4-fos	*Stu*I	70	SP6	10
fGH-GM4	dfGH-GM4	*Msp*I	410	T7	10
mouse GM-CSF	dfGH-GM4	*Msp*I	310	T7	10
GHGM	CMV-GHGM	*Dra*I	230	SP6	10

Table II

Degradation rates of G-CSF and GM-CSF mRNAs in LPS-activated monocytes in the presence and absence of IL-10.

Exponential decay rate constants were calculated in 6 independent experiments. The mean ± SEM is shown for each mRNA. IL-10 destabilised both mRNAs in all 6 experiments.

	G-CSF		GM-CSF	
	- IL-10	+ IL-10	- IL-10	+ IL-10
K value[a]	-0.038±0.043	0.314±0.060	-0.133+/-0.074	0.592±0.206
P[b]		0.003		0.010
half life (h)	-[c]	2.540±0.04	-[c]	1.83±0.44

[a] First order rate constants assuming exponential decay.
[b] Two tailed Student's t test, paired two sample for means.
[c] No degradation was observed.

Table III

Degradation rates of IL-10 mRNA in LPS-activated monocytes in the presence and absence of IL-10.

Exponential decay rate constants were calculated in 5 independent experiments for each duration of exposure to IL-10. The mean ± SEM is shown for each treatment. IL-10 had no significant effect when added for 0.5 h but destabilised the IL-10 mRNA in all 5 experiments when added for 4 h.

	± IL-10 for 0.5 h		± IL-10 for 4 h	
	- IL-10	+ IL-10	-IL-10	+ IL-10
K value[a]	0.101±0.038	0.092±0.107	0.279±0.092	0.652±0.156
P[b]	0.92		0.026	
half life (h)	11.3±4.5	-[c]	8.3±5.9	1.74±0.78

[a] First order rate constants assuming exponential decay

[b] Two tailed Student's t test, paired two sample for means.

[c] No degradation was observed in some experiments, so an average halflife can not be calculated. However, converting the average rate constant to an " average" half life gives 7.5h.

Bibliography

Aghib, D.F., Bishop, J.M., Ottolenghi, S., Guerrasio, A., Serra, A., and Saglio, G. (1990). A 3' truncation of MYC caused by chromosomal translocation in a T-cell leukemia increases mRNA stability. Oncogene *5*, 707-711.

Ahern, S.M., Miyata, T., and Sadler, J.E. (1993). Regulation of human tissue factor expression by mRNA turnover. J. Biol. Chem. *268*, 2154-2159.

Akahane, K. and Pluznik, D.H. (1992). Interleukin-4 inhibits interleukin-1 alpha-induced granulocyte-macrophage colony-stimulating factor gene expression in a murine B-lymphocyte cell line via downregulation of RNA precursor. Blood *79*, 3188-3195.

Akashi, M., Saito, M., and Koeffler, H.P. (1989). Lymphotoxin: stimulation and regulation of colony-stimulating factors in fibroblasts. Blood *74*, 2383-2390.

Akashi, M., Shaw, G., Gross, M., Saito, M., and Koeffler, H.P. (1991). Role of AUUU sequences in stabilization of granulocyte-macrophage colony-stimulating factor RNA in stimulated cells. Blood *78*, 2005-2012.

Akashi, M., Shaw, G., Hachiya, M., Elstner, E., Suzuki, G., and Koeffler, P. (1994). Number and location of AUUUA motifs: role in regulating transiently expressed RNAs. Blood *83*, 3182-3187.

Alberta, J.A., Rundell, K., and Stiles, C.D. (1994). Identification of an activity that interacts with the 3'-untranslated region of c-myc mRNA and the role of its target sequence in mediating rapid mRNA degradation. J. Biol. Chem. *269*, 4532-4538.

Aviv, H., Voloch, Z., Bastos, R., and Levy, S. (1976). Biosynthesis and stability of globin mRNA in cultured erythroleukemic friend cells. Cell *8*, 495-503.

Bagby, G.C., Shaw, G., Heinrich, M.C., Hefeneider, S., Brown, M.A., DeLoughery, T.G., Segal, G.M., and Band, L. (1990). Interleukin-1 stimulation stabilizes GM-CSF mRNA in human vascular endothelial cells: preliminary studies on the role of the 3' AU rich motif. Prog. Clin. Biol. Res. *352*, 233-239.

Baumbach, W.R., Stanley, E.R., and Cole, M.D. (1987). Induction of clonal monocyte-macrophage tumors in vivo by a mouse c-*myc* retrovirus: rearrangement of the CSF-1 gene as a secondary transforming event. Molecular and Cellular Biology *7*, 664-671.

Beelman, C.A. and Parker, R. (1995). Degradation of mRNA in eukaryotes. Cell *81*, 179-183.

Berger, S.L. and Cooper, H.L. (1975). Very short-lived and stable mRNAs from resting human lymphocytes. Proc. Nat. Acad. Sci. USA *72*, 3873-3877.

Bernstein, P.L., Peltz, S.W., and Ross, J. (1989). The poly(A)-poly(A)-binding protein complex is a major determinant of mRNA stability in vitro. Mol. Cell Biol. *9*, 659-670.

Bhasker, C.R., Burgiel, G., Neupert, B., Emery Goodman, A., Kuhn, L.C., and May, B.K. (1993). The putative iron-responsive element in the human erythroid 5-aminolevulinate synthase mRNA mediates translational control. J. Biol. Chem. *268*, 12699-12705.

Bickel, M., Cohen, R.B., and Pluznik, D.H. (1990). Post-transcriptional regulation of GM-CSF synthesis in murine T cells. J. Immunol. *145*, 840-845.

Binder, R., Horowitz, J.A., Basilion, J.P., Koeller, D.M., Klausner, R.D., and Harford, J.B. (1994). Evidence that the pathway of transferrin receptor mRNA degradation involves an endonucleolytic cleavage within the 3' UTR and does not involve poly(A) tail shortening. EMBO J. *13*, 1969-1980.

Bird, T.A., Sleath, P.R., deRoos, P.C., Dower, S.K., and Virca, G.D. (1991). Interleukin-1 represents a new modality for the activation of extracellular signal-regulated kinases/microtubule-associated protein-2 kinases. J. Biol. Chem. *266*, 22661-22670.

Bird, T.A., Kyriakis, J.M., Tyshler, L., Gayle, M., Milne, A., and Virca, G.D. (1994). Interleukin-1 activates p54 mitogen-activated protein (MAP) kinase/stress-activated protein kinase by a pathway that is independent of p21ras, Raf-1, and MAP kinase kinase. J. Biol. Chem. *269*, 31836-31844.

Birnsteil, M.L., Busslinger, M., and Strub, K. (1985). Transcription termination and 3' processing: the end is in site!. Cell *41*, 349-359.

Bogdan, C., Vodovotz, Y., and Nathan, C. (1991). Macrophage deactivation by interleukin 10. J. Exp. Med. *174*, 1549-1555.

Bogdan, C., Paik, J., Vodovotz, Y., and Nathan, C. (1992). Contrasting mechanisms for suppression of macrophage cytokine release by transforming growth factor-beta and interleukin-10. J. Biol. Chem. *267*, 23301-23308.

Bohjanen, P.R., Petryniak, B., June, C.H., Thompson, C.B., and Lindsten, T. (1991). An inducible cytoplasmic factor (AU-B) binds selectively to AUUUA multimers in the 3' untranslated region of lymphokine mRNA. Mol. Cell Biol. *11*, 3288-3295.

Bohjanen, P.R., Petryniak, B., June, C.H., Thompson, C.B., and Lindsten, T. (1992). AU RNA-binding factors differ in their binding specificities and affinities. J. Biol. Chem. *267*,

Brewer, G. (1991). An A + U-rich element RNA-binding factor regulates c-myc mRNA stability in vitro. Mol. Cell Biol. *11*, 2460-2466.

Brewer, G. and Ross, J. (1988). Poly(A) shortening and degradation of the 3' A+U-rich sequences of human c-*myc* mRNA in a cell-free system. Mol. Cell Biol. *8*, 1697-1708.

Broudy, V.C., Kaushansky, K., Segal, G.M., Harlon, J.M., and Adamson, J.W. (1986). Tumor necrosis factor type α stimulates human endothelial cells to produce granulocyte/macrophage colony stimulating factor. Proc. Natl. Acad. Sci. USA *83*, 7467-7471.

Caput, D., Beutler, B., Hartog, K., Thayer, R., Brown-Shimer, S., and Cerami, A. (1986). Identification of a common nucleotide sequence in the 3'-untranslated region of mRNA molecules specifying inflammatory mediators. Proc. Natl. Acad. Sci. U. S. A. *83*, 1670-1674.

Casey, J.L., DiJeso, B., Rao, K., Klausner, K.D., and Harford, J.B. (1988). Two genetic loci participate in the regulation by iron of the gene for the human transferrin receptor. Proc. Natl. Acad. Sci. *85*, 1787-1791.

Casey, J.L., Koeller, D.M., Ramin, V.C., Klausner, R.D., and Harford, J.B. (1989). Iron regulation of transferrin receptor mRNA levels requires iron-responsive elements and a rapid turnover determinant in the 3' untranslated region of the mRNA. EMBO J. *8*, 3693-3699.

Cassatella, M.A., Meda, L., Gasperini, S., Calzetti, F., and Bonora, S. (1994). Interleukin 10 (IL-10) upregulates IL-1 receptor antagonist production from lipopolysaccharide-stimulated human polymorphonuclear leukocytes by delaying mRNA degradation. J. Exp. Med. *179*, 1695-1699.

Castagna, M., Takai, Y., Kaibuchi, K., Sano, K., Kikkawa, U., and Nishizuka, Y. (1982). Direct activation of calcium-activated, phospholipid-dependent protein kinase by tumor-promoting phorbol esters. The Journal of Biological Chemistry *257*, 7847-7851.

Chan, J.Y., Slamon, D.J., Nimer, S.D., Golde, D.W., and Gasson, J.C. (1986). Regulation of expression of human granulocyte/macrophage colony-stimulating factor. Proc. Natl. Acad. Sci. USA *83*, 8669-8673.

Chen, C.Y. and Shyu, A.B. (1994). Selective degradation of early-response-gene mRNAs: functional analyses of sequence features of the AU-rich elements. Mol. Cell Biol. *14*, 8471-8482.

Chen, C.Y.A., Xu, N., and Shyu, A.B. (1995). mRNA decay mediated by two distinct AU-rich elements from c-*fos* and granulocyte-macrophage colony stimulating factor transcripts: different deadenylation kinetics and uncoupling from translation. Molecular and Cellular Biology *15*, 5777-5788.

Chen, F.Y., Amara, F.M., and Wright, J.A. (1993). Mammalian ribonucleotide reductase R1 mRNA stability under normal and phorbol ester stimulating conditions: involvement of a cis-trans interaction at the 3' untranslated region. EMBO J. *12*, 3977-3986.

Chiu, R., Boyle, W.J., Meek, J., Smeal, T., Hunter, T., and Karin, M. (1988). The c-fos protein interacts with c-Jun/AP1 to stimulate transcription of AP-1 responsive genes. Cell *54*, 541-552.

Clark, S.C. and Kamen, R. (1987). The human hematopoietic colony-stimulating factors. Science *236*, 1229-1237.

Conrad, D.H., Waldschmidt, T.J., Lee, W.T., Rao, M., Keegan, A.D., Noelle, R.J., Lynch, R.G., and Kehry, M.R. (1987). Effect of B cell stimulatory factor-1 (interleukin 4) on Fc_{ϵ} and Fc receptor expression on murine B lymphocytes and B cell lines. The Journal of Immunology *139*, 2290-2296.

Cox, T.C., Bawden, M.J., Martin, A., and May, B.K. (1991). Human erythroid 5-aminolevulinate synthase: promoter analysis and identification of an iron-responsive element in the mRNA. EMBO J. *10*, 1891-1902.

Curatola, A.M., Nadal, M.S., and Schneider, R.J. (1995). Rapid degradation of AU-rich element (ARE) mRNAs is activated by ribosome transit and blocked by secondary structure at any position 5' to the ARE. Mol. Cell Biol. *15*, 6331-6340.

D'Andrea, A., Ma, X., Aste Amezaga, M., Paganin, C., and Trinchieri, G. (1995). Stimulatory and inhibitory effects of interleukin (IL)-4 and IL-13 on the production of cytokines by human peripheral blood mononuclear cells: priming for IL-12 and tumor necrosis factor alpha production. J. Exp. Med. *181*, 537-546.

Dandekar, T., Stripecke, R., Gray, N.K., Goossen, B., Constable, A., Johansson, H.E., and Hentze, M.W. (1991). Identification of a novel iron-responsive element in murine and human erythroid delta-aminolevulinic acid synthase mRNA. EMBO J. *10*, 1903-1909.

de Waal Malefyt, R., Abrams, J., Bennett, B., Figdor, C.G., and de Vries, J.E. (1991). Interleukin 10(IL-10) inhibits cytokine synthesis by human monocytes: an autoregulatory role of IL-10 produced by monocytes. J. Exp. Med. *174*, 1209-1220.

de Waal Malefyt, R., Figdor, C.G., Huijbens, R., Mohan Peterson, S., Bennett, B., Culpepper, J., Dang, W., Zurawski, G., and de Vries, J.E. (1993). Effects of IL-13 on phenotype, cytokine production, and cytotoxic function of human monocytes. Comparison with IL-4 and modulation by IFN-gamma or IL-10. J. Immunol. *151*, 6370-6381.

Decker, C.J. and Parker, R. (1993). A turnover pathway for both stable and unstable mRNAs in yeast: evidence for a requirement for deadenylation. Genes Dev. *7*, 1632-1643.

Defrance, T., Aubry, J.P., Rousset, F., Vanbervliet, B., Bonnefoy, J.Y., Arai, N., Takabe, Y., Yokata, T., Lee, F., Arai, K., deVries, J., and Banchereau, J. (1987). Human recombinant interleukin 4 induces Fcϵ receptors (CD23) on normal human B lymphocytes. J. Exp. Med. *165*, 1459-1467.

Dokter, W.H., Esselink, M.T., Sierdsema, S.J., Halie, M.R., and Vellenga, E. (1993). Transcriptional and posttranscriptional regulation of the interleukin-4 and interleukin-3 genes in human T cells. Blood *81*, 35-40.

Donnelly, R.P., Fenton, M.J., Kaufman, J.D., and Gerrard, T.L. (1991). IL-1 expression in human monocytes is transcriptionally and posttranscriptionally regulated by IL-4. J. Immunol. *146*, 3431-3436.

Eckner, R., Ellmeier, W., and Birnstiel, M.L. (1991). Mature mRNA 3' end formation stimulates RNA export from the nucleus. EMBO J. *10*, 3513-3522.

Eick, D., Piechaczyk, M., Henglein, B., Blanchard, J.M., Traub, B., Kofler, E., Wiest, S., Lenoir, G.M., and Bornkamm, W. (1985). Aberrant c-*myc* RNAs of Burkitt's lymphoma cells have longer half-lives. The EMBO Journal *4*, 3717-3725.

Ernst, T.J., Ritchie, A.R., Demetri, G.D., and Griffin, J.D. (1989). Regulation of granulocyte- and monocyte-colony stimulating factor mRNA levels in human blood monocytes is mediated primarily at a post-transcriptional level. J. Biol. Chem. *264*, 5700-5703.

Espevik, T., Figari, I.S., Shalaby, M.R., Lackides, G.A., Lewis, G.D., Shepard, M.H., and Palladino, M.A. (1987). Inhibition of Cytokine Production by Cyclosporin A and Transforming Growth Factor β. J. Exp. Med. *166*, 571-576.

Falkenburg, J.H., Harrington, M.A., de Paus, R.A., Walsh, W.K., Daub, R., Landegent, J.E., and Broxmeyer, H.E. (1991). Differential transcriptional and posttranscriptional regulation of gene expression of the colony-stimulating factors by interleukin-1 and fetal bovine serum in murine fibroblasts. Blood *78*, 658-665.

Fiorentino, D.F., Bond, M.W., and Mossman, T.R. (1989). Two types of mouse helper T cell. IV. Th2 clones secrete a factor that inhibits cytokine production by Th1 clones. J. Exp. Med. *170*, 2081-2095.

Fiorentino, D.F., Zlotnik, A., Mosmann, T.R., Howard, M., and O'Garra, A. (1991). IL-10 inhibits cytokine production by activated macrophages. J. Immunol. *147*, 3815-3822.

Gick, O., Kramer, A., Keller, W., and Birnstiel, M.L. (1986). Generation of histone mRNA 3' ends by endonucleolytic cleavage of the pre-mRNA in a snRNP-dependent *in vitro* reaction. The EMBO Journal *5*, 1319-1326.

Gillis, P. and Malter, J.S. (1991). The adenosine-uridine binding factor recognizes the AU-rich elements of cytokine, lymphokine, and oncogene mRNAs. J. Biol. Chem. *266*, 3172-3177.

Go, N.F., Castle, B.E., Barrett, R., Kastelein, R., Dang, W., Mosmann, T.R., Moore, K.W., and Howard, M. (1990). Interleukin 10, a novel B cell stimulatory factor: unresponsiveness of X chromosome-linked immunodeficiency B cells. J. Exp. Med. *172*, 1625-1631.

Gorospe, M., Kumar, S., and Baglioni, C. (1993). Tumor necrosis factor increases stability of interleukin-1 mRNA by activating protein kinase C. J. Biol. Chem. *268*, 6214-6220.

Greenberg, M.E., Hermanowski, A.L., and Ziff, E.B. (1986). Effect of protein synthesis inhibitors on growth factor activation of c-*fos*, c-*myc*, and actin gene transcription. Molecular and Cellular Biology *6*, 1050-1057.

Greenberg, M.E. and Ziff, E.B. (1984). Stimulation of 3T3 cells induces transcription of the *c-fos* proto-oncogene. Nature *311*, 433-438.

Gruber, M.F., Williams, C.C., and Gerrard, T.L. (1994). Macrophage-colony-stimulating factor expression by anti-CD45 stimulated human monocytes is transcriptionally up-regulated by IL-1 beta and inhibited by IL-4 and IL-10. J. Immunol. *152*, 1354-1361.

Hagan, K.W., Ruiz-Echevarria, M.J., Quan, Y., and Peltz, S.W. (1995). Characterisation of *cis*-acting sequences and decay intermediates involved in nonsense-mediated mRNA turnover. Molecular and Cellular Biology *15*, 809-823.

Hahn, S., Wodnar Filipowicz, A., Nair, A.P., and Moroni, C. (1991). Ras oncogenes amplify lymphokine (interleukin 3, granulocyte-macrophage colony-stimulating factor) induction by calcium ionophore. Oncogene *6*, 2327-2332.

Hamilton, J.A. (1994). Coordinate and noncoordinate colony stimulating factor formation by human monocytes. J. Leukoc. Biol. *55*, 355-361.

Han, J. and Beutler, B. (1990). Endotoxin-responsive sequences control cachectin/tumor necrosis factor biosynthesis at the translational level. J. Exp. Med. *171*, 465-475.

Hart, P.H., Vitti, G.F., Burgess, D.R., Whitty, G.A., Piccoli, D.S., and Hamilton, J.A. (1989). Potential antiinflammatory effects of interleukin 4: suppression of human monocyte tumor necrosis factor α, interleukin 1, and prostaglandin E_2. Proc. Natl. Acad. Sci. USA *86*, 3803-3807.

He, F., Peltz, S.W., Donahue, J.L., Rosbash, M., and Jacobson, A. (1993). Stabilization and ribosome association of unspliced pre-mRNAs in a yeast upf1- mutant. Proc. Natl. Acad. Sci. U. S. A. *90*, 7034-7038.

Hentze, M.W., Caughman, W.S., Roualt, T.A., Barriocanal, J.G., Dancis, A., Harford, J.B., and Klausner, R.D. (1987). Identification of the iron-responsive element for the translational regulation of human ferritin mRNA. Science *231*, 1570-1573.

Herrick, D.J. and Ross, J. (1994). The half-life of c-myc mRNA in growing and serum-stimulated cells: influence of the coding and 3' untranslated regions and role of ribosome translocation. Mol. Cell Biol. *14*, 2119-2128.

Hollis, G.F., Gazdar, A.F., Bertness, V., and Kirsch, I.R. (1988). Complex translocation disrupts c-*myc* regulation in a human plasma cell myeloma. Mol. Cell. Biol. *8*, 124-129.

Horowitz, J.B., Kaye, J., Conrad, P.J., Katz, M.E., and Janeway, C.A. (1986). Autocrine growth inhibition of a cloned line of helper T cells. Proc. Natl. Acad. Sci. U. S. A. *83*, 1886-1890.

Howard, M., Farrar, J., Hilfiker, M., Johnson, B., Takatsu, K., Hamaoka, T., and Paul, W.E. (1982). Identification of a T cell-derived B cell growth factor distinct from interleukin 2. J. Exp. Med. *155*, 914-923.

Hsu, D.H., Moore, K.W., and Spits, H. (1992). Differential effects of IL-4 and IL-10 on IL-2-induced IFN-gamma synthesis and lymphokine-activated killer activity. Int. Immunol. *4*, 563-569.

Hudak, S.A., Gollnick, S.O., Conrad, D.H., and Kehry, M.R. (1987). Murine B-cell stimulatory factor 1 (interleukin 4) increases expression of the Fc receptor for IgE on mouse B cells. Proc. Natl. Acad. Sci. USA *84*, 4606-4610.

Iwai, Y., Bickel, M., Pluznik, D.H., and Cohen, R.B. (1991). Identification of sequences within the murine Granulocyte-Macrophage Colony-stimulating Factor mRNA 3'-untranslated region that mediate mRNA stabilization induced by mitogentreatment of EL-4 thyoma cells. J. Biol. Chem. *266*, 17959-17965.

Iwai, Y., Akahane, K., Pluznik, D.H., and Cohen, R.B. (1993). Ca2+ ionophore A23187-dependent stabilization of granulocyte-macrophage colony-stimulating factor messenger RNA in murine thymoma EL-4 cells is mediated through two distinct regions in the 3'-untranslated region. J. Immunol. *150*, 4386-4394.

Kasama, T., Strieter, R.M., Lukacs, N.W., Burdick, M.D., and Kunkel, S.L. (1994). Regulation of neutrophil-derived chemokine expression by IL-10. J. Immunol. *152*, 3559-3569.

Kikinis, Z., Eisenstein, R.S., Bettany, A.J., and Munro, H.N. (1995). Role of RNA secondary structure of the iron-responsive element in translational regulation of ferritin synthesis. Nucleic. Acids. Res. *23*, 4190-4195.

Klausner, R.D., Rouault, T.A., and Harford, J.B. (1993). Regulating the fate of mRNA: the control of cellular iron metabolism. Cell *72*, 19-28.

Koeffler, H.P., Gasson, J., and Tobler, A. (1988). Transcriptional and posttranscriptional modulation of myeloid colony-stimulationg factor expression by TNF and other agents. Mol. Cell Biol. *8*, 3432-3438.

Krowczynska, A., Yenofsky, R., and Brawerman, G. (1985). Regulation of messenger RNA stability in mouse erythroleukemia cells. J. Mol. Biol. *181*, 231-239.

Lagnado, C.A., Brown, C.Y., and Goodall, G.J. (1994). AUUUA is not sufficient to promote poly(A) shortening and degradation of an mRNA: the functional sequence within AU-rich elements may be UUAUUUA(U/A)(U/A). Mol. Cell. Biol. *14*, 7984-7995.

Larimer, F.W. and Stevens, A. (1990). Disruption of the gene XRN1, coding for a 5'-3' exoribonuclease, restricts yeast cell growth. Gene *95*, 85-90.

Le, J., Weinstein, D., Gubler, U., and Vilcek, J. (1987). Induction of membrane-associated interleukin 1 by tumor necrosis factor in human fibroblasts. The Journal of Immunology *138*, 2137-2142.

Le, P.T., Lazorick, S., Whichard, L.P., Haynes, B.F., and Singer, K.H. (1991). Regulation of cytokine production in the human thymus: epidermal growth factor and transforming growth factor alpha regulate mRNA levels of interleukin 1 alpha (IL-1 alpha), IL-1 beta, and IL-6 in human thymic epithelial cells at a post-transcriptional level. J. Exp. Med. *174*, 1147-1157.

Leeds, P., Wood, J.M., Lee, B.S., and Culbertson, M.R. (1992). Gene products that promote mRNA turnover in Saccharomyces cerevisiae. Mol. Cell Biol. *12*, 2165-2177.

Lieberman, A.P., Pitha, P.M., and Shin, M.L. (1990). Protein kinase regulates tumor necrosis factor mRNA stability in virus-stimulated astrocytes. J. Exp. Med. *172*, 989-992.

Losson, R. and Lacroute, F. (1979). Interference of nonsense mutations with eukaryotic messenger RNA stability. Proc. Natl. Acad. Sci. USA *76*, 5134-5137.

Lowell, J.E., Rudner, D.Z., and Sachs, A.B. (1992). 3'-UTR-dependent deadenylation by the yeast poly(A) nuclease. Genes Dev. *6*, 2088-2099.

Malter, J.S. (1989). Identification of an AUUUA-specific messenger RNA binding protein. Science *246*, 664-666.

Malter, J.S. and Hong, Y. (1991). A redox switch and phosphorylation are involved in the post-translational up-regulation of the adenosine-uridine binding factor by phorbol ester and ionophore. J. Biol. Chem. *266*, 3167-3171.

Meijlink, F., Curran, T., Miller, D., and Verma, I.M. (1985). Removal of a 67-base pair sequence in the noncoding region of protooncogene *fos* converts it to a transforming gene. Proc. Natl. Acad. Sci. U. S. A. *82*, 4987-4991.

Moore, K.W., O'Garra, A., de Waal Malefyt, R., Vieira, P., and Mosmann, T.R. (1993). Interleukin-10. Annu. Rev. Immunol. *11*, 165-190.

Muhlrad, D., Decker, C.J., and Parker, R. (1994). Deadenylation of the unstable mRNA encoded by the yeast MFA2 gene leads to decapping followed by 5'-->3' digestion of the transcript. Genes Dev. *8*, 855-866.

Muhlrad, D., Decker, C.J., and Parker, R. (1995). Turnover mechanisms of the stable yeast PGK1 mRNA. Mol. Cell Biol. *15*, 2145-2156.

Muhlrad, D. and Parker, R. (1994). Premature translational termination triggers mRNA decapping. Nature *370*, 578-581.

Mukaida, A., Kasahara, T., Yagisawa, H., Shioiri-Nakano, K., and Kawai, T. (1987). Signal requirement for interleukin 1-dependent interleukin 2 production by a human leukemia-derived HSB.2 subclone. The Journal of Immunology *139*, 3321-3329.

Mullner, E.W. and Kuhn, K.C. (1988). a stem-loop in the 3' untranslated region mediates iron-dependent regulation of transferrin receptor mRNA stability in the cytoplasm. Cell *53*, 815-825.

Nakagawa, J., Waldner, H., Meyer Monard, S., Hofsteenge, J., Jeno, P., and Moroni, C. (1995). AUH, a gene encoding an AU-specific RNA binding protein with intrinsic enoyl-CoA hydratase activity. Proc. Natl. Acad. Sci. U. S. A. *92*, 2051-2055.

Nanbu, R., Menoud, P.A., and Nagamine, Y. (1994). Multiple instability-regulating sites in the 3' untranslated region of the urokinase-type plasminogen activator mRNA. Mol. Cell Biol. *14*, 4920-4928.

Nielsen, F.C. and Christiansen, J. (1992). Endonucleolysis in the turnover of insulin-like growth factor II mRNA. J. Biol. Chem. *267*, 19404-19411.

Nishizuka, Y. (1984). Role of protein kinase c in cell surface signal transduction and tumour promotion. Nature *308*, 693-698.

Noelle, R., Krammer, P.H., Ohara, J., Uhr, J.W., and Vitetta, E.S. (1984). Increased expression of Ia antigens on resting B cells: an additional role for B-cell growth factor. Proc. Natl. Acad. Sci. USA *81*, 6149-6153.

Ohara, J. and Paul, W.E. (1988). Up-regulation of interleukin 4/B-cell stimulatory factor 1 receptor expression. Proc. Natl. Acad. Sci. USA *85*, 8221-8225.

Ohh, M., Smith, C.A., Carpenito, C., and Takei, F. (1994). Regulation of intercellular adhesion molecule-1 gene expression involves multiple mRNA stabilization mechanisms: effects of interferon-gamma and phorbol myristate acetate. Blood *84*, 2632-2639.

Oswald, I.P., Gazzinelli, R.T., Sher, A., and James, S.L. (1992). IL-10 synergizes with IL-4 and transforming growth factor-beta to inhibit macrophage cytotoxic activity. J. Immunol. *148*, 3578-3582.

Pandey, N.B., Williams, A.S., Sun, J.H., Brown, V.D., Bond, U., and Marzluff, W.F. (1994). Point mutations in the stem-loop at the 3' end of mouse histone mRNA reduce expression by reducing the efficiency of 3' end formation. Mol. Cell Biol. *14*, 1709-1720.

Pandey, N.B. and Marzluff, W.F. (1987). The stem-loop structure at the 3' end of histone mRNA is necessary and sufficient for regulation of histone mRNA stability. Molecular and Cellular Biology *7*, 4557-4559.

Peltz, S.W., Brown, A.H., and Jacobson, A. (1993). mRNA destabilization triggered by premature translational termination depends on at least three cis-acting sequence elements and one trans-acting factor. Genes Dev. *7*, 1737-1754.

Peppel, K., Vinci, J.M., and Baglioni, C. (1991). The AU-rich sequences in the 3' untranslated region mediate the increased turnover of interferon mRNA induced by glucocorticoids. J. Exp. Med. *173*, 349-355.

Piechaczyk, M., Yang, J.Q., Blanchard, J.M., Jeanteur, P., and Marcu, B. (1985). Posttranscriptional mechanisms are responsible for accumulation of truncated c-*myc* RNAs in murine plasma cell tumors. Cell *42*, 589-597.

Powrie, F., Menon, S., and Coffman, R.L. (1993). Interleukin-4 and interleukin-10 synergize to inhibit cell-mediated immunity in vivo. Eur. J. Immunol. *23*, 3043-3049.

Prendergast, G.C. and Cole, M.D. (1989). Posttranscriptional regulation of cellular gene expression by the c-*myc* oncogene. Molecular and Cellular Biology *9*, 124-134.

Pulak, R. and Anderson, P. (1993). mRNA surveillance by the *Caenorhabditis elegans smg* genes. Genes and Development *7*, 1885-1897.

Raj, N.B.K. and Pitha, P.M. (1981). Analysis of interferon mRNA in human fibroblast cells induced to produce interferon. Proc. Natl. Acad. Sci. USA *78*, 7426-7430.

Rajagopalan, L.E. and Malter, J.S. (1994). Modulation of granulocyte-macrophage colony-stimulating factor mRNA stability in vitro by the adenosine-uridine binding factor. J. Biol. Chem. *269*, 23882-23888.

Ramani, M., Ollivier, V., Ternisien, C., Vu, T., Elbim, C., Hakim, J., and de Prost, D. (1993). Interleukin 4 prevents the induction of tissue factor mRNA in human monocytes in response to LPS or PMA stimulation. Br. J. Haematol. *85*, 462-468.

Roehm, N.W., Leibson, H.J., Zlotnik, A., Kappler, J., Marrack, P., and Cambier, J.C. (1984). Interleukin-induced increase in Ia expression by normal mouse B cells. J. Exp. Med. *160*, 679-6994.

Ross, H.J., Sato, N., Ueyama, Y., and Koeffler, H.P. (1991). Cytokine messenger RNA stability is enhanced in tumor cells. Blood *77*, 1787-1795.

Rouault, T.A., Hentze, M.W., Caughman, S.R., Harford, J.B., and Klausner, R.B. (1988). Binding of a cytosolic protein to the iron-responsive element of human ferritin messenger RNA. Science *241*, 1207-1210.

Rousset, F., Garcia, E., Defrance, T., Peronne, C., Vezzio, N., Hsu, D.H., Kastelein, R., Moore, K.W., and Banchereau, J. (1992). Interleukin 10 is a potent growth and differentiation factor for activated human B lymphocytes. Proc. Natl. Acad. Sci. U. S. A. *89*, 1890-1893.

Sachs, A. and Wahle, E. (1993). Poly(A) tail metabolism and function in eucaryotes. J. Biol. Chem. *268*, 22955-22958.

Sanger, F., Nicklens, S., and Coulson, A.R. (1977). DNA sequencing with chain terminating inhibitors. Proc. Natl. Acad. Sci. USA *74*, 5463-5467.

Savant Bhonsale, S. and Cleveland, D.W. (1992). Evidence for instability of mRNAs containing AUUUA motifs mediated through translation-dependent assembly of a > 20S degradation complex. Genes Dev. *6*, 1927-1939.

Schiavi, S.C., Wellington, C.L., Shyu, A.B., Chen, C.Y., Greenberg, M.E., and Belasco, J.G. (1994). Multiple elements in the c-fos protein-coding region facilitate mRNA deadenylation and decay by a mechanism coupled to translation. J. Biol. Chem. *269*, 3441-3448.

Schuler, G.D. and Cole, M.D. (1988). GM-CSF and oncogene mRNA stabilities are independently regulated in *trans* in a mouse monocytic tumor. Cell *55*, 1115-1122.

Shaw, G. and Kamen, S. (1986). A conserved AU sequence from the 3' untranslated region of GM-CSF mRNA mediates selective degradation. Cell *46*, 659-667.

Shyu, A.B., Greenberg, M.E., and Belasco, J.G. (1989). The c-fos transcript is targeted for rapid decay by two distinct mRNA degradation pathways. Genes Dev. *3*, 60-72.

Shyu, A.B., Belasco, J.G., and Greenberg, M.E. (1991). Two distinct destabilizing elements in the c-fos message trigger deadenylation as a first step in rapid mRNA decay. Genes Dev. *5*, 221-231.

Sieff, C.A., Niemeyer, C.M., Mentzer, S.J., and Faller, D.V. (1988). Interleukin-1, tumor necrosis factor, and the production of colony-stimuulating factors by cultured mesenchymal cells. Blood *72*, 1316-1323.

Snapper, C.M. and Paul, W.E. (1987). B cell stimulatory factor-1 (interleukin 4) prepares resting B cells to secrete IgG1 upon subsequent stimulation with bacterial lipopolysaccharide. The Journal of Immunology *139*, 10-17.

Takanaski, S., Nonaka, R., Xing, Z., O'Byrne, P., Dolovich, J., and Jordana, M. (1994). Interleukin 10 inhibits lipopolysaccharide-induced survival and cytokine production by human peripheral blood eosinophils. J. Exp. Med. *180*, 711-715.

te Velde, A.A., Huijbens, R.J.F., Heije, K., de Vries, J.E., and Figdor, C.G. (1990). Interleukin-4 (IL-4) inhibits secretion of IL-1β, tumour necrosis factor α, and IL-6 by human monocytes. Blood *76*, 1392-1397.

Thompson Snipes, L., Dhar, V., Bond, M.W., Mosmann, T.R., Moore, K.W., and Rennick, D.M. (1991). Interleukin 10: a novel stimulatory factor for mast cells and their progenitors. J. Exp. Med. *173*, 507-510.

Thorens, B., Mermod, J.J., and Vassalli, P. (1987). Phagocytosis and inflammatory stimuli induce GM-CSF mRNA in macrophages through posttranscriptional regulation. Cell *48*, 671-679.

Tripp, C.S., Wolf, S.F., and Unanue, E.R. (1993). Interleukin 12 and tumor necrosis factor alpha are costimulators of interferon gamma production by natural killer cells in severe combined immunodeficiency mice with listeriosis, and interleukin 10 is a physiologic antagonist. Proc. Natl. Acad. Sci. U. S. A. *90*, 3725-3729.

Vakalopoulou, E., Schaack, J., and Shenk, T. (1991). A 32-kilodalton protein binds to AU-rich domains in the 3' untranslated regions of rapidly degraded mRNAs. Mol. Cell Biol. *11*, 3355-3364.

Vellenga, E., Rambaldi, A., Ernst, T.J., Ostapovicz, D., and Griffin, J.D. (1988). Independent regulation of M-CSF and G-CSF gene expression in human monocytes. Blood *71*, 1529-1532.

Vietor, I., Schwenger, P., Li, W., Schlessinger, J., and Vilcek, J. (1993). Tumor necrosis factor-induced activation and increased tyrosine phosphorylation of mitogen-activated protein (MAP) kinase in human fibroblasts. J. Biol. Chem. *268*, 18994-18999.

Vitetta, E.S., Ohara, J., Myers, C.D., Layton, J.E., Krammer, P.H., and Paul, W.E. (1985). Serological, biochemical and functional identity of B-cell-stimulatory factor 1 and B cell differentiation factor for IgG1. J. Exp. Med. *162*, 1726-1730.

Wang, P., Wu, P., Siegel, M.I., Egan, R.W., and Billah, M.M. (1994). IL-10 inhibits transcription of cytokine genes in human peripheral blood mononuclear cells. J. Immunol. *153*, 811-816.

Wang, P., Wu, P., Siegel, M.I., Egan, R.W., and Billah, M.M. (1995). Interleukin (IL)-10 inhibits nuclear factor kappa B (NF kappa B) activation in human monocytes. IL-10 and IL-4 suppress cytokine synthesis by different mechanisms. J. Biol. Chem. *270*, 9558-9563.

Weeks, K.M. and Crothers, D.M. (1991). RNA recognition by Tat-derived peptides: interaction in the major groove? [published erratum appears in Cell 1992 Sep 18; 70(6):following 1068]. Cell *66*, 577-588.

Wilimzig, M. (1985). LiCl boiling methods for plasmid mini-preps. Trends in Genetics 158

Williams, A.S. and Marzluff, W.F. (1995). The sequence of the stem and flanking sequences at the 3' end of histone mRNA are critical determinants for the binding of the stem-loop binding protein. Nucleic. Acids. Res. *23*, 654-662.

Wilson, T. and Treisman, R. (1988). Removal of poly(A) and consequent degradation of c-fos mRNA facilitated by 3' AU-rich sequences. Nature *363*, 396-399.

Winstall, E., Gamache, M., and Raymond, V. (1995). Rapid mRNA degradation mediated by the c-fos 3' AU-rich element and that mediated by the granulocyte-macrophage colony-stimulating factor 3' AU-rich element occur through similar polysome-associated mechanisms. Mol. Cell Biol. *15*, 3796-3804.

Wodnar-Filipowitz, A. and Moroni, C. (1990). Regulation of interleukin 3 mRNA expression in mast cells occurs at the posttranscriptional level and is mediated by calcium ions. Proc. Natl. Acad. Sci. USA *87*, 777-781.

Yamato, K., El-Hajjaoui, Z., Kuo, J.F., and Koeffler, H.P. (1989). Granulocyte-Macrophage Colony Stimulating Factor: signals for its mRNA accumulation. Blood *74*, 1314-1320.

Yang, L. and Yang, Y.C. (1994). Regulation of interleukin (IL)-11 gene expression in IL-1 induced primate bone marrow stromal cells. J. Biol. Chem. *269*, 32732-32739.

Ziegler-Heitbrock, H.W.L., Thiel, E., Futterer, A., Herzog, V., Wirtz, A., and Riethmuller, G. (1988). Establishment of a human cell line (monomac 6) with characteristics of mature monocytes. Int. J. Cancer. *41*, 456-461.

Zubiaga, A.M., Belasco, J.G., and Greenberg, M.E. (1995). The nonamer UUAUUUAUU is the key AU-rich sequence motif that mediates mRNA degradation. Mol. Cell Biol. *15*, 2219-2230.

Publications

MOLECULAR AND CELLULAR BIOLOGY, Dec. 1994, p. 7984–7995
0270-7306/94/$04.00+0

Vol. 14, No. 12

AUUUA Is Not Sufficient To Promote Poly(A) Shortening and Degradation of an mRNA: the Functional Sequence within AU-Rich Elements May Be UUAUUUA(U/A)(U/A)

CATHY A. LAGNADO,[1] CHERYL Y. BROWN,[1,2] AND GREGORY J. GOODALL[1]*

Hanson Centre for Cancer Research, Division of Human Immunology, The Institute of Medical and Veterinary Science, Adelaide, South Australia 5000,[1] and Department of Microbiology and Immunology, The University of Adelaide, Adelaide, South Australia 5001,[2] Australia

Received 22 March 1994/Returned for modification 12 May 1994/Accepted 13 July 1994

AU-rich elements (AREs) in the 3′ untranslated regions of several cytokine and oncogene mRNAs have been shown to function as signals for rapid mRNA degradation, and it is assumed that the many other cytokine and oncogene mRNAs that contain AU-rich sequences in the 3′ untranslated region are similarly targeted for rapid turnover. We have used a chimeric gene composed mostly of growth hormone sequences with expression driven by the c-*fos* promoter to investigate the minimal sequence required to act as a functional destabilizing element and to monitor the effect of these sequences on early steps in the degradation pathway. We find that neither AUUUA, UAUUUA, nor AUUUAU can function as a destabilizing element. However, the sequence UAUUUAU, when present in three copies, is sufficient to destabilize a chimeric mRNA. We propose that this sequence functions by virtue of being a sufficient portion of the larger sequence, UUAUUUA(U/A)(U/A), that we propose forms the optimal binding site for a destabilizing factor. The destabilizing effect depends on the number of copies of this proposed binding site and their degree of mismatch in the first two and last two positions, with mismatches in the AUUUA sequence not being tolerated. We found a strict correlation between the effect of an ARE on degradation rate and the effect on the rate of poly(A) shortening, consistent with deadenylation being the first and rate-limiting step in degradation, and the step stimulated by destabilizing AREs. Deadenylation was observed to occur in at least two phases, with an oligo(A) intermediate transiently accumulating, consistent with the suggestion that the degradation processes may be similar in yeast and mammalian cells. AREs that are especially U rich and contain no UUAUUUA(U/A)(U/A) motifs failed to influence the degradation rate or the deadenylation rate, either when downstream of suboptimal destabilizing AREs or when alone.

The half-lives of mRNAs in eukaryotic cells vary widely, ranging from minutes to days, and it is now recognized that the control of mRNA degradation rate is an important level at which gene expression can be regulated (for recent reviews, see references 6 and 43). Many transiently expressed cellular growth regulators (for example, proto-oncogene products and cytokines) are encoded by messages with half-lives as short as 1 h or less. In addition, many cytokine mRNAs can be stabilized considerably, for example, in response to proinflammatory agents (4, 31). Such short but regulatable half-lives, in conjunction with changes in transcription rate, allow these growth factor mRNAs to be produced in a transient burst or reach a new steady-state level very rapidly.

One class of instability element, found in the 3′ untranslated regions (3′UTRs) of many unstable cytokine and oncogene mRNAs, is the AU-rich element (ARE). This is a loosely defined sequence, with the general feature of being U rich with interspersed A's. A regulatory role for AREs was first postulated by Caput et al. (15), who identified a consensus sequence, UUAUUUAU, in a number of cytokine and oncogene mRNA sequences available at that time, although the function of this sequence was not tested. The observation of oncogenic forms of *fos* and *myc* with the region containing the ARE deleted from the gene (1, 26, 37) further suggested a role for these sequences in the control of mRNA stability. This hypothesis was tested by Shaw and Kamen (45), who showed that the 51-nucleotide (nt) ARE from human granulocyte-macrophage colony-stimulating factor mRNA could destabilize the normally stable rabbit β-globin mRNA when inserted into its 3′UTR. This effect was ablated by disrupting the AUUUA motifs within the ARE, directly implicating this sequence in destabilization of mRNA. The AREs from c-*fos*, c-*myc*, beta interferon, and tissue factor have also been shown to be destabilizing (3, 29, 48, 52). However, as AREs vary considerably in size and sequence, the salient features of a functional ARE have not been obvious, and it cannot necessarily be assumed that the presence of an AU-rich region is sufficient to destabilize an mRNA. The motif AUUUA is present in the 3′UTRs of many unstable mRNAs, and the notion that it is a destabilizing sequence has permeated the literature. However, there is to date no direct evidence that this motif alone can function. Indeed, it is possible that the destabilizing function of an ARE is mediated not by the primary sequence but by a secondary structure, since the strings of U present in many AREs could conceivably interact with the poly(A) tail (45, 53). (Precedents for an involvement of 3′ stem-loop structures in the regulation of mRNA stability are found in the transferrin receptor [16] and histone [40] mRNAs.) In addition, the minimal number of motifs required to destabilize an mRNA, whether additional copies have an additive effect, and the effect of the variable spacing observed between individual AU-rich sequences are all largely unknown. Since an understanding of these sequence requirements may contribute to determining the mechanism by which AREs enhance mRNA

* Corresponding author. Mailing address: Hanson Centre for Cancer Research, Division of Human Immunology, IMVS, Frome Rd., Adelaide, S.A. 5000, Australia. Phone: (61 8) 228 7430. Fax: (61 8) 232 4092. Electronic mail address: GGOODALL@IMMUNO.IMVS.SA.GOV.AU.

degradation, we have used a model system to assess the destabilizing potential of various small, defined AU-rich sequences by inserting them into the 3′UTR of a stable mRNA.

A general model for the pathway of mRNA degradation which incorporates the results of recent studies in the yeast *Saccharomyces cerevisiae* (21, 36, 38) has been proposed (21, 38, 43). This model is based on the suggestions that mRNAs are protected from digestion by the binding of poly(A)-binding protein (PABP) to the poly(A) tail (7, 11, 12) and that the first and perhaps rate-limiting phase of degradation is a progressive shortening of the poly(A) tail (12, 47, 53). The yeast poly(A) nuclease requires PABP for its activity, and after a slow initial phase, deadenylation proceeds more rapidly and in a distributive manner until the tail reaches an oligo(A) form, which may be sufficient to still bind one molecule of PABP (36). The body of the mRNA can then either be degraded immediately or first be completely deadenylated, a process called terminal deadenylation (21). In both cases, the degradation of the body of the mRNA occurs very rapidly, as neither poly(A)$^-$ mRNAs nor degradation intermediates are usually detectable (38). Both poly(A) shortening and decay of the oligo(A) species are more rapid in unstable yeast mRNAs (21, 38), with the first step being more processive (36). Degradation of the mRNA body was originally assumed to proceed exonucleolytically from the 3′ end (28), although in *S. cerevisiae*, degradation intermediates lacking the 5′ end (which must result from 5′-3′ exonucleolytic degradation following 5′ cap removal or endonucleolytic cleavage) have been recently identified by impeding the body degradation process (21, 51).

Degradation intermediates of several mammalian mRNAs have been observed, some of which may be products of either 3′ exonucleolytic degradation or endonucleolytic cleavage (12, 32, 49) and others of which are clearly the result of endonucleolytic cleavage in the 3′UTR (9, 13). Various nucleases proposed to be involved in degradation, including a 5′-3′ exonuclease (20), a sequence-specific endonuclease (13), and a nuclear poly(A) nuclease (5), have been purified. Mammalian mRNAs differ from yeast mRNAs in having considerably longer poly(A) tails, but at least for some mRNAs the process of degradation may be similar, and several studies suggest that the instability elements in yeasts and higher eukaryotes may target the same steps in a common degradation pathway (21, 38, 43). Studies of c-*fos* mRNA have suggested that deadenylation is the first step in degradation of this mRNA (53) and that the c-*fos* ARE can stimulate deadenylation of a heterologous mRNA (47). Tumor necrosis factor, c-*myc*, *gro*-α, and beta interferon mRNAs have also been shown to undergo deadenylation as the first stage in their degradation (12, 34, 35, 41, 49). The deadenylation rate decreases when these mRNAs are stabilized either by inhibiting translation (which has been shown to be necessary for degradation of ARE-containing mRNAs [2]) (34, 41, 49, 52, 53), deleting the ARE (48, 53), or inhibiting protein kinase C (35), and thus it has been suggested that AREs increase the degradation rate of an mRNA by increasing the rate of poly(A) shortening. On the other hand, experiments with the c-*fos* ARE have shown that degradation can be uncoupled from deadenylation and raised the possibility that different sequence motifs within the complex c-*fos* ARE may be responsible for the two phases of degradation (47).

We describe here the use of a chimeric gene to assess the effects of a number of simple AU-rich sequences on degradation of an otherwise stable mRNA. We find that some AU-rich sequences, including one which has four copies of the motif AUUUA and others which contain strings of U and could potentially form secondary structures with the poly(A) tail, have no destabilizing effect. We find that UAUUUAU can function when present in three copies and propose that a larger sequence, UUAUUUA(U/A)(U/A), forms the optimal binding site for a degradation factor. Sequences which stimulate degradation have a corresponding stimulatory effect on the rate of poly(A) shortening, both increasing the processivity of the first phase of the deadenylation reaction and increasing the rate of degradation of the oligoadenylated RNA which transiently accumulates prior to body degradation.

MATERIALS AND METHODS

Cell culture and transfection. Mouse NIH 3T3 cells were grown in Dulbecco's modified Eagle's medium (DMEM) with 10% fetal calf serum (FCS; Gibco). Cells (2×10^6 in 0.8 ml) were transfected with 20 μg of plasmid (linearized with *Sal*I) by electroporation (Bio-Rad Gene Pulser, 275 V, 960 μF) and grown for 3 days, and then colonies were selected in 400 μg of G418 sulfate (Geneticin; Gibco) per ml. After 10 to 12 days, colonies were pooled, and the pools were maintained in the presence of 200 μg of G418 sulfate per ml. For analysis of mRNA decay, 0.75×10^6 to 1.0×10^6 cells were plated onto 9-cm-diameter dishes, grown for 48 h in DMEM–10% FCS, then washed three times in phosphate-buffered saline, and serum starved in DMEM–0.5% FCS for 48 h prior to stimulation with DMEM–15% FCS.

Plasmid constructions. Where appropriate, 5′ or 3′ DNA protruding ends were made blunt by treatment with the Klenow fragment of DNA polymerase I or T4 DNA polymerase, respectively. Plasmid pfGH was prepared in multiple steps as follows. Plasmid pRcCMV (Invitrogen) was digested with *Eco*RI and *Kpn*I, blunt ended, and ligated shut to generate plasmid pRcCMVΔ2. Plasmid pG4BGH was prepared by inserting a 241-bp *Pvu*II-*Bcl*I fragment of pRcCMV, containing the bovine growth hormone 3′UTR and polyadenylation signals, into the *Eco*RI site of pGEM4Z (Promega). Plasmid pG4HGHBGH was prepared by inserting a 660-bp *Nco*I-*Sma*I fragment from plasmid pHGH (kindly provided by A. Robins, Bresatec Pty. Ltd., Adelaide, South Australia, Australia), containing the coding region of human growth hormone, into the *Sma*I site of pG4BGH. Plasmid pCMVGH was prepared by insertion of a 1,081-bp *Pvu*I-*Bam*HI fragment from pG4HGHBGH (containing the human growth hormone coding region, bovine growth hormone polyadenylation sequence, and SP6 promoter) into the *Eco*RI site of RcCMVΔ2. Plasmids pCMVGH7 to pCMVGH15 were prepared by insertion of oligonucleotides encoding the various ARE sequences shown in Fig. 1 between the *Kpn*I and *Sac*I sites of plasmid pCMVGH. Plasmids pCMVGH33, pCMVGH44, and pCMVGH55 were prepared by double insertion of oligonucleotides into the *Sac*I site of plasmid pCMVGH to encode the appropriate ARE sequences as shown in Fig. 1. These plasmids were digested with *Nru*I and *Hin*dIII to delete the cytomegalovirus promoter, and a 700-bp *Eco*RI-*Hin*dIII fragment of plasmid pfos3CAT (kindly provided by H. Iba and D. Cohen), containing the chicken c-*fos* promoter, was inserted to yield plasmids pfGH7 to pfGH15, pfGH33, pfGH44, and pfGH55. Plasmid pfGH733 was prepared by ligating a 1.4-kb *Sac*I fragment of pfGH7 to a 4.4-kb *Kpn*I fragment of pfGH33. Plasmids pfGH833 and pfGH1033 were prepared by ligating a 3.5-kb *Sac*I-*Pvu*I fragment of plasmids pfGH8 and pfGH10, respectively to a 3.6-kb *Kpn*I-*Pvu*I fragment of plasmid fGH33. All inserted ARE sequences were confirmed by dideoxynucleotide sequencing.

Plasmid pGAPM, containing a portion of the coding region of the human *GAPDH* cDNA, was prepared by inserting a 400-bp *Sac*II-*Hin*dIII fragment of plasmid pHcGAP (ATCC

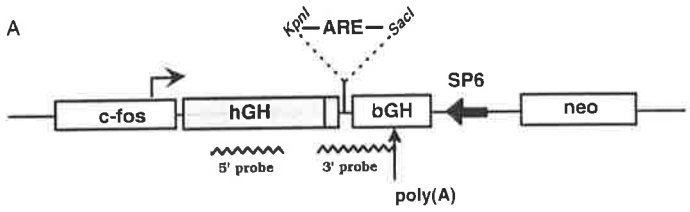

B

	KpnI ... SacI
ARE7	gguaccAUUUAUUUAUUUAUUUAUUUACUCgagcuc
ARE8	gguaccAUUUAAUUUAAUUUAAUUUAAUUUACUCgagcuc
ARE9	gguaccAUUAUUAUUAUUAUUAUUACUCgagcuc
ARE10	gguaccGGACGACAUUUAUUUAUUUACUCgagcuc
ARE11	gguaccCGAGCUGACGACAUUUAUUUACUCgagcuc
ARE12	gguaccUAUAUUAUAUUUAUUUAUAUUACUCgagcuc
ARE13	gguaccAUUUAUCACACAUUUAUCACACAUUUAUCUCgagcuc
ARE14	gguaccUAUUUACACACUAUUUACACACUAUUUACUCgagcuc
ARE15	gguaccUAUUUAUCACACUAUUUAUCACACUAUUUAUCUCgagcuc
ARE33	gagcugCAGUUUUUAUUUUUAUUUUUgagcugCAGUUUUUAUUUUUAUUUUUgagcuc
ARE44	gagcugCAGUUUUUUUUUAUUUUUUUUgagcugCAGUUUUUUUUUAUUUUUUUUgagcuc
ARE55	gagcugCAGAUUUAAAAAUUUAgagcugCAGAUUUAAAAAUUUAgagcuc

FIG. 1. The fGH gene and sequences of the various AREs inserted in the 3'UTR. (A) Schematic representation of the fGH gene. Boxes indicate segments of the gene that were derived from the chicken *c-fos* gene (c-fos), human growth hormone cDNA (hGH), and bovine growth hormone cDNA (bGH); plasmid-derived sequences are indicated by a line. The translated region is indicated by shading. The transcription start site, site of insertion of AREs, and the polyadenylation site are indicated. Also shown are the relative location of the SP6 promoter, used to make 3' probes for RNase protection assays, and the neomycin resistance gene. The regions protected by the 5' and 3' RNase protection probes are shown as zigzag lines. (B) Sequences of AREs inserted between the *Kpn*I and *Sac*I sites (ARE7 to ARE15) or into the *Sac*I site (ARE33 to ARE55). AUUUA motifs are underlined, and sequences from restriction sites used to insert the AREs are shown in lowercase.

57090) between the *Hin*cII and *Hin*dIII sites of plasmid pGEM-1 (Promega).

Analysis of mRNA decay and deadenylation. Total RNA was isolated at various times after serum stimulation of NIH 3T3 cells by the guanidine thiocyanate procedure of Chomczynski and Sacchi (18). Transcripts derived from transfected DNA and cellular *GAPDH* were detected by RNase protection analysis using in vitro-synthesized complementary RNA probes. The various fGH (growth hormone chimeric gene; Fig. 1) mRNAs were detected by using probes synthesized from the appropriate pfGH plasmids digested with *Pvu*II, using SP6 RNA polymerase and 200 Ci of [α-^{32}P]UTP per mmol (23). Depending on the size of the ARE inserted in the pfGH plasmid, the probes were complementary to 165 to 211 nt of the 3' terminus of the mRNA. The *GAPDH* mRNA was detected by using a probe complementary to a 120-nt internal fragment of the mouse *GAPDH* mRNA, synthesized from *Dde*I-digested plasmid pGAPM, using T7 RNA polymerase and 100 Ci of [α-^{32}P]UTP per mmol. Poly(A)$^-$ mRNA was prepared by using oligo(dT) and RNase H as described previously (12).

RNase protection assays were performed essentially as described previously (23), using 10 μg of RNA and digestion with RNase A (10 μg/ml) at 0°C, and analyzed on 6% polyacrylamide–8 M urea gels. For analysis of poly(A) tail length, the digestion products were dissolved in 10 μl of loading dye (0.04% bromophenol blue, 0.04% xylene cyanol, 10% glycerol, 1× Tris-borate-EDTA) and electrophoresed on nondenaturing 6% polyacrylamide gels in 1× Tris-borate-EDTA. It was not possible to measure actual poly(A) tail lengths on these gels, as appropriate fGH constructs encoding mRNAs with poly(A) tails of defined lengths were not available. Gels were run for appropriate times to ensure that the poly(A)$^-$ markers migrated to identical positions.

The amount of specific mRNA was quantitated by PhosphorImager analysis using Imagequant version 3.21 (Molecular Dynamics, Sunnyvale, Calif.) and normalized with respect to the *GAPDH* internal standard. Since the amount of *GAPDH* mRNA increased linearly for 8 h following serum stimulation, a regression line was fitted to the pooled *GAPDH* mRNA data and used to calculate the expected *GAPDH* mRNA level in each sample. Levels of fGH mRNA were normalized by multiplying by the ratio expected *GAPDH*/observed *GAPDH*. This correction avoids overestimating the instability of individual mRNAs and does not change the relative destabilizing effect of the various AREs.

RESULTS

A model system for studying the effects of AU-rich sequences on mRNA stability. To compare the effects on mRNA stability of various 3'UTR sequences, we constructed a chimeric gene (fGH; Fig. 1) containing the promoter and 5'UTR from *c-fos*, a translated region encoding human growth hormone, and a 3'UTR and downstream polyadenylation signals from bovine growth hormone. The *fos* promoter responds transiently to a shift from low to high serum in the culture medium, resulting in a pulse of transcription lasting less than 1 h, and has been used by others in studies of mRNA degradation (3, 17, 47, 48). This inducible promoter was used in preference to a constitutive promoter to allow mRNA degradation rates to be mea-

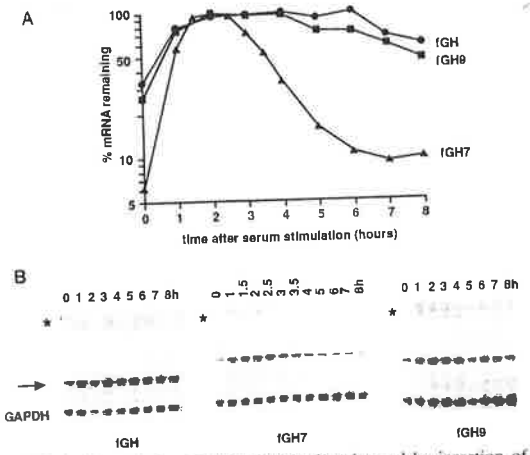

FIG. 2. Degradation of fGH mRNA is enhanced by insertion of ARE7. RNA was isolated at the times indicated following serum stimulation of NIH 3T3 cells stably expressing the fGH transcript with ARE7 (fGH7), ARE9 (fGH9), or no ARE (fGH) in the 3'UTR. (A) Time course of degradation. Specific mRNAs were quantitated by PhosphorImager analysis. (B) Phosphorimage of RNase protection gels. The fGH mRNA protection product is indicated by an arrow. The asterisk indicates the position of a larger transcript believed to result from usage of a downstream polyadenylation site.

sured without using transcription inhibitors, which have been shown in a number of situations to prolong the life of unstable mRNAs (3, 33, 46, 48, 52). A short synthetic sequence containing unique restriction sites was included within the 3'UTR to allow the insertion of various chemically synthesized oligonucleotides. For simplicity, we call each inserted sequence ARE*n*, with insertion of ARE*n* into fGH, generating fGH*n*. All sequences are presented in the RNA form. Polyclonal NIH 3T3 lines expressing the various chimeric genes were established, and the stability of the mRNAs was determined by using RNase protection analysis to quantitate the amount of specific transcript remaining at various times after induction of transcription.

The fGH transcript, which contains no AU-rich insert, decayed little during the 8 h of the time course (Fig. 2). This was expected since growth hormone mRNA, which makes up most of the transcript, has a half-life greater than 9 h (25, 39). To confirm that insertion of an ARE could destabilize the fGH mRNA, we inserted ARE7 (Fig. 1), containing the sequence AUUUAUUUAUUUAUUUAUUUA. This sequence is part of the granulocyte-macrophage colony-stimulating factor ARE that has been shown to destabilize β-globin mRNA when inserted into its 3'UTR (45). We used Northern (RNA) blot analysis to confirm that these and all other fGH variants used in this study express a single major mRNA species of the expected size (data not shown). As expected, the fGH7 mRNA was unstable; transcript levels were maximal between 1.5 and 2.5 h after induction with serum and declined rapidly thereafter (Fig. 2). Since the pulse of transcription lasts only 40 min (data not shown), there is a significant lag before the onset of degradation. We confirmed that the degradation rate of the 3'UTR measured in these experiments using the 3' RNase protection probe accurately reflected the degradation rate of the transcript by repeating the assays with a coding-region probe (Fig. 1). Since the rates obtained with the two probes were identical and no smaller degradation intermediates were detected (data not shown), it appears that once degradation of the body of the mRNA has commenced, it occurs very rapidly. With these, as with all fGH variants analyzed, a faint band was visible on the RNase protection gel at the position of full-length probe. This band is not due to incomplete RNase digestion and probably represents a small proportion of transcripts that are not cleaved at the growth hormone polyadenylation site, an interpretation supported by Northern blot analysis (data not shown). These longer transcripts degraded at the same rate as the major form of the mRNA.

To verify that the instability of the fGH7 mRNA was not due to disruption of sequences at the insertion site, or the result of a change in the spacing between stop codon and poly(A) tail, we inserted a different AU-rich sequence of similar length (AUUAUUAUUAUUAUUAUUA, ARE9; Fig. 1). The fGH9 mRNA was stable (Fig. 2), indicating that the effect of ARE7 was sequence dependent. This system was therefore considered suitable for analysis of the effects on mRNA stability of insertion of various AREs into the 3'UTR and was further used to define the sequence requirements of such destabilizing elements.

Multiple isolated copies of AUUUA do not destabilize. The motif AUUUA is present in the 3'UTRs of many unstable cytokine mRNAs and is often assumed to be the sequence within the ARE that is responsible for targeting the mRNA for rapid degradation. To test whether the sequence AUUUA in any context can target an mRNA for degradation, we prepared ARE55, which contains four copies of AUUUA separated by three to nine bases (GAUUUAAAAAUUUAGAGCUGCA GAUUUAAAAAUUUAG), and ARE8, in which five copies of AUUUA lie adjacent to each other (CAUUUAAUUUAA UUUAAUUUAAUUUAC). The choice of sequence to separate the AUUUA motifs in ARE55 was arbitrary, in that it was not based on any naturally occurring sequences; the central region is largely derived from restriction sites used in the construction of the ARE, and the AAA sequences were chosen to maintain AU richness in the region without creating a sequence similar to ARE7.

Little degradation of fGH55 mRNA was observed during 8 h (Fig. 3), showing that an appropriate context is required for the sequence AUUUA to affect the stability of an mRNA. The fGH8 mRNA was unstable but did not degrade as rapidly as fGH7 mRNA (Fig. 3) even though both AREs have five copies of AUUUA, further indicating that the effect of an ARE on mRNA stability is not determined solely by the number of AUUUA motifs that are present but depends on the context in which the AUUUA motifs reside. Since the sequence AUUUA alone is not sufficient to destabilize an mRNA, the flanking sequences in fGH7 and fGH8 must somehow contribute to their destabilizing effect. These flanking sequences may either contribute to the destabilizing sequence or provide a more optimal spacing between two such sequences, perhaps allowing a cooperative effect between the binding of two proteins, or both.

ARE7 and ARE8 increase the rate of poly(A) tail removal. By analyzing the poly(A) distribution profiles of mRNAs at various times after serum induction, it is possible to correlate the effects of different AREs on both deadenylation and degradation of the fGH mRNA and thus draw conclusions about whether the same sequences direct both shortening and degradation and about the relationship between these two processes. We therefore compared the rates of deadenylation of the unstable mRNAs, fGH7 and fGH8, with those of the stable mRNAs, fGH, fGH55, and fGH9.

To compare poly(A) shortening rates, the products of the

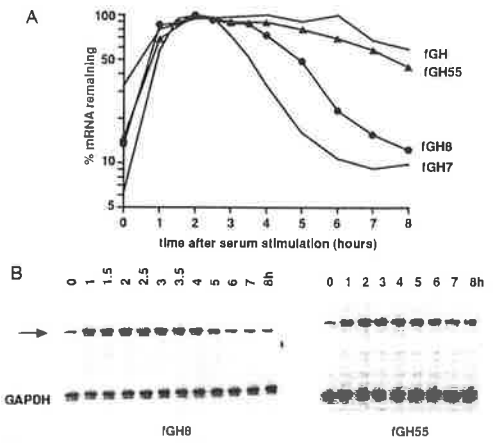

FIG. 3. Degradation of fGH mRNA is enhanced by ARE8 but not ARE55. RNA was isolated at the times indicated following serum stimulation of stably transfected NIH 3T3 cells expressing the fGH transcript with ARE55 (fGH55) or ARE8 (fGH8) in the 3′UTR. (A) Time course of degradation of the fGH55 and fGH8 mRNAs. Specific mRNAs were quantitated by PhosphorImager analysis. For comparison, the time courses of degradation of fGH and fGH7, from Fig. 2, are also shown. (B) Phosphorimage of RNase protection gels. The fGH8 mRNA protection product is indicated by an arrow.

RNase protection assays were run on nondenaturing gels. Because the probes used protected the 3′ end of the mRNA up to the polyadenylation site, and RNase A does not cleave the poly(A) tail, the migration of the protected digestion products on a nondenaturing gel depends on the length of the tail. The stable mRNAs fGH, fGH55, and fGH9 were deadenylated very slowly (Fig. 4). RNA synthesized in the first hour following serum stimulation of the cells ran as a high-molecular-weight band, indicating the presence of a long poly(A) tail. During the subsequent 4 to 5 h, the tail length of these transcripts progressively decreased. During this time, the band appeared to broaden, which could indicate some increase in the heterogeneity of tail length during shortening or could be a consequence of the enhanced separation of smaller compared with larger molecules during gel electrophoresis. Between 6 and 8 h after serum stimulation, an accumulation of transcripts with short tails was evident; however, little or no poly(A)$^-$ mRNA was seen. This result suggests that this oligo(A) form is either degraded directly or further deadenylated to poly(A)$^-$ mRNA which does not accumulate because it is rapidly degraded.

There are several differences in the profile of deadenylation of the unstable fGH7 mRNA compared with the stable mRNAs. The fGH7 mRNA was rapidly deadenylated compared with the slow rate of poly(A) tail shortening seen with fGH, fGH55, and fGH9 (Fig. 4). To visualize steps in the rapid deadenylation of fGH7, samples were prepared at half-hourly intervals, instead of hourly as for the stable mRNAs. The heterogeneity of fGH7 poly(A) tail lengths increased markedly as shortening proceeded. The broadening of the band with time was greater than that seen with the stable fGH, fGH9, and fGH55 transcripts and so cannot be ascribed solely to the greater separation of smaller molecules by gel electrophoresis. This increase in heterogeneity could result from a more processive mechanism of exonucleolytic shortening of the fGH7 poly(A) tails. Some accumulation of oligo(A) mRNA could be seen between 2.5 to 4 h after stimulation, but little remained at 5 h poststimulation, and the shortest transcripts

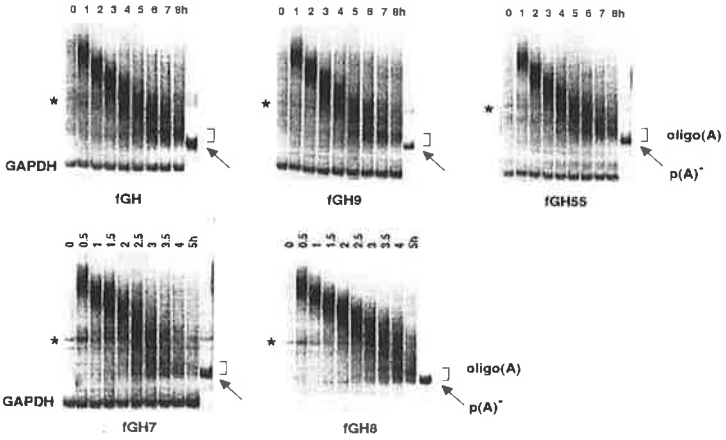

FIG. 4. Deadenylation of fGH7 and fGH8 mRNAs is rapid compared with that of the stable mRNAs fGH, fGH9, and fGH55. RNA was isolated at the times indicated following serum stimulation of NIH 3T3 cells stably transfected with the indicated constructs and was analyzed by RNase protection assay under conditions that do not cleave the poly(A) tail. The products were electrophoresed on nondenaturing polyacrylamide gels and visualized by PhosphorImager analysis. A *GAPDH* coding region probe was included as an internal quantitation standard except for the fGH8 experiment shown here, where its omission demonstrates that it does not obscure degradation products. The last track of each gel shows the migration of poly(A)$^-$ mRNA [p(A)$^-$], generated by treating RNA from serum-stimulated cells with RNase H in the presence of oligo(dT). The bracket indicates the position of the oligo(A) intermediate that can been seen late in the time courses. The asterisk indicates the position of a band that is not an intermediate in the deadenylation process but results from protection of full-length probe by a transcript believed to result from usage of a downstream polyadenylation site.

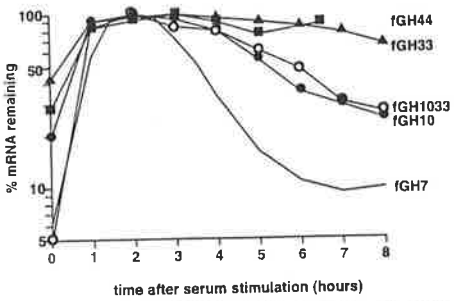

FIG. 5. Degradation of fGH mRNA is enhanced similarly by ARE10 and ARE1033 but not by ARE33 or ARE44. RNA was isolated at the times indicated following serum stimulation of NIH 3T3 cells stably transfected with the constructs indicated. For comparison, the time course of degradation of fGH7 mRNA, from Fig. 2, is also shown.

comigrated with the poly(A)$^-$ marker rather than as oligo(A) (Fig. 4). Thus, both the initial rate of poly(A) shortening and the degradation of the oligo(A) form are faster than the rates of these two steps seen with the stable transcripts, fGH, fGH55, and fGH9.

The other unstable mRNA, fGH8, was also deadenylated rapidly, although at a slightly slower rate than fGH7. In both cases, transcripts with no or very short poly(A) tails first appeared at approximately 2.5 h, correlating well with the end of the lag preceding the onset of rapid degradation (Fig. 2 and 3). This observation is consistent with the hypothesis that deadenylation is required before degradation of the body of the mRNA can occur (12, 21, 38, 47, 53) and that AREs increase the overall degradation rate by increasing the rate of poly(A) shortening.

U tracts do not destabilize. ARE55 contains AUUUA motifs but does not destabilize. Are the AUUUA motifs in ARE7 and ARE8 essential for their destabilizing effects, or may it be some other feature of these AREs, such as the preponderance of U residues, that was responsible for destabilization? Indeed, a common feature of cytokine and oncogene AREs is that they are primarily U rich with interspersed A's (for compilations of ARE sequences, see references 19 and 45). Our results with fGH7, fGH8, fGH9, fGH55, and fGH (Fig. 2 and 3) were consistent with the possibility that AREs act by forming stem-loop structures with the poly(A) tail, since the sequences that were most effective at both promoting poly(A) removal and destabilizing the mRNA (ARE7 and to a lesser extent ARE8) were those that could potentially form the strongest base-pairing interactions with the poly(A) tail.

We tested whether AREs that contain strings of U but no AUUUA motifs can promote degradation by making ARE33 and ARE44 (Fig. 1). The fGH33 and fGH44 mRNAs were quite stable, however (Fig. 5), and were subject to poly(A) shortening at the same slow rate (Fig. 6 and data not shown) as the other stable mRNAs (Fig. 4). Thus, strings of U, and by implication a secondary structure involving the poly(A) tail, are not likely to be the crucial feature that promotes the degradation of the mRNA; the sequence AUUUA, while not in itself sufficient, appears to be necessary for destabilization.

Although the U-rich sequences that we tested had no effect on degradation of the mRNA, it is conceivable that the U strings present in many cytokine and oncogene AREs enhance the effects of proximal AUUUA-containing motifs. We considered this possibility following a report by Shyu et al. (47), who showed that mutation of the c-*fos* AUUUA motifs had only a small effect on the rate of deadenylation of a chimeric mRNA. This raised the possibility that one or both of the U-rich regions in the c-*fos* ARE act as an enhancer of deadenylation. Since our ARE33 contains a duplication of a sequence very similar to the c-*fos* U-rich element that lies downstream of the AUUUA motifs, we tested whether ARE33 could enhance deadenylation of several fGH variants. ARE33 was inserted downstream of ARE7, ARE8, and a truncated, less destabilizing form of ARE7 called ARE10 (see below), generating fGH733, fGH833, and fGH1033, respectively. Insertion of the extra U-rich sequences did not enhance either the degradation rate (Fig. 5 and data not shown) or the rate of poly(A) shortening (Fig. 6 and data not shown).

Delineation of a minimal functional sequence. The functional element that marks the mRNA for rapid turnover does not seem to be a stem-loop structure formed by base pairing between the poly(A) tail and U-rich sequences in the ARE. Furthermore, secondary structure predictions from cytokine and oncogene 3'UTR sequences did not reveal any common secondary structures in the vicinity of the AU-rich regions (data not shown). Thus, the AREs probably provide binding sites for one or more degradation factors that recognize a single-stranded RNA sequence. Since this sequence, or a close match to the sequence, must be present in ARE7, but not in

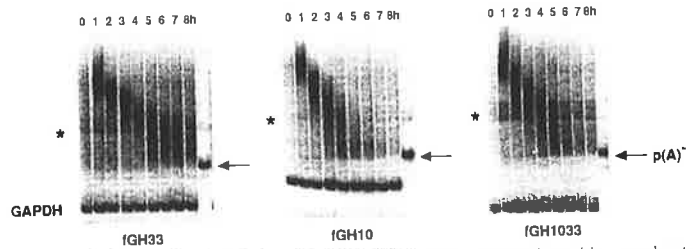

FIG. 6. A U-rich ARE does not influence deadenylation rate, either alone or in conjunction with a moderately destabilizing AUUUA-containing ARE. RNA was isolated at the times indicated following serum stimulation of NIH 3T3 cells stably transfected with the indicated constructs and analyzed by RNase protection assay under conditions that do not cleave the poly(A) tail. The products were electrophoresed on nondenaturing polyacrylamide gels and visualized by PhosphorImager analysis. The last track of each gel shows the migration of poly(A)$^-$ mRNA [p(A)$^-$], generated by treating the sample with RNase H in the presence of oligo(dT). The asterisk indicates the position of a band that is not an intermediate in the deadenylation process but results from protection of full-length probe by a transcript believed to result from usage of a downstream polyadenylation site.

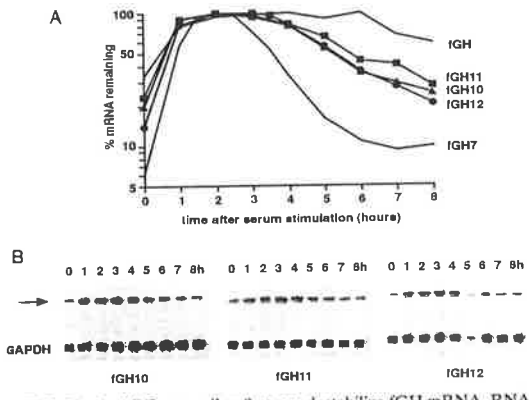

FIG. 7. An ARE as small as 9 nt can destabilize fGH mRNA. RNA was isolated at the times indicated following serum stimulation of NIH 3T3 cells stably transfected with the indicated constructs. (A) Time course of degradation of the mRNAs. Specific mRNAs were quantitated by PhosphorImager analysis. For comparison, the time courses of degradation of fGH and fGH7, from Fig. 2, are also shown. (B) Phosphorimage of RNase protection gels. The mRNA protection product is indicated by an arrow.

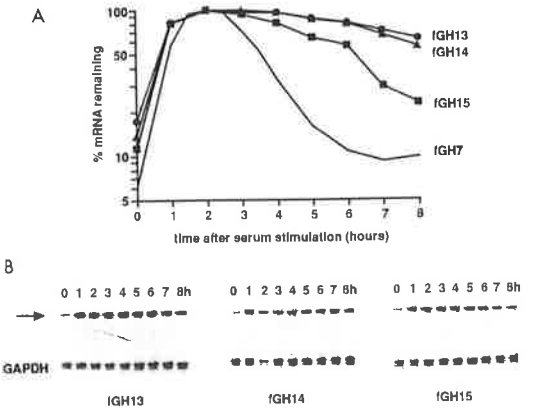

FIG. 8. UAUUUAU is the smallest sequence from ARE7 that can destabilize. RNA was isolated at the times indicated following serum stimulation of NIH 3T3 cells stably transfected with the indicated constructs. (A) Time course of degradation of the mRNAs. Specific mRNAs were quantitated by PhosphorImager analysis. For comparison, the time course of degradation of fGH7 mRNA, from Fig. 2, is also shown. (B) Phosphorimage of RNase protection gels. The mRNA protection product is indicated by an arrow.

the AREs that do not destabilize (ARE33, ARE44, ARE55, and ARE9), some short sequences can be eliminated from consideration at this stage. ARE7 contains a repeating motif that can be equally expressed as $(AUUU)_n$, $(UAUU)_n$, $(UUAU)_n$, or $(UUUA)_n$, but multiple copies of all these tetranucleotide sequences are present in ARE33 and ARE44, which do not destabilize. Similarly, the pentanucleotide sequences UAUUU, UUAUU, and UUUAU that are present in multiple copies in ARE7 are present in multiple copies in ARE33 and ARE44, and the AUUUA sequence is present in ARE55. Thus, the minimal functional sequence within ARE7 must be more than 5 nt in length and must contain AUUUA. However, strict adherence to a unique sequence longer than 6 nt is not likely to be necessary for destabilizing activity, since the longest sequence that is highly conserved in cytokine and oncogene AREs is UAUUUA (33).

To more closely delimit the functional sequence, we made shorter forms of ARE7, creating ARE10 (AUUUAUUUAU UUA) and ARE11 (AUUUAUUUA) (Fig. 1). Both of these AREs increased the degradation rate of the mRNA, showing that a sequence as short as 9 nt can destabilize, although not as effectively as ARE7 (Fig. 7). If AREs function as factor binding sites, the greater efficiency of ARE7 than of ARE10 and ARE11 could result from ARE7 containing a single, larger and therefore higher-affinity site or could be due to the presence of multiple sites. If ARE7 contains a single site, this could be composed of an essential core sequence plus less specific AU-rich flanking sequences which contribute to the affinity of the site. To investigate this possibility, we included extra AU-rich sequences flanking the AUUUAUUUA sequence of fGH11 to increase the size of the ARE to that of ARE7, generating fGH12 (Fig. 1). The presence of the extra flanking AU-rich sequences had at most a small effect on the stability (Fig. 7) and did not produce an ARE as destabilizing as ARE7. The greater effectiveness of ARE7 than of ARE10, ARE11, and ARE12 is therefore probably due to the presence of more functional motifs in ARE7 than in ARE10, ARE11, and ARE12.

Three copies of UAUUUAU can destabilize. Since the 5-nt sequence AUUUA was necessary but not alone sufficient to destabilize, we tested whether a 6- or 7-nt sequence from ARE7 could function. To ensure that small effects would be detectable, we inserted three copies of each of these short sequences, separated by the sequence CACAC. Neither AUUUAU (ARE13) nor UAUUUA (ARE14) destabilized the fGH transcript (Fig. 8); however, three copies of UAUUUAU (ARE15) did destabilize (Fig. 8), suggesting that UAUUUAU is the smallest sequence from within ARE7 that is sufficient to destabilize an mRNA. Since ARE8 and ARE11 do not contain exact copies of UAUUUAU but are nevertheless destabilizing, it must be concluded that the sequences flanking AUUUA in these larger AREs in some way obviate a strict requirement for the UAUUUAU sequence. This conclusion is consistent with the observation that UAUUUA is the longest highly conserved sequence in cytokine and proto-oncogene AREs (33).

AREs appear to increase degradation by increasing the deadenylation rate. We showed above that the destabilizing ARE7 and ARE8 increase the rate of poly(A) shortening compared with nondestabilizing AREs (ARE55, ARE9, ARE33, and ARE44), or no ARE (fGH). To examine further the relationship between effects on deadenylation versus degradation, we analyzed the effects of all of the ARE sequences on both processes. Because the unstable mRNAs become rapidly heterogeneous in poly(A) tail length and we cannot measure actual poly(A) tail length on our nondenaturing gels, it is difficult to calculate a meaningful shortening rate. Instead, we quantitated the whole tail length profile at various times after serum stimulation (Fig. 9 and data not shown). The individual plots were normalized by using the *GAPDH* internal standard to correct for any variation in the amount of RNA run on the gel. To reduce the distortion resulting from the read-through product (Fig. 2) and the small contribution from the heterogeneous smear due to basal transcription, the steady-state profile from unstimulated cells (time zero in Fig. 4 and 6) was subtracted from each profile obtained after serum stimulation.

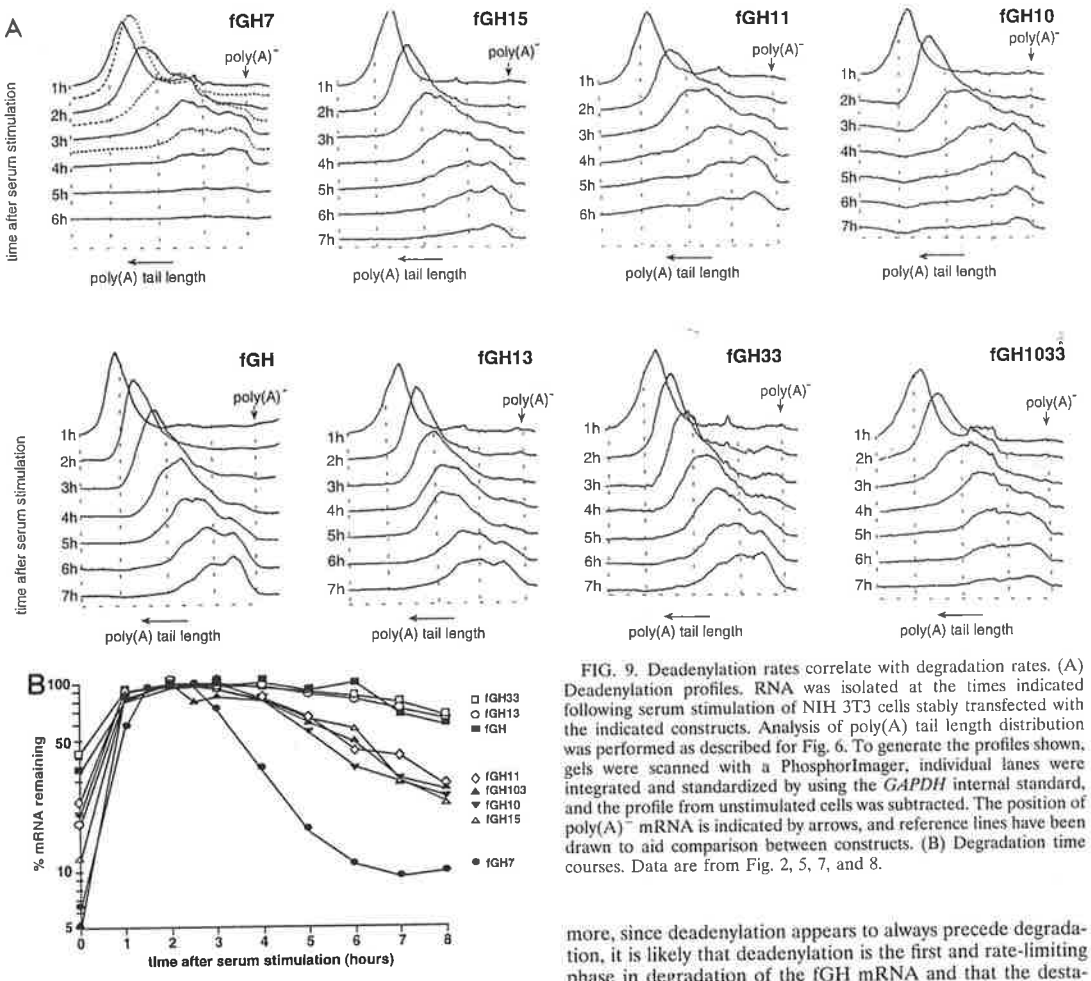

FIG. 9. Deadenylation rates correlate with degradation rates. (A) Deadenylation profiles. RNA was isolated at the times indicated following serum stimulation of NIH 3T3 cells stably transfected with the indicated constructs. Analysis of poly(A) tail length distribution was performed as described for Fig. 6. To generate the profiles shown, gels were scanned with a PhosphorImager, individual lanes were integrated and standardized by using the *GAPDH* internal standard, and the profile from unstimulated cells was subtracted. The position of poly(A)$^-$ mRNA is indicated by arrows, and reference lines have been drawn to aid comparison between constructs. (B) Degradation time courses. Data are from Fig. 2, 5, 7, and 8.

This minimizes overrepresentation of the read-through transcripts, the protected products of which run as a discrete band rather than as a smear because the antisense RNA probe does not protect the 3′ end of these longer transcripts, resulting in removal of the poly(A) tail. The time intervals were hourly except for fGH7, which because of its more rapid deadenylation was sampled half-hourly.

The profiles in Fig. 9 show that the correlation between deadenylation rate and degradation rate (Fig. 2, 3, 5, 7, and 8; summarized in Fig. 9B) is maintained without exception, with those mRNAs which degraded more rapidly undergoing more rapid poly(A) shortening. The length of the lag before degradation of the mRNA body begins (varying from 1 h for fGH7 to 4.5 h for fGH) also correlates well with the time at which transcripts with no or very small poly(A) tails first appear.

Since the ARE sequences that we constructed were mostly simple reiterated sequences, the most likely explanation for this correlation is that the same putative ARE-binding factor was influencing both deadenylation and degradation. Furthermore, since deadenylation appears to always precede degradation, it is likely that deadenylation is the first and rate-limiting phase in degradation of the fGH mRNA and that the destabilizing effect of the inserted AREs results largely from their ability to increase the deadenylation rate.

DISCUSSION

A model system with which to study the effects of synthetic AREs on mRNA stability. Chimeric genes have been used in a number of studies to assess the destabilizing effect of various elements within the 3′UTRs of natural mRNAs (3, 17, 21, 45, 47, 48). Such systems have several advantages: by using a coding region from a stable mRNA (which presumably does not contain a destabilizing element such as those identified in the coding regions of the c-*fos* [30, 48] and c-*myc* [54] mRNAs) and by inserting all sequences at a fixed location in the 3′UTR, other influences on mRNA stability can be minimized, allowing the observed effects to be attributed to the insertion of these sequences. We have used such a chimeric gene, with various synthetic AU-rich sequences inserted into the 3′UTR, to analyze the sequence requirements for ARE-mediated mRNA destabilization. To perform these experiments, we found it preferable to use the inducible c-*fos* promoter, rather

than a constitutive promoter, to drive expression. In initial experiments using a constitutive promoter, we found that certain AREs reduced the steady-state level of the mRNA; however, when the mRNA half-life was measured following transcription inhibition with actinomycin D, the mRNA did not appear as unstable as expected. Subsequent experiments using the *fos* promoter confirmed that actinomycin D treatment decreased the degradation rate of the mRNA (33). Actinomycin D has also been shown to prolong the life of several other ARE-containing mRNAs (3, 46, 48, 52). On the other hand, stimulation of cells with serum (used to induced expression from the *fos* promoter) did not change the apparent half-life of an unstable ARE-containing mRNA driven from a constitutive promoter (14). The pulse of transcription from the *fos* promoter also makes it possible to determine precursor-product relationships for early intermediates in the degradation pathway, facilitating analysis of changes in poly(A) tail length during mRNA degradation.

AUUUA and oligo(U) do not destabilize, but multiple copies of UAUUUAU do. From inspection of cytokine and oncogene 3′UTR sequences, we concluded that a common feature was the presence of strings of 3 to 6 U's, often flanked by single A's. Because of this, the hypothesis that guided the initial design of AU sequences to be tested was that U richness was the functional feature of AREs, perhaps because it promoted the formation of a hairpin structure by base pairing with the poly(A) tail (45, 53). Alternatively, You et al. (55) have proposed that some U-rich AREs may be recognized on the basis of their U richness, but as single-stranded rather than double-stranded RNA. Nevertheless, in our experiments with mRNAs containing AREs with strings of U of various lengths, we found no effect of the U-rich AREs on the stability of the mRNA and concluded it was unlikely that AREs function by forming a hairpin structure. In subsequent experiments, we assumed that the ARE functioned as a single-stranded binding site for a degradation factor, and the following discussion therefore uses the terms destabilizing sequence and binding site interchangeably, although the notion that the destabilizing sequence is a factor binding site remains unproven.

We found that the sequence AUUUA is not sufficient to confer instability on an mRNA, even when present in multiple copies. The smallest sequence that destabilized in multiple copies was UAUUUAU, although this sequence is probably not optimal since ARE15, containing three separated copies of this sequence, was not as effective as ARE7, which contains only two nonoverlapping copies. For simplicity, we consider here only nonoverlapping copies of the motif because steric hindrance is likely to prevent the simultaneous binding of potential destabilizing factors to two overlapping copies of a binding site. The use of overlapping sites cannot be ruled out but would not change the conclusions that follow. The greater efficiency of ARE7 than of ARE15 could result from one or both of the two putative binding sites in ARE7 providing a better match to the full binding-site sequence. It is also possible that the greater efficiency is due to ARE7 having a more optimal spacing between its two sites, allowing cooperative interactions in the binding of two factors, or a single dimeric factor, or to a combination of better spacing and better matches to the sequence.

The full motif may be UUAUUUA(U/A)(U/A). In Fig. 10, we have attempted to deduce a consensus sequence for the putative optimal binding site, based on the relative destabilizing efficiencies of the different AREs tested in this study. Since we do not know the degree of cooperativity, if any, resulting from multiple sites, the optimal spacing between sites, or the relative effects of different mismatches in the site, our conclusions remain somewhat speculative. Nevertheless, the relative efficiencies of the various AREs tested are consistent with (i) the binding site being UUAUUUAUU, (ii) the AUUUA core being necessary but not sufficient, and (iii) a total of no more than two mismatches being tolerated in the flanking positions, where their presence reduces the efficiency of the site.

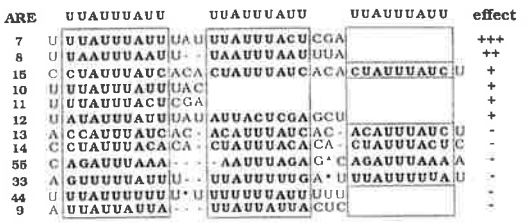

FIG. 10. Matches within different AREs to the motif UUAUUU AUU and their relative destabilizing effects. ARE sequences are aligned to maximize the fit to UUAUUUAUU. Only sequences within the AREs are shown, and matches to the motif are indicated by stippling. The asterisks in ARE55, ARE33, and ARE44 represent 3, 9, and 11 nt, respectively. ARE12 can alternatively be described as UUAUUUAUA; ARE55 has a fourth AUUUA-containing motif that is not shown.

The proposed requirement for AUUUA as a necessary core is based on several observations. ARE33 and ARE44 both contain at least two copies of the proposed UUAUUUAUU motif with just one or two mismatches, but the mismatches occur in the AUUUA core, and these AREs do not destabilize. Similarly, three mismatches to this motif occur in ARE9, two of which are within the AUUUA core, and this ARE also does not destabilize. The frequency with which AUUUA occurs in the 3′UTRs of unstable cytokine and oncogene mRNAs also suggests it has an important role, and in several studies in which point mutations were introduced into the AUUUA motifs of destabilizing AREs, disruption of the AUUUA sequences abolished the destabilizing effect (45, 47, 50).

The argument for inclusion of the extra U's flanking the UAUUUAU motif is based in part on the relative efficiencies of ARE8, ARE11, and ARE12 compared with ARE15. ARE15 has three UAUUUAU motifs but is no more destabilizing than ARE11 and ARE12, which probably have only one binding site (Fig. 10) and, in the case of ARE11, an incomplete UAUUUAU motif. This observation suggests that, while sufficient, the UAUUUAU motif may not be optimal. Additionally, ARE8 has no complete UAUUUAU sequences yet is more destabilizing than ARE15, indicating that UAUUUAU cannot be necessary for destabilization. The common feature between ARE8, ARE11, and ARE12 that is absent in ARE15 is U at one or both positions flanking the UAUUUAU, suggesting that U at these positions contributes to the effectiveness of the sequence as a destabilizing motif.

One copy of the proposed binding site, as in ARE10, ARE11, and ARE12, is clearly sufficient to produce a destabilizing effect, although multiple copies, as in ARE7 and ARE8, are more effective. Furthermore, the effectiveness of individual motifs probably depends on the degree of mismatching in the first two and last two positions (compare ARE7 with ARE15). Thus, AREs can potentially confer on mRNAs a wide range of half-lives, and this appears to be reflected in the variety of ARE sequences found in different cytokine and oncogene mRNAs.

A survey of 42 different cytokine and oncogene 3′UTR sequences from human and mouse genomes, containing 230

TABLE 1. Relative nucleotide frequencies at positions flanking AUUUA sequences[a]

Base	Relative frequency (%) at indicated position in the sequence NNAUUUANN			
	1	2	8	9
U	44.3	77.4	69.1	44.8
A	26.1	16.1	26.1	31.7
C	15.7	5.7	2.2	7.8
G	13.9	0.9	2.7	15.7

[a] Derived from 42 cytokine and oncogene 3′UTR sequences from human and mouse genomes, containing 230 AUUUA motifs.

AUUUA motifs, is consistent with the functional motif being UUAUUUAUU. Where the sequence NNAUUUANN occurs, U is the preferred base at positions 1, 2, 8, and 9 (Table 1). In addition, the sequence UAUUUAU occurs at least once in 39 of the 42 3′UTRs. When U is not present at positions 8 or 9, there is a strong bias for A, suggesting that A at one or both of these positions may contribute to the affinity of the binding site, or at least be less disruptive than G or C. Since the results of experiments in which a segment from the 3′UTR of granulocyte colony-stimulating factor was inserted into fGH also suggest that A is an acceptable substitution for U at position 8 or 9 (14), we propose that the functional element is more correctly defined as UUAUUUA(U/A)(U/A). The destabilizing ability of ARE8 is also consistent with A being an acceptable substitution for U at position 8.

Since the sequence AUUUA is the essential core of a destabilizing motif but is not in itself sufficient to destabilize an mRNA, it is not necessarily correct to assume, without measurement of the half-life, that an mRNA containing AUUUA in the 3′UTR will be unstable. The larger motif that we have described should be a better indicator of the likely stability of newly identified AUUUA-containing mRNAs.

Implications for studies of binding proteins. A number of AU-binding proteins have been identified by using UV cross-linking and gel shift assays (8, 10, 22, 24, 27, 42, 50, 56). Some of these proteins bind poly(U) as well as AUUUA-containing RNAs (10, 27, 42, 50, 56), suggesting that the binding to the AUUUA-containing probes may result from affinity for oligo(U) stretches. Since the oligo(U) containing ARE33 and ARE44 did not destabilize the fGH mRNA, the primary destabilizing factor is probably not a U-binding protein. Two proteins identified by Bohjanen et al. (10) in stimulated T cells (AU-B and AU-C) appear to have binding characteristics consistent with our destabilizing data and do not bind poly(U). Thus, our data support the proposal that these proteins may have a role in ARE-mediated degradation (10).

Destabilizing AREs enhance the rate of deadenylation. We have examined the effects of various ARE sequences on both deadenylation and degradation of fGH mRNA and found that poly(A) shortening preceded degradation of both stable and unstable variants of this mRNA. In all cases, there was a correlation between the rate of deadenylation and degradation of the mRNA; all destabilizing AREs enhanced the deadenylation rate, and no ARE stimulated just one of these processes. We cannot distinguish from these experiments whether the destabilizing effect of UUAUUUA(U/A)(U/A) motifs results from stimulation of deadenylation alone (which could be rate limiting in degradation) or whether steps subsequent to deadenylation are also stimulated.

The poly(A) tails of stable mRNAs were slowly and rather uniformly shortened over a period of several hours until the tails reached an oligo(A) form (which presumably binds at least one molecule of PABP). The transient accumulation of this species indicates that a subsequent step in its degradation is slow. Although no poly(A)$^-$ mRNA was evident during degradation of the fGH mRNA or the other stable variants, it cannot be concluded that these mRNAs are not terminally deadenylated. The difference between the slow rate of conversion of oligo(A) mRNA to poly(A)$^-$ mRNA and the rate of the subsequent degradation of poly(A)$^-$ mRNA may be too great for any significant accumulation of the poly(A)$^-$ form to occur.

The more unstable mRNAs, especially fGH7, became shorter and more heterogeneous in length early in the time course compared with the stable mRNAs, consistent with deadenylation being faster and more processive, as observed for rapidly deadenylated yeast mRNAs (21, 38). Less oligo(A) mRNA accumulated, indicating that this intermediate was also more rapidly degraded. Since a poly(A)$^-$ form of the fGH7 mRNA was detected, a portion at least of this unstable mRNA undergoes terminal deadenylation.

Our data show that deadenylation precedes mRNA body degradation and proceeds in at least two phases, consistent with the suggestion that the mRNA degradation pathways are similar in yeast and mammalian cells (21, 38). The simplest explanation for our observations is that AREs destabilize mRNAs by enhancing the rates of both poly(A) shortening and terminal deadenylation. However, degradation without terminal deadenylation has been observed for two yeast mRNAs by the artificial stabilization of degradation intermediates, which were found to have short oligo(A) tails (21). Thus, it could well be that not all mammalian mRNAs are terminally deadenylated prior to degradation: in addition to stimulating deadenylation, AREs may also stimulate the rate of decapping or endonucleolytic cleavage of deadenylated or oligoadenylated mRNAs.

U-rich sequences do not enhance deadenylation. Single substitutions of A for U in the AUUUA motifs of the ARE from c-*fos* have been shown to inhibit its ability to stimulate mRNA degradation but to have only a slight effect on the deadenylation rate (47). These studies suggested that in the more complex c-*fos* ARE, the AUUUA motif is required for degradation of the mRNA body but not for deadenylation, whereas our studies indicate that the UUAUUUA(U/A)(U/A) motif stimulates both processes. Another implication of the observations of Shyu et al. (47) was that the U-rich sequences proximal to the AUUUA motifs in the complex c-*fos* ARE may play a role in stimulating deadenylation. Since we found that two synthetic U-rich AREs (ARE33 and ARE44) had no stimulatory effect on deadenylation of the fGH mRNA, we tested whether ARE33, the sequence most resembling the downstream U-rich region of the c-*fos* ARE, stimulated deadenylation when placed 3′ of either our most destabilizing (fGH7) or less destabilizing AREs (fGH10 and fGH8). However, no enhancement of deadenylation or degradation of these chimeric mRNAs was observed, leading us to conclude that in this context a U-rich sequence has no effect.

A further analysis of the c-*fos* ARE was published while our manuscript was in the final stages of preparation (17) and has shown, consistent with our findings, that the AUUUA-containing region is sufficient to promote deadenylation and degradation of a heterologous mRNA, while the downstream U-tract alone is not. In contrast to our findings, however, this U tract was found to have an enhancing effect on deadenylation when placed either 5′ or 3′ of the AUUUA motifs. It therefore appears that the precise nature and context of such U-rich

sequences in individual complex AREs may determine their influence on deadenylation.

Using simple synthetic AREs, we have identified a motif, UUAUUUA(U/A)(U/A), which we suggest is the binding site for a destabilizing factor that promotes two phases of mRNA deadenylation. This information should aid the understanding of the function of the more complex AREs that occur in some natural mRNAs.

ACKNOWLEDGMENTS

We thank D. Cohen and H. Iba for the gift of the plasmid pfos3CAT, L. Ashman for the gift of plasmid pHcGAP, A. Robins for the gift of plasmid pHGH, R. Bryant (Royal Adelaide Hospital Medical Illustration Unit) for assistance with figure preparation, and L. Coles, T. Gonda, Y. Khew-Goodall, and F. Shannon for critical reading of the manuscript.

C. Brown is the recipient of an Overseas Postgraduate Research Scholarship from the University of Adelaide, and G. Goodall is the Poseidon Fellow of the Hanson Centre for Cancer Research. This work was supported by the National Health and Medical Research Council of Australia and the Royal Adelaide Hospital Research Review Committee.

REFERENCES

1. **Aghib, D. F., J. M. Bishop, S. Ottolenghi, A. Guerrasio, A. Serra, and G. Saglio.** 1990. A 3′ truncation of *MYC* caused by chromosomal translocation in a human T-cell leukemia increases mRNA stability. Oncogene **5:**707–711.
2. **Aharon, T., and R. J. Schneider.** 1993. Selective destabilization of short-lived mRNAs with the granulocyte-macrophage colony-stimulating factor AU-rich 3′ noncoding region is mediated by a cotranslational mechanism. Mol. Cell. Biol. **13:**1971–1980.
3. **Ahern, S. M., T. Miyata, and J. E. Sadler.** 1993. Regulation of human tissue factor expression by mRNA turnover. J. Biol. Chem. **268:**2154–2159.
4. **Akashi, M., A. H. Loussararian, D. C. Adelman, M. Saito, and H. P. Koeffler.** 1990. Role of lymphotoxin in expression of interleukin 6 in human fibroblasts. Stimulation and regulation. J. Clin. Invest. **85:**121–129.
5. **Astrom, J., A. Astrom, and A. Virtanen.** 1992. Properties of a HeLa cell 3′ exonuclease specific for degrading poly(A) tails of mammalian mRNA. J. Biol. Chem. **267:**18154–18159.
6. **Belasco, J., and G. Brawerman.** 1993. Control of messenger RNA stability. Academic Press, San Diego, Calif.
7. **Bernstein, P., S. W. Peltz, and J. Ross.** 1989. The poly(A)-poly(A)-binding protein complex is a major determinant of mRNA stability in vitro. Mol. Cell. Biol. **9:**659–670.
8. **Bickel, M., I. Yoshitaka, D. H. Pluznik, and R. B. Cohen.** 1992. Binding of sequence-specific proteins to the adenosine- plus uridine-rich sequences of the murine granulocyte/macrophage colony-stimulating factor mRNA. Proc. Natl. Acad. Sci. USA **89:** 10001–10005.
9. **Binder, R., S.-P. L. Hwang, R. Ratnasabapathy, and D. L. Williams.** 1989. Degradation of apolipoprotein II mRNA occurs via endonucleolytic cleavage at 5′-AAU-3′/5′-UAA-3′ elements in single-stranded loop domains of the 3′-noncoding region. J. Biol. Chem. **264:**16910–16918.
10. **Bohjanen, P. R., B. Petryniak, C. H. June, C. B. Thompson, and T. Lindsten.** 1992. AU RNA-binding factors differ in their binding specificities and affinities. J. Biol. Chem. **267:**6302–6309.
11. **Brawerman, G.** 1989. mRNA Decay: finding the right targets. Cell **57:**9–10.
12. **Brewer, G., and J. Ross.** 1988. Poly(A) shortening and degradation of the 3′ -A+U-rich sequences of human c-*myc* mRNA in a cell-free system. Mol. Cell. Biol. **8:**1697–1708.
13. **Brown, B. D., I. D. Zipkin, and R. M. Harland.** 1993. Sequence-specific endonucleolytic cleavage and protection of mRNA in *Xenopus* and *Drosophila*. Genes Dev. **7:**1620–1631.
14. **Brown, C. Y., C. A. Lagnado, and G. J. Goodall.** Unpublished data.
15. **Caput, D., B. Beutler, K. Hartog, R. Thayer, S. Brown-Shimer, and A. Cerami.** 1986. Identification of a common nucleotide sequence in the 3′-untranslated region of mRNA molecules specifying inflammatory mediators. Proc. Natl. Acad. Sci. USA **83:**1670–1674.
16. **Casey, J. L., D. M. Koeller, V. C. Ramin, R. D. Klausner, and J. B. Harford.** 1989. Iron regulation of transferrin receptor mRNA levels requires iron-responsive elements and a rapid turnover determinant in the 3′ untranslated region of the mRNA. EMBO J. **8:**3693–3699.
17. **Chen, C.-Y. A., T.-M. Chen, and A.-B. Shyu.** 1994. Interplay of two functionally and structurally distinct domains of the c-*fos* AU-rich element specifies its mRNA-destabilizing function. Mol. Cell. Biol. **14:**416–426.
18. **Chomczynski, P., and N. Sacchi.** 1987. Single-step method of RNA isolation by acid guanidinium thiocyanate-phenol-chloroform extraction. Anal. Biochem. **162:**156–159.
19. **Cosman, D.** 1987. Control of messenger RNA stability. Immunol. Today **8:**16–17.
20. **Coutts, M., and G. Brawerman.** 1993. A 5′ exoribonuclease from cytoplasmic extracts of mouse sarcoma 180 ascites cells. Biochim. Biophys. Acta **1173:**57–62.
21. **Decker, C. J., and R. Parker.** 1993. A turnover pathway for both stable and unstable mRNAs in yeast: evidence for a requirement for deadenylation. Genes Dev. **7:**1632–1643.
22. **Gillis, P., and J. S. Malter.** 1991. The adenosine-uridine binding factor recognizes the AU-rich elements of cytokine, lymphokine, and oncogene mRNAs. J. Biol. Chem. **266:**3172–3177.
23. **Goodall, G. J., and W. Filipowicz.** 1989. The AU-rich sequences present in the introns of plant nuclear pre-mRNAs are required for splicing. Cell **58:**473–483.
24. **Hamilton, B. J., E. Nagy, J. S. Malter, B. A. Arrick, and W. F. C. Rigby.** 1993. Association of heterogeneous nuclear ribonucleoprotein A1 and C proteins with reiterated AUUUA sequences. J. Biol. Chem. **268:**8881–8887.
25. **Helms, S. R., and F. M. Rottman.** 1990. Characterization of an inducible promoter system to investigate decay of stable mRNA molecules. Nucleic Acids Res. **18:**255–259.
26. **Hollis, G. F., A. F. Gazdar, V. Bertness, and I. R. Kirsch.** 1988. Complex translocation disrupts c-*myc* regulation in a human plasma cell myeloma. Mol. Cell. Biol. **8:**124–129.
27. **Huang, L.-Y., B. G. Tholanikunnel, E. Vakalopoulou, and C. C. Malbon.** 1993. The M_r 35,000 β-adrenergic receptor mRNA-binding protein induced by agonists requires both an AUUUA pentamer and U-rich domains for RNA recognition. J. Biol. Chem. **268:**25769–25775.
28. **Jackson, R. J., and N. Standart.** 1990. Do the poly(A) tail and 3′ untranslated region control mRNA translation? Cell **62:**15–24.
29. **Jones, T. R., and M. D. Cole.** 1987. Rapid cytoplasmic turnover of c-*myc* mRNA: requirement of the 3′ untranslated sequences. Mol. Cell. Biol. **7:**4513–4521.
30. **Kabnick, K. S., and D. E. Housman.** 1988. Determinants that contribute to cytoplasmic stability of human c-*fos* and β-globin mRNAs are located at several sites in each mRNA. Mol. Cell. Biol. **8:**3244–3250.
31. **Koeffler, H. P., J. Gasson, and A. Tobler.** 1988. Transcriptional and posttranscriptional modulation of myeloid colony-stimulating factor expression by tumor necrosis factor and other agents. Mol. Cell. Biol. **8:**3432–3438.
32. **Kowalski, J., and D. T. Denhardt.** Regulation of the mRNA for monocyte-derived neutrophil-activating peptide in differentiating HL60 promyelocytes. Mol. Cell. Biol. **9:**1946–1957.
33. **Lagnado, C. A., and G. J. Goodall.** Unpublished data.
34. **Laird-Offringa, I. A., C. L. de Wit, P. Elfferich, and A. J. van der Eb.** 1990. Poly(A) tail shortening is the translation-dependent step in c-*myc* mRNA degradation. Mol. Cell. Biol. **10:**6132–6140.
35. **Lieberman, A. P., P. M. Pitha, and M. L. Shin.** 1992. Poly(A) removal is the kinase-regulated step in tumor necrosis factor mRNA decay. J. Biol. Chem. **267:**2123–2126.
36. **Lowell, J. E., D. Z. Rudner, and A. B. Sachs.** 1992. 3′-UTR-dependent deadenylation by the yeast poly(A) nuclease. Genes Dev. **6:**2088–2099.
37. **Meijlink, F., T. Curran, A. D. Miller, and I. M. Verma.** 1985. Removal of a 67-base-pair sequence in the noncoding region of protooncogene *fos* converts it to a transforming gene. Proc. Natl. Acad. Sci. USA **82:**4987–4991.

38. **Muhlrad, D., and R. Parker.** 1992. Mutations affecting stability and deadenylation of the yeast MFA2 transcript. Genes Dev. **6:** 2100–2111.
39. **Paek, I., and R. Axel.** 1987. Glucocorticoids enhance stability of human growth hormone mRNA. Mol. Cell. Biol. **7:**1496–1507.
40. **Pandey, N. B., and W. F. Marzluff.** 1987. The stem-loop structure at the 3′ end of histone mRNA is necessary and sufficient for regulation of histone mRNA stability. Mol. Cell. Biol. **7:**4557–4559.
41. **Peppel, K., and C. Baglioni.** 1991. Deadenylation and turnover of interferon-β mRNA. J. Biol. Chem. **266:**6663–6666.
42. **Raj, N. B. K., and P. M. Pitha.** 1993. 65-kDa protein binds to destabilizing sequences in the IFN-β mRNA coding and 3′UTR. FASEB J. **7:**702–710.
43. **Sachs, A. B.** 1993. Messenger RNA degradation in eukaryotes. Cell **74:**413–421.
44. **Schiavi, S. C., J. G. Belasco, and M. E. Greenberg.** 1992. Regulation of proto-oncogene mRNA stability. Biochim. Biophys. Acta **1114:**95–106.
45. **Shaw, G., and R. Kamen.** 1986. A conserved AU sequence from the 3′ untranslated region of GM-CSF mRNA mediates selective mRNA degradation. Cell **46:**659–667.
46. **Shaw, J., K. Meerovitch, R. C. Bleackley, and V. Paetkau.** 1988. Mechanisms regulating the level of IL-2 mRNA in T lymphocytes. J. Immunol. **140:**2243–2248.
47. **Shyu, A-B., J. G. Belasco, and M. E. Greenberg.** 1991. Two distinct destabilizing elements in the c-*fos* message trigger deadenylation as a first step in rapid mRNA decay. Genes Dev. **5:**221–231.
48. **Shyu, A.-B., M. E. Greenberg, and J. G. Belasco.** 1989. The c-*fos* transcript is targeted for rapid decay by two distinct mRNA degradation pathways. Genes Dev. **3:**60–72.
49. **Stoeckle, M. Y., and L. Guan.** 1993. High-resolution analysis of *gro* α poly(A) shortening: regulation by interleukin-1β. Nucleic Acids Res. **21:**1613–1617.
50. **Vakalopoulou, E., J. Schaack, and T. Shenk.** 1991. A 32-kilodalton protein binds to AU-rich domains in the 3′ untranslated regions of rapidly degraded mRNAs. Mol. Cell. Biol. **11:**3355–3364.
51. **Vreken, P., and H. A. Raue.** 1992. The rate-limiting step in yeast *PGK1* mRNA degradation is an endonucleolytic cleavage in the 3′-terminal part of the coding region. Mol. Cell. Biol. **12:**2986–2996.
52. **Whittemore, L.-A., and T. Maniatis.** 1990. Postinduction turnoff of beta-interferon gene expression. Mol. Cell. Biol. **10:**1329–1337.
53. **Wilson, T., and R. Treisman.** 1988. Removal of poly(A) and consequent degradation of c-*fos* mRNA facilitated by 3′ AU-rich sequences. Nature (London) **336:**396–399.
54. **Wisdom, R., and W. Lee.** 1991. The protein-coding region of c-*myc* mRNA contains a sequence that specifies rapid mRNA turnover and induction by protein synthesis inhibitors. Genes Dev. **5:**232–243.
55. **You, Y., C.-Y. A. Chen, and A.-B. Shyu.** 1992. U-rich sequence-binding proteins (URBPs) interacting with a 20-nucleotide U-rich sequence in the 3′ untranslated region of c-*fos* mRNA may be involved in the first step of c-*fos* mRNA degradation. Mol. Cell. Biol. **12:**2931–2940.
56. **Zhang, W., B. J. Wagner, K. Ehrenman, A. W. Schaefer, C. T. deMaria, D. Crater, K. deHaven, L. Long, and G. Brewer.** 1993. Purification, characterization, and cDNA cloning of an AU-rich element RNA-binding protein, AUF1. Mol. Cell. Biol. **13:**7652–7665.

Brown, C.Y., Lagnado, C.A., Vadas, M.A. & Goodall, G.J. (1996) Differential regulation of the stability of cytokine mRNAs in lipopolysaccharide-activated blood monocytes in response to interleukin-10.
Journal of Biological Chemistry, v. 271(August), pp. 20108-20112

Submitted to Science

A cytokine mRNA-destabilising stem-loop that is functionally distinct from AU-rich elements

Cheryl Y. Brown, Cathy A. Lagnado and Gregory J. Goodall*

Hanson Centre for Cancer Research
Institute of Medical and Veterinary Science
Frome Road
Adelaide S.A. 5000
Australia

*To whom correspondence should be addressed

Abstract

The control of mRNA stability is crucial to the regulation of cytokine expression. Described here is a novel potent destabilising element, termed the stem-loop destabilising element (SLDE), found in the 3' untranslated region (3'UTR) of G-CSF mRNA. Evidence is presented that functionally equivalent elements also exist in the IL-2 and IL-6 mRNAs. The SLDE is functionally distinct from the AU-rich elements, which are also present in these and other cytokine mRNAs, since it destabilises a chimeric mRNA in a tumour cell line in which AU-rich elements do not function. In addition the effect of the SLDE is insensitive to calcium ionophore, and is therefore regulated independently of AU destabilising elements. The existence of two distinct mRNA destabilising elements provides an additional mechanism for the differential regulation of cytokine expression.

The control of mRNA degradation rate is a major factor in the regulation of expression of many cytokines and proto-oncogenes. The mRNAs of various hemopoietic cytokines, including G-CSF, GM-CSF, IL-1, IL-2, IL-3, IL-6 and TNFα, are unstable in unstimulated cells, but are stabilised for a period of time following cellular activation (1-5). The AU destabilising elements (AUDEs) present in the 3'UTRs of all these mRNAs clearly play a part in the degradation of these mRNAs in unstimulated cells (6,7), but how these mRNAs are stabilised is not known. Experiments with chimeric genes containing regions of the GM-CSF or the IL-11 3'UTRs have suggested that additional sequence elements may be necessary for mRNA stability to be fully regulated (8,9). Although the presence of an AUDE in an mRNA confers an instability that is sensitive to Ca^{2+} ionophore (10,11), the AUDE alone is not sufficient for stabilisation in response to natural inducers of cytokines such as IL-1 and TNF, or in response to phorbol ester (8,12,13). We had previously established a system for identifying the functional destabilising element within AU-rich sequences (14), and sought to apply the system to search for additional regulatory elements in the G-CSF mRNA. We describe here the identification of a novel destabilising element in the 3'UTR of the G-CSF mRNA, and present evidence that similar destabilising elements occur in the 3'UTRs of IL-2 and IL-6 mRNAs.

To identify regulatory elements in cytokine mRNAs we have used a reporter mRNA, termed fGH (Fig.1)(14), which is composed mostly of growth hormone sequences. Transcription of fGH is driven by the fos promoter, so that a brief transcriptional pulse can be generated by serum stimulation, without the use of transcriptional inhibitors. The fGH mRNA is normally stable, but can be made unstable by the insertion of a destabilising element at unique restriction sites in the 3'UTR , as is shown by the insertion of the synthetic AU-rich sequence in fGH-AU1 (Figs. 1, 2). Similarly, insertion of the AU-rich region from the G-CSF 3'UTR rendered the reporter mRNA unstable (fGH-AU2, Figs. 1, 2). As expected for instability conferred by AU-rich elements, both mRNAs could be stabilised by addition of the calcium ionophore,

A23187 (Fig. 2). To our surprise however, when the entire 3'UTR of G-CSF was inserted into the reporter gene, the resulting mRNA (fGH-GCSF) remained unstable in cells treated with the calcium ionophore (Fig. 3).

Many tumour cells constitutively express one or more cytokines, due at least in part to the abnormal stability of the cytokine mRNA in these cells (16). We transfected 5637 bladder carcinoma cells with the AUDE-containing reporter genes fGH-AU1 and fGH-AU2 and found that these mRNAs were constitutively stable (Fig. 2), indicating that the AU-mediated system of mRNA degradation does not function in these cells. However, the fGH-GCSF mRNA, which contains the entire 3'UTR of G-CSF, was relatively unstable in 5637 cells (Fig. 3). These results, together with the experiments with calcium ionophore, suggest that the 3'UTR of G-CSF contains a destabilising element that functions independently of the AU-mediated degradation system.

To identify candidate sequences for such an element we compared the sequences of the human and mouse G-CSF mRNAs. We noticed that the 3'UTRs (approximately 850 nt) were rather dissimilar, except for three segments of 50, 40 and 20 nt. The 50 nt segment contains the AU-rich region, which we had inserted to make fGH-AU2. The conserved 40 and 20 nt regions each contained sequences capable of forming a stem-loop structure, which we call stem-loop A and stem-loop B, respectively (Fig 4). We inserted a 183 nt segment (SL1), encompassing both the 40 nt and 20 nt conserved sequences, into fGH to create fGH-SL1. The fGH-SL1 mRNA, like the fGH-GCSF mRNA, was unstable (Fig. 5), suggesting that the 183 nt SL1 region contained the additional instability element. However, the interpretation was slightly complicated by the fact that the SL1 region includes two sequences that almost match the AUDE sequence, UUAUUUA(U/A)(U/A), one in the putative stem of stem-loop A, the other in the stem and loop of stem-loop B. We therefore made point mutations to ensure these potential AUDEs were not functional, creating fGHSL2 (Fig. 4). To maintain the potential for stem-loop formation in fGHSL2 we simultaneously introduced

complementary changes to maintain base pairing in the stems. The fGHSL2 mRNA was at least as unstable as fGHSL1, was not stabilised in the presence of ionophore (Fig. 5), and functioned in 5637 cells (data not shown), indicating that the instability element(s) were still intact and were not regulated by calcium. On the other hand, disruption of the stem-loops by uncompensated mutations in both stems, but leaving the potential AUDEs intact (fGHSL3, Fig. 4) removed the destabilising effect (Fig. 5). Thus the presence of one or both stem-loops, but not of the AUDE-like sequences, is necessary for the destabilising effect of this region. In fGHSL5 we changed the sequence of both loops, changing loop A from CAA to GCG and loop B from UAU to ACA (Fig 4). This eliminated the destabilising effect, indicating that at least some part of the loop sequence(s) is essential (Fig. 5).

To determine whether only one or both of the conserved stem-loops acts as a destabilising element we made fGHSL6 and fGHSL7, in which mutations were made to disrupt stem A and stem B, respectively (Fig. 4). The fGHSL6 mRNA, with stem A eliminated, remained unstable (Fig. 5), indicating that stem-loop A is not necessary for destabilisation, although the fGHSL6 mRNA was not quite as unstable as the fGHSL1 mRNA. However, disruption of stem B caused a marked increase in the stability of the mRNA (fGHSL7, Fig 5), indicating that stem-loop B is essential for instability. Finally, to test whether the region between the stem-loops is part of the destabilising element we made fGHSL2D, in which the 124 nt interloop region of fGHSL2 was replaced by just 12 nt. The fGHSL2D mRNA was stable (Fig. 5), indicating that part of the interloop region, or at least some sequence flanking the stem-loop, is required for the destabilising effect. Taken together, these results show that a region of the G-CSF 3'UTR that includes the conserved stem-loop B functions as a destabilising element and is responsible for the instability of fGH-GCSF mRNA in ionophore-treated cells and in 5637 cells.

To investigate whether cytokines in addition to G-CSF may contain similar non-AU instability elements, we made a series of chimeric genes in which entire 3'UTRs from various AUDE-containing cytokine genes replaced the 3'UTR of fGH. We compared the stabilities of the resulting mRNAs in NIH3T3 cells in the presence and absence of calcium ionophore. The fGH-GMCSF and fGH-IL4 mRNAs, containing the 3'UTR from GM-CSF and IL-4, respectively, were significantly stabilised by ionophore (data not shown), suggesting that for these mRNAs instability is primarily due to the AU-rich regions. In contrast, the fGH-IL2 and fGH-IL6 mRNAs were only modestly stabilised in the presence of ionophore (Fig. 6). Thus the IL-2 and IL-6 mRNAs appear to contain instability elements with functionally similar properties to the stem-loop element of G-CSF. Further experiments are required to locate these instability elements in the IL-2 and IL-6 mRNAs. Nevertheless, our results suggest that a class of potent instability element structurally and functionally distinct from AU-rich elements participates in the regulation of G-CSF, IL-2 and IL-6 mRNAs and suggests a mechanism for the differential regulation of cytokine mRNA stability.

Legends

Figure 1. The fGH gene and two of the sequences inserted into the 3'UTR. Boxes indicate regions derived from the chicken c-*fos* gene and growth hormone cDNA, while lines indicate vector-derived sequences. The translated region is shaded and the polyadenylation site is indicated.

Figure 2. AUDE-containing mRNAs are stable in 5637 bladder carcinoma cells and in NIH3T3 cells treated with the calcium ionophore A23187. RNA was isolated at various times after serum stimulation of cells stably transfected with chimeric fGH genes containing (A) a synthetic AU destabilising sequence (fGH-AU1) or (B) the AU-rich region from G-CSF (fGH-AU2), inserted in the 3'UTR. Specific mRNAs were quantitated by RNase protection assay. Both mRNAs were unstable in NIH3T3 cells but stable in 5637 cells, and both were stabilised in NIH3T3 cells treated with A23187. The data shown are means ± SEM from 3 experiments.

Figure 3. An mRNA containing the entire 3'UTR of G-CSF is unstable in 5637 cells, and is not stabilised in NIH3T3 cells treated with the calcium ionophore A23187. RNA was isolated at various times after serum stimulation of cells stably transfected with the fGH-GCSF gene. The data shown are means ± SEM from 2 experiments.

Figure 4. Various sequences inserted into the 3'UTR of the fGH gene. SL1, from the 3'UTR of human G-CSF, includes two putative stem-loops that are conserved in the mouse and human mRNAs. The 124 base sequence between the stems and 8 bases 3' of stem-loop B are not shown. The other sequences were derived from SL1 as shown.

Figure 5. The effects of SL1 and its derivatives on the stability of the fGH mRNA. The sequences inserted into fGH are described in Fig. 4. RNA was isolated at various times after serum stimulation of NIH3T3 cells stably transfected with variants of the

fGH gene containing the indicated sequences inserted in the 3'UTR. The stability of the fGHSL2 mRNA was unchanged by treatment of the cells with the calcium ionophore A23187 (dotted line in A). In B the SL1 data (dashed line) is replotted for comparison.

Figure 6. The 3' UTRs of IL-2 and IL-6 destabilise the fGH mRNA in the presence and absence of the calcium ionophore A23187. The entire 3'UTR of IL-2 or IL-6 was inserted near the termination codon of the fGH gene, generating fGH-IL2 and fGH-IL6 respectively. RNA was isolated at various times after serum stimulation of NIH3T3 cells stably transfected with either gene and quantitated by RNase protection assay. The data shown are means ± SEM from 2 experiments. Addition of A23187 at the time of serum stimulation resulted in only a modest increase in the survival of the mRNAs compared to the effect on mRNAs containing only AU-rich insertions (see Fig. 2).

References

1. H. P. Koeffler, J. Gasson, A. Tobler, *Mol. Cell Biol.* **8**, 3432 (1988).

2. T. Lindsten, C. H. June, J. A. Ledbetter, G. Stella, C. B. Thompson, *Science* **244**, 339 (1989).

3. S. C. Guba, G. Stella, L. A. Turka, C. H. June, C. B. Thompson, et al, *J. Clin. Invest.* **84**, 1701 (1989).

4. M. Akashi, A. H. Loussararian, D. C. Adelman, M. Saito, H. P. Koeffler, *J. Clin. Invest.* **85**, 121 (1990).

5. J. A. Elias, V. Lentz, *J. Immunol.* **145**, 161 (1990).

6. G. Shaw, S. Kamen, *Cell* **46**, 659 (1986).

7. T. Wilson, R. Treisman, *Nature* **363**, 396 (1988).

8. Y. Iwai, M. Bickel, D. H. Pluznik, R. B. Cohen, *J. Biol. Chem.* **266**, 17959 (1991).

9. L. Yang, Y. C. Yang, *J. Biol. Chem.* **269**, 32732 (1994).

10. A. Wodnar Filipowicz, C. Moroni, *Proc. Natl. Acad. Sci. U. S. A.* **87**, 777 (1990).

11. Y. Iwai, K. Akahane, D. H. Pluznik, R. B. Cohen, *J. Immunol.* **150**, 4386 (1993).

12. M. Akashi, G. Shaw, M. Hachiya, E. Elstner, G. Suzuki, et al, *Blood* **83**, 3182 (1994).

13. M. Akashi, G. Shaw, M. Gross, M. Saito, H. P. Koeffler, *Blood* **78**, 2005 (1991).

14. C. A. Lagnado, C. Y. Brown, G. J. Goodall, *Mol. Cell. Biol.* **14**, 7984 (1994).

15. Plasmids were constructed by insertion of the sequences described below into the Sac I site, or between the Kpn I and Sac I sites, of pfGH (14). pfGH-AU1 contains the sequence shown in Fig.1 generated by annealing of chemically synthesised oligonucleotides. pfGH-AU2 and pfGH-GCSF contain the sequence shown in Fig. 1 and the full 3'UTR of human G-CSF, respectively, generated by PCR amplification from a plasmid containing the human G-CSF cDNA (kindly provided by F. Shannon). PCR primers for generation of fGH variants SL1, SL2, SL3, SL6 and SL7 inserted, in addition to sequences shown in Fig. 3, the 5' sequence [Sac I]-AAGCTT and the downstream sequence ...TGTTCCCC-[Sac I]. The PCR amplification to generate the insert for fGHSL5 included Kpn I and Sac I sites immediately flanking the sequence

shown in Fig. 3. fGHSL2D was created by insertion of annealed oligonucleotides generating the sequence shown in Fig. 3 immediately flanked by Kpn I and Sac I sites. To prepare pfGH-IL2 and pfGH-IL6 the full 3'UTRs of human IL-2 and IL-6 cDNAs, respectively, flanked by 5'-Kpn I and 3'-Sac I sites, were PCR amplified from plasmids pAT153hIL2 (kindly provided by W. Fiers) and pBSF2.3.8.1 (kindly provided by T. Hirano).

Polyclonal NIH3T3 cultures transfected by electroporation with variants of the pfGH plasmid were established and cultured as described previously (14). Cultures of stably transfected 5637 cells were prepared similarly, but using electroporation settings of 270 V and 500 μF. Serum stimulation was performed as described (14) except that, where indicated, 2 μM A23187 was included in the medium containing 15% fetal calf serum.

RNA was isolated at various times after serum stimulation by the method of Chomczynski and Sacchi (17) and subjected to RNase protection assay using an RNA probe complementary to the growth hormone translated region and pGAPDH as an internal quantitation standard, as described (14).

16. H. J. Ross, N. Sato, Y. Ueyama, H. P. Koeffler, *Blood* **77**, 1787 (1991).

17. P. Chomczynski, N. Sacchi, *Anal. Biochem.* **162**, 156 (1987).

18. We thank Justin Dibbens, Leeanne Coles, Tom Gonda and Mathew Vadas for helpful comments on the manuscript. This work was supported by a program grant from the NH&MRC of Australia.

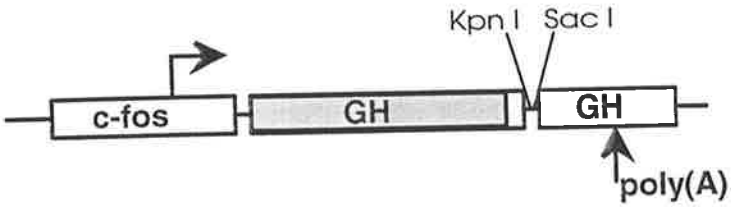

Kpn I Sac I

fGH-AU1 GGAUCCAUUUAUUUAUUUAUUUAUUUACUCAGCUGCAGUUUAUUUAUUUAUUUAUUUCUCGAGCUC

fGH-AU2 GGUACCUGAGCCAAGCCCUCCCCAUCCCAU
GUAUUUAUCUCUAUUUAAUAUUUAUGUCUAUUUAAGCCUCAUAUUUAAAGACAGAGCUC

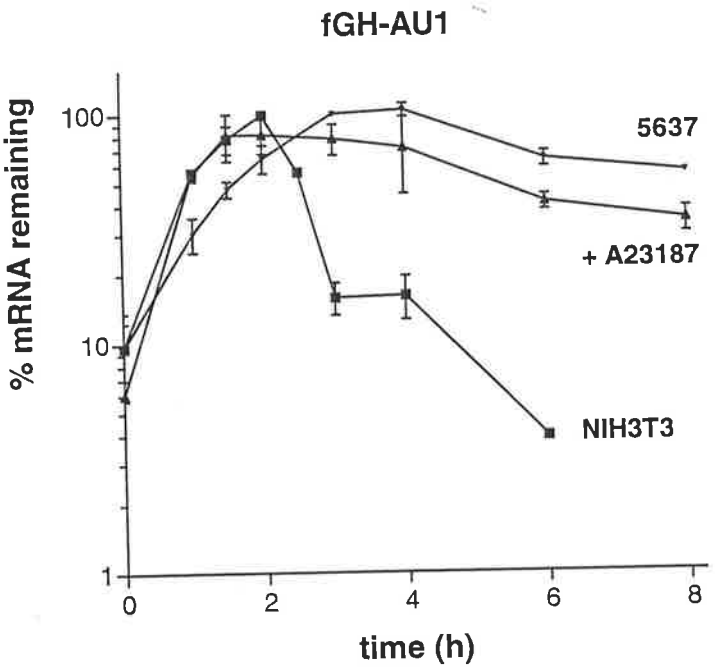
fGH-AU1
% mRNA remaining
100
10
1
0
2
4
6
8
time (h)
5637
+ A23187
NIH3T3

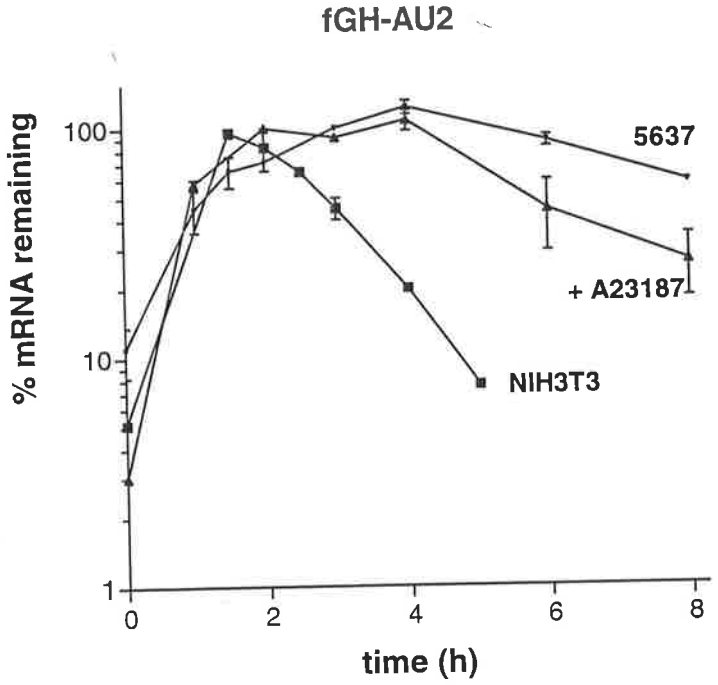
fGH-AU2
% mRNA remaining
100
10
1
0
2
4
6
8
time (h)
5637
+ A23187
NIH3T3

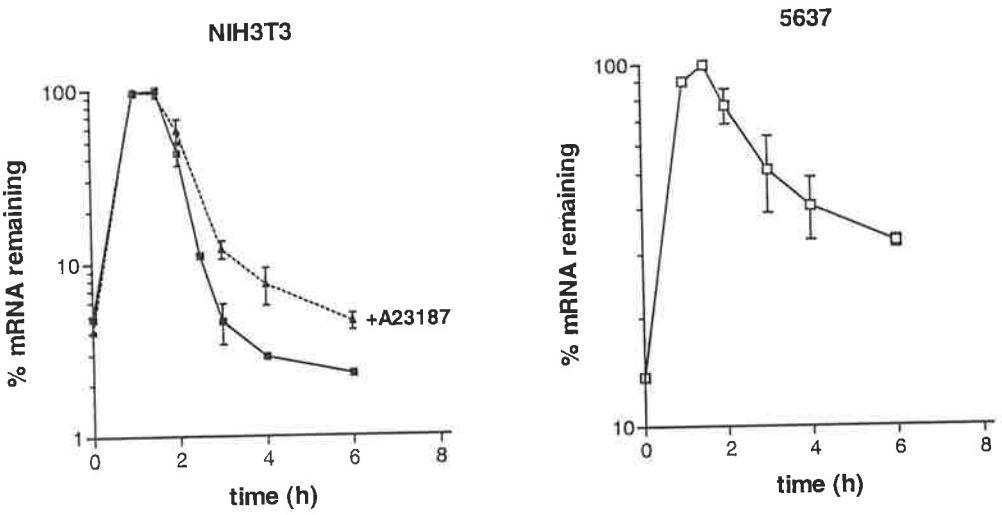
NIH3T3
5637
100
10
1
% mRNA remaining
+A23187
0
2
4
6
8
time (h)

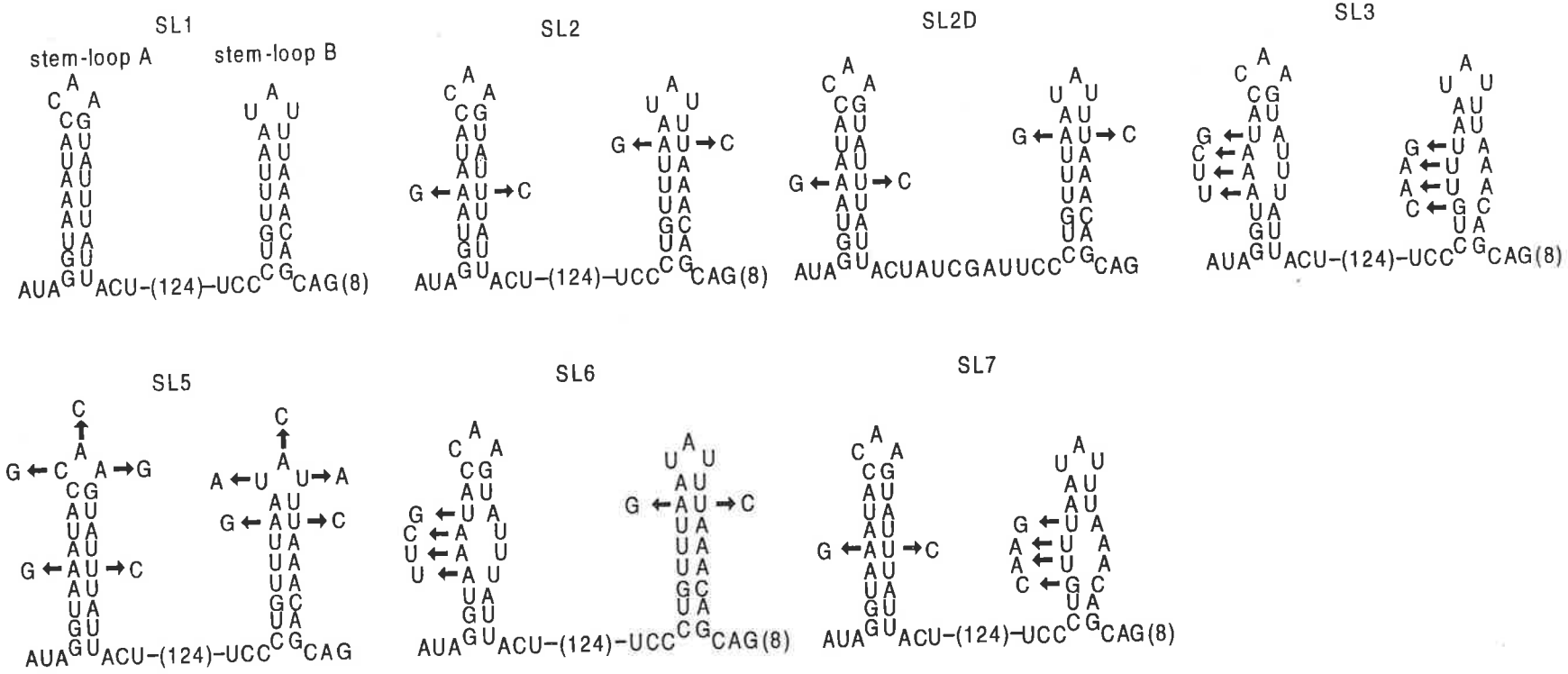
SL1
stem-loop A
stem-loop B
AUAGUACU-(124)-UCCCGCAG(8)
SL2
AUAGUACU-(124)-UCCCGCAG(8)
SL2D
AUAGUACUAUCGAUUCCCGCAG
SL3
AUAGUACU-(124)-UCCCGCAG(8)
SL5
AUAGUACU-(124)-UCCCGCAG
SL6
AUAGUACU-(124)-UCCCGCAG(8)
SL7
AUAGUACU-(124)-UCCCGCAG(8)

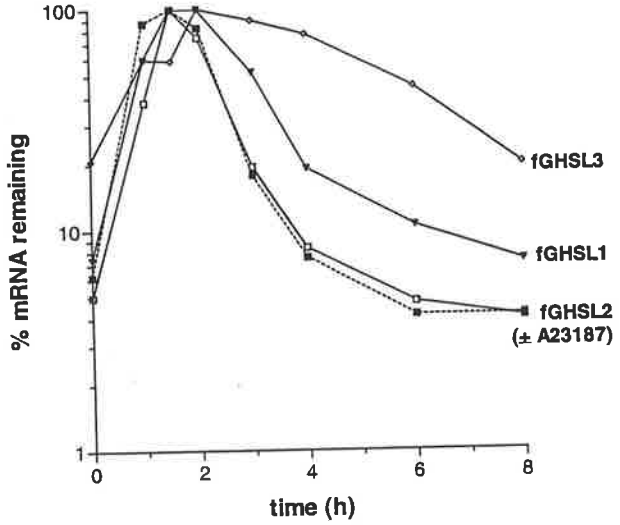
100
10
1
% mRNA remaining
0
2
4
6
8
time (h)
fGHSL3
fGHSL1
fGHSL2
(± A23187)

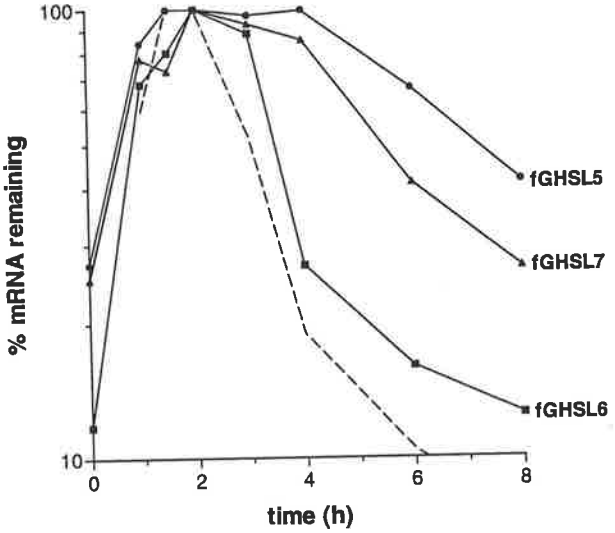
100
10
% mRNA remaining
0
2
4
6
8
time (h)
fGHSL5
fGHSL7
fGHSL6

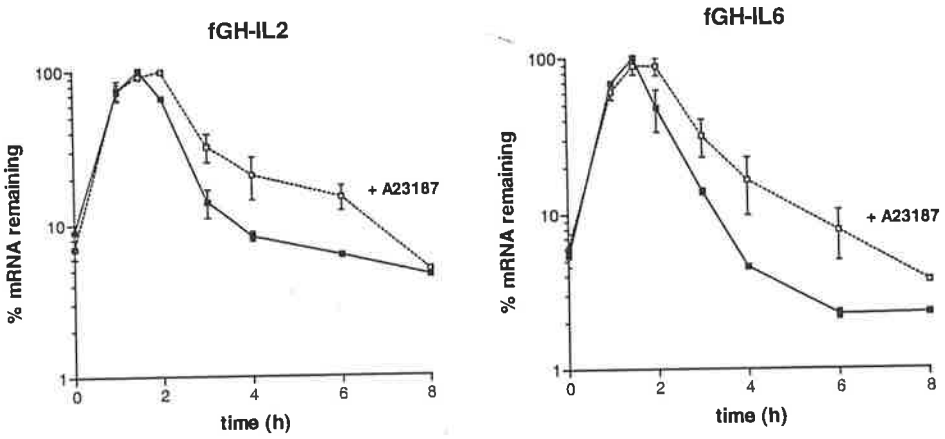
fGH-IL2
% mRNA remaining
100
10
1
0
2
4
6
8
time (h)
+ A23187
fGH-IL6
% mRNA remaining
100
10
1
0
2
4
6
8
time (h)
+ A23187